In vitro Liposomen-Rekonstitution intrazellulärer Signaltransduktion kleiner GTPasen

Inaugural-Dissertation

zur

Erlangung des Doktorgrades der

Mathematisch-Naturwissenschaftlichen Fakultät

der Heinrich-Heine-Universität Düsseldorf

vorgelegt von

Si-Cai Zhang

Aus Hubei, China

Düsseldorf, May 2014

Aus dem Institut für Biochemie und Molekularbiologie II
der Heinrich-Heine-Universität Düsseldorf

Gedruckt mit der Genehmigung der
Mathematisch-Naturwissenschaftlichen Fakultät der
Heinrich-Heine-Universität Düsseldorf

Referent: PD Dr. Reza Ahmadian
Koreferent: Prof. Dr. Johannes Hegemann

Tag der mündlichen Prüfung:

Eidesstattliche Erklärung

Hiermit erkläre ich an Eides statt, dass ich die hier vorgelegte Dissertation eigenständig und ohne unerlaubte Hilfe angefertigt habe. Es wurden keinerlei andere Quellen und Hilfsmittel, außer den angegebenen, benutzt. Zitate aus anderen Arbeiten wurden kenntlich gemacht. Diese Dissertation wurde in der vorgelegten oder einer ähnlichen Form noch bei keiner anderen Institution eingereicht und es wurden bisher keine erfolglosen Promotionsversuche von mir unternommen.

Düsseldorf, December 2013

_____

Si-Cai Zhang

Table of Contents

Table of Figures

Introduction

1. Small GTPases

Ras was discovered from the murine leukaemia retroviruses at very beginning (Scolnick et al., 1973; Hager et al., 1979; Tsuchida and Uesugi, 1981), which can induce tumor in new-born rodents (Harvey, 1964; Kirsten and Mayer, 1967). Until 1982, the first human RAS gene was isolated and characterized from human bladder carcinoma cell line (Goldfarb et al., 1982; Pulciani et al., 1982; Shih and Weinberg, 1982) and found to be related with *v-ras* oncogen (Parada et al., 1982). Biochemical studies showed that Ras bound with guanine nucleotides (Scolnick et al., 1979) and located at inner leaflet of plasma membrane (Willingham et al., 1980). Later it was found that it is a GDP/GTP binding and GTP hydrolyzing protein (Gibbs et al., 1984), which is regulated by guanine nucleotide exchange factor (GEF) (Shou et al., 1992; Wei et al., 1992) as an activator (Kamata and Feramisco, 1984) and by GTPase-activating protein (GAP) as an inactivator (Trahey et al., 1988; Vogel et al., 1988; Ballester et al., 1990; Xu et al., 1990). Thus, Ras acts as a molecular switch in the cell, by cycling between an active GTP-bound and an inactive GDP-bound conformation (Rommel and Hafen, 1998).
It is known that EGF (epithelial growth factor) mediated Ras activation is linked via EGFR (EGF receptor), the adaptor protein Grb2 (Growth factor receptor-bound protein 2) and the RasGEF SOS1 (son of sevenless homolog 1) (Bowtell et al., 1992). Grb2 binds to tyrosine-phosphorylated EGFR through its SH2 (Src-homology-2) domain and to SOS1 through its SH3 (Src-homology-3) domain (Clark et al., 1992; Lowenstein et al., 1992; McCormick, 1993). Ras function in signal transduction was established with the discovery of several binding partners of Ras, called downstream effectors, such as RAF (Rapidly Accelerated Fibrosarcoma) (Han et al., 1993), a kinase in mitogen-activated protein kinase (MAPK) pathway, PI3K (phosphatidylinositol 3-kinase) and RAL-GDS (Ral guanine nucleotide dissociation stimulator) (Kikuchi et al., 1994; Rodriguez-Viciana et al., 1994; Harris and McCormick, 2010).

1.1.Classification of Ras Small GTPases

Until now, over 150 human Ras-like proteins are identified, which belong to the Ras superfamily. They are grouped into five subfamilies according to their sequence-structure-property relationships (Macara et al., 1996; Wennerberg et al., 2005), including Ras, Rho, Rab, Arf and Ran families (Takai et al., 2001) (Fig. 1).

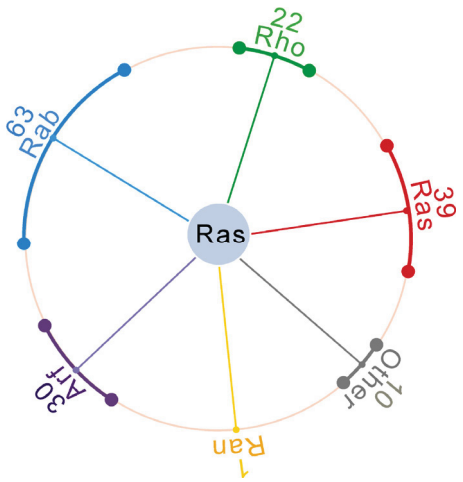

Figure 1: The Ras superfamily. Ras superfamily is divided into five families, including Ras, Rho, Rab, Arf, and Ran. The numbers indicate total number of the members to each family in humans.

1.2.Motifs and structural properties

All members of the Ras superfamily share a GDP/GTP binding (G**)** domain. Although the length and sequence of the G domains are different (e.g. H-Ras residues 1-166), they harbor 5 characteristic guanine nucleotide binding (G) motifs: G1 box, GX_4GKS/T (residues 10-17 in H-Ras) or phosphate binding (P) loop; G2 box (residues 32-40 in H-Ras) also called effector binding site or switch I, containing an almost invariant threonine, which coordinates the magnesium (Mg^{2+}) ion and the γ-phosphate of GTP; G3 box (DX_2G; residues 53-62 in H-Ras) with the conserved aspartate and glycine coordinating the Mg^{2+} ion and γ-phosphate of GTP, respectively; G4 box N/TKXD (residues 112-119 in H-Ras), with the aspartate binding to the guanine ring and the asparagine and the lysine contacting the G1 box; G5 box (S/CAK/K/T; residues 144-146 in H-Ras), with the alanine binding to guanine nucleotide (Bourne et al., 1991; Wennerberg et al., 2005). The conformations of two regions (called switch I and II) change dramatically when the G domain cycles between the GTP-bound and GDP-bound states. Switch I region overlaps with G2 box and locates between α1 helix and β2 strand. Switch II region contains part of α2 helix and G3 motif. Such GTP-induced conformation changes are critical for its function of molecular switch, which favors to downstream effectors interaction (Vetter and Wittinghofer, 2001) (Fig. 2).

The G domain is not only conserved in Ras superfamily and also in other guanine nucleotide binding proteins, like the elongation factor Tu and the α subunit of the heterotrimeric signal-transducing G proteins (Bourne et al., 1991). The homology of G domain between different members is even higher within each family. For example, the identity among the G domain of the Ras isoforms (H-Ras, K-Ras and N-Ras) in Ras family or the Rac isoforms (Rac1, Rac2 and Rac3) in Rho family is over 90% (Cox and Der, 2010) (ten Klooster and Hordijk, 2007). The main difference comes from the carboxyl (C) terminal hypervariable region (HVR; residues 165-185 in

H-Ras; 173-189 in RhoA; 181-212 in Rab5) (Ali et al., 2004; Karnoub and Weinberg, 2008; Lartey and Lopez Bernal, 2009). HVR associates small GTPases with the cell membrane and also play important role in selectivity for different binding partner (Lam and Hordijk, 2013). In Ras family, K-Ras4B contains a positively charged HVR, which is crucial for membrane binding (Hancock et al., 1990) and also transforming activity (Jackson et al., 1994). The HVR in Rho GTPases is sufficient to associate the proteins with the membrane in the absence of posttranslational modification (Michaelson et al., 2001) (see next paragraph). Rac1 HVR has been suggested to activate the downstream effecter p21-activated kinase1 (PAK1) (Knaus et al., 1998). A similar strategy is also used by the members of the Rab family. The C-terminal HVRs are the determinants for membrane localization for Rab GTPases (Chavrier et al., 1991) (Stenmark et al., 1994). These regions are also responsible for interaction with effectors and regulatory proteins, like TIP47 (tail-interacting protein of 47 kDa) and guanine nucleotide dissociation inhibitor (GDI) (Rak et al., 2003; Aivazian et al., 2006).

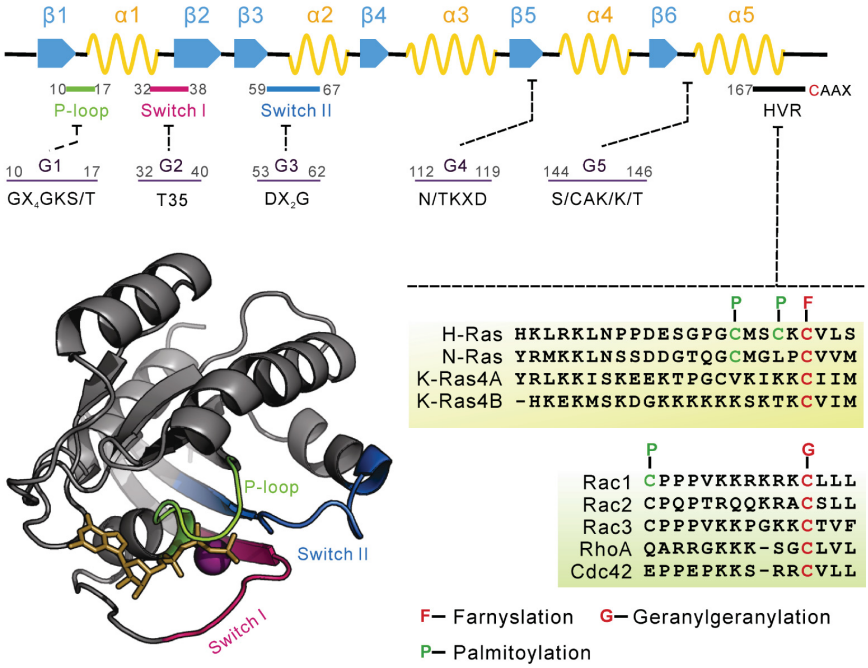

Figure 2: Motifs and structure of the Ras protein. Secondary structure of Ras proteins is shown at the top. Colored lines highlight the relative positions of motifs critical for the nucleotide binding (G1-G5), including P-loop (green), switch I (pink) and switch II (blue), which correspond the colors shown in the crystal structure of Ras (PDB code: 4EFL). The amino acid sequence of the HVR of Ras and Rho proteins are shown along with the posttranslational modification site.

A critical motif downstream of HVR is the CAAX (C = Cys, A = aliphatic, X = any amino acid) box, which dictates membrane localization of most small GTPases. For Rab family, this motif also could be CC, CXC, CCX, CCXX or CCXXX (Newman and Magee, 1993).The cysteine in this motif is modified either by farnesylation (15-carbon isoprenoid) or geranylgeranylation (20-carbon isoprenoid).

1.3.Posttranslational modification of Small GTPases

Small GTPases are posttranslationally modified in addition to farnesylation and geranylgeranylation at their carboxyl terminus also by palmitoylation, myristoylation, methylation, ubiquitylation, ADP-ribosylation, sumoylation, acetylation, and phosphorylation (Newman and Magee, 1993; Ahearn et al., 2012).

Amongst all the modifications, the best investigated one is the prenylation of the CAAX box of Ras proteins. The very last amino acid (at the position X of the CAAX motif) determines the type of prenylation (farnesylation or geranylgeranylation). The proteins are farnesylated if it is a serine or a methionine, and geranylgeranylated if it is leucine or phenyalanine. Some GTPases are also palmitoylated within the HVR, such as H-Ras, N-Ras TC10 and RhoB (Wennerberg and Der, 2004).

The CAAX modification involves three enzymatic reactions. Farnesyl transferase (FTase) modifies the cysteine of Ras with a farnysl group (Clarke et al., 1988). Farnesylated Ras proteins are attached to ER (endoplasmic reticulum), where an endoprotease, designated Ras-converting enzyme 1 (RCE1), cleaves the last three AAX residues (Kim et al., 1999). Immediately following the proteolysis, the isopenylcysteine is methylated by the enzyme called ICMT1 (isoprenylcysteine carboxylmethyl transterase 1) (Dai et al., 1998). K-Ras, which is not palmitoylated, will be transported to plasma membrane destinations, most probably by PDEδ (phosphodiesterase δ) (Weise et al., 2012). Farnesyl group contributes weakly plasma membrane binding but is significantly stabilized by positively charged HVR of K-Ras. H-Ras and N-Ras are further palmitoylated at the GN (Golgi network) by palmitoyl acyltransferase (Swarthout et al., 2005) and are transported to plasma membrane via recycling endosomes (Misaki et al., 2010; Ahearn et al., 2012). Most Rho family proteins, e.g. RhoA, Rac1 and Cdc42, are geranylgeranylated by geranylgeranyl transferase I (GGTase I) instead of FTase (Zhang and Casey, 1996).

1.4.Function of Small GTPases

Ras superfamily GTPases act as a molecular switches in the cell (Rommel and Hafen, 1998). As mentioned above, each GTPase family has its own unique biochemical and biological function in the cell due to structural differences.

It is hard to characterize the unique function of a specified small GTPase family alone because in most cases a biological process is achieved by the crosstalk of different proteins (Mitin et al., 2005; Iden and Collard, 2008). In general, Ras family controls the cell proliferation, differentiation, apoptosis and survival, (Malumbres and Barbacid, 2003). Rho family is known for its function in the reorganization of actin cytoskeleton and regulates the cellular structure, motility, adhesion and cell cycles (Wennerberg and Der, 2004; Amin et al., 2013). Rab family is the largest branch in the Ras superfamily and mainly regulates vesicular transport and protein trafficking between different organelles (Zerial and McBride, 2001). The ADP ribosylation factor (Arf) family also regulates the transport of vesicle but acts on the cargo sorting, vesicle formation and release (Nie et al., 2003). The Ras-like nuclear (Ran) protein is

a single member of the Ran family and controls the nucleocytoplasmic transport of RNAs and proteins through NPC (nuclear pore complex) and regulates the microtubule organization (Li et al., 2003; Weis, 2003).

2. Plasma membrane

Plasma membrane is a 30Å biologic film that separates the cytosolic constituents and external environment (van Meer et al., 2008). This was described by Singer and Nicolson as "fluid mosaic" model 40 years ago,: the cellular membranes are homologous lipid bilayers and global proteins intercalate thoroughly or partially in such fluidic bilayers (Singer and Nicolson, 1972). It is clear that plasma membrane is asymmetric and compose of different amphipathic lipids, which has the propensity for self-association (Bretscher, 1973). Transmembrane proteins across and some other proteins attach the lipid bilayers and associate with lipids in the membrane to form different compartments, for example the eisosomal proteins (Berchtold et al., 2012). Such interaction processes are highly dynamic and can be achieved in millisecond (Eggeling et al., 2009).

2.1.Composition and structure of plasma membrane

Lipids are basic building units of the cellular membranes. Lipid molecules contain hydrophobic tails, which consist of either unsaturated or saturated carbon chains and hydrophilic head groups. Such physical property of lipids dictates the creation of bilayers by spontaneous aggregation.

There are multitudes of lipids synthesized in the eukaryotic cell (Sud et al., 2007) but only some of them are used as structural lipids of the cell membrane. Those lipid components of membrane can be divided into three categories (Fig. 3): glycerophospholipids, sphingolipids and cholesterol (van Meer et al., 2008). Structural glycerophospholipids in membrane include phosphatidylcholine (PC), phosphatidylethanolamine (PE), phosphatidylserine (PS), phosphatidylinositol (PI) and phosphatidic acid (PA). These groups of lipids share the same hydrophobic portion, diacylglycerol (DAG), and differ in both head group and the types of fatty acids. PC accounts for more than 50% total phospholipids in eukaryotic cell membrane. PE inclusion in the membrane imposes a curvature stress favoring for budding on membrane. The major sphingolipids in eukaryotic membrane are sphingomyelin (SM) and glycosphingolipids (GSL) (van Meer and Lisman, 2002). The backbone of sphingolipids is ceramide. SM is found mainly at the outer leaflet of membrane and accounts for about 10% lipids of extracellular layer (Sonnino and Prinetti, 2013). The fatty acyl chains of sphingolipids are saturated, which confer them narrower and taller cylinder shape and the ability to pack tightly compared to phospholipids. Cholesterol constitutes the third class of lipids which has preferential interaction with sphiongolipids (Ramstedt and Slotte, 2002). Cholesterol is synthesized in ER and regulated strictly in the cell. It is thought that cholesterol can decrease the fluidity of fluid membrane (Ohvo-Rekila et al., 2002). Studies also show

that cholesterol involves in the assembly of lipid raft (Schroeder et al., 1998).
Lipid bilayers can exist in two states, a solid or "gel" state below their melting temperature (Tm), and a fluid or "liquid" state above their Tm. For biological membranes, they always stay in liquid state in which lipids or embedded proteins are dynamic. Dependent on the content of cholesterol, the fluid membrane can form different phases: liquid disordered (I_d) phase with low content of cholesterols, which has higher fluidity, and a more permeable and liquid ordered (I_o) phase contain more cholesterols, in which cholesterols and sphingolipids are packed tightly (Ipsen et al., 1987). It is noteworthy that there are surely lateral compartments within plasma membrane exhibit a composition, structure and biological function distinct from the surrounding membrane. These areas are called "microdomains" (Ziolkowska et al., 2012), such as clathrin-coated pits, caveolae, cilia, focal adhesions and synapses. The term "lipid rafts" is donated to the liquid ordered microdomains in plasma membrane, which are enriched in sphingolipids, cholesterol and proteins. Until now even though the intact lipid rafts are not detected and their existence is still questionable, the concept of "lipid rafts" are accepted generally by scientists (Zurzolo et al., 2003) (Fig. 3).

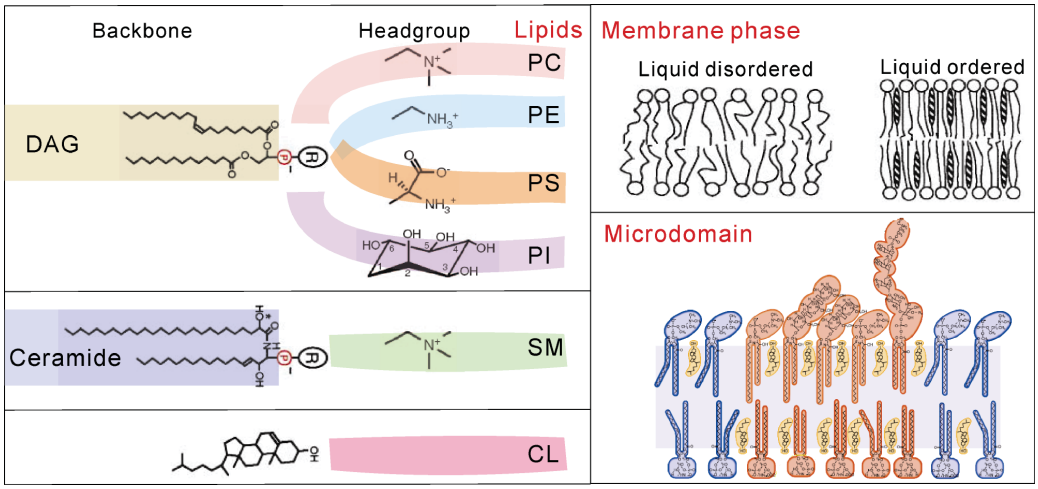

Figure 3: Lipids and structure of the plasma membrane. Six lipids are shown, which are divided in three groups. "R" indicates the head group of the phospholipids. PC, PE, PS, PI, SM and CL stand for phosphatidylcholine, phosphatidylethanolamine, phosphatidylserine, phosphatidylinositol, sphingomyelin and cholesterol. Lipids bilayer exists in two different physiological membrane phases, such as liquid disordered (I_d) and liquid ordered (I_o). I_o is usually composed of sphingolipids containing saturated backbone and cholesterol. Membrane micodomains are compact cholesterol-rich structures in I_o phase. Modified from (Simons and Ikonen, 2000; Munro, 2003; Lee, 2011).

2.2.**Function of plasma membrane**

Plasma membrane functions as physical barrier to separate the aqueous environments from the both sides of the cellular membrane. This barrier delimits the cell as a living unit and keeps a stable space for different biological processes. Biological membranes

also serve as a hydrophobic milieu behaving like a solvent for transmembrane proteins or small molecules.
More importantly, membranes supply the platforms, where signals are transduced, like the raft based microdomains or caveolae and also other microdomains in plasma membrane (Lemaire-Ewing et al., 2012). Studies have shown that lipid rafts are involved in plenty of biological phenomena. Lipid rafts is indicated to activate T cell through T cell receptor (TCR) and to participate in the inflammation process (Luo et al., 2008). Nitric oxide (NO) production in endothelial cell is also regulated by microdomain through caveolin-1 (Mason et al., 2004). In monocytic THP-1 cells, 7-ketocholesterol incorporation with lipid rafts can induce the recruitment of transient receptor potential channel-1 (TPCR-1), which leads the increase of calcium in cytoplasm. Such increase of free calcium activates calcineurin, a phosphatase activating pro-apoptotic Bad protein that triggers apoptosis pathway in mitochondria (Berthier et al., 2004). Lipid rafts are also involved in the regulation of apoptosis by Fas, a member of tumor necrosis factor. Fas can aggregate within the lipid rafts and become activated independent of its ligands. Fas activation results in recruitment of additional pro-apoptotic proteins into lipid raft domains and hence initiates caspase cascade or JNK apoptotic pathway (Wu et al., 2002; Bang et al., 2003).

2.3.Liposomes

In order to study membrane functions in vitro, model membranes are generally used, one of which is liposome. Liposomes are close lipid structures providing both a membrane matrix and an internal volume separated from the medium (Eytan, 1982). Different methods are used to produce liposomes. Regardless of the preparation methodology, the underlying principle for the formation of liposomes is the hydrophilic/hydrophobic interaction between lipid-lipid and lipid-water molecules (Mozafari, 2005). A simple way to achieve this is the input of energy, such as sonication and heating. The disadvantage of these methods is the size heterogeneity of the liposomes. A better way to obtain relatively unified liposomes is using extruder by mechanic method to obtain liposomes with defined diameters. In many cases liposomes are prepared from mixtures of different phospholipids, such as phophatidylcholine, phophatidylserine and phosphatidylethanolamine (Szoka and Papahadjopoulos, 1980). To simulate the physiological membrane, synthetic lipids mixture with defined composition usually are used for the formation of liposomes (Maier et al., 2000). In addition, lipids purified from tissues are also often used for liposome preparation (Boura and Hurley, 2012), including Folch I and Folch III lipids which are isolated from brain of bovine (Folch, 1942).

3. Small GTPases of the Ras family

As a prototypic family of small GTPases, the members of Ras family are expanded to 39 members, including Ras, Rap, Ral and Rheb subfamily (Cox and Der, 2010). Among these Ras proteins, H-Ras, K-Ras and N-Ras are most studied isoforms

because of their crucial roles in human cancer. The best characterized Ras signaling pathway, which contributes to oncogenesis, is the aberrant Ras-Raf-Mek1/2-Erk1/2 cascade (Repasky et al., 2004). In this pathway, Raf is the downstream effector of active Ras, which conveys the signal from Ras to serial kinases in the cell. In addition to Raf, a spectrum of effectors is identified to be involved in distinct pathways which are associates with progression of cancer if dysregulated.

After the identification of Raf as the effector of Ras proteins, the guanine nucleotide-exchange factors for the Ras-like small GTPases (Ral guanine nucleotide dissociation stimulator, RalGDS) is also determined as one of the Ras effectors (Kikuchi et al., 1994). Upregulation of RalGDS-Ral pathway promotes cellular proliferation (Hamad et al., 2002; Chien and White, 2003). Another effector is phosphoinositide 3-kinases (PI3K) (Rodriguez-Viciana et al., 1994). Activation of PI3K leads to cell survival through AKT and transcription nuclear factor-κB (NF-κB) (Rodriguez-Viciana et al., 1994; Marte and Downward, 1997; Mayo et al., 1997). The RacGEF T-cell lymphoma invasion and metastasis 1 (Tiam1) has been shown to be an effector of Ras and its deletion in mice is demonstrated to be resistant to Ras induced skin tumors (Lambert et al., 2002; Malliri et al., 2002). Phospholipase ε (PLCε) has been demonstrated as direct binding partner of Ras proteins and has been shown to activate Ras-mediated MAPK pathway (Kelley et al., 2001; Lopez et al., 2001). In contrary with above effectors, Ras association domain-containing family protein 5 (Rassf5 or Nore1) is demonstrated as a Ras effector (Makbul et al., 2013) but behaves like a tumor suppressor (Tommasi et al., 2002). The multiplicity of Ras effectors indicates that signaling in tumorigenesis mediated by Ras might be cooperative (Repasky et al., 2004) (Fig. 4).

3.1.Ras proteins and human diseases

Somatic mutations of *RAS* genes are observed in 32% of human cancers, in which K-Ras, N-Ras and H-Ras account for 85%, 12% and 3%, respectively (Harris and McCormick, 2010). The hotspots of these Ras mutations are mainly in codons 12, 13 and 61, which contribute to the dominant active Ras proteins (Cox and Der, 2010). Each mutated Ras has its preference for different tumors. K-Ras mutations are frequently detected in pancreatic and colonic carcinomas; N-Ras alterations are mainly observed in lymphoid cancers and melanomas; H-Ras mutations are predominantly found in bladder carcinomas (Karnoub and Weinberg, 2008).

Unlike the somatic mutations, a group of germline Ras mutations and components of the Ras/MAPK cascade have been found to be associated with several developmental syndromes, including Costello syndrome (CS), cardio-facio-cutaneous syndrome (CFCS) and Noonan syndrome (NS) (Tidyman and Rauen, 2009; Cox and Der, 2010). Usually these Ras mutations cause mild gain-of-function (Cirstea et al., 2010; Gremer et al., 2011; Cirstea et al., 2013; Flex et al., 2014), which are well-tolerated compared with somatic mutations and represent non-lethal phenotypes with facial dysmorphism, cardiac defect and cutaneous abnormality (Tidyman and Rauen, 2008). In addition to Ras mutations, a spectrum of alterations in Ras regulators, effectors and upstream

transducers are also associated with above developmental disorders. Since their close involvement with Ras/MAPK pathway, these diseases and related syndromes are referred as RASopathy (Cizmarova et al., 2013; Rauen, 2013) (Fig. 4).

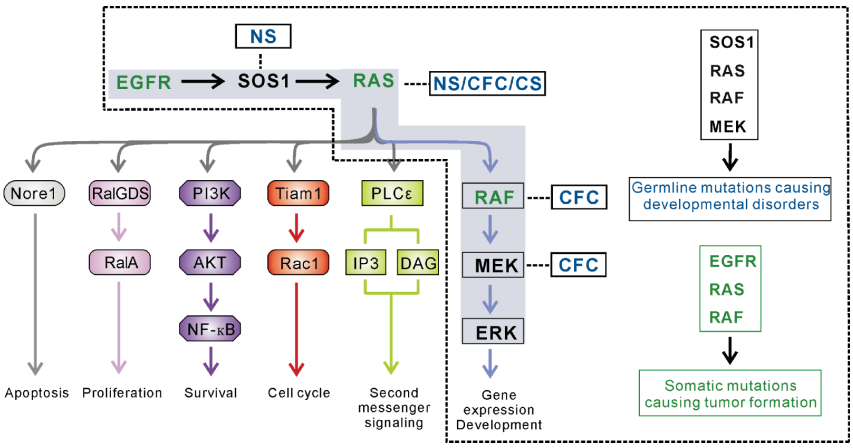

Figure 4: Ras signaling pathways associated with human diseases. Ras mediates several signaling pathways through its downstream effectors. Somatic and germline mutations of the components of the MAPK pathway (boxed) to cause developmental disorders and tumor formation, respectively. Developmental disorders include Noonan syndrome (NS), Cardio-Facio-Cutanous syndrome (CFC) and Costello syndrome (CS).

An interesting feature of mutations in RASopathy is that the signal output is clearly different and milder as compared to the somatic mutations leading to cancer. Two mutations of H-Ras at G12 and G13 are identified to cause the CS (Aoki et al., 2005). For K-Ras, two unusual mutations (G60R and D153V) are found together with other eight substitutions in its effector BRAF to lead CFCS (Niihori et al., 2006); three *de novo* germline mutations (V14I, T58I and D153V) are discovered to cause NS (Schubbert et al., 2006; Gremer et al., 2011). Two substitutions (T50I and G60E) in N-Ras are also identified in the patients with NS. Biochemical analysis *in vitro* for N-Ras carrying these two mutations exhibits mild activation of MAPK pathway compared with oncogenic N-Ras mutants (Cirstea et al., 2010). The similar biochemical characteristics are observed for two K-Ras mutants (Y71H and K147E) which associated NS and CFCS (Cirstea et al., 2013). In this context, K-Ras^{K147E} sustains the similar level of active state with oncogenic K-Ras but exhibits sensitivity to GAP and low affinity with RAF1 which leads mild activation of Ras signaling. A recent work has demonstrated that R-Ras carrying two germline mutations (G39dup and V55M) are involved in RASopathy through enhanced Ras/MAPK cascade (Flex et al., 2014).

3.2.Ras proteins and membrane interaction

In fact, the GTPases in one family have their own favored effectors and their mutations and dysregulations are related with special disorders and diseases, like H-, K- and N-Ras proteins. Since these proteins have similar effector loop, it is difficult to

explain such discrepancy from the structural point of view. Various studies reveal that the specific localization of Ras proteins in the plasma membrane might be one reason (Hancock, 2003; Prior and Hancock, 2012). It has been reported that H-Ras and K-Ras exist in both raft-based microdmains of plasma membranes and non-raft plasma membranes In the microdomain caveolae, there is more H-Ras than K-Ras where, H-Ras moves out of the ordered membrane upon activation (Prior et al., 2001). Contrary to H-Ras, K-Ras predominantly localizes outside of the microdomain. Such distinct localizations are modulated with different mechanisms, by which K-Ras associated with acidic area in liquid-disordered lipid domain of plasma membrane through its positively charged HVR (Villalonga et al., 2001; Weise et al., 2011) and H-Ras shuttling between microdomains is probably mediated by scaffolding protein galectin-1 (Paz et al., 2001). N-Ras shows different interaction patterns with plasma membrane compared to H-Ras and K-Ras, in which active N-Ras preferentially clusters into raft of plasma membrane (Eisenberg et al., 2011).

Except lateral movement of Ras protein in plasma membrane, membrane attached Ras proteins can also orientate on plasma membrane upon nucleotide loading. It has been observed that G-domain of H-Ras orientates on plasma membrane through Helix α4 and HVR dependent on different nucleotide bound states (Abankwa et al., 2008). When H-Ras is GTP loaded, R128 and R135 located at Helix α4 interact with membrane and stabilize active H-Ras for cellular signaling. In contrast, R169 and K170 in HVR associate with membrane when H-Ras is inactive, GDP-load state. In this conformational changes, D47 and E49 in the loop region between β2 and β3 strands are supposed to bind membrane and serve as a supporting point for this orientation (Abankwa et al., 2008). Another study has shown that β2-β3 loop of N-Ras is involved in its dimerization and enhance its nanoclustering in PC membrane (Guldenhaupt et al., 2012). In the same region of N-Ras, T50 is supposed to interact with plasma membrane and substitution of threonine to isoleucine disrupts this interaction (Cirstea et al., 2010). As a common observation of different studies, residue mutations in this β2-β3 loop region lead to the enhanced Ras signaling (Abankwa et al., 2008; Cirstea et al., 2010). In spite of the enhancement of signaling output, the exact mechanism is still in speculation. One possible explanation is that the conformation changes in plasma membrane may favor specific regulators or effectors to bind with Ras proteins.

3.3. Role of PDEδ in the modulation of Ras proteins

Phosphodiesterase δ (PDEδ) was originally identified as a component of cyclic GMP phosphodiesterase from retinal rod cells (Florio et al., 1996). Yeast two-hybrid assay showed that PDEδ interacts with H-Ras, Rap1A and Rap2B but not K-Ras (Nancy et al., 2002). The interaction of PDEδ and Ras proteins is dependent on the farnesyl group at the C-terminus of Ras but independent of their nucleotide-bound state. Further experiment revealed that Rheb, Arl2, N-Ras and K-Ras4B also interact with PDEδ (Hanzal-Bayer et al., 2002; Alexander et al., 2009; Weise et al., 2012). Cellular study have shown that PDEδ may be involved in Ras trafficking in the cell and

function as a prenyl-binding proteins with high affinity to farnesylated proteins (Nancy et al., 2002; Zhang et al., 2004).

Since PDEδ and RhoGDI share high structural similarity, it is speculated that PDEδ might function as a guanine nucleotide dissociation inhibitor for Ras family like RhoGDI for Rho GTPases. The following facts should be noted: (1) from structure aspect, the interacting ways between RhoGDI, PDEδ and their binding partners are different. This is reported by the structural studies of Rheb-PDEδ and Rac1-RhoGDI complexes (Fig.5), that Rheb and PDEδ interaction is solely through the hydrophobic interaction of farnesyl group of Rheb at its C-terminus and the binding pocket of PDEδ (Grizot et al., 2001; Ismail et al., 2011). Within comparision with Rheb-PDEδ, RhoGDI has an additional N-terminal regulatory arm, which harbors the switch region of Rac1 except the hydrophobic interaction between geranylgeranyl group of Rac1 and C-terminal barrel of RhoGDI. (2) RhoGDI exhibits preferentially higher affinity to GDP-bound Rho GTPases which is not observed in the case of PDEδ (Nancy et al., 2002). (3) From the functional point of view, RhoGDI extracts Rho GTPases from plasma membrane and sequesters them in cytosol in the inactive state. For PDEδ, it becomes clearer that it delivers Ras to rather than extracts it from the plasma membrane (Weise et al., 2012). The regulatory mechanisms of Ras proteins delivery to the plasma membrane are rather complicated (Chandra et al., 2011). PDEδ specifically interacts with non-palmitoylated Ras proteins and hence regulates their distribution between membranes. Co-expression of PDEδ with Ras proteins that containing polycationic motif such as K-Ras, showed more significant solubilizing effects (Chandra et al., 2011).

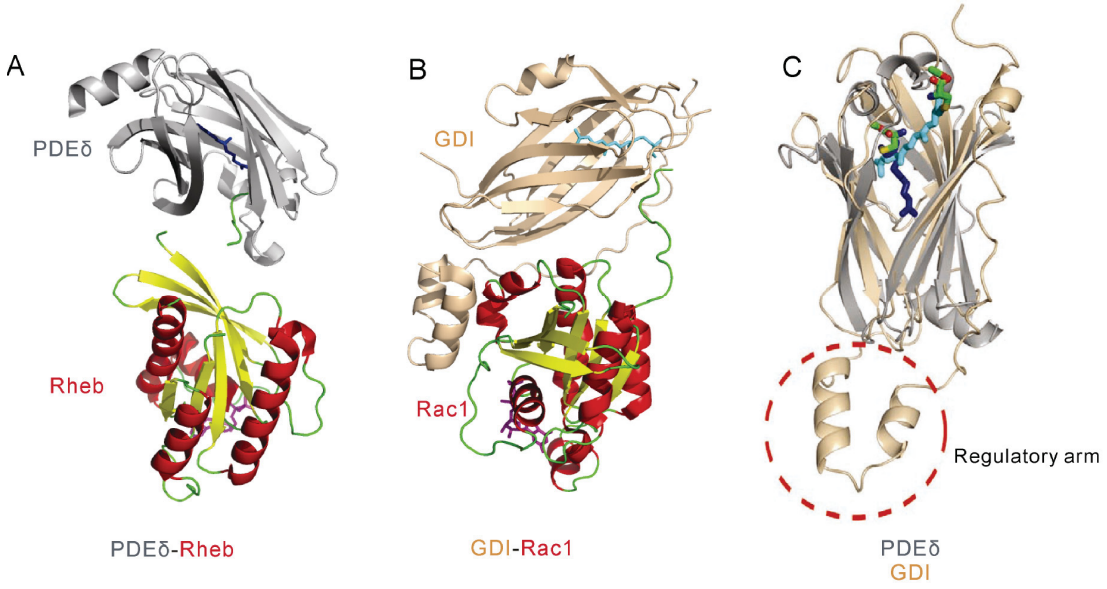

Figure 5: Comparison of PDEδ and RhoGDI. The structures of PDEδ-Rheb (A, PDB code: 3T5G) and RhoGDI-Rac1 (B, PDB code: 1HH4) and their overlay (C) show the similarity and differences between PDEδ and RhoGDI. In contrast to PDEδ, RhoGDI interacts with additional regions of Rac1 using different domains, including an N-terminal regulatory arm (red circle in C). Modified from (Ismail et al., 2011).

Available structures of PDEδ and Ras proteins have shown that PDEδ and Ras interaction is not specific. How such a complex is released is unclear. Active Arl GTPases are shown to displace Rheb from PDEδ (Ismail et al., 2011). This process is modulated by the conformational change, in which the binding pocket is switch off and cannot bury the farnesyl group any more (Ismail et al., 2011; Watzlich et al., 2013).

4. The Rho family of small GTPases

The role of the Rho family proteins as signaling molecules in the control of a large number of fundamental cellular processes is largely dependent on a functional molecular switch which cycles between a GDP-bound, inactive state and a GTP-bound, active state (Dvorsky and Ahmadian, 2004). Similar to Ras family proteins, the cellular regulation of this cycle also involves GEFs, which accelerate the intrinsic nucleotide exchange, and GAPs, which accelerate the intrinsic GTP hydrolysis activity (Cherfils and Zeghouf, 2013). Rho protein functions require both posttranslational modification by isoprenyl groups and membrane association. Rho GTPase underlay, therefore, a further control mechanism that pinpoints their membrane targeting to specific subcellular sites. This mechanism is achieved by the function of guanine nucleotide dissociation inhibitors (GDIs), which bind selectively to prenylated Rho proteins and control their cycle between cytosol and membrane (Fig. 6). Activation of Rho proteins results in their association with effector molecules that subsequently activate a wide variety of downstream signaling cascades (Bishop and Hall, 2000; Burridge and Wennerberg, 2004), consequently regulate several important physiological and pathophysiological processes in all eukaryotic cells (Etienne-Manneville and Hall, 2002; Heasman and Ridley, 2008). Following, the biochemical properties of the Rho proteins and their regulatory cycles will be described in detail.

Unlike Ras GTPases , Rho proteins possess an additional α helix insertion composed of 13 amino acids between β strand 5 and α helix 4, which is a unique feature among most of the Rho small GTPases members (Thapar et al., 2002). The Rho family members of the GTP binding proteins have emerged as key regulatory molecules that couple changes in the extracellular environment to intracellular signal transduction pathways. So far, 20 human members of the Rho family have been identified, which can be, based on their sequence homology, divided into six distinct subfamilies: (1) Rho (RhoA, RhoB, RhoC); (2) Rac (Rac1, Rac1b, Rac2, Rac3, RhoG); (3) Cdc42 (Cdc42, G25K, TC10, TCL, RhoU/Wrch1, RhoV/Chp); (4) RhoD (RhoD, Rif); (5) Rnd (Rnd1, Rnd2, Rnd3); (6) RhoH/TTF (Wennerberg and Der, 2004; Boureux et al., 2007).

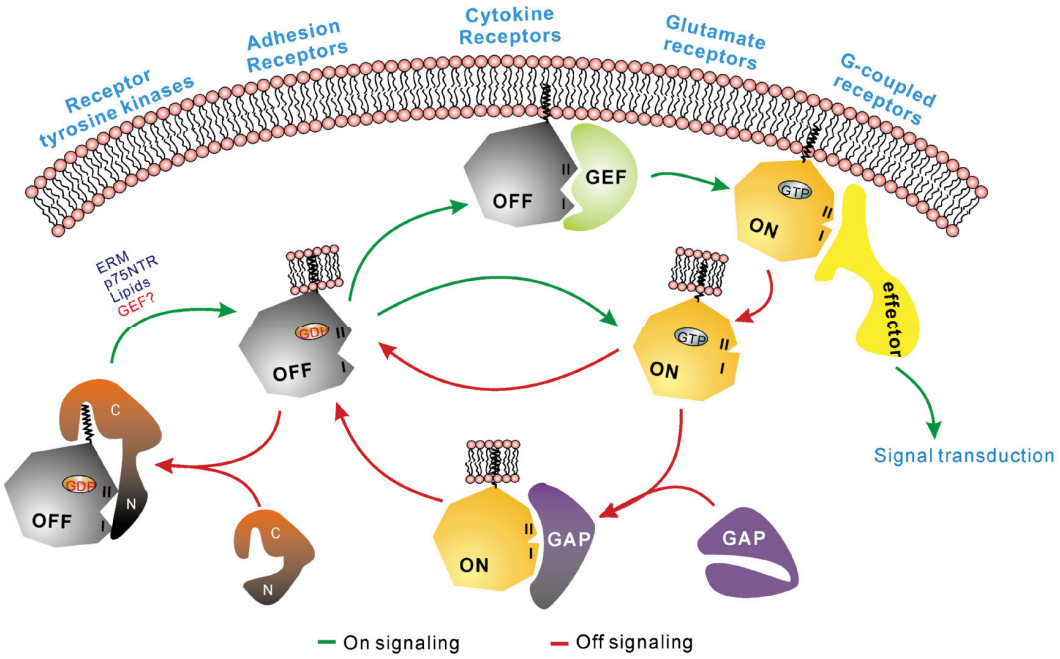

Figure 6: Regulation of Rho GTPases. Rho GTPases are regulated by three proteins, GEF (Guanine nucleotide exchange factor), GAP (GTPase activating protein) and GDI (Guanine nucleotide dissociation inhibitor). RhoGDI solubilizes prenylated Rho proteins in cytosol and keeps it in inactive state. Some factors, for example, $p75^{NTR}$, ERM proteins and lipids have been implicated to disrupt RhoGDI and Rho interaction. GEFs accelerate the GDP/GTP exchange of the Rho GTPases leading to their activation. Active Rho GTPases associate with downstream effectors and mediate signal transduction. GAPs accelerate hydrolysis of GTP to GDP and switch off Rho GTPase signaling. As indicated, all these processes are mediated by different receptors across the plasma membrane.

4.1.Regulators of Rho proteins

GEFs are able to selectively bind to their substrate Rho proteins and accelerate the exchange of the tightly bound GDP to GTP. Common mechanism utilized by GEFs is strongly reducing the affinity of the bound GDP, leading to its displacement and the subsequent association of GTP (Cherfils and Chardin, 1999; Guo et al., 2005). This reaction involves several steps, leading to an intermediate state of the GEF in the complex with the nucleotide-free Rho protein. This intermediate does not accumulate in the cell and rapidly dissociate because of the high intracellular GTP concentration leading to the formation of the active Rho·GTP complex. Therefore, the main reason is that the binding affinity of nucleotide-free Rho protein is significantly higher for GTP than for the GEF proteins (Cherfils and Chardin, 1999; Hutchinson and Eccleston, 2000). Cellular activation of the Rho proteins and their cellular signaling can be selectively uncoupled from the GEFs by overexpressing dominant negative mutants of the Rho proteins (e.g. threonine 17 in Rac1 and Cdc42 or threonine 19 in RhoA to asparagine) (Heasman and Ridley, 2008). Such a mutation decreases affinity of the Rho protein to bound nucleotide resulting in a so-called `dominant negative´ behavior (Rossman et al., 2002). As a consequence, dominant negative mutants

undergo a tight complex with their cognate GEFs and thus sequestrate them from activating the endogenous substrate Rho proteins.

The diffuse B-cell lymphoma (Dbl) family of RhoGEFs directly activates the proteins of the Rho family (Cook et al., 2013; Jaiswal et al., 2013). The prototype of this GEF family is Dbl protein, which has been reported to act on Cdc42 (Hart et al., 1991). The members of Dbl family are characterized by an unique Dbl homology (DH) domain, which is often preceded by a pleckstrin homology (PH) domain indicating an essential and conserved function (Hoffman and Cerione, 2002; Erickson and Cerione, 2004; Rossman and Sondek, 2005; Aittaleb et al., 2010; Jaiswal et al., 2011; Viaud et al., 2012). The DH domain is highly efficient catalytic machine (Rossman et al., 2005) which is able to accelerate the nucleotide exchange of Rho proteins up to 107-fold (Jaiswal et al., 2011; Jaiswal et al., 2013), as efficiently as the RanGEF RCC1 (Klebe et al., 1995) and *Salmonella typhimurium* effector SopE (see below) (Rudolph et al., 1999; Bulgin et al., 2010). The nearly invariant domain organization of the DH-PH tandem in Dbl family proteins presumes a conserved function for the PH domain. However, a clear role of the tandem PH domain has not yet been established. A model for PH domain-assisted nucleotide exchange has been proposed for some GEFs, such as Dbl, Dbs and Trio (Rossman et al., 2005). Herein the PH domain serves multiple roles in signaling events such as anchoring GEFs to the membrane (via phosphoinositides) and directing them towards their interacting GTPases which are already attached to the membrane.

Apart from conventional Dbl family RhoGEFs, there are two additional proteins families, which do not share any sequence and structural similarity with each other. The dedicator of cytokinesis (DOCK) or CDM-zizimin homology (CZH) family RhoGEFs, which are characterized by two conserved regions, is known as the DOCK-homology regions 1 and 2 (DHR1 and DHR2) domains (Meller et al., 2005; Rittinger, 2009). This type of GEFs employs their DHR2 domain to activate specially Rac and Cdc42 proteins (Meller et al., 2005). The third Rho protein-specific GEF family, represented by the SopE/WxxxE-type exchange factors, is classified as type III effector proteins of bacterial pathogens (Bulgin et al., 2010). They functionally, but not structurally, mimic eukaryotic GEFs by efficiently activating Rac1 and Cdc42 and thus induce "the trigger mechanism of cell entry (Rudolph et al., 1999; Bulgin et al., 2010).

Hydrolysis of the bound GTP is the timing mechanism that terminates signal transduction of the Rho family proteins and returns them to their GDP-bound inactive state (Jaiswal et al., 2012). The intrinsic GTP hydrolysis (GTPase) reaction usually is slow, but can be stimulated by several orders of magnitude through interaction of the Rho proteins with Rho-specific GAPs (Zhang and Zheng, 1998; Fidyk and Cerione, 2002; Eberth et al., 2005). The RhoGAP family defines by the presence of conserved catalytic GAP domain which is sufficient for the interaction with Rho proteins, mediating accelerated catalysis (Scheffzek and Ahmadian, 2005). The GAP domain supplies a conserved arginine residue, termed `arginine finger´, to stabilize the transition state and catalyze the GTP hydrolysis reaction (Rittinger et al., 1997; Nassar et al., 1998). RhoGAP insensitivity can be achieved by the substitution of

either the catalytic arginine of the GAP domain (Graham et al., 1999; Fidyk and Cerione, 2002) or amino acids critical for the GTP hydrolysis in Rho proteins, e.g. Glycine 12 and glutamine 61 in Rac1 and Cdc42 or glycine 14 and glutamine 63 in RhoA, which are known as the constitutive active mutants (Ahmadian et al., 1997; Graham et al., 1999).

The first RhoGAP, p50RhoGAP, was identified by biochemical analysis of human spleen cell extracts with recombinant RhoA (Garrett et al., 1989). Since then more than 80 RhoGAP containing proteins have been identified in eukaryotes, ranging from yeast to human (Lancaster et al., 1994; Moon and Zheng, 2003). The RhoGAP domain (also known as Bcr-homology, BH domain) containing proteins are present throughout the genome and rarely cluster in specific chromosomal regions (Peck et al., 2002). Most of the RhoGAP family members are frequently accompanied by several other functional domains and motifs implicated in tight regulation and membrane targeting (Moon and Zheng, 2003; Tcherkezian and Lamarche-Vane, 2007; Eberth et al., 2009). Numerous mechanisms have been shown to affect the specificity and the catalytic activity of the RhoGAPs e.g. intramolecular autoinhibition (Eberth et al., 2009), post-translational modification (Minoshima et al., 2003) and regulation by interaction with lipid membrane (Ligeti et al., 2004) and proteins (Yang et al., 2009; Jaiswal et al., *in prep*.).

RhoGDI (GDP dissociation inhibitor) was identified as an inhibitory GDP/GTP exchange protein for Rho family small GTPases (Ueda et al., 1990; Hori et al., 1991; Hiraoka et al., 1992), which interacts with and keeps Rho GTPases in their GDP-bound state (Hancock and Hall, 1993). There are three Rho-specific GDI isoforms found in human: RhoGDI (GDIα/GDI1), which is expressed ubiquitously (Fukumoto et al., 1990); Ly/D4GDI (or GDIβ/GDI2), which is specifically expressed in hematopoietic tissues and predominately in lymphocyte cell lines (Leonard et al., 1992; Scherle et al., 1993); RhoGDIγ (or GDI3) associates contrary to the other two RhoGDIs, with plasma membrane and is specifically expressed in lung, brain and testis (Zalcman et al., 1996; Adra et al., 1997).

RhoGDI interacts with Rho GTPases via two regions: a carboxyl terminal β-sandwich forms a hydrophobic pocket, which interacts with isoprenes on carboxyl terminal of Rho GTPases; an amino terminal regulatory arm, which binds to the switch I and II region of Rho GTPases (Gosser et al., 1997; Hoffman et al., 2000; Scheffzek et al., 2000). The former contact contributes to the high affinity of RhoGDI-Rho GTPases interaction (Tnimov et al., 2012) and the latter affects the GDP/GTP nucleotide exchange of Rho GTPase and hence inhibit GDP dissociation (Dvorsky and Ahmadian, 2004).

Interaction of RhoGDI and Rho GTPases can be disrupted by several ways. Rac1 can be released from Rac1 and RhoGDI complex by liposomes containing phosphatidylinositol 3,4,5-trisphosphate (Robbe et al., 2003; Ugolev et al., 2008). Another mechanism for disruption of RhoGTPases and RhoGDI is by specific protein interaction. For example, p75 neurotrophin receptor ($p75^{NTR}$) and ezrin/radixin/moesin (ERM) proteins have been shown to displace RhoGDI-Rho GTPase complex resulting in membrane association of the Rho GTPases (Takahashi

et al., 1997; Yamashita and Tohyama, 2003). A recent study indicates merlin may sequester RhoGDI by its C-terminal region to activate Rho A in axon and a patient merlin mutant loses binding to RhoA resulting in reduced RhoA activity (Schulz et al., 2013). A third regulatory mechanism is RhoGDI phosphorylation. RhoGDI can be phosphorylated by the serine/threonine p21-activated kinase 1 (PAK1) and the tyrosine kinase Src. GDI phosphorylation leads to a dramatic decrease in the ability of RhoGDI to form complex with Rho GTPases, including RhoA, Rac1 and cdc42 (DerMardirossian et al., 2004; DerMardirossian et al., 2006). Despite intensive research over the last two decades, the mechanisms by which GDI associates and displaces the Rho GTPases from the membrane remains to be investigated.

4.2.Roles of Rho proteins in Cells

Rho GTPases are famous in the regulation of cellular actin cytoskeleton organization by three well studied members, RhoA, Cdc42 and Rac1 (Hall, 1998) (Fig. 7). RhoA regulates the assembly of contractile actomyosin filaments and stimulates the formation of stress fibers in the cell. Rac1 promotes the organization of peripheral F-actin and hence is responsible for the production of membrane sheet and lamellipodia, and Cdc42 is involved in the formation of thin-structural filopodia by inducing peripheral actin-rich microspike (Wherlock and Mellor, 2002). Concomitant with their special biological function, these GTPases localize in different compartment of the cell. In migrating cells, active Rac1 functions in the leading area of the cell, but active Rho acts at the rear of the cell to generate contractile forces (Jaffe and Hall, 2005). Cdc42, maybe not all in cells, probably also localizes in the leading area of moving cells. Studies showed that Cdc42 is crucial for directional migration of cells towards chemoattractant (Simon et al., 1995; Allen et al., 1998). These different consequences are controlled by the interaction of Rho GTPase members with diverse effector proteins. Active Cdc42 directly binds to N-WASP, a member of Wiskott-Aldrich syndrome proteins (WASPs) family, and relieves its autoinhibition between VCA domain (Verprolin homology, central and acidic region) and GBD (GTPase binding domain). VCA in opened conformation can interact with Arp2/3 and initiate polymerization of actin (Bompard and Caron, 2004). Active Rac1 can release WAVE (WASP verprolin homologous), another WASP family member, from an inhibited WAVE-PIR121-Nap1-Abi-HSPC300 complex and facilitate its VCA domain binding to Arp2/3 (Chen et al., 2010). RhoA regulates actin organization by activating mDia1, a forming family member, which interacts with barbed end of actin filament and profilin/actin complex alternately to elongate the actin filaments through its two FH (Formin homology) domains in the active state (Zigmond, 2004).

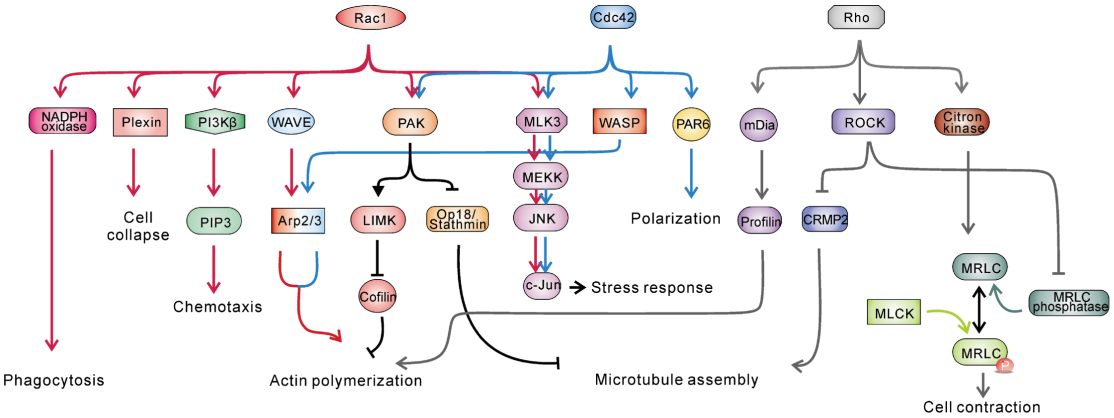

Figure 7: Signaling processes regulated by Rho GTPases. Rho GTPases mediate multiple signaling pathways. As indicated, each pathway controls a specific biochemical process. Rac1 and Cdc42 share several effectors and regulate similar functions. See more details in paragraph 4.2.

Other proteins downstream of Rho GTPases also show importance and complexity in cytoskeleton organization. Cofilin, an actin depolymerization factor, regulates actin filaments from two sides. It severs actin filaments and associates actin polymerization and elongation from the uncapped end (Arter et al., 2004). On the other hand, it also may lead to the disassembly of actin filament (Pollard and Borisy, 2003). Cofilin is under the regulation of LIM kinase (LIMK) which phosphorylates and inactivates cofilin. In turn, LIMK is phosphorylated and activated by PAK downstream of Rac1 and Cdc42 (Yang et al., 1998). In a similar way, cofilin also can be phosphorylated and inactivated by ROCK downstream of RhoA (Ohashi et al., 2000). MLCK (myosin light chain kinase) is a kinase which can phosphorylate myosin II regulatory light chain (MRLC) and leads to the contract activity. Consequently, MLCK is phosphorylated by PAK and results in reduced MRLC phosphorylation (Sanders et al., 1999). In another way, active RhoA promotes MRLC phosphorylation by phosphorylating and inactivating MRLC phosphatase through its downstream effecter ROCK (Kimura et al., 1996).

Rho GTPases regulate microtubule cytoskeleton through two ways, one is modulation of microtubule assembly and another one is stabilizing the plus end of microtubule by capture proteins. Two proteins can mediate microtubule assembly in contrary way, Op18/stathmin promotes microtubule disassembly but collapsin responses mediator protein-2 (CRMP-2) facilitates microtubule assembly. Op18/stathmin can be phosphorylated on one of the four susceptive residues by PAK, and be inactivated, and finally result in elongation of microtubules (Daub et al., 2001). PAK is the downstream effector of Rac1 and Cdc42, both of which can bind directly to GBD domain of PAK and relieve its autoinhibition (Manser et al., 1994). Such release results in its autophosphorylation and activation (Chong et al., 2001). In neuron, CRMP-2 is phosphorylated and inactivated by ROCK, which leads to the cone collapse (Arimura et al., 2000). ROCK is regulated by RhoA via binding to its RBD domain and thus interrupting the interaction of catalytic kinase domain and the C-terminal region (Ishizaki et al., 1996).

Similar to Ras family members, Rho GTPases also regulate gene expression. A transcription factor, serum response factor (SRF), controls growth-factor-immediate-early genes. Its activation requires a co-activator, MAL, which is modulated dependent on actin polymerization regulated by Rho GTPases (Miralles et al., 2003). The stress activated kinase, c-Jun N-terminal kinase (JNK) is regulated by Rho GTPases in different ways. RhoA directly binds to the N-terminus of MAP/ERK kinase 1 (MEKK1) and activates it, and sequentially resulting in JNK activation (Gallagher et al., 2004). Rac1 and Cdc42 interacts directly with mix lineage kinase 3 (MLK3) which activates MEKK and finally induces JNK activation (Teramoto et al., 1996). Rac1 and Cdc42 also can activate another MAP kinase, p38, through its effector PAK1 (Zhang et al., 1995).

Rho small GTPases are also involved in different cell cycle progressions. In the G_1 phase, Rac1 and Cdc42 are reported to stimulate cyclin D1 transcription, and Rac1 controls cyclin D1 mRNA translation after triggering by integrin activation (Westwick et al., 1997; Mettouchi et al., 2001). Rho is necessary for normal cyclin D expression, but this is Rac1 dependent as well (Welsh et al., 2001). In the late G_1, Cdc42 is indicated to stimulate cyclin E expression through its effector p70 S6 kinase (Chou et al., 2003). In mitosis phase, Rho plays important role in centrosome positioning through its effector ROCK (Rosenblatt et al., 2004). Cdc42 is crucial for asymmetric cell division through its effector Par6, which is an important element of polarization complex (Gotta et al., 2001). In the late mitosis, citron kinase, a Rho dependent kinase, controls the cytokinesis via phosphorylating MLC (myosin light chain) (Yamashiro et al., 2003).

The phagocyte NADPH oxidase (nicotinamide adenine dinucleotide phosphate-oxidase) is one of the first effectors of Rac identified (Abo et al., 1991). Rac is involved in the assembly and activation of NADPH oxidase by directly binding to $p67^{phox}$ and probably $gp91^{phox}$ (Lapouge et al., 2000). The mechanism of Rac involvement in this oxidase complex is controversial but proposed that Rac modulates the electron transfer from NADPH to oxygen which finally forms superoxide (Diebold and Bokoch, 2001; Gorzalczany et al., 2002).

Plexins belong to the receptors of semaphorins and are transmembrane proteins which bind semaphorins (Kruger et al., 2005). It contains several conservative domains, like extracellular Sema domain, a split intracellular Ras-like GAP domain and a middle segment which split the GAP domain and is responsible for Rho GTPases binding (Tong et al., 2007). Besides, Plexin-B subgroup has an additional PDZ which can interact with two RhoGEFs, leukaemia-associated RhoGEF (LARG) and PDZ-RhoGEF (PRG) (Aurandt et al., 2002; Perrot et al., 2002). It has been reported that Rac1 binding to Plexin-A1 disrupts autoinhibited conformation of the split GAP domain which stimulates cell collapse (Turner et al., 2004). Another Rho member, Rnd1 is also demonstrated to bind to Plexin-A1 and promote its RasGAP activity (Rohm et al., 2000), which is blocked by RhoD (Zanata et al., 2002). How these different Rho GTPases interplay to bind to Plexin and regulate different cellular process is still unclear.

4.3.Rho proteins and human diseases

Since Rho GTPases regulate a spectrum of biochemical process, deregulation of Rho GTPases and its regulators or effectors in any process may lead to different disorders or diseases in human.

A dominant negative Rac2 mutation is found in patient who displayed chronic granulomatous disease (CGD) (Williams et al., 2000). This disorder may result in activation failure of NADPH oxidase for reactive oxygen species (ROS) production, which is vital for neutrophils to kill invading microorganisms (Diebold and Bokoch, 2001).

Actually Rho members are quite conserved and seldom mutated with exception of above example and RhoH which is mutated in a non-Hodgkin's lymphomas (Preudhomme et al., 2000). It involved extensively in a spectrum of cancers with alteration at the level of expression and/or activation. Increased RhoA expression is observed in liver, skin, and colon cancers; RhoC is over-expressed in breast and skin cancer; In contrary, RhoB is downregulated in human cancer which is supposed to be a suppressor in tumorigenesis; Rac1 expression is elevated in testicular, gastric and breast cancer (Parri and Chiarugi, 2010). In addition, aberrant expressions of a cohort of RhoGEFs are also detected in human cancers together with or probably leading to the deregulation of Rho GTPases (Cook et al., 2013). In addition to their roles in tumorigenesis, Rho GTPases and their effectors are well defined to regulate cytoskeleton reorganization and hence contribute to cancer invasion and metastasis, Cardiovascular disease, pulmonary hypertension, and hepatic disease (Toksoz and Merdek, 2002; Firth et al., 2012).

Up to date, more and more studies found out that Rho GTPases play fundamental role in nerve cell functions, which include neuronal specification and polarization, axon guidance, survival and nerve growth. RhoA are reported to antagonize Rac1 activity in inhibition of nerve growth due to injury (Niederost et al., 2002). Based on these, dysfunction of Rho members are associated with several neurodegenerative diseases such as amyotrophic lateral sclerosis (ALS), Alzheimer's disease, Huntington's disease and Parkinson's disease. These neuronal disorders usually represent reductive or increasing expression or activity of Rho GTPases, and their regulators or effectors (DeGeer and Lamarche-Vane, 2013).

Chapter 1: Liposome reconstitution and modulation of recombinant prenylated human Rac1 by GEFs, GDI1 and Pak1*

Zhang, S.C., Gremer, L., Heise, H., Janning, P., Symanets, A., Cirstea, I.C., Krause, E., Nürnberg, B., Ahmadian, M.R. (2014) submitted to PLoS One. 9(7):e102425..

Background: Subcellular localization of Rho GTPases to different cellular membranes is known to be critical for their biological activity. This is achieved by a hypervariable region (HVR) and geranylgeranylation or farnesylation at the CAAX motif. However, the last decades in research of small GTPases under cell-free conditions were prevalently dominated by non-membranous systems such as soluble, mostly C-terminally truncated GTPases as well as shortened regulatory and effector proteins, mostly comprised of either the minimal catalytically active regulatory domains (GAPs, GEFs) or, in the case of effectors, the GTPase-binding domains (GBDs). Since the basic molecular mechanism of GTPase regulation and effector interaction is largely elucidated, it is in fact necessary now to move from these simplified soluble systems to more physiological and complex systems, i.e. multi-domain binding proteins acting on prenylated GTPases bound to the lipid membranes, the site at which they normally achieve their function in cells. A crucial prerequisite is, therefore, the availability of large quantities of purified, posttranslationally modified GTPases.

Result: A baculovirus-insect cell expression system was employed to produce recombinant prenylated human Rac1. Recombinant Rac1 proteins localized predominantly on plasma membrane of *Spodoptera frugiperda* (*Sf*9) cell, which is a characteristic property of prenylated GTPases. Out of eighteen detergents, CHAPS showed the best quality to extract intact, GDP-bound Rac1 from the membrane fraction of *Sf*9 cells. Accordingly, large amount of Rac1 was purified from *Sf*9 cell and the C-terminal geranylgeranyl modification was identified by mass spectrometry. Prenylated GDP-bound and GppNHp-bound Rac1 showed interaction with RhoGDI1 and synthetic liposomes, as well as Folch I and III liposomes. A RhoGDI1-mediated Rac1 extraction from the liposomes was competitively blocked in the presence of RacGEFs (Vav2, Dbl, TrioN, Tiam1 and P-Rex1) and the Rac1 effector Pak1. Results demonstrate that Rac1 activation counteracts its extraction from liposomes by RhoGDI1 and shifted the equilibrium of Rac1 from cytoplasm to plasma membrane.

Conclusion: Previous studies have shown that conserved residues of the switch regions of Rac1 do not only contribute to the interaction with the GDI but also to the interaction with other regulators, such as GEFs and GAPs, as well as with effectors. However, it is important to note that GDI1 has to compete in cells with the latter, which selectively bind to the active, GTP-bound forms of the Rho GTPases. Under this environmental condition on the surface of the plasma membrane GDI does probably not undergo any interaction with Rac1-GTP because it, as long as it is not switched off by GAPs, may preferentially exist in complex with various

* ***Enclosure 1***

signal-transducing effectors, such as Pak1. We also found that dissociation of Rac1-GDP from its complex with RhoGDI1 strongly correlated with two distinct activities of the DHPH of especially Dbl and Tiam1, including PH-mediated association with liposomes and DH-mediated GDP/GppNHp exchange of Rac1. The fact that GEFs can disrupt Rac1 and GDI complex and hence activate Rac1 indicates that the Rho GTPase-GDI complex may not be as tight as it has been suggested previously.

Significance: The cell membrane is a platform for signal transduction through transmembrane receptors and membrane-associated proteins, including heterotrimeric G proteins and small GTPases of the Ras superfamily. To achieve their function these proteins are essentially dependent on posttranslational modifications by isoprenylation, palmitoylation or myristoylation. In addition to studies of structural and chemical aspects of the individual proteins and components of signaling pathways, the new challenge is now to investigate the influence of the lipid membrane surface environment on the temporal and spatial regulation of signaling events. In our study, we used detergent screening strategy to purify prenylated Rac1 from insect cell and reconstituted its activation on liposomes. Our data showed more details about the protein interactions which are more close to their physiological situation in the cell. This study has opened a new window into future mechanistic studies.

Author contribution: The author of this dissertation has performed 95% of this study on the in vitro liposome reconstitution of Rac1 regulation and signaling by establishing three different approaches, including expression and purification of prenytaled human Rac1, preparation of composition-dependent synthetic liposomes, and Rac1-liposome sedimentation assay in order to perform in vitro liposome reconstitution of Rac1 regulation and signaling. In addition, he has interpreted and discussed the data, and wrote the initial version of the manuscript, which has been recently published in PLOS one.

Chapter 2: An electrostatic switch mechanism controls the Rho-GDI selectivity and function

Zhang, S.C., Nouri, K., Amin, E., Dvorsky, R., Nguyen, B.N., Gremer, L., Heise, H., Ahmadian, M.R. (in preparation)

Background: Rho small GTPases are regulated by three different regulators, GEF, GAP and RhoGDI, of which RhoGDI has been shown to bind to GDP-bound RhoGTPases in a non-selective manner and to keep them in their inactive state. Up to date, the crystal structures of geranylgeranylated Rac1, RhoA and Cdc42 in complex with RhoGDI are known. Accordingly, the interactions between RhoGDI and these three Rho GTPases are mainly achieved by two contacts. One is through the interaction of N-terminal regulatory arm of RhoGDI to the switch regions of the Rho proteins. The second is between the C-terminal hydrophobic pocket of RhoGDI and the C-termnal prenyl group of the Rho proteins. We have reported that RhoGDI interacts and extracts prenylated Rac1 from plasma membrane. However, the molecular mechanism how this process is modulated is still unclear. The N-terminal region of RhoGDI has been recently reported to inhibit its membrane translocation. This indicates the N-terminus of RhoGDI might be critical in the extraction of Rac1 from membrane.

Result: We have shown that prenylated Rac1 bound to RhoGDI with a slightly higher affinity as compared to the unprenylated Rac1. Further analysis demonstrated that RhoGDI revealed distinct interaction properties to diverse Rho proteins. It specifically bound to unprenylated full length Rac1, Rac3 and RhoA but neither to full length Rac2 and Cdc42 not to C-terminal truncated Rac1 and RhoA. Kinetic analysis demonstrated that positively charged residues of Rac1 C-terminus of are essential for the RhoGDI function. Replacing these residues with glutamic acids resulted in loss of Rac1-RhoGDI interaction (Fig. 1). Structural analysis reveals that two residues in RhoGDI, E163 and E164, in the proximity of the hydrophobic binding pocket might be involved in the interaction with positively charged hypervariable region of the Rho proteins. A RhoGDI mutant with the substitution of E163 and E164 to lysines exhibited a drastic decrease in binding to unprenylated full length Rac1 and Rac3 but a 3-fold increase in RhoA binding. Liposome extraction assay showed that this RhoGDI mutant almost lost its extraction ability for prenylated Rac1. In contrast to kinetic measurements for the interaction between prenylated Rac1 and diverse RhoGDI proteins, which did not show significant differences, the extraction of prenylated Rac1 from the liposomes was largely affected. RhoGDI1 lacking the N-terminal 25 residues was disabled to extract Rac1 from the liposomes. This effect is not observed with RhoGDI1 lacking the N-terminal 15 residues. Notably, RhoGDI $^{E163K/164K}$ and RhoGDI$^{\Delta N25}$ bind to prenylated Rac1 even though its Rac1 extraction ability was completely abolished (Fig. 2).

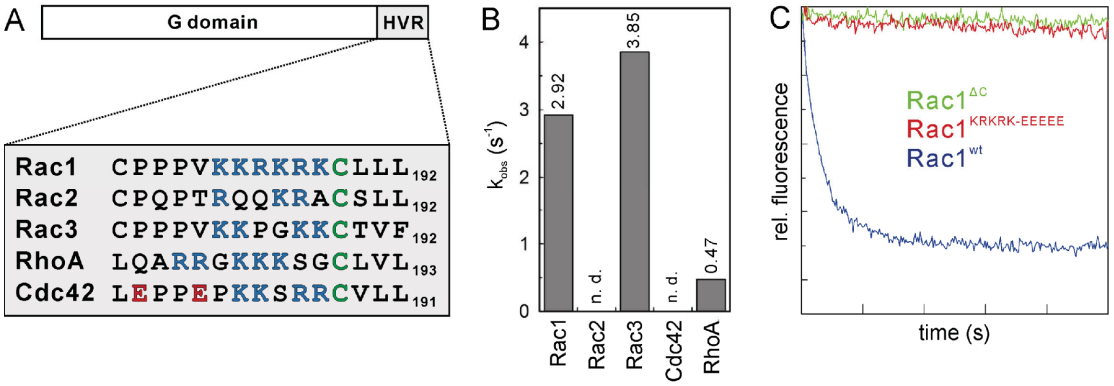

Figure 1. C-terminus of Rho GTPases contributed to selective interaction with RhoGDI. (A) Domain organization and sequence alignment of hypervariable region (HVR) of Rho GTPases. (B) Kinetics of RhoGDI association with various Rho GTPases. Rac1 and Rac3 exhibited similar association rates, which are 6-8 fold fat´ster than that of Cdc42RhoA. Rac2 and Cdc42 did not show any detectable association with RhoGDI (n. d.) (n. d.). (C) Critical role of the Rac1 C-terminus in the RhoGDI interaction. Deletion of Rac1 HRV or its mutation (KRKRK to EEEEE) completely abolished RhoGDI association with Rac1.

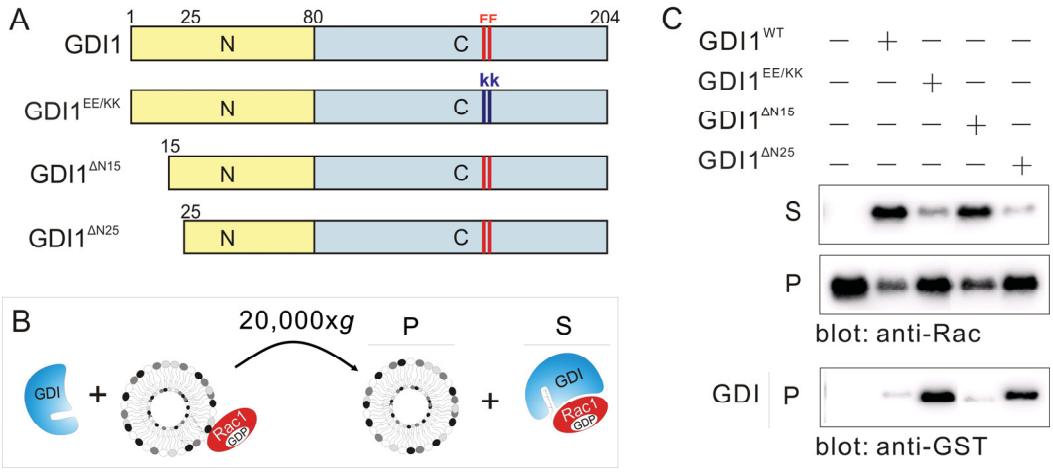

Figure 2. Negatively charged residues of RhoGDI displayed crucial role in extracting Rac1 from liposomes. (A) GDI variants used in this study. GDI1$^{EE/KK}$, GDI1$^{\Delta N15}$ and GDI1$^{\Delta N25}$ indicated variants with substitutions of E163 and E164 to lysines, deletion of first 15 and 25 residues at the N-terminus of RhoGDI1, respectively. (B) Schematic representation of Rac1^{wt} extraction assay by RhoGDI. (C) Differential Extraction of Rac1 variants by RhoGDI. Rac1 and GDI were detected by Western blotting using Rac1 and GST antibodies. P and S indicated pellet and supernatant, respectively.

Conclusion: This study elucidated distinct new binding pattern for the RhoGDI interaction with the Rho GTPases. For unprenylated Rho proteins, it has specific interaction with Rac1 and RhoA but not Cdc42. A positively charged hypervariable region of Rac1 and RhoA is essential for this interaction. More importantly, it has been demonstrated that E163, E164, and residues between the amino acids 15 and 25

at the N-terminus of RhoGDI play critical role for its RhoGDI extraction ability even they don't contribute to the Rac1binding affinity. Taking these results together, the extraction of Rac1 from membrane by RhoGDI underlies an electrostatic interaction of the C-terminal HVR of Rac1 with the C-terminal and very N-terminal domains of RhoGDI.

Significance: The RhoGDI-Rho GTPases interaction has been studied more than 20 years and it is commonly believed that the interactions between these two proteins are via two non-selective interactions. Our work showed now that additional interactions exist and shed lights on the mechanism of how RhoGDI specifically extracts Rho GTPases from plasma membrane. This process is probably modulated by the electrostatic interaction between polybasic region of Rho proteins and regions near the hydrophobic pocket in RhoGDI.

Author contribution: The author of this dissertation has performed 85% of this study by analyzing successfully the interaction between prenylted Rho Proteins and various GDIs using different methods, including stopped-flow fluorescence spectrometry, fluorescence polarization, *in vitro* liposome reconstitution. In addition, he wrote the initial version of the manuscript by interpreting and discussing the data, and preparing a first version of the manuscript, which is going to be submitted for publication.

Chaper 3: Molecular mechanism of N-Ras integration at the plasma membrane

Zhang, S.C., Nouri, K., Amin, E., Dvorsky, R., Ahmadian, M.R. (in preparation)

Background: Somatic mutation of NRAS, a prominent member of the Ras family GTPases, is often observed in lymphoid cancers and melanomas with the hotspot in codons 12, 13 and 61. Two germline mutations of NRAS, T50I and G60E, have been reported to cause Noonan syndrome through enhancement of MAPK pathway. In contrast to G60E, which massively affected the intrinsic and extrinsic functions of NRAS G domain, T50I is suggested to affect NRAS interaction with plasma membrane. Similarly, two residues in HRAS, D47 and E49, are assumed to interact with plasma membrane and serve as supporting point to assist its conformational change depending on the bound nucleotide. Mutations of residues also led to elevated MAPK signaling. As T50, D47 and E49 are located in the same region in NRAS, namely in the loop between β2 and β3 strands, it has been proposed that interaction of this region with the plasma membrane may block Sos1 accessibility and consequently a Sos1-catalyzed Ras activation. However, a direct association of the RAS proteins, e.g. NRAS, with the lipid membrane and modulation of their signal transduction remains to be investigated.

Result: By using laser scanning confocal microscopy, $NRAS^{wt}$ was observed to mainly localize at Golgi complex and in the plasma membrane. Inspected different picture was observed for $NRAS^{D47K/E49K/T50I}$ which was distributed in the cytoplasm but not at Golgi complex and plasma membrane (Fig. 1).

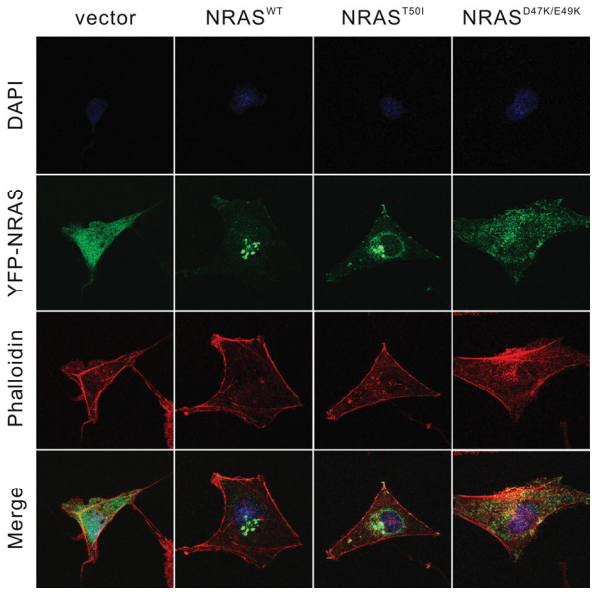

Figure 1. **Confocal imaging of YFP-fused NRAS variants transiently transfected in Cos-7 cells.** Cos-7 cells were fixed with acetone/methanol (1:1) at 48 h posttransfection. Slides were detected by using excitation wavelength at 364 nm (DAPI in blue), 488 nm (YFP in green) and 543 nm (Phalloidin in red) on a Zeiss laser scanning microscope (LSM 510).

Cellular analysis demonstrates that $NRAS^{D47K/E49K/T50I}$ led to enhanced MAPK signaling in Cos-7 cells compared to $NRAS^{wt}$. The activation of the MAPK pathway by NRAS triple mutant was comparable to oncogenic $NRAS^{G12V}$. Interestingly, the same level of active NRASNRAS triple mutant and wildtype were detected (Fig. 2).

By cotransfecting NRASNRAS and PDEδ, NRAS$^{D47K/E49K/T50I}$ showed a relatively higher GTP-bound, active state as compared to NRASNRASNRAS^{wt}. *In vitro* experiment exhibits that PDEδ bound to NRAS^{wt} but do not extract it from the liposomes.

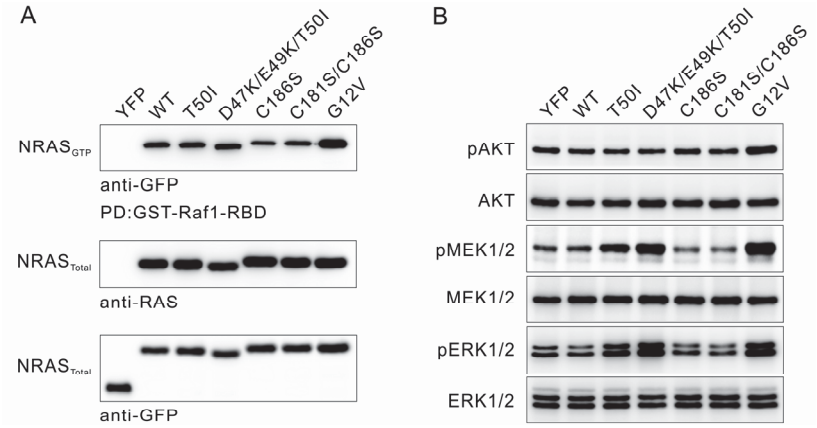

Figure 2. **Differential signaling activities of the NRAS variants in Cos-7 cells.** Lysates of Cos-7 cells, transiently transfected with different NRAS variants in the presence of 10% serum were used for both pull down assay using GST-Raf1-RBD (A) and visualization of the downstream pathways (B). (A) Active, GTP-bound YFP-fused NRAS variants were pulled down using GST-Raf1-RBD. NRAS variants exhibited a similar activation state as NRAS^{WT} when compared to the constitutive NRAS^{G12V}. (B) NRAS^{T50I} and NRAS$^{D47K/E49K/T50I}$ variants revealed a significant increase in the levels of phosphorylated MEK1/2 and ERK1/2, as compared to NRAS^{WT} and NRAS^{G12V}, leading to stronger downstream MAPK signaling but not PI3K signaling. Farnesylation-deficient (NRAS^{C186S}) and palmitoylation/farnesylation-deficient (NRAS$^{C181S/C186S}$) variants were used as negative controls and the constitutive active NRAS^{G12V} as positive control.

Conclusion: Previous studies have suggested that β2-β3 loop in NRAS involved in its membrane integration. D47, E49 and T50 in this loop might play important role in NRAS interaction with membrane and its activation. Our experiments by substituting D47 and E49 to positively charged lysines in the context of the patient mutation T50I clearly showed impaired association of NRAS with plasma membrane. This disruption ultimately resulted in an enhanced MAPK activation. PDEδ has been reported to deliver KRAS to plasma membrane. Cotransfection of NRAS and PDEδ in cells has shown that PDEδ exacerbates distinction of activation of NRAS mutants upon EGF induction. It implies that PDEδ might interfere in NRAS activation and membrane association in cell by additional mechanism.

Significance: RAS proteins have been thought to anchor to membrane by its C-terminal prenyl group. Our data proves that G-domain of NRAS might also associate with membrane. Such an association may interfere with its activation on plasma membrane. Except RAS compartmental localization, association of G-domain with membrane could be another mechanism, e.g. such as scaffolding function; in regulation of RAS signaling.

Author contribution: The author of this dissertation has performed 90% of this study

by analyzing successfully a set of N-Ras mutations regarding their membrane interaction, subcellular localization, and signal transduction. In addition, he purified N-Ras and its variants for liposome binding assays and activation by its activator Sos1 on liposomes. The data of this study is under preparation for publication.

Chapter 4: Interaction characteristics of Plexin-B1 with Rho family proteins*

Fansa, E.K., Dvorsky, R., Zhang, S.C., Fiegen, D., and Ahmadian, M.R. (2013) Biochem Biophys Res Commun. 434(4):785-90.

Background: Plexin-B1 is a transmembrane receptor, which regulates several cellular processes upon stimulation of semaphorin at the extracellular domain. Members of Rho family, including Rnd1, Rac1 and RhoD, have been reported to associate directly with the Rho-binding domain of Plexin-B1 (B1RBD). How Plexin-B1 selectively interacts with the spectrum of Rho GTPases was unclear.

Result: B1RBD interaction with 11 different Rho proteins was investigated in this study. Among these representative members, Rac isoforms, Rnd isoforms and RhoD were detected to interact with B1RBD in their active states. Rnd1 displayed with 3.2 μM the highest binding affinity followed by Rac1, which showed strongest interaction with B1RBD among Rac isoforms. Isothermal titrated calorimeter (ITC) experiments and analytical size exclusion chromatography (aSEC) revealed that Rnd1 displaced Rac1 from its B1RBD complex, but not vise verse. Structure analysis of B1RBD in complex with Rac1 and Rnd1 showed that the B1RBD-binding amino acids on the surface of Rac1 and Rnd1 are conserved. A negatively charged patch composed of four acidic amino acids of Rac and Rnd isoforms were supposed to be responsible for selective interaction with B1RBD. Finally, the C-terminal hypervariable region (HVR) was identified to contribute to the interaction with B1RBD through electrostatic interaction.

Conclusion: In this study, a large number of Rho proteins were investigated comprehensively for their interaction with B1RBD. Rac and Rnd isoforms as well as RhoD have been shown to specifically interact with B1RBD. Even with similar affinity to B1RBD, Rnd1 can displace Rac1 from B1RBD complex. A loop region consisting of 31 residues in B1RBD (amino acids 1854-1885) may facilitate selective interaction with the Rho proteins at the plasma membrane. The latter most likely provide positively charged residues from their C-terminal tail to bind B1RBD.

Significance: This extensive *in vitro* study provided fundamental insights into the crosstalk between plexin-B1 and diverse Rho proteins. For example, Rnd2 was shown to bind to Plexin-D1 and inhibit axon outgrowth of cortical neurons and down regulation of R-Ras activity. This work also indicated that other interacting mechanism between Plexin-B1 and Rho proteins may exist in addition to the observed contacts, which were obtained from the structural analysis. This may include the HVR in Rho or B1RBD association with plasma membrane.

Author contribution: The author of this dissertation has performed 10% of this study by obtaining materials and UTC data for the interaction of Plexin B1 with Rho GTPases and their variants.

* ***Enclosure 2***

Chapter 5: Diverging gain-of-function mechanisms of two novel KRAS mutations associated with Noonan and cardio-facio-cutaneous syndromes*

Cirstea, I.C., Gremer, L., Dvorsky, R., Zhang, S.C., Piekorz, R.P., Zenker, M., Ahmadian, M.R. (2013) Hum Mol Genet. 22(2):262-70.

Background: The germline mutations in RAS proteins are identified in a group of RAS-MAPK-related disorders. These disorders include Noonan syndrome (NS), Costello syndrome (CS) and cardio-facio-cutaneous syndrome (CFCS). Two KRAS mutations (Y71H and K147E) are identified to be associated with NS and CFCS. The molecular impact of these mutations on the regulation and signal transduction of KRAS remained to be investigated.

Result: $KRAS^{wt}$, $KRAS^{Y71H}$, $KRAS^{K147E}$ and $KRAS^{G12V}$ were transfected into COS-7 cell and active RAS and its downstream signaling in MAPK pathway were analyzed. In the presence of serum, the level of active RAS^{Y71H} was comparable with RAS^{wt}, whereas active $KRAS^{K147E}$ was comparable with oncogenic mutant $KRAS^{G12V}$, although they are not GAP resistant as compared to $KRAS^{G12V}$. Under serum-free condition, $KRAS^{K147E}$ led to moderate MEK1/2 activation and slight ERK1/2 activation compared to $KRAS^{Y71H}$ that showed no significant difference. EGF stimulation in a time-dependent manner revealed that $KRAS^{Y71H}$ and $KRAS^{K147E}$ upregulated MAPK pathway with higher ERK1/2 phosphorylation compared with $KRAS^{wt}$. Biochemical analysis indicated that $KRAS^{K147E}$ has high intrinsic nucleotide dissociation ability and $KRAS^{Y71H}$ has higher RAF1 binding affinity even though it shows similar intrinsic nucleotide dissociation as compared to $KRAS^{wt}$. Structural analysis demonstrated that Lys147 interacts with Phe28 and Asp119 which bind to guanine base and this interaction indirectly contributes to stabilization of nucleotide binding. Disruption of Lys147 will increase nucleotide dissociation and facilitate GTP binding.

Conclusion: In this study, two KRAS variants were characterized *in vivo*, *in vitro* and *in silico*. $KRAS^{Y71H}$ showed similar level of active proteins but it led a mild increased activation of downstream signaling because it exhibited an enhanced binding affinity to RAF1. In contrast, $KRAS^{K147E}$ exhibited accumulated active protein in the cell which was similar with oncogenic KRAS. This phenomenon is resulted from its self-activating property with enhanced nucleotide exchange. An increased signaling output in the cell can be explained by its biochemical characters and structure organizations.

Significance: This work dissects the mechanisms by which different RAS mutations play their roles in development disorders. $KRAS^{Y71H}$ belongs to the wild type mutation associated with NS and $KRAS^{K147E}$ can be placed in severe mutation. Both of the mutations are tolerated in the germline. The moderate activation of MAPK pathway resulted by these mutations is determined directly by its fundamental structure. The data in this study clearly elucidate the diversity of reasons for the

* ***Enclosure 3***

variable pathogenesis, for example the developmental disorder and cancer.

Author contribution: The author of this dissertation has performed 10% of this study by analyzing EGF-induced effects of the K-Ras mutants on downstream signaling pathways.

Chapter 6: Functional crosstalk between Ras and Rho pathways: p120RasGAP competitively inhibits the RhoGAP activity of Deleted in Liver Cancer (DLC) tumor suppressors by masking its catalytic arginine finger*

Jaiswal, M., Dvorsky, R., Amin, E., Risse, S.L., Fansa, E.K., Zhang, S.C., Taha, M.S., Gauhar, A.R., Nakhaei-Rad, S., Kordes, C., Koessmeier, K.T., Cirstea, I.C., Olayioye, M.A., Haeussinger, D., Ahmadian, M.R. (2014) J Biol Chem. 289(10):6839-49.

Background: GAPs are regulators of Ras and Rho proteins by stimulating their inefficient intrinsic GTP hydrolysis reaction. Increasing evidence suggests that there are cross talks between Ras and Rho GAPs. Association of p120 RasGAP with p190 and DCL1 has been shown to conversely regulate their RhoGAP activity leading to p190 activation and DLC1 inhibition. The mechanism by which how p120 interferes DLC1 RhoGAP activity was unclear.

Result: Kinetic measurements of RhoGAP activities of DLC1 isoforms, DLC1, DLC2 and DLC3, demonstrated that they are inefficient RhoGAPs as compared to other other RhoGAP, including p50 and p190. Kinetic measurements revealed that a low catalytic activity, rather than the binding affinity, exclusively contributed to the low RhoGAP function of the DLC proteins. Interestingly, SH3 domain of p120 RasGAP almost completely inhibited the RhoGAP activity of DLC1, which resulted form a high affinity interaction. Detailed analysis of various other SH3 and RhoGAP proteins revealed that the p120 SH3 interaction with the DLC1 RhoGAP domain is highly selective. A detailed structural analysis of of the interaction between the DLC1 RhoGAP and p120 SH3 determined three critical amino acids in p120 SH3 contributing to the inhibition of DLC1 RhoGAP activity by contacting and masking the catalytic arginine finger. Mutation at theses residues abolished both p120-DLC1 interaction and p120-mediated inhibition of the DLC1 RhoGAP activity.

Conclusion: This study has shown that p120 SH3 domain utilizes a novel binding mode to selectively interact with the DLC1 RhoGAP domain and to potently inhibit its RhoGAP activity. This interaction represents three remarkable characteristics, such as high affinity, high selectivity and a novel non-canonical binding mode. Unlike the canonical interaction between SH3 domain and PXXP motif, three amino acids in p120 SH3 domain contribute its high affinity to DLC1 GAP domain and inhibit GAP activity by masking the catalytic arginine in GAP domain.

Significance: This study provided mechanistic and structural insights into a selective regulation of DLC1 RhoGAP activity and shed light onto the role of multifunctional p120 RasGAP. It is interesting to note that p120 also act as an “effector” linking Ras and Rho signaling pathways in addition to its classical RasGAP activity. The novel findings suggest a functional crosstalk between Ras and Rho proteins at the level of

* ***Enclosure 4***

regulatory proteins.

Author contribution: The author of this dissertation has performed 10% of this study by analyzing the autoinhibition DLC1 full length. Therefore, he has expressed and purified various DLC1 proteins, including the full length.

Chapter 7: Activating mutations in RRAS underlie a phenotype within the RASopathy spectrum and contribute to leukaemogenesis*

Flex, E., Jaiswal, M., Pantaleoni, F., Martinelli, S., Strullu, M., Fansa, E.K., Caye, A., De Luca, A., Lepri, F., Dvorsky, R., Pannone, L., Paolacci, S., Zhang, S.C., Fodale, V., Bocchinfuso, G., Rossi, C., Burkitt-Wright, E.M., Farrotti, A., Stellacci, E., Cecchetti, S., Ferese, R., Bottero, L., Castro, S., Fenneteau, O., Brethon, B., Sanchez, M., Roberts, A.E., Yntema, H.G., Van Der Burgt, I., Cianci, P., Bondeson, M.L., Cristina Digilio, M., Zampino, G., Kerr, B., Aoki, Y., Loh, M.L., Palleschi, A., Di Schiavi, E., Carè, A., Selicorni, A., Dallapiccola, B., Cirstea, I.C., Stella, L., Zenker, M., Gelb, B.D., Cavé, H., Ahmadian, M.R., Tartaglia, M. (2014) Hum Mol Genet. 23 (16):4315-27.

Background: RASopathies are referred as a group of diseases affecting development and growth, in which germline and somatic mutations in a number of genes encoding transducers and modulatory proteins participating in the Ras/MAPK signaling pathway are usually identified. It has been also reported that these disorders are related with certain haematological malignances and other paediatric cancers. Even though many genes are found to be aberrant to cause these abnormalities, still a significant fraction is missing which could be the causal factor.

Result: By using protein interaction/functional association network analysis to select candidate genes involved in RAS signaling for Noonan syndrome or related RASopathy, two mutations (Val55Met and Gly39dup) in RRAS, another member of the Ras family, were identified. The latter is also identified in the patient with juvenile myelomonocytic leukaemia (JMML). Structure analysis indicated that Val55Met have enhanced GDP releasing ability resulting in faster nucleotide exchange and increased interaction with GEF. Biochemical assays demonstrated dramatic increase in intrinsic GDP dissociation rate for $RRAS^{G39dup}$ and GEF-stimulated nucleotide exchange for $RRAS^{G39dup}$ and $RRAS^{V55M}$. $RRAS^{G39dup}$ also showed significantly reduced intrinsic and GAP-stimulated GTP hydrolysis.

Conclusion: This work demonstrated that the dysregulation of RRAS protein is associated with the RASopathy syndrome and two germline mutations in RRAS occur in an aggressive form of JMML, a rare childhood myeloproliferative/myelodysplastic neoplasm. Structural and functional studies have demonstrated that the mutations in RRAS cause remarkably diverse biochemical effects with a common outcome, namely a rather moderate gain-of-function.

Significance: Data in this study elucidated that upregulated RRAS function represents a novel event contributing to JMML pathogenesis. It further extend the concept of 'RASopathy gene' to a transducer whose dysregulated function perturbs signal flow through the MAPK pathway but does not belong to the core RAS/MAPK signaling cassette.

* ***Enclosure 5***

Author contribution: The author of this dissertation has performed 5% of this study by analyzing the downstream signaling pathways of the R-Ras mutants.

Summary

The Ras and Rho family of small GTPases function as a molecular switch in the cell and regulate a spectrum of biochemical pathways and biological processes. Their activation and inactivation are modulated by two distinct regulators, GEF and GAP, respectively. Active small GTPases accomplish transduction of extracellular signal to downstream effectors through anchoring to plasma membrane via posttranslational modification, such as C-terminal geranylgeranylation. Geranylgeranylated Rho GTPases, e.g. Rac1, are modulated by an additional regulator, the GDI, which displaces them from the plasma membrane by specific binding to GDP-bound Rho GTPases and to the geranylgeranyl moiety. The dissociation of the Rho GTPase-GDI complex is thought to be modulated by p75NTR, ERM proteins and phospholipids. The role of such GDI displacement factors (GDF) remains to be demonstrated *in vitro*.

The germline Ras mutations are associated with diverse developmental disorders, collectively referred as RASopathies. Detailed analysis of an N-Ras mutation (T50I) provided novel insights into additional Ras interaction with membrane. Two other adjacent residues, D47 and E49, have been proposed also to interact with the membrane. How such membrane association affects the cellular signaling of N-Ras is still unclear.

In this thesis, Rac1 and N-Ras are investigated in details regarding to their interaction with lipid membranes, regulators and effectors under cell-free conditions and in cells. The latter allowed exploring a causal relationship between germline Ras mutations and the RASopathies. We showed that prenylated human Rac1, purified from insect cells interacts with the liposomes in a nucleotide independent manner. GDI efficiently bound to an extracted Rac1 from liposomes, which was blocked in the presence of Rac1-specific GEFs. Rac1 activation by GEFs positively modulated Rac1 association to the liposomes. Further mechanistic studies provided an unexpected new insight for elucidating an electrostatic interaction between the positively charged Rac1 C-terminus and distinct negatively charged regions of the terminal ends of GDI that is responsible for Rac1 extraction from the membrane.

Furthermore, the impacts of various germline Ras mutations were characterized in detail. T50I together with two additional mutations (D47K and E49K) clearly affected additional N-Ras interaction with plasma membrane and consequently caused an enhanced activation of the MAPK pathway. These data suggest that Ras interaction with the membrane via D47, E49 and T50 most probably suppresses Ras activation. In contrast, two germline K-Ras mutations, Y71H and K147E, led to mild gain-of-function due to changes of the effector and nucleotide binding properties. Another type of mutation in R-Ras, G39dup (duplication of G39), showed higher MAPK signaling because of reduced intrinsic and GAP-stimuated GTP hydrolysis. Our findings clearly emphasize that individual RAS mutations, despite being associated with comparable phenotypes of developmental disorders in patients, can remarkably cause diverse biochemical effects with a common outcome, namely a rather moderate gain-of-function.

Zusammenfassung

Die GTPasen der Ras- und Rho-Familien fungieren als molekulare Schalter in der Zelle und regulieren ein breites Spektrum an biochemischen Signalwegen und biologischen Prozessen. Ihre Aktivierung und Deaktivierung werden durch zwei verschiedenen Regulatoren (GEF und GAP) reguliert. Kleine aktive GTPasen ermöglichen die Transduktion von extrazellulären Signalen zu nachgeschalteten Effektoren, in dem sie sich durch posttranslationale Modifikationen, z.B. durch die C-terminale Geranylgeranylierung, an die Plasmamembran anheften. Geranylgeranylierte Rho GTPasen, z.B. Rac1, werden durch einen zusätzlichen Regulator, dem GDI, reguliert. Durch spezifische Bindung an die GDP-gebundene Rho GTPase und die geranylgeranyl-Gruppe veranlasst GDI die Dissoziation der Rac1 von der Plasmamembran. Es wird angenommen, dass die Dissoziation des Rho GTPase-GDI-Komplexes durch p75NTR, ERM Proteine und Phospholipide reguliert wird. Die Rolle dieser so-genannten GDIDdisplacement-Faktoren (GDF) muss *in vitro* noch gezeigt werden.

Die Ras Keimbahn-Mutationen sind assoziiert mit diversen Entwicklungsstörungen, die auch als RASopathien bezeichnet werden. Detaillierte Analysen einer N-Ras Mutation (T50I) haben weitere Einblicke in die Ras Interaktion mit Membranen gezeigt. Es wird angenommen, dass zwei weitere angrenzende Residuen, D47 und E49, ebenfalls mit der Membran interagieren. Wie sich die Membran Assoziation auf den zellulären Signalweg der N-Ras auswirkt, ist nicht bekannt.

In dieser Doktorarbeit wurden Rac1 und N-Ras hinsichtlich ihrer Interaktion mit Lipid-Membranen, Regulatoren und Effektoren unter zellfreien Bedingungen und in Zellen detailliert untersucht. Letzteres ermöglicht uns weitere Einblicke in die Beziehung zwischen Ras-Keimbahn-Mutationen und RASopathien. Es wurde gezeigt, dass das prenylierte Rac1 des Menschen, welche aus Insektenzellen isoliert und gereinigt wurde, mit den Liposomen in einer Nukleotid-unabhängigen Weise interagiert.

GDI bindet und extrahiert effektiv Rac1 von den Liposomen, welches in Anwesenheit von Rac1-spezifischen GEFs blockiert wird. Die .Rac1-Aktivierung durch GEFs wirkt sich positiv auf die Regulation von Rac1-Assoziation mit Liposomen aus. Weitere mechanistische Studien haben einen unerwarteten neuen Einblick in die elektrostatische Interaktion zwischen positiv geladener C-Terminus von Rac1 und negativ geladene Regionen terminaler Enden von GDI gezeigt, welche verantwortlich für die Rac1-Extraktion von der Membran sind.

Des Weiteren werden die Auswirkungen von diversen Ras-Keimbahn-Mutationen in Detail charakterisiert. Zusammen mit zwei zusätzlichen Mutationen (D47 und E49K) beeinflusst T50I die N-Ras-Interaktion mit der Plasmamembran und sorgt folglich für die Aktivierung der MAPK-Signalweg. Dies deutet darauf hin, dass die Ras-nteraktion mit der Membran durch D47, E49 und T50 höchst wahrscheinlich die Ras-Aktivierung unterdrückt. Demgegenüber stehen zwei K-Ras-Keimbahn-Mutationen, Y71H und K147E, die durch Veränderungen der Effektoren-Interaktionen und Nucleotid-bindenden Eigenschaften zu einem mäßigen

Funktionsgewinn (Gain-of-Function) beisteuern.
Ein anderer Mutationstyp in R-Ras ist G39dup (Verdopplung von G39). Es wurde gezeigt, dass dieser Mutationstyp höhere MAPK-Signale erzeugt, da grundlegende und GAP-stimulierende GTP-Hydrolyse reduziert werden. Unsere Daten unterstützen die Aussage, dass individuelle Ras Mutationen, obwohl sie mit vielen Phänotypen von Entwicklungsstörungen in Patienten in Zusammenhang stehen, diverse bemerkenswerte biochemische Effekte mit einem gemeinsamen Ergebnis erzielen können, und zwar dem mäßigem Funktionsgewinn (Gain-of-Function).

Abbreviations

AML	Acute myeloid leukaemia
Arp2/3	Actin-related protein-2/3
aSEC	Analytical size exclusion chromatography
B1RBD	Ras binding domain of Plexin-B1
CFCS	Cardio-facio-cutaneous syndrome
CGD	Chronic granulomatous disease
CRMP-2	Collapsin response mediator protein-2
CS	Costello syndrome
DLC	Deleted in liver cancer
EGF	Epithelial growth factor
ER	Endoplasmic reticulum
FH	Formin homology
FTase	Farnesyltransferase
GAP	GTPase activating proteins
GBD	GTPase binding domain
GC	Golgi complex
GDI	GDP dissociation inhibitor
GEF	Guanine nucleotide exchange factors
GGTase I	Geranylgeranyl transferase I
GGTase II	Geranylgeranyl transferase II
GSL	Glycosphingolipid
HVR	Hypervariable region
Icmt	Isoprenylcysteine carboxyl methyl transferase
JMML	Juvenile myelomonocytic leukaemia
MAPK	mitogen-activated protein kinase
MLC	Myosin light chain
NADPH oxidase	Nicotinamide adenine dinucleotide phosphate-oxidase
NF-κB	Nuclear factor-κB

NPC	Nuclear pore complex
NS	Noonan syndrome
PA	Phosphatidic acid
PAK	P21-activated kinase
PAT	Palmitoyl acyltransferase
PC	Phosphatidylcholine
PDEδ	Phophodiesterase δ
PE	phosphatidylethanolamine
PI	Phosphatidylinositol
PI3K	Phosphoinositide 3-kinase
PS	Phosphatidylserine
RAF	Rapidly Accelerated Fibrosarcoma
RalGDS	Ral guanine nucleotide dissociation stimulator
Rce1	Ras-converting enzyme 1
ROS	Reactive oxygen species
SM	Sphingomeylin
SH2	Src-homology-2 domain
SH3	Src-homology-3 domain
SOS1	Son of sevenless homolog 1
TIP47	Tail-interacting protein of 47 kDa
VCA	Verprolin homology, central and acidic region
WASPs	Wiskott-Aldrich syndrome proteins
WAVE	WASP verprolin homologues

References

Abankwa, D., Gorfe, A. A. and Hancock, J. F. (2008). "Mechanisms of Ras membrane organization and signalling: Ras on a rocker." Cell Cycle **7**(17): 2667-2673.

Abankwa, D., Hanzal-Bayer, M., Ariotti, N., Plowman, S. J., Gorfe, A. A., Parton, R. G., McCammon, J. A. and Hancock, J. F. (2008). "A novel switch region regulates H-ras membrane orientation and signal output." EMBO J **27**(5): 727-735.

Abo, A., Pick, E., Hall, A., Totty, N., Teahan, C. G. and Segal, A. W. (1991). "Activation of the NADPH oxidase involves the small GTP-binding protein p21rac1." Nature **353**(6345): 668-670.

Adra, C. N., Manor, D., Ko, J. L., Zhu, S. C., Horiuchi, T., VanAelst, L., Cerione, R. A. and Lim, B. (1997). "RhoGDI gamma: A GDP-dissociation inhibitor for Rho proteins with preferential expression in brain and pancreas." Proc Natl Acad Sci U S A **94**(9): 4279-4284.

Ahearn, I. M., Haigis, K., Bar-Sagi, D. and Philips, M. R. (2012). "Regulating the regulator: post-translational modification of RAS." Nat Rev Mol Cell Biol **13**(1): 39-51.

Ahmadian, M. R., Mittal, R., Hall, A. and Wittinghofer, A. (1997). "Aluminum fluoride associates with the small guanine nucleotide binding proteins." FEBS Lett. **408**(3): 315-318.

Aittaleb, M., Boguth, C. A. and Tesmer, J. J. (2010). "Structure and function of heterotrimeric G protein-regulated Rho guanine nucleotide exchange factors." Mol Pharmacol **77**(2): 111-125.

Aivazian, D., Serrano, R. L. and Pfeffer, S. (2006). "TIP47 is a key effector for Rab9 localization." J Cell Biol **173**(6): 917-926.

Alexander, M., Gerauer, M., Pechlivanis, M., Popkirova, B., Dvorsky, R., Brunsveld, L., Waldmann, H. and Kuhlmann, J. (2009). "Mapping the isoprenoid binding pocket of PDEdelta by a semisynthetic, photoactivatable N-Ras lipoprotein." Chembiochem **10**(1): 98-108.

Ali, B. R., Wasmeier, C., Lamoreux, L., Strom, M. and Seabra, M. C. (2004). "Multiple regions contribute to membrane targeting of Rab GTPases." J Cell Sci **117**(Pt 26): 6401-6412.

Allen, W. E., Zicha, D., Ridley, A. J. and Jones, G. E. (1998). "A role for Cdc42 in macrophage chemotaxis." J Cell Biol **141**(5): 1147-1157.

Amin, E., Dubey, B. N., Zhang, S. C., Gremer, L., Dvorsky, R., Moll, J. M., Taha, M. S., Nagel-Steger, L., Piekorz, R. P., Somlyo, A. V. and Ahmadian, M. R. (2013). "Rho-kinase: regulation, (dys)function, and inhibition." Biological Chemistry **394**(11): 1399-1410.

Aoki, Y., Niihori, T., Kawame, H., Kurosawa, K., Ohashi, H., Tanaka, Y., Filocamo, M., Kato, K., Suzuki, Y., Kure, S. and Matsubara, Y. (2005). "Germline mutations in HRAS proto-oncogene cause Costello syndrome." Nat Genet **37**(10): 1038-1040.

Arimura, N., Inagaki, N., Chihara, K., Menager, C., Nakamura, N., Amano, M., Iwamatsu, A., Goshima, Y. and Kaibuchi, K. (2000). "Phosphorylation of collapsin response mediator protein-2 by Rho-kinase. Evidence for two separate signaling pathways for growth cone collapse." J Biol Chem **275**(31): 23973-23980.

Arter, J. L., Chi, D. S., M, G., Fitzgerald, S. M., Guha, B. and Krishnaswamy, G. (2004). "Obstructive sleep apnea, inflammation, and cardiopulmonary disease." Front Biosci **9**: 2892-2900.

Aurandt, J., Vikis, H. G., Gutkind, J. S., Ahn, N. and Guan, K. L. (2002). "The semaphorin receptor plexin-B1 signals through a direct interaction with the Rho-specific nucleotide exchange factor, LARG." Proc Natl Acad Sci U S A **99**(19): 12085-12090.

Ballester, R., Marchuk, D., Boguski, M., Saulino, A., Letcher, R., Wigler, M. and Collins, F. (1990). "The NF1 locus encodes a protein functionally related to mammalian GAP and yeast IRA

proteins." Cell **63**(4): 851-859.

Bang, B., Gniadecki, R., Larsen, J. K., Baadsgaard, O. and Skov, L. (2003). "In vivo UVB irradiation induces clustering of Fas (CD95) on human epidermal cells." Exp Dermatol **12**(6): 791-798.

Berchtold, D., Piccolis, M., Chiaruttini, N., Riezman, I., Riezman, H., Roux, A., Walther, T. C. and Loewith, R. (2012). "Plasma membrane stress induces relocalization of Slm proteins and activation of TORC2 to promote sphingolipid synthesis." Nature Cell Biology **14**(5): 542-547.

Berthier, A., Lemaire-Ewing, S., Prunet, C., Monier, S., Athias, A., Bessede, G., Pais de Barros, J. P., Laubriet, A., Gambert, P., Lizard, G. and Neel, D. (2004). "Involvement of a calcium-dependent dephosphorylation of BAD associated with the localization of Trpc-1 within lipid rafts in 7-ketocholesterol-induced THP-1 cell apoptosis." Cell Death Differ **11**(8): 897-905.

Bishop, A. L. and Hall, A. (2000). "Rho GTPases and their effector proteins." The Biochemical journal **348 Pt 2**: 241-255.

Bompard, G. and Caron, E. (2004). "Regulation of WASP/WAVE proteins: making a long story short." J Cell Biol **166**(7): 957-962.

Boura, E. and Hurley, J. H. (2012). "Structural basis for membrane targeting by the MVB12-associated beta-prism domain of the human ESCRT-I MVB12 subunit." Proc Natl Acad Sci U S A **109**(6): 1901-1906.

Boureux, A., Vignal, E., Faure, S. and Fort, P. (2007). "Evolution of the Rho family of ras-like GTPases in eukaryotes." Mol Biol Evol **24**(1): 203-216.

Bourne, H. R., Sanders, D. A. and McCormick, F. (1991). "The GTPase superfamily: conserved structure and molecular mechanism." Nature **349**(6305): 117-127.

Bowtell, D., Fu, P., Simon, M. and Senior, P. (1992). "Identification of murine homologues of the Drosophila son of sevenless gene: potential activators of ras." Proc Natl Acad Sci U S A **89**(14): 6511-6515.

Bretscher, M. S. (1973). "Membrane structure: some general principles." Science **181**(4100): 622-629.

Bulgin, R., Raymond, B., Garnett, J. A., Frankel, G., Crepin, V. F., Berger, C. N. and Arbeloa, A. (2010). "Bacterial guanine nucleotide exchange factors SopE-like and WxxxE effectors." Infect Immun **78**(4): 1417-1425.

Burridge, K. and Wennerberg, K. (2004). "Rho and Rac take center stage." Cell **116**(2): 167-179.

Chandra, A., Grecco, H. E., Pisupati, V., Perera, D., Cassidy, L., Skoulidis, F., Ismail, S. A., Hedberg, C., Hanzal-Bayer, M., Venkitaraman, A. R., Wittinghofer, A. and Bastiaens, P. I. (2011). "The GDI-like solubilizing factor PDEdelta sustains the spatial organization and signalling of Ras family proteins." Nature Cell Biology **14**(2): 148-158.

Chavrier, P., Gorvel, J. P., Stelzer, E., Simons, K., Gruenberg, J. and Zerial, M. (1991). "Hypervariable C-terminal domain of rab proteins acts as a targeting signal." Nature **353**(6346): 769-772.

Chen, Z., Borek, D., Padrick, S. B., Gomez, T. S., Metlagel, Z., Ismail, A. M., Umetani, J., Billadeau, D. D., Otwinowski, Z. and Rosen, M. K. (2010). "Structure and control of the actin regulatory WAVE complex." Nature **468**(7323): 533-538.

Cherfils, J. and Chardin, P. (1999). "GEFs: structural basis for their activation of small GTP-binding proteins." Trends Biochem Sci **24**(8): 306-311.

Cherfils, J. and Zeghouf, M. (2013). "Regulation of small GTPases by GEFs, GAPs, and GDIs." Physiol Rev **93**(1): 269-309.

Chien, Y. and White, M. A. (2003). "RAL GTPases are linchpin modulators of human tumour-cell

proliferation and survival." Embo Reports **4**(8): 800-806.

Chong, C., Tan, L., Lim, L. and Manser, E. (2001). "The mechanism of PAK activation. Autophosphorylation events in both regulatory and kinase domains control activity." J Biol Chem **276**(20): 17347-17353.

Chou, M. M., Masuda-Robens, J. M. and Gupta, M. L. (2003). "Cdc42 promotes G1 progression through p70 S6 kinase-mediated induction of cyclin E expression." J Biol Chem **278**(37): 35241-35247.

Cirstea, I. C., Gremer, L., Dvorsky, R., Zhang, S. C., Piekorz, R. P., Zenker, M. and Ahmadian, M. R. (2013). "Diverging gain-of-function mechanisms of two novel KRAS mutations associated with Noonan and cardio-facio-cutaneous syndromes." Hum Mol Genet **22**(2): 262-270.

Cirstea, I. C., Kutsche, K., Dvorsky, R., Gremer, L., Carta, C., Horn, D., Roberts, A. E., Lepri, F., Merbitz-Zahradnik, T., Konig, R., Kratz, C. P., Pantaleoni, F., Dentici, M. L., Joshi, V. A., Kucherlapati, R. S., Mazzanti, L., Mundlos, S., Patton, M. A., Silengo, M. C., Rossi, C., Zampino, G., Digilio, C., Stuppia, L., Seemanova, E., Pennacchio, L. A., Gelb, B. D., Dallapiccola, B., Wittinghofer, A., Ahmadian, M. R., Tartaglia, M. and Zenker, M. (2010). "A restricted spectrum of NRAS mutations causes Noonan syndrome." Nat Genet **42**(1): 27-29.

Cizmarova, M., Kostalova, L., Pribilincova, Z., Lasabova, Z., Hlavata, A., Kovacs, L. and Ilencikova, D. (2013). "Rasopathies - dysmorphic syndromes with short stature and risk of malignancy." Endocr Regul **47**(4): 217-222.

Clark, S. G., Stern, M. J. and Horvitz, H. R. (1992). "C. elegans cell-signalling gene sem-5 encodes a protein with SH2 and SH3 domains." Nature **356**(6367): 340-344.

Clarke, S., Vogel, J. P., Deschenes, R. J. and Stock, J. (1988). "Posttranslational modification of the Ha-ras oncogene protein: evidence for a third class of protein carboxyl methyltransferases." Proc Natl Acad Sci U S A **85**(13): 4643-4647.

Cook, D. R., Rossman, K. L. and Der, C. J. (2013). "Rho guanine nucleotide exchange factors: regulators of Rho GTPase activity in development and disease." Oncogene **16**(10): 362.

Cox, A. D. and Der, C. J. (2010). "Ras history: The saga continues." Small GTPases **1**(1): 2-27.

Dai, Q., Choy, E., Chiu, V., Romano, J., Slivka, S. R., Steitz, S. A., Michaelis, S. and Philips, M. R. (1998). "Mammalian prenylcysteine carboxyl methyltransferase is in the endoplasmic reticulum." J Biol Chem **273**(24): 15030-15034.

Daub, H., Gevaert, K., Vandekerckhove, J., Sobel, A. and Hall, A. (2001). "Rac/Cdc42 and p65PAK regulate the microtubule-destabilizing protein stathmin through phosphorylation at serine 16." J Biol Chem **276**(3): 1677-1680.

DeGeer, J. and Lamarche-Vane, N. (2013). "Rho GTPases in neurodegeneration diseases." Exp Cell Res **319**(15): 2384-2394.

DerMardirossian, C., Rocklin, G., Seo, J. Y. and Bokoch, G. M. (2006). "Phosphorylation of RhoGDI by Src regulates Rho GTPase binding and cytosol-membrane cycling." Mol Biol Cell **17**(11): 4760-4768.

DerMardirossian, C., Schnelzer, A. and Bokoch, G. M. (2004). "Phosphorylation of RhoGDI by Pak1 mediates, dissociation of Rac GTPase." Mol Cell **15**(1): 117-127.

Diebold, B. A. and Bokoch, G. M. (2001). "Molecular basis for Rac2 regulation of phagocyte NADPH oxidase." Nat Immunol **2**(3): 211-215.

Dvorsky, R. and Ahmadian, M. R. (2004). "Always look on the bright site of Rho: structural implications for a conserved intermolecular interface." EMBO Rep **5**(12): 1130-1136.

Eberth, A., Dvorsky, R., Becker, C. F., Beste, A., Goody, R. S. and Ahmadian, M. R. (2005). "Monitoring the real-time kinetics of the hydrolysis reaction of guanine nucleotide-binding proteins." Biol. Chem. **386**(11): 1105-1114.

Eberth, A., Lundmark, R., Gremer, L., Dvorsky, R., Koessmeier, K. T., McMahon, H. T. and Ahmadian, M. R. (2009). "A BAR domain-mediated autoinhibitory mechanism for RhoGAPs of the GRAF family." Biochem J **417**(1): 371-377.

Eggeling, C., Ringemann, C., Medda, R., Schwarzmann, G., Sandhoff, K., Polyakova, S., Belov, V. N., Hein, B., von Middendorff, C., Schonle, A. and Hell, S. W. (2009). "Direct observation of the nanoscale dynamics of membrane lipids in a living cell." Nature **457**(7233): 1159-1162.

Eisenberg, S., Beckett, A. J., Prior, I. A., Dekker, F. J., Hedberg, C., Waldmann, H., Ehrlich, M. and Henis, Y. I. (2011). "Raft protein clustering alters N-Ras membrane interactions and activation pattern." Mol Cell Biol **31**(19): 3938-3952.

Erickson, J. W. and Cerione, R. A. (2004). "Structural elements, mechanism, and evolutionary convergence of Rho protein-guanine nucleotide exchange factor complexes." Biochemistry **43**(4): 837-842.

Etienne-Manneville, S. and Hall, A. (2002). "Rho GTPases in cell biology." Nature **420**(6916): 629-635.

Eytan, G. D. (1982). "Use of liposomes for reconstitution of biological functions." Biochim Biophys Acta **694**(2): 185-202.

Fidyk, N. J. and Cerione, R. A. (2002). "Understanding the catalytic mechanism of GTPase-activating proteins: demonstration of the importance of switch domain stabilization in the stimulation of GTP hydrolysis." Biochemistry **41**(52): 15644-15653.

Firth, A. L., Choi, I. W. and Park, W. S. (2012). "Animal models of pulmonary hypertension: Rho kinase inhibition." Prog Biophys Mol Biol **109**(3): 67-75.

Flex, E., Jaiswal, M., Pantaleoni, F., Martinelli, S., Strullu, M., Fansa, E. K., Caye, A., De Luca, A., Lepri, F., Dvorsky, R., Pannone, L., Paolacci, S., Zhang, S. C., Fodale, V., Bocchinfuso, G., Rossi, C., Burkitt-Wright, E. M., Farrotti, A., Stellacci, E., Cecchetti, S., Ferese, R., Bottero, L., Castro, S., Fenneteau, O., Brethon, B., Sanchez, M., Roberts, A. E., Yntema, H. G., Van Der Burgt, I., Cianci, P., Bondeson, M. L., Cristina Digilio, M., Zampino, G., Kerr, B., Aoki, Y., Loh, M. L., Palleschi, A., Di Schiavi, E., Care, A., Selicorni, A., Dallapiccola, B., Cirstea, I. C., Stella, L., Zenker, M., Gelb, B. D., Cave, H., Ahmadian, M. R. and Tartaglia, M. (2014). "Activating mutations in RRAS underlie a phenotype within the RASopathy spectrum and contribute to leukaemogenesis." Hum Mol Genet **15**: 15.

Florio, S. K., Prusti, R. K. and Beavo, J. A. (1996). "Solubilization of membrane-bound rod phosphodiesterase by the rod phosphodiesterase recombinant delta subunit." J Biol Chem **271**(39): 24036-24047.

Folch, J. (1942). "Brain Cephalin, a mixture of Phosphatides. Separation from it of Phosphatidyl serine, Phosphatidyl ethanolamine, and a fraction containing an inositol Phosphatide." J Biol Chem. **146**: 35-44.

Fukumoto, Y., Kaibuchi, K., Hori, Y., Fujioka, H., Araki, S., Ueda, T., Kikuchi, A. and Takai, Y. (1990). "Molecular-Cloning and Characterization of a Novel Type of Regulatory Protein (Gdi) for the Rho Proteins, Ras P21-Like Small Gtp-Binding Proteins." Oncogene **5**(9): 1321-1328.

Gallagher, E. D., Gutowski, S., Sternweis, P. C. and Cobb, M. H. (2004). "RhoA binds to the amino terminus of MEKK1 and regulates its kinase activity." J Biol Chem **279**(3): 1872-1877.

Garrett, M. D., Self, A. J., van Oers, C. and Hall, A. (1989). "Identification of distinct cytoplasmic targets for ras/R-ras and rho regulatory proteins." J Biol Chem **264**(1): 10-13.

Gibbs, J. B., Sigal, I. S., Poe, M. and Scolnick, E. M. (1984). "Intrinsic GTPase activity distinguishes normal and oncogenic ras p21 molecules." Proc Natl Acad Sci U S A **81**(18): 5704-5708.

Goldfarb, M., Shimizu, K., Perucho, M. and Wigler, M. (1982). "Isolation and preliminary characterization of a human transforming gene from T24 bladder carcinoma cells." Nature **296**(5856): 404-409.

Gorzalczany, Y., Alloul, N., Sigal, N., Weinbaum, C. and Pick, E. (2002). "A prenylated p67phox-Rac1 chimera elicits NADPH-dependent superoxide production by phagocyte membranes in the absence of an activator and of p47phox: conversion of a pagan NADPH oxidase to monotheism." J Biol Chem **277**(21): 18605-18610.

Gosser, Y. Q., Nomanbhoy, T. K., Aghazadeh, B., Manor, D., Combs, C., Cerione, R. A. and Rosen, M. K. (1997). "C-terminal binding domain of Rho GDP-dissociation inhibitor directs N-terminal inhibitory peptide to GTPases." Nature **387**(6635): 814-819.

Gotta, M., Abraham, M. C. and Ahringer, J. (2001). "CDC-42 controls early cell polarity and spindle orientation in C. elegans." Curr Biol **11**(7): 482-488.

Graham, D. L., Eccleston, J. F. and Lowe, P. N. (1999). "The conserved arginine in rho-GTPase-activating protein is essential for efficient catalysis but not for complex formation with Rho.GDP and aluminum fluoride." Biochemistry **38**(3): 985-991.

Gremer, L., Merbitz-Zahradnik, T., Dvorsky, R., Cirstea, I. C., Kratz, C. P., Zenker, M., Wittinghofer, A. and Ahmadian, M. R. (2011). "Germline KRAS mutations cause aberrant biochemical and physical properties leading to developmental disorders." Hum Mutat **32**(1): 33-43.

Grizot, S., Faure, J., Fieschi, F., Vignais, P. V., Dagher, M. C. and Pebay-Peyroula, E. (2001). "Crystal structure of the Rac1-RhoGDI complex involved in nadph oxidase activation." Biochemistry **40**(34): 10007-10013.

Guldenhaupt, J., Rudack, T., Bachler, P., Mann, D., Triola, G., Waldmann, H., Kotting, C. and Gerwert, K. (2012). "N-Ras forms dimers at POPC membranes." Biophys J **103**(7): 1585-1593.

Guo, Z., Ahmadian, M. R. and Goody, R. S. (2005). "Guanine nucleotide exchange factors operate by a simple allosteric competitive mechanism." Biochemistry **44**(47): 15423-15429.

Hager, G. L., Chang, E. H., Chan, H. W., Garon, C. F., Israel, M. A., Martin, M. A., Scolnick, E. M. and Lowy, D. R. (1979). "Molecular cloning of the Harvey sarcoma virus closed circular DNA intermediates: initial structural and biological characterization." J Virol **31**(3): 795-809.

Hall, A. (1998). "Rho GTPases and the actin cytoskeleton." Science **279**(5350): 509-514.

Hamad, N. M., Elconin, J. H., Karnoub, A. E., Bai, W., Rich, J. N., Abraham, R. T., Der, C. J. and Counter, C. M. (2002). "Distinct requirements for Ras oncogenesis in human versus mouse cells." Genes Dev **16**(16): 2045-2057.

Han, M., Golden, A., Han, Y. and Sternberg, P. W. (1993). "C. elegans lin-45 raf gene participates in let-60 ras-stimulated vulval differentiation." Nature **363**(6425): 133-140.

Hancock, J. F. (2003). "Ras proteins: different signals from different locations." Nat Rev Mol Cell Biol **4**(5): 373-384.

Hancock, J. F. and Hall, A. (1993). "A Novel Role for Rhogdi as an Inhibitor of Gap Proteins." EMBO J **12**(5): 1915-1921.

Hancock, J. F., Paterson, H. and Marshall, C. J. (1990). "A polybasic domain or palmitoylation is required in addition to the CAAX motif to localize p21ras to the plasma membrane." Cell

63(1): 133-139.

Hanzal-Bayer, M., Renault, L., Roversi, P., Wittinghofer, A. and Hillig, R. C. (2002). "The complex of Arl2-GTP and PDE delta: from structure to function." EMBO J **21**(9): 2095-2106.

Harris, T. J. and McCormick, F. (2010). "The molecular pathology of cancer." Nat Rev Clin Oncol **7**(5): 251-265.

Hart, M. J., Eva, A., Evans, T., Aaronson, S. A. and Cerione, R. A. (1991). "Catalysis of guanine nucleotide exchange on the CDC42Hs protein by the dbl oncogene product." Nature **354**(6351): 311-314.

Harvey, J. J. (1964). "An Unidentified Virus Which Causes the Rapid Production of Tumours in Mice." Nature **204**: 1104-1105.

Heasman, S. J. and Ridley, A. J. (2008). "Mammalian Rho GTPases: new insights into their functions from in vivo studies." Nat Rev Mol Cell Biol **9**(9): 690-701.

Hiraoka, K., Kaibuchi, K., Ando, S., Musha, T., Takaishi, K., Mizuno, T., Asada, M., Menard, L., Tomhave, E., Didsbury, J., Snyderman, R. and Takai, Y. (1992). "Both Stimulatory and Inhibitory Gdp/Gtp Exchange Proteins, Smg Gds and Rho Gdi, Are Active on Multiple Small Gtp-Binding Proteins." Biochem. Biophys. Res. Commun **182**(2): 921-930.

Hoffman, G. R. and Cerione, R. A. (2002). "Signaling to the Rho GTPases: networking with the DH domain." FEBS Lett **513**(1): 85-91.

Hoffman, G. R., Nassar, N. and Cerione, R. A. (2000). "Structure of the Rho family GTP-binding protein Cdc42 in complex with the multifunctional regulator RhoGDI." Cell **100**(3): 345-356.

Hori, Y., Kikuchi, A., Isomura, M., Katayama, M., Miura, Y., Fujioka, H., Kaibuchi, K. and Takai, Y. (1991). "Post-translational modifications of the C-terminal region of the rho protein are important for its interaction with membranes and the stimulatory and inhibitory GDP/GTP exchange proteins." Oncogene **6**(4): 515-522.

Hutchinson, J. P. and Eccleston, J. F. (2000). "Mechanism of nucleotide release from Rho by the GDP dissociation stimulator protein." Biochemistry **39**(37): 11348-11359.

Iden, S. and Collard, J. G. (2008). "Crosstalk between small GTPases and polarity proteins in cell polarization." Nat Rev Mol Cell Biol **9**(11): 846-859.

Ipsen, J. H., Karlstrom, G., Mouritsen, O. G., Wennerstrom, H. and Zuckermann, M. J. (1987). "Phase equilibria in the phosphatidylcholine-cholesterol system." Biochim Biophys Acta **905**(1): 162-172.

Ishizaki, T., Maekawa, M., Fujisawa, K., Okawa, K., Iwamatsu, A., Fujita, A., Watanabe, N., Saito, Y., Kakizuka, A., Morii, N. and Narumiya, S. (1996). "The small GTP-binding protein Rho binds to and activates a 160 kDa Ser/Thr protein kinase homologous to myotonic dystrophy kinase." EMBO J **15**(8): 1885-1893.

Ismail, S. A., Chen, Y. X., Rusinova, A., Chandra, A., Bierbaum, M., Gremer, L., Triola, G., Waldmann, H., Bastiaens, P. I. and Wittinghofer, A. (2011). "Arl2-GTP and Arl3-GTP regulate a GDI-like transport system for farnesylated cargo." Nat Chem Biol **7**(12): 942-949.

Jackson, J. H., Li, J. W., Buss, J. E., Der, C. J. and Cochrane, C. G. (1994). "Polylysine domain of K-ras 4B protein is crucial for malignant transformation." Proc Natl Acad Sci U S A **91**(26): 12730-12734.

Jaffe, A. B. and Hall, A. (2005). "Rho GTPases: biochemistry and biology." Annu Rev Cell Dev Biol **21**: 247-269.

Jaiswal, M., Dubey, B. N., Koessmeier, K. T., Gremer, L. and Ahmadian, M. R. (2012). "Biochemical

assays to characterize Rho GTPases." Methods Mol Biol **827**: 37-58.

Jaiswal, M., Dvorsky, R. and Ahmadian, M. R. (2013). "Deciphering the molecular and functional basis of Dbl family proteins: a novel systematic approach toward classification of selective activation of the Rho family proteins." J Biol Chem **288**(6): 4486-4500.

Jaiswal, M., Gremer, L., Dvorsky, R., Haeusler, L. C., Cirstea, I. C., Uhlenbrock, K. and Ahmadian, M. R. (2011). "Mechanistic insights into specificity, activity, and regulatory elements of the regulator of G-protein signaling (RGS)-containing Rho-specific guanine nucleotide exchange factors (GEFs) p115, PDZ-RhoGEF (PRG), and leukemia-associated RhoGEF (LARG)." J Biol Chem **286**(20): 18202-18212.

Jaiswal, M., Risse, S., Cirstea, I. C., Olayioye, M. A. and Ahmadian, M. R. (*in prep*.). "Identification of structural and functional determinants of the inhibition of DLC tumor suppressor protein by p120 RasGAP."

Kamata, T. and Feramisco, J. R. (1984). "Epidermal growth factor stimulates guanine nucleotide binding activity and phosphorylation of ras oncogene proteins." Nature **310**(5973): 147-150.

Karnoub, A. E. and Weinberg, R. A. (2008). "Ras oncogenes: split personalities." Nat Rev Mol Cell Biol **9**(7): 517-531.

Kelley, G. G., Reks, S. E., Ondrako, J. M. and Smrcka, A. V. (2001). "Phospholipase C(epsilon): a novel Ras effector." EMBO J **20**(4): 743-754.

Kikuchi, A., Demo, S. D., Ye, Z. H., Chen, Y. W. and Williams, L. T. (1994). "ralGDS family members interact with the effector loop of ras p21." Mol Cell Biol **14**(11): 7483-7491.

Kim, E., Ambroziak, P., Otto, J. C., Taylor, B., Ashby, M., Shannon, K., Casey, P. J. and Young, S. G. (1999). "Disruption of the mouse Rce1 gene results in defective Ras processing and mislocalization of Ras within cells." J Biol Chem **274**(13): 8383-8390.

Kimura, K., Ito, M., Amano, M., Chihara, K., Fukata, Y., Nakafuku, M., Yamamori, B., Feng, J., Nakano, T., Okawa, K., Iwamatsu, A. and Kaibuchi, K. (1996). "Regulation of myosin phosphatase by Rho and Rho-associated kinase (Rho- kinase)." Science **273**(5272): 245-248.

Kirsten, W. H. and Mayer, L. A. (1967). "Morphologic responses to a murine erythroblastosis virus." J Natl Cancer Inst **39**(2): 311-335.

Klebe, C., Prinz, H., Wittinghofer, A. and Goody, R. S. (1995). "The kinetic mechanism of Ran--nucleotide exchange catalyzed by RCC1." Biochemistry **34**(39): 12543-12552.

Knaus, U. G., Wang, Y., Reilly, A. M., Warnock, D. and Jackson, J. H. (1998). "Structural requirements for PAK activation by Rac GTPases." J Biol Chem **273**(34): 21512-21518.

Kruger, R. P., Aurandt, J. and Guan, K. L. (2005). "Semaphorins command cells to move." Nat Rev Mol Cell Biol **6**(10): 789-800.

Lam, B. D. and Hordijk, P. L. (2013). "The Rac1 hypervariable region in targeting and signaling: a tail of many stories." Small GTPases **4**(2): 78-89.

Lambert, J. M., Lambert, Q. T., Reuther, G. W., Malliri, A., Siderovski, D. P., Sondek, J., Collard, J. G. and Der, C. J. (2002). "Tiam1 mediates Ras activation of Rac by a PI(3)K-independent mechanism." Nature Cell Biology **4**(8): 621-625.

Lancaster, C. A., Taylor-Harris, P. M., Self, A. J., Brill, S., van Erp, H. E. and Hall, A. (1994). "Characterization of rhoGAP. A GTPase-activating protein for rho-related small GTPases." J Biol Chem **269**(2): 1137-1142.

Lapouge, K., Smith, S. J., Walker, P. A., Gamblin, S. J., Smerdon, S. J. and Rittinger, K. (2000). "Structure of the TPR domain of p67phox in complex with Rac.GTP." Mol Cell **6**(4): 899-907.

Lartey, J. and Lopez Bernal, A. (2009). "RHO protein regulation of contraction in the human uterus." Reproduction **138**(3): 407-424.

Lee, A. G. (2011). "Biological membranes: the importance of molecular detail." Trends Biochem Sci **36**(9): 493-500.

Lemaire-Ewing, S., Lagrost, L. and Neel, D. (2012). "Lipid rafts: a signalling platform linking lipoprotein metabolism to atherogenesis." Atherosclerosis **221**(2): 303-310.

Leonard, D., Hart, M. J., Platko, J. V., Eva, A., Henzel, W., Evans, T. and Cerione, R. A. (1992). "The identification and characterization of a GDP-dissociation inhibitor (GDI) for the CDC42Hs protein." J Biol Chem **267**(32): 22860-22868.

Li, H. Y., Cao, K. and Zheng, Y. (2003). "Ran in the spindle checkpoint: a new function for a versatile GTPase." Trends Cell Biol **13**(11): 553-557.

Ligeti, E., Dagher, M. C., Hernandez, S. E., Koleske, A. J. and Settleman, J. (2004). "Phospholipids can switch the GTPase substrate preference of a GTPase-activating protein." J Biol Chem **279**(7): 5055-5058.

Lopez, I., Mak, E. C., Ding, J., Hamm, H. E. and Lomasney, J. W. (2001). "A novel bifunctional phospholipase c that is regulated by Galpha 12 and stimulates the Ras/mitogen-activated protein kinase pathway." J Biol Chem **276**(4): 2758-2765.

Lowenstein, E. J., Daly, R. J., Batzer, A. G., Li, W., Margolis, B., Lammers, R., Ullrich, A., Skolnik, E. Y., Bar-Sagi, D. and Schlessinger, J. (1992). "The SH2 and SH3 domain-containing protein GRB2 links receptor tyrosine kinases to ras signaling." Cell **70**(3): 431-442.

Luo, C., Wang, K., Liu de, Q., Li, Y. and Zhao, Q. S. (2008). "The functional roles of lipid rafts in T cell activation, immune diseases and HIV infection and prevention." Cell Mol Immunol **5**(1): 1-7.

Macara, I. G., Lounsbury, K. M., Richards, S. A., McKiernan, C. and Bar-Sagi, D. (1996). "The Ras superfamily of GTPases." Faseb J **10**(5): 625-630.

Maier, U., Babich, A., Macrez, N., Leopoldt, D., Gierschik, P., Illenberger, D. and Nurnberg, B. (2000). "Gbeta 5gamma 2 is a highly selective activator of phospholipid-dependent enzymes." J Biol Chem **275**(18): 13746-13754.

Makbul, C., Constantinescu Aruxandei, D., Hofmann, E., Schwarz, D., Wolf, E. and Herrmann, C. (2013). "Structural and thermodynamic characterization of Nore1-SARAH: a small, helical module important in signal transduction networks." Biochemistry **52**(6): 1045-1054.

Malliri, A., van der Kammen, R. A., Clark, K., van der Valk, M., Michiels, F. and Collard, J. G. (2002). "Mice deficient in the Rac activator Tiam1 are resistant to Ras-induced skin tumours." Nature **417**(6891): 867-871.

Malumbres, M. and Barbacid, M. (2003). "RAS oncogenes: the first 30 years." Nat Rev Cancer **3**(6): 459-465.

Manser, E., Leung, T., Salihuddin, H., Zhao, Z. S. and Lim, L. (1994). "A brain serine/threonine protein kinase activated by Cdc42 and Rac1." Nature **367**(6458): 40-46.

Marte, B. M. and Downward, J. (1997). "PKB/Akt: connecting phosphoinositide 3-kinase to cell survival and beyond." Trends Biochem Sci **22**(9): 355-358.

Mason, R. P., Walter, M. F. and Jacob, R. F. (2004). "Effects of HMG-CoA reductase inhibitors on endothelial function: role of microdomains and oxidative stress." Circulation **109**(21 Suppl 1): II34-41.

Mayo, M. W., Wang, C. Y., Cogswell, P. C., Rogers-Graham, K. S., Lowe, S. W., Der, C. J. and

Baldwin, A. S., Jr. (1997). "Requirement of NF-kappaB activation to suppress p53-independent apoptosis induced by oncogenic Ras." Science **278**(5344): 1812-1815.

McCormick, F. (1993). Signal transduction. How receptors turn Ras on, Nature. 1993 May 6;363(6424):15-6.

Meller, N., Merlot, S. and Guda, C. (2005). "CZH proteins: a new family of Rho-GEFs." J Cell Sci **118**(Pt 21): 4937-4946.

Mettouchi, A., Klein, S., Guo, W., Lopez-Lago, M., Lemichez, E., Westwick, J. K. and Giancotti, F. G. (2001). "Integrin-specific activation of Rac controls progression through the G(1) phase of the cell cycle." Mol Cell **8**(1): 115-127.

Michaelson, D., Silletti, J., Murphy, G., D'Eustachio, P., Rush, M. and Philips, M. R. (2001). "Differential localization of Rho GTPases in live cells: regulation by hypervariable regions and RhoGDI binding." J Cell Biol **152**(1): 111-126.

Minoshima, Y., Kawashima, T., Hirose, K., Tonozuka, Y., Kawajiri, A., Bao, Y. C., Deng, X., Tatsuka, M., Narumiya, S., May, W. S., Jr., Nosaka, T., Semba, K., Inoue, T., Satoh, T., Inagaki, M. and Kitamura, T. (2003). "Phosphorylation by aurora B converts MgcRacGAP to a RhoGAP during cytokinesis." Developmental cell **4**(4): 549-560.

Miralles, F., Posern, G., Zaromytidou, A. I. and Treisman, R. (2003). "Actin dynamics control SRF activity by regulation of its coactivator MAL." Cell **113**(3): 329-342.

Misaki, R., Morimatsu, M., Uemura, T., Waguri, S., Miyoshi, E., Taniguchi, N., Matsuda, M. and Taguchi, T. (2010). "Palmitoylated Ras proteins traffic through recycling endosomes to the plasma membrane during exocytosis." J Cell Biol **191**(1): 23-29.

Mitin, N., Rossman, K. L. and Der, C. J. (2005). "Signaling interplay in Ras superfamily function." Curr Biol **15**(14): R563-574.

Moon, S. Y. and Zheng, Y. (2003). "Rho GTPase-activating proteins in cell regulation." Trends Cell Biol **13**(1): 13-22.

Mozafari, M. R. (2005). "Liposomes: an overview of manufacturing techniques." Cell Mol Biol Lett **10**(4): 711-719.

Munro, S. (2003). "Lipid rafts: elusive or illusive?" Cell **115**(4): 377-388.

Nancy, V., Callebaut, I., El Marjou, A. and de Gunzburg, J. (2002). "The delta subunit of retinal rod cGMP phosphodiesterase regulates the membrane association of Ras and Rap GTPases." J Biol Chem **277**(17): 15076-15084.

Nassar, N., Hoffman, G. R., Manor, D., Clardy, J. C. and Cerione, R. A. (1998). "Structures of Cdc42 bound to the active and catalytically compromised forms of Cdc42GAP." Nat Struct Biol **5**(12): 1047-1052.

Newman, C. M. and Magee, A. I. (1993). "Posttranslational processing of the ras superfamily of small GTP-binding proteins." Biochim Biophys Acta **25**(1): 79-96.

Nie, Z., Hirsch, D. S. and Randazzo, P. A. (2003). "Arf and its many interactors." Curr Opin Cell Biol **15**(4): 396-404.

Niederost, B., Oertle, T., Fritsche, J., McKinney, R. A. and Bandtlow, C. E. (2002). "Nogo-A and myelin-associated glycoprotein mediate neurite growth inhibition by antagonistic regulation of RhoA and Rac1." J Neurosci **22**(23): 10368-10376.

Niihori, T., Aoki, Y., Narumi, Y., Neri, G., Cave, H., Verloes, A., Okamoto, N., Hennekam, R. C., Gillessen-Kaesbach, G., Wieczorek, D., Kavamura, M. I., Kurosawa, K., Ohashi, H., Wilson, L., Heron, D., Bonneau, D., Corona, G., Kaname, T., Naritomi, K., Baumann, C., Matsumoto,

N., Kato, K., Kure, S. and Matsubara, Y. (2006). "Germline KRAS and BRAF mutations in cardio-facio-cutaneous syndrome." Nat Genet **38**(3): 294-296.

Ohashi, K., Nagata, K., Maekawa, M., Ishizaki, T., Narumiya, S. and Mizuno, K. (2000). "Rho-associated kinase ROCK activates LIM-kinase 1 by phosphorylation at threonine 508 within the activation loop." J Biol Chem **275**(5): 3577-3582.

Ohvo-Rekila, H., Ramstedt, B., Leppimaki, P. and Slotte, J. P. (2002). "Cholesterol interactions with phospholipids in membranes." Prog Lipid Res **41**(1): 66-97.

Parada, L. F., Tabin, C. J., Shih, C. and Weinberg, R. A. (1982). "Human EJ bladder carcinoma oncogene is homologue of Harvey sarcoma virus ras gene." Nature **297**(5866): 474-478.

Parri, M. and Chiarugi, P. (2010). "Rac and Rho GTPases in cancer cell motility control." Cell Commun Signal **8**: 23.

Paz, A., Haklai, R., Elad-Sfadia, G., Ballan, E. and Kloog, Y. (2001). "Galectin-1 binds oncogenic H-Ras to mediate Ras membrane anchorage and cell transformation." Oncogene **20**(51): 7486-7493.

Peck, J., Douglas, G. t., Wu, C. H. and Burbelo, P. D. (2002). "Human RhoGAP domain-containing proteins: structure, function and evolutionary relationships." FEBS Lett **528**(1-3): 27-34.

Perrot, V., Vazquez-Prado, J. and Gutkind, J. S. (2002). "Plexin B regulates Rho through the guanine nucleotide exchange factors leukemia-associated Rho GEF (LARG) and PDZ-RhoGEF." J Biol Chem **277**(45): 43115-43120.

Pollard, T. D. and Borisy, G. G. (2003). "Cellular motility driven by assembly and disassembly of actin filaments." Cell **112**(4): 453-465.

Preudhomme, C., Roumier, C., Hildebrand, M. P., Dallery-Prudhomme, E., Lantoine, D., Lai, J. L., Daudignon, A., Adenis, C., Bauters, F., Fenaux, P., Kerckaert, J. P. and Galiegue-Zouitina, S. (2000). "Nonrandom 4p13 rearrangements of the RhoH/TTF gene, encoding a GTP-binding protein, in non-Hodgkin's lymphoma and multiple myeloma." Oncogene **19**(16): 2023-2032.

Prior, I. A. and Hancock, J. F. (2012). "Ras trafficking, localization and compartmentalized signalling." Semin Cell Dev Biol **23**(2): 145-153.

Prior, I. A., Harding, A., Yan, J., Sluimer, J., Parton, R. G. and Hancock, J. F. (2001). "GTP-dependent segregation of H-ras from lipid rafts is required for biological activity." Nature Cell Biology **3**(4): 368-375.

Pulciani, S., Santos, E., Lauver, A. V., Long, L. K., Robbins, K. C. and Barbacid, M. (1982). "Oncogenes in human tumor cell lines: molecular cloning of a transforming gene from human bladder carcinoma cells." Proc Natl Acad Sci U S A **79**(9): 2845-2849.

Rak, A., Pylypenko, O., Durek, T., Watzke, A., Kushnir, S., Brunsveld, L., Waldmann, H., Goody, R. S. and Alexandrov, K. (2003). "Structure of Rab GDP-dissociation inhibitor in complex with prenylated YPT1 GTPase." Science **302**(5645): 646-650.

Ramstedt, B. and Slotte, J. P. (2002). "Membrane properties of sphingomyelins." Febs Letters **531**(1): 33-37.

Rauen, K. A. (2013). "The RASopathies." Annu Rev Genomics Hum Genet **14**: 355-369.

Repasky, G. A., Chenette, E. J. and Der, C. J. (2004). "Renewing the conspiracy theory debate: does Raf function alone to mediate Ras oncogenesis?" Trends Cell Biol **14**(11): 639-647.

Rittinger, K. (2009). "Snapshots form a big picture of guanine nucleotide exchange." Sci Signal **2**(91): pe63.

Rittinger, K., Walker, P. A., Eccleston, J. F., Smerdon, S. J. and Gamblin, S. J. (1997). "Structure at

1.65 A of RhoA and its GTPase-activating protein in complex with a transition-state analogue." Nature **389**(6652): 758-762.

Robbe, K., Otto-Bruc, A., Chardin, P. and Antonny, B. (2003). "Dissociation of GDP dissociation inhibitor and membrane translocation are required for efficient activation of Rac by the Dbl homology-pleckstrin homology region of Tiam." J Biol Chem **278**(7): 4756-4762.

Rodriguez-Viciana, P., Warne, P. H., Dhand, R., Vanhaesebroeck, B., Gout, I., Fry, M. J., Waterfield, M. D. and Downward, J. (1994). "Phosphatidylinositol-3-OH kinase as a direct target of Ras." Nature **370**(6490): 527-532.

Rohm, B., Rahim, B., Kleiber, B., Hovatta, I. and Puschel, A. W. (2000). "The semaphorin 3A receptor may directly regulate the activity of small GTPases." Febs Letters **486**(1): 68-72.

Rommel, C. and Hafen, E. (1998). "Ras--a versatile cellular switch." Curr Opin Genet Dev **8**(4): 412-418.

Rosenblatt, J., Cramer, L. P., Baum, B. and McGee, K. M. (2004). "Myosin II-dependent cortical movement is required for centrosome separation and positioning during mitotic spindle assembly." Cell **117**(3): 361-372.

Rossman, K. L., Der, C. J. and Sondek, J. (2005). "GEF means go: turning on RHO GTPases with guanine nucleotide-exchange factors." Nat Rev Mol Cell Biol **6**(2): 167-180.

Rossman, K. L. and Sondek, J. (2005). "Larger than Dbl: new structural insights into RhoA activation." Trends Biochem Sci **30**(4): 163-165.

Rossman, K. L., Worthylake, D. K., Snyder, J. T., Cheng, L., Whitehead, I. P. and Sondek, J. (2002). "Functional analysis of cdc42 residues required for Guanine nucleotide exchange." J Biol Chem **277**(52): 50893-50898.

Rudolph, M. G., Weise, C., Mirold, S., Hillenbrand, B., Bader, B., Wittinghofer, A. and Hardt, W. D. (1999). "Biochemical analysis of SopE from Salmonella typhimurium, a highly efficient guanosine nucleotide exchange factor for RhoGTPases." J Biol Chem **274**(43): 30501-30509.

Sanders, L. C., Matsumura, F., Bokoch, G. M. and de Lanerolle, P. (1999). "Inhibition of myosin light chain kinase by p21-activated kinase." Science **283**(5410): 2083-2085.

Scheffzek, K. and Ahmadian, M. R. (2005). "GTPase activating proteins: structural and functional insights 18 years after discovery." Cell Mol Life Sci **62**(24): 3014-3038.

Scheffzek, K., Stephan, I., Jensen, O. N., Illenberger, D. and Gierschik, P. (2000). "The Rac-RhoGDI complex and the structural basis for the regulation of Rho proteins by RhoGDI." Nat Struct Biol **7**(2): 122-126.

Scherle, P., Behrens, T. and Staudt, L. M. (1993). "Ly-Gdi, a Gdp-Dissociation Inhibitor of the Rhoa Gtp-Binding Protein, Is Expressed Preferentially in Lymphocytes." Proc Natl Acad Sci U S A **90**(16): 7568-7572.

Schroeder, R. J., Ahmed, S. N., Zhu, Y., London, E. and Brown, D. A. (1998). "Cholesterol and sphingolipid enhance the Triton X-100 insolubility of glycosylphosphatidylinositol-anchored proteins by promoting the formation of detergent-insoluble ordered membrane domains." J Biol Chem **273**(2): 1150-1157.

Schubbert, S., Zenker, M., Rowe, S. L., Boll, S., Klein, C., Bollag, G., van der Burgt, I., Musante, L., Kalscheuer, V., Wehner, L. E., Nguyen, H., West, B., Zhang, K. Y., Sistermans, E., Rauch, A., Niemeyer, C. M., Shannon, K. and Kratz, C. P. (2006). "Germline KRAS mutations cause Noonan syndrome." Nat Genet **38**(3): 331-336.

Schulz, A., Baader, S. L., Niwa-Kawakita, M., Jung, M. J., Bauer, R., Garcia, C., Zoch, A., Schacke, S.,

Hagel, C., Mautner, V.-F., Hanemann, C. O., Dun, X.-P., Parkinson, D. B., Weis, J., Schroder, J. M., Gutmann, D. H., Giovannini, M. and Morrison, H. (2013). "Merlin isoform 2 in neurofibromatosis type 2-associated polyneuropathy." Nature Neuroscience **16**(4): 426-433.

Scolnick, E. M., Papageorge, A. G. and Shih, T. Y. (1979). "Guanine nucleotide-binding activity as an assay for src protein of rat-derived murine sarcoma viruses." Proc Natl Acad Sci U S A **76**(10): 5355-5359.

Scolnick, E. M., Rands, E., Williams, D. and Parks, W. P. (1973). "Studies on the nucleic acid sequences of Kirsten sarcoma virus: a model for formation of a mammalian RNA-containing sarcoma virus." J Virol **12**(3): 458-463.

Shih, C. and Weinberg, R. A. (1982). "Isolation of a transforming sequence from a human bladder carcinoma cell line." Cell **29**(1): 161-169.

Shou, C., Farnsworth, C. L., Neel, B. G. and Feig, L. A. (1992). "Molecular cloning of cDNAs encoding a guanine-nucleotide-releasing factor for Ras p21." Nature **358**(6384): 351-354.

Simon, M. N., De Virgilio, C., Souza, B., Pringle, J. R., Abo, A. and Reed, S. I. (1995). "Role for the Rho-family GTPase Cdc42 in yeast mating-pheromone signal pathway." Nature **376**(6542): 702-705.

Simons, K. and Ikonen, E. (2000). "How cells handle cholesterol." Science **290**(5497): 1721-1726.

Singer, S. J. and Nicolson, G. L. (1972). "The fluid mosaic model of the structure of cell membranes." Science **175**(4023): 720-731.

Sonnino, S. and Prinetti, A. (2013). "Membrane domains and the "lipid raft" concept." Curr Med Chem **20**(1): 4-21.

Stenmark, H., Valencia, A., Martinez, O., Ullrich, O., Goud, B. and Zerial, M. (1994). "Distinct structural elements of rab5 define its functional specificity." EMBO J **13**(3): 575-583.

Sud, M., Fahy, E., Cotter, D., Brown, A., Dennis, E. A., Glass, C. K., Merrill, A. H., Jr., Murphy, R. C., Raetz, C. R., Russell, D. W. and Subramaniam, S. (2007). "LMSD: LIPID MAPS structure database." Nucleic Acids Res **35**(Database issue): D527-532.

Swarthout, J. T., Lobo, S., Farh, L., Croke, M. R., Greentree, W. K., Deschenes, R. J. and Linder, M. E. (2005). "DHHC9 and GCP16 constitute a human protein fatty acyltransferase with specificity for H- and N-Ras." J Biol Chem **280**(35): 31141-31148.

Szoka, F., Jr. and Papahadjopoulos, D. (1980). "Comparative properties and methods of preparation of lipid vesicles (liposomes)." Annu Rev Biophys Bioeng **9**: 467-508.

Takahashi, K., Sasaki, T., Mammoto, A., Takaishi, K., Kameyama, T., Tsukita, S., Tsukita, S. and Takai, Y. (1997). "Direct interaction of the Rho GDP dissociation inhibitor with ezrin/radixin/moesin initiates the activation of the Rho small G protein." J Biol Chem **272**(37): 23371-23375.

Takai, Y., Sasaki, T. and Matozaki, T. (2001). "Small GTP-binding proteins." Physiol Rev **81**(1): 153-208.

Tcherkezian, J. and Lamarche-Vane, N. (2007). "Current knowledge of the large RhoGAP family of proteins." Biol Cell **99**(2): 67-86.

ten Klooster, J. P. and Hordijk, P. L. (2007). "Targeting and localized signalling by small GTPases." Biol Cell **99**(1): 1-12.

Teramoto, H., Coso, O. A., Miyata, H., Igishi, T., Miki, T. and Gutkind, J. S. (1996). "Signaling from the small GTP-binding proteins Rac1 and Cdc42 to the c-Jun N-terminal kinase/stress-activated protein kinase pathway. A role for mixed lineage kinase 3/protein-tyrosine kinase 1, a novel member of the mixed lineage kinase family." J Biol Chem

271(44): 27225-27228.

Thapar, R., Karnoub, A. E. and Campbell, S. L. (2002). "Structural and biophysical insights into the role of the insert region in Rac1 function." Biochemistry **41**(12): 3875-3883.

Tidyman, W. E. and Rauen, K. A. (2008). "Noonan, Costello and cardio-facio-cutaneous syndromes: dysregulation of the Ras-MAPK pathway." Expert Rev Mol Med **9**(10).

Tidyman, W. E. and Rauen, K. A. (2009). "The RASopathies: developmental syndromes of Ras/MAPK pathway dysregulation." Curr Opin Genet Dev **19**(3): 230-236.

Tnimov, Z., Guo, Z., Gambin, Y., Nguyen, U. T. T., Wu, Y. W., Abankwa, D., Stigter, A., Collins, B. M., Waldmann, H., Goody, R. S. and Alexandrov, K. (2012). "Quantitative Analysis of Prenylated RhoA Interaction with Its Chaperone, RhoGDI." J Biol Chem **287**(32): 26549-26562.

Toksoz, D. and Merdek, K. D. (2002). "The Rho small GTPase: functions in health and disease." Histol Histopathol **17**(3): 915-927.

Tommasi, S., Dammann, R., Jin, S. G., Zhang, X. F., Avruch, J. and Pfeifer, G. P. (2002). "RASSF3 and NORE1: identification and cloning of two human homologues of the putative tumor suppressor gene RASSF1." Oncogene **21**(17): 2713-2720.

Tong, Y., Chugha, P., Hota, P. K., Alviani, R. S., Li, M., Tempel, W., Shen, L., Park, H. W. and Buck, M. (2007). "Binding of Rac1, Rnd1, and RhoD to a novel Rho GTPase interaction motif destabilizes dimerization of the plexin-B1 effector domain." J Biol Chem **282**(51): 37215-37224.

Trahey, M., Wong, G., Halenbeck, R., Rubinfeld, B., Martin, G. A., Ladner, M., Long, C. M., Crosier, W. J., Watt, K., Koths, K. and et al. (1988). "Molecular cloning of two types of GAP complementary DNA from human placenta." Science **242**(4886): 1697-1700.

Tsuchida, N. and Uesugi, S. (1981). "Structure and functions of the Kirsten murine sarcoma virus genome: molecular cloning of biologically active Kirsten murine sarcoma virus DNA." J Virol **38**(2): 720-727.

Turner, L. J., Nicholls, S. and Hall, A. (2004). "The activity of the plexin-A1 receptor is regulated by Rac." J Biol Chem **279**(32): 33199-33205.

Ueda, T., Kikuchi, A., Ohga, N., Yamamoto, J. and Takai, Y. (1990). "Purification and characterization from bovine brain cytosol of a novel regulatory protein inhibiting the dissociation of GDP from and the subsequent binding of GTP to rhoB p20, a ras p21-like GTP-binding protein." J Biol Chem **265**(16): 9373-9380.

Ugolev, Y., Berdichevsky, Y., Weinbaum, C. and Pick, E. (2008). "Dissociation of Rac1(GDP).RhoGDI complexes by the cooperative action of anionic liposomes containing phosphatidylinositol 3,4,5-trisphosphate, Rac guanine nucleotide exchange factor, and GTP." J Biol Chem **283**(32): 22257-22271.

van Meer, G. and Lisman, Q. (2002). "Sphingolipid transport: rafts and translocators." J Biol Chem **277**(29): 25855-25858.

van Meer, G., Voelker, D. R. and Feigenson, G. W. (2008). "Membrane lipids: where they are and how they behave." Nat Rev Mol Cell Biol **9**(2): 112-124.

Vetter, I. R. and Wittinghofer, A. (2001). "The guanine nucleotide-binding switch in three dimensions." Science **294**(5545): 1299-1304.

Viaud, J., Gaits-Iacovoni, F. and Payrastre, B. (2012). "Regulation of the DH-PH tandem of guanine nucleotide exchange factor for Rho GTPases by phosphoinositides." Adv Biol Regul **52**(2): 303-314.

Villalonga, P., Lopez-Alcala, C., Bosch, M., Chiloeches, A., Rocamora, N., Gil, J., Marais, R., Marshall, C. J., Bachs, O. and Agell, N. (2001). "Calmodulin binds to K-Ras, but not to H- or N-Ras, and modulates its downstream signaling." Mol Cell Biol **21**(21): 7345-7354.

Vogel, U. S., Dixon, R. A., Schaber, M. D., Diehl, R. E., Marshall, M. S., Scolnick, E. M., Sigal, I. S. and Gibbs, J. B. (1988). "Cloning of bovine GAP and its interaction with oncogenic ras p21." Nature **335**(6185): 90-93.

Watzlich, D., Vetter, I., Gotthardt, K., Miertzschke, M., Chen, Y. X., Wittinghofer, A. and Ismail, S. (2013). "The interplay between RPGR, PDEdelta and Arl2/3 regulate the ciliary targeting of farnesylated cargo." Embo Reports **14**(5): 465-472.

Wei, W., Mosteller, R. D., Sanyal, P., Gonzales, E., McKinney, D., Dasgupta, C., Li, P., Liu, B. X. and Broek, D. (1992). "Identification of a mammalian gene structurally and functionally related to the CDC25 gene of Saccharomyces cerevisiae." Proc Natl Acad Sci U S A **89**(15): 7100-7104.

Weis, K. (2003). "Regulating access to the genome: nucleocytoplasmic transport throughout the cell cycle." Cell **112**(4): 441-451.

Weise, K., Kapoor, S., Denter, C., Nikolaus, J., Opitz, N., Koch, S., Triola, G., Herrmann, A., Waldmann, H. and Winter, R. (2011). "Membrane-mediated induction and sorting of K-Ras microdomain signaling platforms." J Am Chem Soc **133**(4): 880-887.

Weise, K., Kapoor, S., Werkmuller, A., Mobitz, S., Zimmermann, G., Triola, G., Waldmann, H. and Winter, R. (2012). "Dissociation of the K-Ras4B/PDEdelta complex upon contact with lipid membranes: membrane delivery instead of extraction." J Am Chem Soc **134**(28): 11503-11510.

Welsh, C. F., Roovers, K., Villanueva, J., Liu, Y., Schwartz, M. A. and Assoian, R. K. (2001). "Timing of cyclin D1 expression within G1 phase is controlled by Rho." Nature Cell Biology **3**(11): 950-957.

Wennerberg, K. and Der, C. J. (2004). "Rho-family GTPases: it's not only Rac and Rho (and I like it)." J Cell Sci **117**(Pt 8): 1301-1312.

Wennerberg, K., Rossman, K. L. and Der, C. J. (2005). "The Ras superfamily at a glance." J Cell Sci **118**(Pt 5): 843-846.

Westwick, J. K., Lambert, Q. T., Clark, G. J., Symons, M., Van Aelst, L., Pestell, R. G. and Der, C. J. (1997). "Rac regulation of transformation, gene expression, and actin organization by multiple, PAK-independent pathways." Mol Cell Biol **17**(3): 1324-1335.

Wherlock, M. and Mellor, H. (2002). "The Rho GTPase family: a Racs to Wrchs story." J Cell Sci **115**(Pt 2): 239-240.

Williams, D. A., Tao, W., Yang, F., Kim, C., Gu, Y., Mansfield, P., Levine, J. E., Petryniak, B., Derrow, C. W., Harris, C., Jia, B., Zheng, Y., Ambruso, D. R., Lowe, J. B., Atkinson, S. J., Dinauer, M. C. and Boxer, L. (2000). "Dominant negative mutation of the hematopoietic-specific Rho GTPase, Rac2, is associated with a human phagocyte immunodeficiency." Blood **96**(5): 1646-1654.

Willingham, M. C., Pastan, I., Shih, T. Y. and Scolnick, E. M. (1980). "Localization of the src gene product of the Harvey strain of MSV to plasma membrane of transformed cells by electron microscopic immunocytochemistry." Cell **19**(4): 1005-1014.

Wu, S., Loke, H. N. and Rehemtulla, A. (2002). "Ultraviolet radiation-induced apoptosis is mediated by Daxx." Neoplasia **4**(6): 486-492.

Xu, G. F., O'Connell, P., Viskochil, D., Cawthon, R., Robertson, M., Culver, M., Dunn, D., Stevens, J.,

Gesteland, R., White, R. and et al. (1990). "The neurofibromatosis type 1 gene encodes a protein related to GAP." Cell **62**(3): 599-608.

Yamashiro, S., Totsukawa, G., Yamakita, Y., Sasaki, Y., Madaule, P., Ishizaki, T., Narumiya, S. and Matsumura, F. (2003). "Citron kinase, a Rho-dependent kinase, induces di-phosphorylation of regulatory light chain of myosin II." Mol Biol Cell **14**(5): 1745-1756.

Yamashita, T. and Tohyama, M. (2003). "The p75 receptor acts as a displacement factor that releases Rho from Rho-GDI." Nature Neuroscience **6**(5): 461-467.

Yang, N., Higuchi, O., Ohashi, K., Nagata, K., Wada, A., Kangawa, K., Nishida, E. and Mizuno, K. (1998). "Cofflin phosphorylation by LIM-kinase 1 and its role in Rac-mediated actin reorganization." Nature **393**(6687): 809-812.

Yang, X. Y., Guan, M., Vigil, D., Der, C. J., Lowy, D. R. and Popescu, N. C. (2009). "p120Ras-GAP binds the DLC1 Rho-GAP tumor suppressor protein and inhibits its RhoA GTPase and growth-suppressing activities." Oncogene **28**(11): 1401-1409.

Zalcman, G., Closson, V., Camonis, J., Honore, N., RousseauMerck, M. F., Tavitian, A. and Olofsson, B. (1996). "RhoGDI-3 is a new GDP dissociation inhibitor (GDI) - Identification of a non-cytosolic GDI protein interacting with the small GTP-binding proteins rhoB and rhoG." J Biol Chem **271**(48): 30366-30374.

Zanata, S. M., Hovatta, I., Rohm, B. and Puschel, A. W. (2002). "Antagonistic effects of Rnd1 and RhoD GTPases regulate receptor activity in Semaphorin 3A-induced cytoskeletal collapse." J Neurosci **22**(2): 471-477.

Zerial, M. and McBride, H. (2001). "Rab proteins as membrane organizers." Nat Rev Mol Cell Biol **2**(2): 107-117.

Zhang, B. and Zheng, Y. (1998). "Regulation of RhoA GTP hydrolysis by the GTPase-activating proteins p190, p50RhoGAP, Bcr, and 3BP-1." Biochemistry **37**(15): 5249-5257.

Zhang, F. L. and Casey, P. J. (1996). "Protein prenylation: molecular mechanisms and functional consequences." Annu Rev Biochem **65**: 241-269.

Zhang, H., Liu, X. H., Zhang, K., Chen, C. K., Frederick, J. M., Prestwich, G. D. and Baehr, W. (2004). "Photoreceptor cGMP phosphodiesterase delta subunit (PDEdelta) functions as a prenyl-binding protein." J Biol Chem **279**(1): 407-413.

Zhang, S., Han, J., Sells, M. A., Chernoff, J., Knaus, U. G., Ulevitch, R. J. and Bokoch, G. M. (1995). "Rho family GTPases regulate p38 mitogen-activated protein kinase through the downstream mediator Pak1." J Biol Chem **270**(41): 23934-23936.

Zigmond, S. H. (2004). "Formin-induced nucleation of actin filaments." Curr Opin Cell Biol **16**(1): 99-105.

Ziolkowska, N. E., Christiano, R. and Walther, T. C. (2012). "Organized living: formation mechanisms and functions of plasma membrane domains in yeast." Trends Cell Biol **22**(3): 151-158.

Zurzolo, C., van Meer, G. and Mayor, S. (2003). "The order of rafts. Conference on microdomains, lipid rafts and caveolae." Embo Reports **4**(12): 1117-1121.

Curriculum Vitae

Personal details

Name:	Sicai Zhang
Date of Birth:	April 5th 1980
Place of Birth	Hubei, China
Nationality:	Chinese

Education

2010-2014	PhD student (Institute for Biochemistry and Molecular Biology II, Heinrich-Heine-University, Düsseldorf, Germany)
2006-2010	Research associate (structural biology group, Institute of Biochemistry and Cell Biology, Chinese Academy of Sciences, Shanghai, China)
2003-2006	M.Sc. in Agronomy (Yunnan Agricultural University, Kunming and Institute of Biochemistry and Cell Biology, Chinese Academy of Sciences, Shanghai, China)
1999-2003	B.Sc. in Agronomy (Yangtze University, Jinzhou, China)

Publications

Zhang, S. C., Sun, M., Li, T., Wang, Q. H., Hao, J. H., Han, Y., Hu, X. J., Zhou, M., Lin, S. X. (2011). Structure analysis of a new psychrophilic marine protease. PLoS One 6(11): e26939.

Zhang, S.C., Gremer, L., Heise, H., Janning, P., Symanets, A., Cirstea, I.C., Krause, E., Nürnberg, B., Ahmadian, M.R. (2014). Liposome reconstitution and modulation of recombinant prenylated human Rac1 by GEFs, GDI1 and Pak1. PLoS One 9(7):e102425.

Cirstea, I. C., Gremer, L., Dvorsky, R., **Zhang, S. C.**, Piekorz, R. P., Zenker, M., Ahmadian, M. R. (2013). Diverging gain-of-function mechanisms of two novel KRAS mutations associated with Noonan and cardio-facio-cutaneous syndromes. Hum Mol Genet 22(2): 262-270.

Fansa, E. K., Dvorsky, R., **Zhang, S. C.**, Fiegen, D., Ahmadian, M. R. (2013). Interaction characteristics of Plexin-B1 with Rho family proteins. Biochem Biophys Res Commun 434(4): 785-790.

Jaiswal, M., Dvorsky, R., Amin, E., Risse, S. L., Fansa, E. K., **Zhang, S. C.**, Taha, M. S., Gauhar, A. R., Nakhaei-Rad, S., Kordes, C., Koessmeier, K. T., Cirstea, I. C., Olayioye, M. A., Haeussinger, D. and Ahmadian, M. R. (2014). Functional crosstalk between Ras and Rho pathways: p120RasGAP competitively inhibits the RhoGAP activity of Deleted in Liver Cancer (DLC) tumor suppressors by masking its catalytic arginine finger. J Biol Chem 24: 24.

Flex, E., Jaiswal, M., Pantaleoni, F., Martinelli, S., Strullu, M., Fansa, E. K., Caye, A.,

De Luca, A., Lepri, F., Dvorsky, R., Pannone, L., Paolacci, S., **Zhang, S. C.**, Fodale, V., Bocchinfuso, G., Rossi, C., Burkitt-Wright, E. M., Farrotti, A., Stellacci, E., Cecchetti, S., Ferese, R., Bottero, L., Castro, S., Fenneteau, O., Brethon, B., Sanchez, M., Roberts, A. E., Yntema, H. G., Van Der Burgt, I., Cianci, P., Bondeson, M. L., Cristina Digilio, M., Zampino, G., Kerr, B., Aoki, Y., Loh, M. L., Palleschi, A., Di Schiavi, E., Care, A., Selicorni, A., Dallapiccola, B., Cirstea, I. C., Stella, L., Zenker, M., Gelb, B. D., Cave, H., Ahmadian, M. R. and Tartaglia, M. (2014). Activating mutations in RRAS underlie a phenotype within the RASopathy spectrum and contribute to leukaemogenesis. Hum Mol Genet 15: 15.

Amin, E., Dubey, B. N., **Zhang, S. C.**, Gremer, L., Dvorsky, R., Moll, J. M., Taha, M. S., Nagel-Steger, L., Piekorz, R. P., Somlyo, A. V. and Ahmadian, M. R. (2013). "Rho-kinase: regulation, (dys)function, and inhibition." Biological Chemistry 394(11): 1399-1410.

Book chapter in press

Zhang, S. C., Nouri, K., Amin, E., Taha, M. S., Nakhaeizadeh, H., Nakhaei-Rad, S., Dvorsky, R., and Ahmadian, M. R. (2014). Classical Rho proteins: Biochemistry of molecular switch function and regulation. In: Ras Superfamily Small G Proteins: Biology and Mechanisms 1, Heidelberg: Springer.

Manuscript in preparation

Zhang S. C., Nouri K., Amin E., Gierschik P, and Ahmadian, M. R. An electrostatic switch mechanism controls the Rho-GDI selectivity and function.

Zhang S. C., Nouri K., Amin E., Hahaeizadeh, H., and Ahmadian, M. R. Mechanism of N‐Ras integration at the plasma membrane.

Acknowledgement

I would like to give my very first and deepest thanks to my supervisor Reza Ahmadian. I thank him to give me the chance to join his group and do leading level scientific research. Before I come to his group, I know nothing about cell signaling and am blind at the professional research. He illuminates my scientific career and leads my way to the right direction for future. He imparts his knowledge to me selflessly. The sense of him to me is a spiritual mentor and will accompany me in my whole life.

Besides my supervisor, I would like to thank Prof. Johannes Hegemann to be my secondary supervisor and also for his support in reviewing my thesis.

I would like to express my heartful gratitude to my current fellow labmates in Reza's group: Mohamed Saleh, Saeideh Nakhaeirad, Kazem Nouri, Ehsan Amin, Hossein Nakhaeizadeh, Radovan Dvorsky, Bach-Ngan Nguyen, Nirina Sivakumar, Marcel Buchholz, Oliver Krumbach and my previous colleagues: Eyad Fansa, Mamta Jigsaw, Badri Dubey, for the kind help from social and scientific aspects, for the unforgettable days we have stay together.

The special appreciation will be given to Ion Cirstea, even most of time he is a naughty guy in my mind. But he does really have helped me in my work and give me support from both scientific and social point. This appreciation will also be given to Lothar Gremer who never hesitates to help me when I ask for.

I'm also grateful to all the members in the institute of Biochemistry and Molecular biology II. Thanks for continuous support from Dr. Roland Piekorz and Prof. Jürgen Scheller.

My sincere thanks also go to my close friend Dr. Zhaoping Ding. Thanks for his constructive discussion with me about fascinating cardio biology. I really cherish the friendship with Dr. Guanghui Zhang, who is the closest partner in my private life here.

I would like to appreciate all the days on this land since August 7th, 2010 which is the first day I land at Germany. I would never forget the educated life and people here and keep them all in my deep inside.

This thesis is dedicated to my beloved woman, my wife Meijie Cao (Sarah). I would like to thank her for her persistence on waiting for me and comprehensive support in this period. Life is short but she contributed her most precious days for just waiting for me. In my heart, she is the greatest woman in this world. I wish I can give the best words in this world to describe my gratitude for her. The last, I would like to thank my family at my hometown. Thank them for encouraging me and support all the time. I really miss them.

OPEN ACCESS Freely available online

PLOS ONE

Liposome Reconstitution and Modulation of Recombinant Prenylated Human Rac1 by GEFs, GDI1 and Pak1

Si-Cai Zhang[1], Lothar Gremer[1,2,3], Henrike Heise[2,3], Petra Janning[4], Aliaksei Shymanets[5], Ion C. Cirstea[1,6], Eberhard Krause[7], Bernd Nürnberg[5], Mohammad Reza Ahmadian[1]*

1 Institute of Biochemistry and Molecular Biology II, Medical Faculty of the Heinrich-Heine University, Düsseldorf, Germany, **2** Institute of Physical Biology, Heinrich-Heine University, Düsseldorf, Germany, **3** Institute of Complex Systems, ICS-6, Research Center Jülich GmbH, Jülich, Germany, **4** Department of Chemical Biology, Max-Planck Institute of Molecular Physiology, Dortmund, Germany, **5** Institute of Experimental and Clinical Pharmacology and Toxicology, Tübingen Medical School, Tübingen, Germany, **6** Leibniz Institute for Age Research, Jena, Germany, **7** Laboratory of Mass Spectrometry, Leibniz Institute of Molecular Pharmacology, Berlin, Germany

Abstract

Small Rho GTPases are well known to regulate a variety of cellular processes by acting as molecular switches. The regulatory function of Rho GTPases is critically dependent on their posttranslational modification at the carboxyl terminus by isoprenylation and association with proper cellular membranes. Despite numerous studies, the mechanisms of recycling and functional integration of Rho GTPases at the biological membranes are largely unclear. In this study, prenylated human Rac1, a prominent member of the Rho family, was purified in large amount from baculovirus-infected *Spodoptera frugiperda* insect cells using a systematic detergent screening. In contrast to non-prenylated human Rac1 purified from *Escherichia coli*, prenylated Rac1 from insect cells was able to associate with synthetic liposomes and to bind Rho-specific guanine nucleotide dissociation inhibitor 1 (GDI1). Subsequent liposome reconstitution experiments revealed that GDI1 efficiently extracts Rac1 from liposomes preferentially in the inactive GDP-bound state. The extraction was prevented when Rac1 was activated to its GTP-bound state by Rac-specific guanine nucleotide exchange factors (GEFs), such as Vav2, Dbl, Tiam1, P-Rex1 and TrioN, and bound by the downstream effector Pak1. We found that dissociation of Rac1-GDP from its complex with GDI1 strongly correlated with two distinct activities of especially Dbl and Tiam1, including liposome association and the GDP/GTP exchange. Taken together, our results provided first detailed insights into the advantages of the *in vitro* liposome-based reconstitution system to study both the integration of the signal transducing protein complexes and the mechanisms of regulation and signaling of small GTPases at biological membranes.

Citation: Zhang S-C, Gremer L, Heise H, Janning P, Shymanets A, et al. (2014) Liposome Reconstitution and Modulation of Recombinant Prenylated Human Rac1 by GEFs, GDI1 and Pak1. PLoS ONE 9(7): e102425. doi:10.1371/journal.pone.0102425

Editor: Ed Manser, Institute of Molecular and Cell Biology (IMCB), Singapore

Received April 17, 2014; **Accepted** June 18, 2014; **Published** July 11, 2014

Data Availability: The authors confirm that all data underlying the findings are fully available without restriction. All relevant data are within the paper and its Supporting Information files.

Funding: This research was gratefully supported in part by the German Research Foundation (Deutsche Forschungsgemeinschaft or DFG) through the Collaborative Research Center 974 (SFB 974) "Communication and Systems Relevance during Liver Injury and Regeneration", and the International NRW Research School BioStruct, granted by the Ministry of Innovation, Science and Research of the State North Rhine-Westphalia, the Heinrich-Heine-University of Düsseldorf, and the Entrepreneur Foundation at the Heinrich-Heine-University of Düsseldorf. The funders had no role in study design, data collection and analysis, decision to publish, or preparation of the manuscript.

Competing Interests: The authors have declared that no competing interests exist.

* Email: reza.ahmadian@uni-duesseldorf.de

Introduction

The Rho family GTPases are known to play an important role in diverse cellular processes and progression of different diseases, such as cardiovascular diseases, developmental and neurological disorders, as well as in tumor invasion and metastasis [1]. Rho GTPases share two common functional characteristics, membrane anchorage and an on/off switch cycle [2,3].

Subcellular localization of Rho GTPases to different cellular membranes is known to be critical for their biological activity. This is achieved by a hypervariable region (HVR) [4] and a lipid anchor in their C-terminal tail at a distinct cysteine residue in the CAAX motif (C is cysteine, A is any aliphatic amino acid, and X is any amino acid) [2,5,6,7]. In addition to either geranylgeranylation or farnesylation at the CAAX motif, some members of the Rho family, such as Rac1, require the C-terminal polybasic region and palmitoylation, essential for plasma membrane targeting and interaction with multiple lipids [8,9].

Rho GTPase function is dependent on the guanine nucleotide-binding (G) domain that contains the principle binding center for GDP and GTP and binds depending on its nucleotide-bound state various regulators and effectors [3]. Thus, membrane-associated Rho GTPases act, with some exceptions [10], as molecular switches by cycling between an inactive GDP-bound state and an active GTP-bound state [10]. This cycle underlies two critical intrinsic functions, the GDP-GTP exchange and GTP hydrolysis [10] and is controlled by at least three classes of regulatory proteins [3]: (i) Guanine nucleotide exchange factors (GEFs), especially those of the diffuse B-cell lymphoma (Dbl) family, which catalyze the exchange of GDP to GTP and activate the GTPase [11,12]; ii)

GTPase activating proteins (GAPs), which enhance the GTP hydrolysis and convey the GTPase in its inactive conformation [13,14]; (iii) Guanine nucleotide dissociation inhibitors (GDIs), which bind to prenylated Rho GTPases and extract them from the membranes into the cytoplasm [15,16,17]. The formation of the active GTP-bound state of Rho GTPases is accompanied by a conformational change in two regions (known as switch I and II; [3] which provide a platform for the selective interaction with structurally and functionally diverse effectors, *e.g.* p21-activated kinase α (Pak1). This class of proteins activate a wide variety of downstream signaling cascades [18,19,20] thereby regulating many important physiological and pathophysiological processes in eukaryotic cells [21,22].

The last decades in research of small GTPases under cell-free conditions were prevalently dominated by non-membranous systems such as soluble, mostly C-terminally truncated GTPases as well as shortened regulatory and effector proteins, mostly comprised of either the minimal catalytically active regulatory domains (GAPs, GEFs) or, in the case of effectors, the GTPase-binding domains (GBDs). Since the basic molecular mechanism of GTPase regulation and effector interaction is largely elucidated, it is in fact necessary now to move from these simplified soluble systems to more physiological and complex systems, *i.e.* multi-domain binding proteins acting on prenylated GTPases bound to the lipid membranes, the site at which they normally achieve their function in cells. A crucial prerequisite is, therefore, the availability of large quantities of purified, posttranslationally modified GTPases. Several different strategies have been developed to obtain lipid-modified proteins. It has been shown that Cdc42 purified from human platelets and insect cells can be extracted from the liposomes by RhoGDI1 (called here GDI1) [23,24]. Rac1 alone was purified from insect cells by using detergents [25,26]. Robbe *et al*. have purified prenylated Rac1 in complex with GDI1 that stabilized Rac1 in aqueous solution [27,28]. A similar strategy was used for the purification and structural determination of the Cdc42·GDP·GDI1 complex as well as of RhoA [29,30]. Ugolev *et al*. have used an enzymatic method to modify Rac1 *in vitro* by using geranylgeranyl transferase I [31]. They have shown that Rac1 dissociated from GDI1 by the cooperative action of RacGEFs and phosphatidylinositol (3, 4, 5)-trisphosphate (PIP3) containing liposomes. Gureasko *et al*. have directly attached Ras covalently to liposomes by using chemical cross linking [32]. The latter strategy avoids difficulties inherent in purifying lipid-modified proteins but is not useful for extraction experiments of membrane-bound GTPases using GDIs [27] or, alternatively, the δ subunit of phosphodiesterase (PDEδ) [33,34,35]. A large number of studies have utilized the advantage of a chemical ligation of a synthesized, lipidated C-terminal peptide with the purified G domain of different small GTPases [36], such as Rab proteins [37,38,39], K-Ras [35] and RhoA [17]. However, the question of how naturally modified, liposome-bound small GTPases, *e.g.* Rac1, interact with their regulators and effectors remains to be unveiled.

In this study we established a novel protocol for the extraction and purification of recombinant, prenylated, functionally active human Rac1 using a baculovirus-insect cell expression system and a detergent screening. Subsequently, *in vitro* liposome reconstitution studies were performed to gain insights into the Rac1 association with liposomes of different lipid compositions, and the extraction of Rac1 by GDI1. Rac1 extraction was prevented by a GEF-mediated Rac1 activation and Pak1 interaction.

Materials and Methods

Constructs

Human *Rac1* (GenBank accession no. NM_006908.4) was subcloned into pFastBacHTB vector (Invitrogen, Carlsbad, CA) and fused with an N-terminal hexa-histidine (6xHis) tag. For bacterial expression, full-length *Rac1* and *GDI1* (GenBank accession no. D13989) were cloned into pGEX-4T1 vector. DHPH constructs of human *Vav2* (aa 168–543), human *Dbl* (aa 498–825), *TrioN* (aa 1226–1535), murine *Tiam1* (aa 1033–1404), human *P-Rex1* (aa 34–415), and human *Pak1*-GBD (aa 57–141) have been reported before [11,40].

Antibodies, media and reagents

Anti-His-tag (mouse), anti-Rac (mouse), anti-E-cadherin (rabbit), anti-GAPDH (rabbit), anti-histone H3 (rabbit), anti-α-tubulin (rabbit), anti-rabbit IgG (goat), anti-mouse IgG conjugated with Alexa Fluor® 488 (goat), anti-Rabbit IgG conjugated with Alexa Fluor® 594 (goat) were purchased from Invitrogen (Oregon, USA); anti-mouse IgG was obtained from Dako (rabbit, California, USA). GDP and a non-hydrolyzable GTP analogue, guanosine 5′-[β,γ-imido]triphosphate (GppNHp), were obtained from Jena Bioscience GmbH (Jena, Germany). TC100 insect cell media, fetal bovine serum, antibiotics (penicillin and streptomycin) and 10% Pluronic F-68 were obtained from PAN-Biotech GmbH (Aidenbach, Germany). Phosphatidylserine (PS), Phosphatidylcholine (PC), phosphatidylethanolamine (PE) and sphingomyelin (SM), phosphatidylinositol 4,5-bisphosphate (PIP2), and Folch I and Folch III brain lipid extracts were purchased from Sigma-Aldrich (Munich, Germany). PIP_3 is from Merck (Darmstadt, Germany). All other standard reagents, including detergents (Table S1 in File S1) were obtained from Carl Roth GmbH (Karlsruhe, Germany) or Merck-Millipore (Darmstadt, Germany).

Baculoviruses and insect cell culture

Human *Rac1* gene subcloned into pFastBacHTB vector (Invitrogen, Carlsbad, CA) was transformed into DH10BAC strain. Agar plates containing kanamycin, gentamycin, tetracycline, X-gal and isopropyl-β-D-thiogalactoside were used to select recombinant *Rac1* clones. The *Rac1*-positive clones underwent two more purification steps before recombinant *Rac1* bacmid were extracted. The baculoviruses (passage 1) were generated by infecting *Sf*9 insect cells using recombinant *Rac1* bacmids. Viruses were ready to use for large scale Rac1 expression after two more amplification steps (passages 2 and 3).

*Sf*9 were cultured in TC-100 medium, containing 10% fetal bovine serum, penicillin, streptomycin and pluronic F-68 solution at 27°C. The titer of baculoviruses was determined by the $ITCD_{50}$ method [41,42]. The multiplicity of infection (MOI) and Rac1 expression time were optimized by infecting the *Sf*9 cells at different MOIs and different culture time points. Samples of infected cells (1 ml) were harvested; the cell pellets were lysed in Laemmli buffer, containing 60 mM Tris-HCl pH 6.8, 2% SDS, 10% glycerol, 5% β-mercaptoethanol, 0.01% bromophenol blue and analyzed by immunoblotting using an anti-His-tag antibody.

Confocal laser scanning microscopy (cLSM)

Insect cells were fixed with acetone/methanol (1:1) at 24 hours after seeding in 12 well plates. Cells were incubated first with antibodies against Rac1 and α-tubulin and then with secondary anti-mouse and anti-rabbit antibodies conjugated with Alexa Fluor® 488 and Alexa Fluor® 594 as well as DAPI (Danvers, USA). All steps were carried out at room temperature. Specimens were

visualized and photographed using a confocal laser scanning microscope (LSM510META; Zeiss, Jena, Germany).

Cell fractionation

*Sf*9 cells were harvested, resuspended in a buffer, containing 10 mM HEPES-NaOH pH 7.9, 1.5 mM $MgCl_2$, 10 mM KCl, 0.5 mM dithiothreitol (DTT), 1 tablet EDTA-free protease inhibitors (Roche, Mannheim, Germany), and disrupted under detergent-free conditions using pre-chilled Dounce homogenizer for 20 strokes with a tight pestle. Disrupted cells were centrifuged at 300x*g* for 5 min at 4°C. The supernatant was removed and centrifuged at 50000x*g* for 2 h at 4°C to separate the membrane (pellet) and the cytosolic fractions (supernatant). The pellet, containing enriched nuclei, was resuspended in 0.25 mM sucrose, 10 mM $MgCl_2$ and a cushion of 0.88 mM sucrose and 0.5 mM $MgCl_2$ was laid over. This sample was centrifuged at 2800x*g* for 10 min at 4°C to obtain the nuclear pellet. Protein samples from different fractions were analyzed by immunoblotting. Anti-Rac1 antibody was used to detect distribution of recombinant human Rac1 in all the fractions. Antibodies against E-cadherin, GAPDH and Histone H3 were used as marker for membrane, cytoplasmic and nuclear fractions, respectively.

Detergent screening

Eighteen different detergents (Table S1 in File S1) were used to extract Rac1 from the membrane fraction of *Sf*9 insect cells. Detergents were used at 20% (w/v) stock solution in buffer, containing 50 mM Tris-HCl pH 7.5, 100 mM NaCl, 2 mM $MgCl_2$, 10% glycerol, 20 mM β-glycerolphosphate, 1 mM ortho-Na_3VO_4 and 1 tablet EDTA-free inhibitor cocktail. The detergents at 1% and 0.5% (w/v) final concentrations were added into the suspension of membrane fractions, containing recombinant human Rac1. The mixtures were incubated at room temperature for 30 min and centrifuged at 20000x*g* for 10 min. The pellets and small amounts of supernatants were collected for immunoblot analysis. Residual supernatants were used further for pull-down assays with glutathione S-transferase (GST)-GDI1.

Thin layer chromatography

To check the lipid composition of the liposomes thin-layer chromatography was conducted using a thin layer chromatography plate (silica, 20×20 cm; Macherey-Nagel GmbH, Düren, Germany) and a chloroform/methanol/water/acetic acid (60:50:4:1) as eluting solvent system. Lipids were detected by molybdophosphoric acid spray.

Protein purification and nucleotide exchange

Large scale *Rac1* expression was conducted according to the established protocol described above. *Sf*9 insect cells were inoculated at a density of 1.5×10^6 cells/ml under optimized MOI and culture time. Cells were resuspended in lysis buffer, containing 50 mM HEPES-NaOH pH 7.4, 150 mM NaCl, 2 mM β-mercaptoethanol, 5 mM $MgCl_2$, 0.1 mM GDP, 10 mM imidazole and the optimized detergents according to the screening procedure described above. Cells were disrupted by sonication in ice-water mixture. Supernatants were collected by centrifugation and loaded on a Ni-NTA Superflow column (Qiagen, Hilden, Germany). High salt buffer (50 mM HEPES-NaOH pH 7.4, 150 mM NaCl, 2 mM β-mercaptoethanol, 5 mM $MgCl_2$, 0.1 mM GDP, 10 mM imidazole, 350 mM KCl and 1 mM ATP) was used to remove impurities from the target proteins. Rac1 protein was eluted using an imidazole gradient ranging from 10 to 500 mM. The protein solution was concentrated and further purified on a Superdex 75 column (10/300 GL, GE-Healthcare, Uppsala, Sweden) with 50 mM HEPES-NaOH pH 7.4, 150 mM NaCl, 3 mM DTT, 5 mM $MgCl_2$ and 0.5% (w/v) Na-cholate as buffer system. GppNHp-bound Rac1 proteins as well as human GDI1, RacGEFs, Pak1, full length and C-terminal truncated Rac1 proteins were prepared from *E. coli* as described previously [11,43].

Pull-down assay

GST-fused human GDI1 bound to glutathione beads was used to pull-down prenylated Rac1 from supernatants in the detergent screening procedure. Because of a detergent-induced nucleotide depletion of Rac1 it was important to determine the content of GDP-bound Rac1 proteins. The respective supernatants and beads were mixed and rotated at 4°C for 30 min. Samples were centrifuged at 500x*g* for 30 sec. Beads were washed three times using the buffers described above and containing the corresponding detergents. The beads and supernatant were analyzed by immunoblotting using anti-Rac antibody.

Liposome preparation

Liposome assays were performed by mixing and incubating the liposomes and purified Rac1 proteins. The mixtures were incubated for different time points and centrifuged at different speeds to separate the liposome pellets and supernatants for optimizing the centrifuging force. The liposomes were prepared as described previously [44]. Briefly, a lipid mixture (194 µg), containing 39% (w/w) PE, 16% (w/w) PC, 36% (w/w) PS, 4% (w/w) SM, and 5% (w/w) PIP2 or PIP3, was dried using light nitrogen stream. Obtained lipid film was hydrated with 300 µl of a buffer, containing 30 mM HEPES-NaOH pH 7.4, 50 mM NaCl, 3 mM DTT, 5 mM $MgCl_2$. Sonication (20 s with minimal power, 50% off and 50% on) was employed finally to form liposomes. Folch I and Folch III brain lipids extracts were prepared in methanol and chloroform at a concentration of 25 mg/ml. Folch I contains different phosphoinositides, PS, and cerebrosides in a ratio of 1:5:4 [45]. Folch III is composed of 80% PS, 10% PE, 5% cerebrosides and 5% unidentified membrane lipids [46]. Folch I or Folch III liposomes (250 µg, respectively) were prepared under the same conditions in 300 µl of the HEPES buffer. Liposomes with increasing PS or PC were prepared by either PS/PE or PC/PE to analyze lipid composition of Folch III. PC was used as control. Total lipids used for each liposome preparation were constantly 250 µg in 300 µl buffer.

Results

Subcellular localization of human Rac1 overexpressed in insect cells

The baculovirus-*Spodoptera frugiperda* (*Sf*9) insect cell expression system was used to express and purify human Rac1 in a prenylated form. In order to obtain optimal Rac1 expression, the tissue culture infectious dose 50 ($TCID_{50}$) method was utilized to determine titers of the baculovirus stocks as described before [41,42]. A striking characteristic of baculovirus-infected *Sf*9 cells is the so-called cytopathic effect, which is observed as a reduction of cell numbers and swollen cell size depending on the extent of infection as compared to the non-infected, highly confluent culture (Fig. S1A in File S1). *Sf*9 cells were next infected at different MOIs and culture time length. Increasing amounts of baculovirus resulted in a slight, dose-dependent increase in Rac1 expression with a peak around 36 and 48 h post-infection, especially at a MOI of 4 or 5 (Fig. S1B in File S1). Confocal imaging analysis revealed that human Rac1 is predominantly localized at the

plasma membrane (Fig. S1C in File S1). Cell fractionation experiments showed that Rac1 was mainly found in the membrane and endoplasmic reticulum-enriched nuclear fractions (Fig. S1D in File S1). These data clearly show that human Rac1 produced in insect cells exhibits similar characteristics as compared to endogenous Rac1 in mammalian cells, such as mouse embryonic fibroblasts and HeLa [47], regarding its cellular distribution [48].

Detergent extraction and purification of prenylated human Rac1 overexpressed in insect cells

An important issue to be considered for the extraction of nucleotide-bound, prenylated human Rac1 from *Sf*9 membrane fractions was the choice of an appropriate detergent. First attempts using deoxycholate and cholate as detergents were not successful. The former did not solubilize Rac1, while the latter did extract Rac1 but considerable amounts of extracted Rac1 proteins were depleted of their bound nucleotide (data not shown) indicating partial unfolding upon cholate treatment. It is of importance to note that a stoichiometric ratio of bound GDP is mandatory to avoid aggregation and precipitation of penylated Rac1, which means that the GDP-bound state must be monitored at every purification step, including detergent extraction from the cell membrane. Therefore, we tested sixteen additional detergents regarding their properties to extract fully functional Rac1 from the insect cell membrane fractions (Table S1 in File S1). Considering that the high amounts of detergent may also impair the quality of proteins, we used two different detergent concentrations (0.5% and 1% (w/v), respectively). Figure 1A illustrates a workflow with the corresponding steps of Rac1 extraction from the membrane and its pull-down by GST-GDI1. Seven detergents, *i.e.* Triton X-100, Triton X-114, Igepal CA 630, CHAPS, n-dodecyl-β-D-maltoside, Zwittergent 3–12 and Zwittergent 3–14 extracted similar amounts Rac1 from the membrane fraction at 0.5 and 1% concentrations (see supernatant fractions S1 in Fig. 1B, upper panel). In contrast, higher concentrations (1%) of cholate, n-octyl-β-D-glucopyranoside, n-nonyl-β-D-glucopyranoside, n-octyl-β-D-thioglucopyranoside, Zwittergent 3–10 and Zwittergent 3–16 were required to quantitatively extract Rac1 (Fig. 1B, upper panel). Tween 20, n-hexyl-β-D-glucopyranoside, n-heptyl-β-D-glucopyranoside and Zwittergent 3-08 were not useful at any concentrations (see pellet fractions P1 in Fig. 1B, upper panel).

After Rac1 was solubilized into the S1 fractions, purified GST fusion protein GST-GDI1 was employed to assess the functionality of soluble Rac1 in pull-down (PD) experiments, since only prenylated and GDP-bound Rac1 proteins are useful to study the RhoGDI interaction. From the seven detergents described above, CHAPS at 0.5% revealed the best property in extracting Rac1 from the insect cell membrane in its native, GDP-bound state (see P2 in Fig. 1B, lower panel). Almost all Rac1 proteins from the supernatant 1 (S1) were pulled down. In contrast, considerable amounts of Rac1 extracted by the other six detergents (Triton X-100, Triton X-114, Igepal CA 630, n-dodecyl-β-D-maltoside, Zwittergent 3–12 and Zwittergent 3–14) remained in the S2 fraction indicating that these Rac1 proteins are nucleotide-depleted or in incorrect conformation and thus inactive in binding to GST-GDI1 (Fig. 1B, lower panel).

Taken together, CHAPS displayed the two criteria required for further studies, namely to quantitatively solubilize Rac1 from insect cell membranes and to fully retain the GDI-binding activity of Rac1. Accordingly, 0.5% CHAPS was used to extract Rac1 from the membrane before successively applying the protein solution on two chromatography columns (Ni-NTA and size exclusion, respectively), in order to purify human Rac1 from insect cells (called from now $Rac1^{Ic}$) at high quantities. Mass spectrometric analysis of intact $Rac1^{Ic}$, compared to human Rac1 full length purified from *E. coli* ($Rac1^{Ec}$), revealed a fully modified protein by geranylgeranylation with a modified most likely phosphorylated population (Fig. S2 in File S1).

Human Rac1 purified from insect cells associates with liposomes

To analyze the membrane-binding properties of $Rac1^{Ic}$ synthetic liposomes were prepared and sedimentation experiments were conducted according to the workflow illustrated in Figure S3A in File S1. To setup $Rac1^{Ic}$ sedimentation by the liposomes various conditions were tested and optimized. One aspect was the incubation time after mixing $Rac1^{Ic}$ with liposomes. Under the given conditions a weak binding of $Rac1^{Ic}$ to the liposomes was observed, which was not significantly changed with increasing incubation time (Fig. S3B in File S1). We next analyzed the sedimentation force to avoid disruption of $Rac1^{Ic}$-liposome interactions by incubating the samples for 30 min and using different centrifugation speeds to spin down the liposomes. Figure S3C in File S1 shows that increasing sedimentation force from 20,000x*g* to 60,000x*g* led to dissociation of $Rac1^{Ic}$ from the liposomes suggesting that the sedimentation force should not exceed 20,000x*g*. In the next step we varied the ratio of Rac1 (1.5 µg) and liposomes (10 to 60 µl), and found out that as lower the ratio of $Rac1^{Ic}$ to liposome is as larger are the $Rac1^{Ic}$ amounts associated with the liposomes (Fig. S3D in File S1). The data clearly indicate that mixing of 1.5 µg $Rac1^{Ic}$ with 20 µl liposomes for 20 min and centrifuging the sample at 20,000x*g* for 30 min provides optimal conditions for $Rac1^{Ic}$ sedimentation with liposomes, which are used in following experiments.

The question of whether the lipid compositions of the liposomes may affect the liposome association of $Rac1^{Ic}$ was next addressed using the optimized conditions described above. Data shown in Figure S3E in File S1 reveal that $Rac1^{Ic}$-liposome interaction was only marginally affected upon depletion of the liposomes by individual phospholipids, especially PS and PIP2, by comparing the amounts of $Rac1^{Ic}$ in the supernatants. As a control, we used $Rac1^{Ec}$, which does not bind to the liposomes at all (Fig. S3E in File S1). Taken together, our data clearly demonstrate that $Rac1^{Ic}$ is a lipidated protein and fulfills all criteria for the subsequent *in vitro* liposome reconstitution analysis.

GDI1 interacts with and extracts $Rac1^{Ic}$ from liposomes

GDI1 is reported to solubilize Rac1 in living cells and inhibit GDP dissociation from Rac1 [23], for which a C-terminal geranylgeranylation of Rac1 is required [48]. Therefore, we examined the properties of $Rac1^{Ic}$ interaction with liposomes and GDI1 by combining liposome sedimentation and GST-GDI1 pull-down assays. As controls, $Rac1^{Ec}$ was used. In addition, we prepared also inactive GDP-bound and stable active GppNHp-bound forms of the Rac1 proteins. GppNHp is a non-hydrolysable analogue of GTP. As shown in Figure 2A, GST-GDI1 pulled down only $Rac1^{Ic}$ but neither $Rac1^{Ec}$. Data obtained from the immunoblotting analysis of the supernatant and pellet fractions after liposome sedimentation showed that equal amounts of $Rac1^{Ic}$ in GDP-bound and GppNHp-bound states were associated with the liposomes (Fig. 2B). Under these conditions, we did not observe any liposome binding of $Rac1^{Ec}$. Association of $Rac1^{Ic}$, but not $Rac1^{Ec}$, with both GDI1 and liposomes clearly support the mass spectrometric data and proved that human Rac1 purified from insect cells is posttranslationally modified by geranylgeranylation.

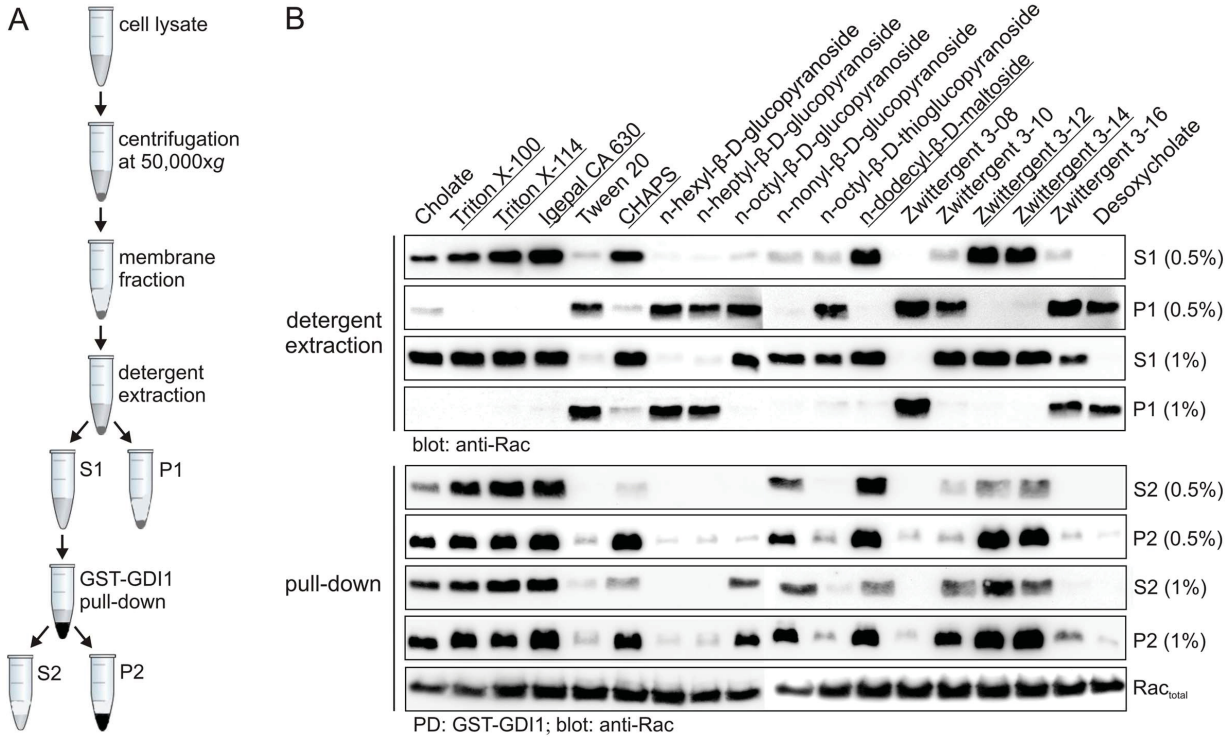

Figure 1. Detergent screening for optimal extraction of GDP-bound Rac1 from the insect cell membrane. (**A**) Schematic workflow for the isolation of insect cell membrane fraction, detergent extraction and pull-down assay using GST-GDI1. (**B**) Effects of eighteen various detergents on Rac1 extraction from the membrane fraction of insect cells (upper panel) and inspection of Rac1 prenylation *via* pull-down with GST-GDI1 (lower panel). Membrane fractions mixed with two different concentrations (0.5% and 1%) of the respective detergents (Table S1 in File S1) were incubated at room temperature for 30 min, separated in supernatants (S1) and pellets (P1) by centrifugation and immunoblotted using anti-Rac1 antibody. The Supernatants S1 were used in pull-down assays (PD) by using GST-GDI1, which selectively binds to the intact, nucleotide-bound Rac1. Resulted pellets (P2, corresponding to the GSH beads) and supernatant (S2) were visualized by anti-Rac1 antibody in immunoblots. Underlined detergents, especially CHAPS, showed the best properties in the extraction of GDP-bound Rac1 from the insect cell membranes.
doi:10.1371/journal.pone.0102425.g001

GDI1 is known to extract inactive, GDP-bound Rho GTPases, such as Rac1, from membranes and hold them in a complex in the cytosol away from their sites of action at membranes [16,23,49,50]. To test this issue on liposomes *in vitro* in more detail, we performed two types of experiments. In the first approach, liposomes, GDI1 and Rac proteins were mixed together and incubated for 20 min at room temperature. Subsequently, the samples were centrifuged at 20,000x*g* for 30 min, and the respective supernatants and liposome pellets were immunoblotted using an anti-Rac antibody. The majority of the Rac1^{Ic} proteins remained in the supernatant most likely in complex with GDI1 regardless of the nature of the bound nucleotide (Fig. 2C). Only a trace amount of Rac1^{Ic} protein, especially the GppNHp-bound form, was found in the liposome fraction. These data shows that GDI1 dominantly competes with the liposomes in binding Rac1^{Ic}. In the second approach, we firstly prepared Rac1^{Ic}-bound liposomes under the same condition as in the previous experiment but in the absence of GDI1, then mixed the sample with GDI1 and performed the liposome sedimentation experiment again. Figure 2D shows that GDI1 is able to extract Rac1^{Ic} from liposomes preferentially in the GDP-bound from. To further prove this observation we repeated these experiments using increasing concentrations of GDI1 of 2- to 20-fold molar excess above Rac1^{Ic}, associated with liposomes. A 2-fold excess of GDI1 was sufficient to displace all "extractable" GDP-bound Rac1^{Ic} from the liposomes (Fig. 2E). In contrast, about 10-fold larger amounts of GDI1 were required to extract Rac1^{Ic}-GppNHp from the liposomes (Figs. 2E). Taken together, our result clearly demonstrates that the majority of the membrane-bound Rac1 protein is extracted by GDI1 and remains GDI1 associated.

Rac1^{Ic} activation counteracts its extraction from the liposomes by GDI1

We have shown above that GDI1 also binds Rac1^{Ic}-GppNHp and extracts it from the liposomes (Fig. 2). To examine the interrelationship of this interaction, we conducted a series of liposome sedimentation experiments in the presence of the GTPase-binding domain (GBD) of Pak1 (called here Pak1). Mixing the Rac1^{Ic} proteins with liposomes, GDI1 and Pak1, respectively, revealed that Pak1 did neither influence the association of the GDP-bound Rac1^{Ic} proteins with the liposomes nor with GDI1 (Fig. 3A, lane 5). This data were comparable to the conditions when GDI1 was present and Pak1 absent (Fig. 2C, lane1). In contrast, Pak1 strongly counteracted a GDI1-mediated displacement of GppNHp-bound Rac1^{Ic} from the liposomes (Fig. 2C, lane2 and Fig. 3A, lane 6). In the next experiments we used liposome-associated Rac1^{Ic} proteins and showed that GDI1 extracted Rac1^{Ic} in both nucleotide-bound states from the liposomes in the absence of Pak1 (Fig. 3B, lane 1 and 2). Addition of Pak1 efficiently blocked GDI1-driven Rac1 extraction of GppNHp-bound Rac1^{Ic} from the liposomes (Fig. 3B, lane 4) but not that of the GDP-bound Rac1^{Ic} (Fig. 3B, lane 3). In agreement with the structural data [3,28,51,52], our results suggest that Pak1

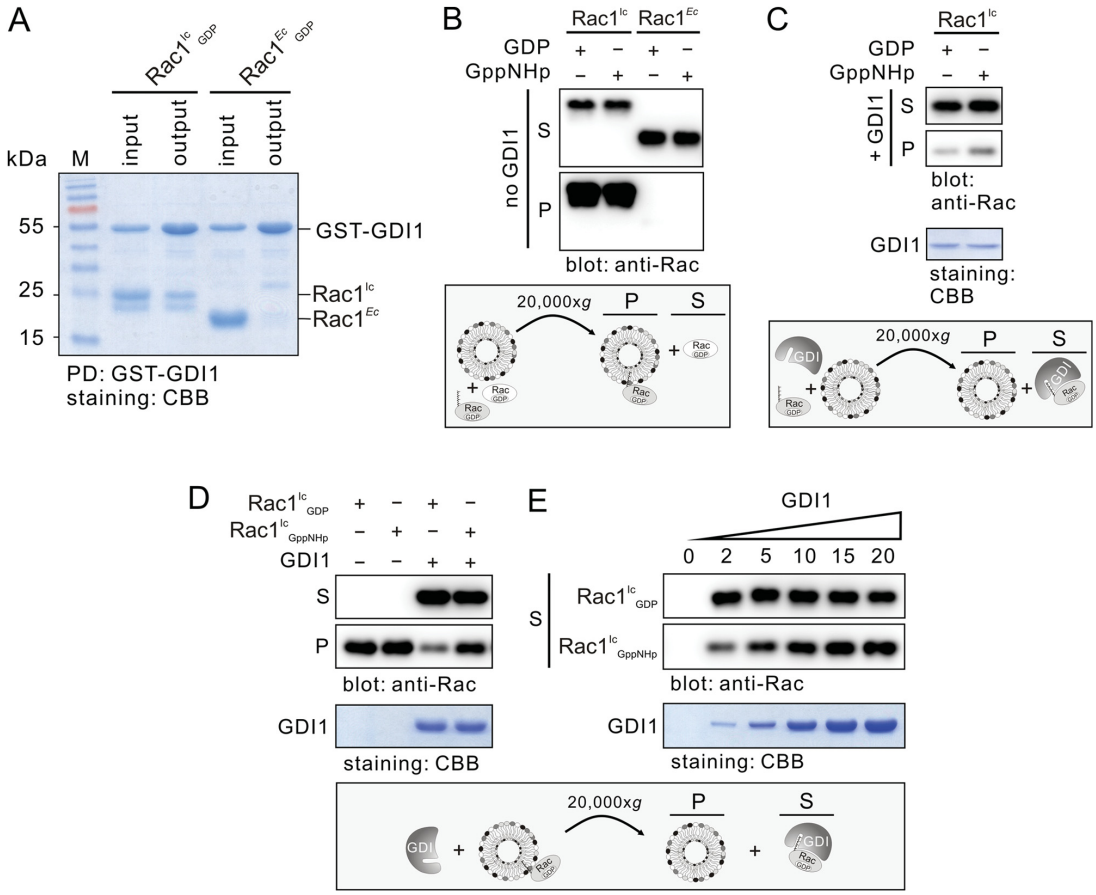

Figure 2. Nucleotide-independent extraction of Rac1^{Ic} from the liposomes by GDI1. (**A**) GST-GDI1 pull-down of Rac1^{Ic} but not of Rac1^{Ec}. Input is the total mixture of beads and proteins, and output is the pull-down (PD). (**B**) Liposome binding of Rac1^{Ic} but not of Rac1^{Ec}. In the liposome sedimentation assay, Rac1^{Ic} efficiently binds to liposomes in the absence of GDI1 and independent of whether it was loaded with GDP or GppNHp, a non-hydrolysable GTP analog. Rac1^{Ec} failed to bind to liposomes under the same conditions. (**C**) Preferential binding Rac1^{Ic} to GDI1 than to liposomes. GDI1 binds to both GDP-bound and GppNHp-bound Rac1^{Ic} proteins and prevents their association with the liposomes. (**D**, **E**) GDI1 efficiently extracted GDP-bound Rac1^{Ic} from the liposomes and to a lower extend also Rac1^{Ic}-GppNHp. Same amount of GDP-bound and GppNHp-bound forms of Rac1^{Ic} associated with the liposomes were prepared before incubation with 5-fold molar excess of GDI1 and sedimentation at 20,000x*g* (**D**). Using increasing molar excess of GDI1 (2-, 5-, 10-, 15- and 20-fold) showed that higher concentrations of GDI1 are required to extract Rac1^{Ic}-GppNHp from the liposomes to supernatants in comparison to Rac1^{Ic}-GDP (**E**). CBB, coomassie brilliant blue; *Ec*, *E. coli*; Ic, insect cells; P, liposome pellet; S, supernatant.
doi:10.1371/journal.pone.0102425.g002

binding to the switch regions of active Rac1 competitively blocks the GDI1 association with the same regions of Rac1.

We next set out to analyze Rac1^{Ic} activation on the liposomes in the presence and in the absence of Pak1 and GDI1. We first prepared GDP-bound Rac1^{Ic} associated with liposomes, which were then incubated with free GppNHp and the DHPH domains of the RacGEF Tiam1 to accelerate the nucleotide exchange of Rac1^{Ic}, leading to membrane bound Rac1^{Ic}-GppNHp. GST-DHPH of Tiam1 as a minimal RacGEF protein contains the catalytic (Dbl homology or DH) and the lipid membrane binding (pleckstrin homology or PH) domains. GST-Pak1 was mixed in the samples as a marker for activated Rac1^{Ic} as it selectively binds to the active, GppNHp-bound state of Rac1 [53]. After incubation, the mixture was spun down and GST fusion in the pellet was visualized by immunobloting using anti-GST antibody. Results shown in Figure 3C revealed that Pak1 could be detected predominatantly in the liposome pellet only when both Tiam1 and GppNHp were present. In addition, DHPH was also detected in the pellet fraction. These data clearly indicate that Tiam1 DHPH was able to activate Rac1^{Ic} on the liposomes.

The next question we addressed was the ratio of soluble and liposome-bound Rac1 in the presence of GDI1, the RacGEF Tiam1 and the Rac effector Pak1. The majority of GDP-bound Rac1 appeared in complex with GDI1 (Fig. 3D, lane 1) indicating again that GDI1 efficiently extract Rac1^{Ic} from the liposomes. The picture slightly changed when the experiment was repeated also in the presence of Pak1 and GppNHp (Fig. 3D, lane 2) or Pak1 and Tiam1 (Fig. 3D, lane 3). There was, however, a significant limitation of the GDI-mediated Rac1 extraction from the liposomes observable when all components were in the sample (Fig. 3D, lane 4). This clearly demonstrates that a Tiam1-mediated exchange of the bound GDP for GppNHp resulted in the Rac1^{Ic}-GppNHp-Pak1 complex formation on the liposomes as shown by Pak1 blotting (Fig. 3D, lane 4). This significantly blocked GDI1 association with and extraction of Rac1^{Ic} from the liposomes. This result suggests that Rac1 activation by Tiam1 largely counteracted

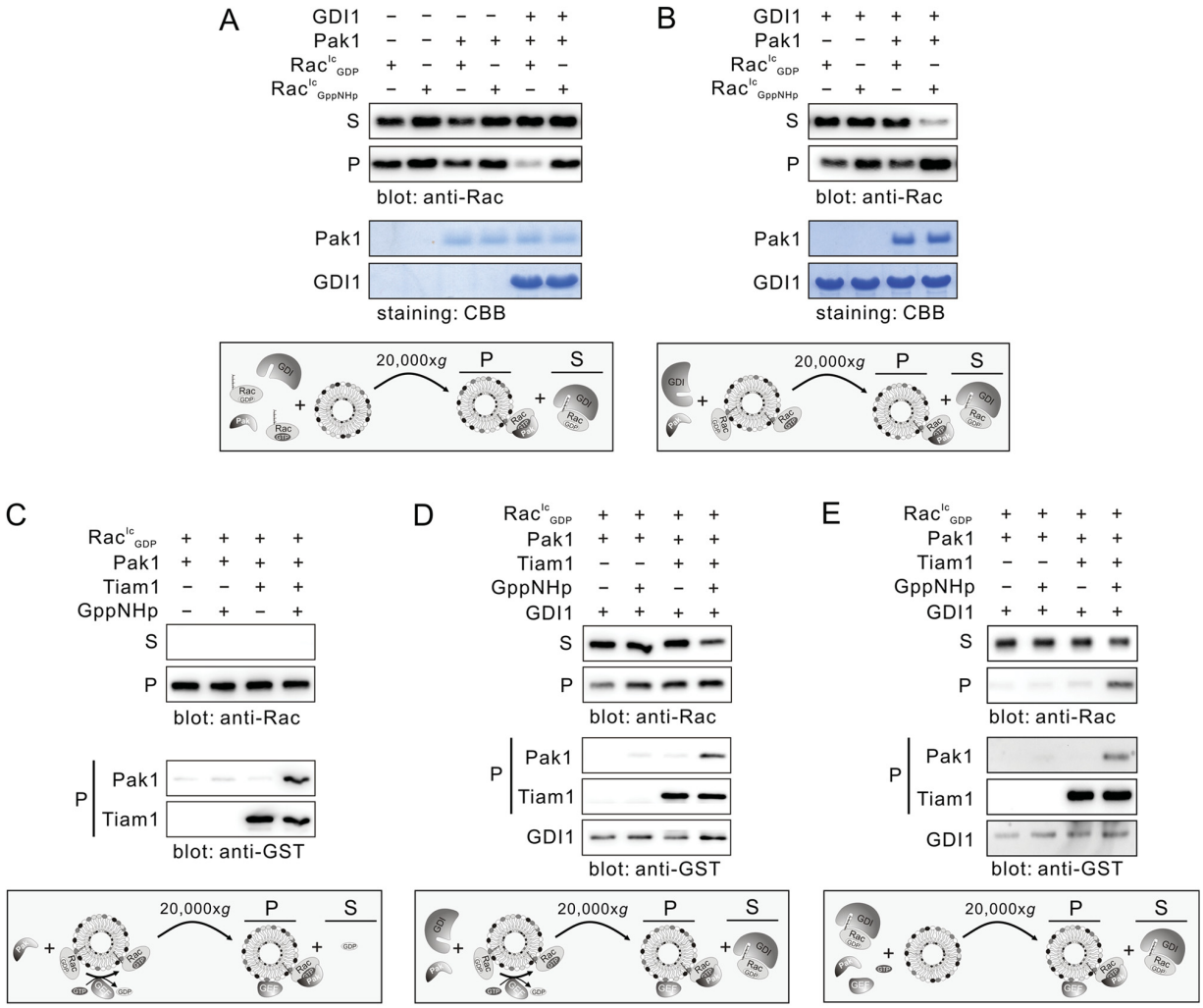

Figure 3. Pak1 binding to activated Rac1^{lc} counteracting its extraction from the liposomes by GDI1. (**A**) Pak1 interferes with GDI1 binding to GppNHp-bound Rac1^{lc} and potentiates Rac1^{lc}-GppNHp association with the liposomes. An excess amount of 20-fold of Pak1 was used in liposome sedimentation assay. (**B**) Competitive inhibition of the GDI1-mediated Rac1^{lc}-GppNHp extraction from the liposomes by Pak1. (**C**) Tiam1-mediated Rac1^{lc} activation on the liposomes. Liposome-bound Rac1^{lc}-GDP was incubated with Pak1 in the presence or absence of Tiam1-DHPH and an excess of GppNHp. Rac1^{lc} activation on liposome was evaluated by detecting Pak1 in the pellet, which is bound to Tiam1-activated Rac1^{lc}. (**D**) Tiam1-mediated Rac1^{lc} activation on the liposomes in the presence of GDI1. (**E**) Partial displacement from the GDI1 complex, activation by Tiam1 and association of Rac1^{lc} with liposomes and Pak1. CBB, coomassie brilliant blue; *Ec*, *E. coli*; Ic, insect cells; P, liposome pellet; S, supernatant.
doi:10.1371/journal.pone.0102425.g003

the extraction of Rac1 from the liposomes by RhoGDI and shifts Rac1 towards a signaling-competent state.

However, the scenario substantially changes when Rac1^{lc}-GDP was not liposome-bound, like in the previous experiments, but in the complex with GDI (Fig. 3E). Under this condition, the presence of Tiam1, GppNHp and Pak1 was required to significantly release Rac1^{lc}-GDP from its GDI complex, to catalyze the nucleotide exchange by Tiam1 and to generate a liposome-bound Rac1^{lc}-GppNHp-Pak1 complex. This result clearly indicate that Tiam1 and Pak1 are certainly able to quantitatively displace the Rac1-GDP-GDI complex.

Rac1^{lc} activation by liposome-associating RacGEFs

The RhoGEFs of the Dbl family have been commonly implicated as lipid membrane binding modules [54]. The experiments described above have shown that Tiam1 DHPH activates liposome-bound Rac1, which can be atributed to the lipid membrane-binding PH domain [27,55,56]. Recently, we have shown that in addition to Tiam1 also Vav2, P-Rex1, Dbl, and TrioN are Rac1-specific GEFs [11]. These experiments have been performed under cell-free conditions in the absence of liposomes using nonprenylated Rac1 protein. Prior to the analysis of these Dbl proteins towards Rac1^{lc}, we analyzed their liposome-binding properties using the respective GST-DHPH proteins expressed and purified from *E. coli*. Therefore, we used four different types of liposomes, synthetic liposomes comprising in addition to PS, PC, PE and SM, either PIP2 (Lipo^{+PIP2}) or PIP3 (Lipo^{+PIP3}), as well liposomes derived from bovine brain type I and III Folch membrane lipids (see Materials and Methods). Figure 4A shows different liposome-binding capabilities of the five different Dbl proteins. Vav2, Dbl and P-Rex1 differently bound to all types of liposomes. TrioN and Tiam1 were hardly detected in Lipo^{+PIP2} but differently bound to the other liposomes. Interestingly, Tiam1 tightly bound to Folch III liposomes.

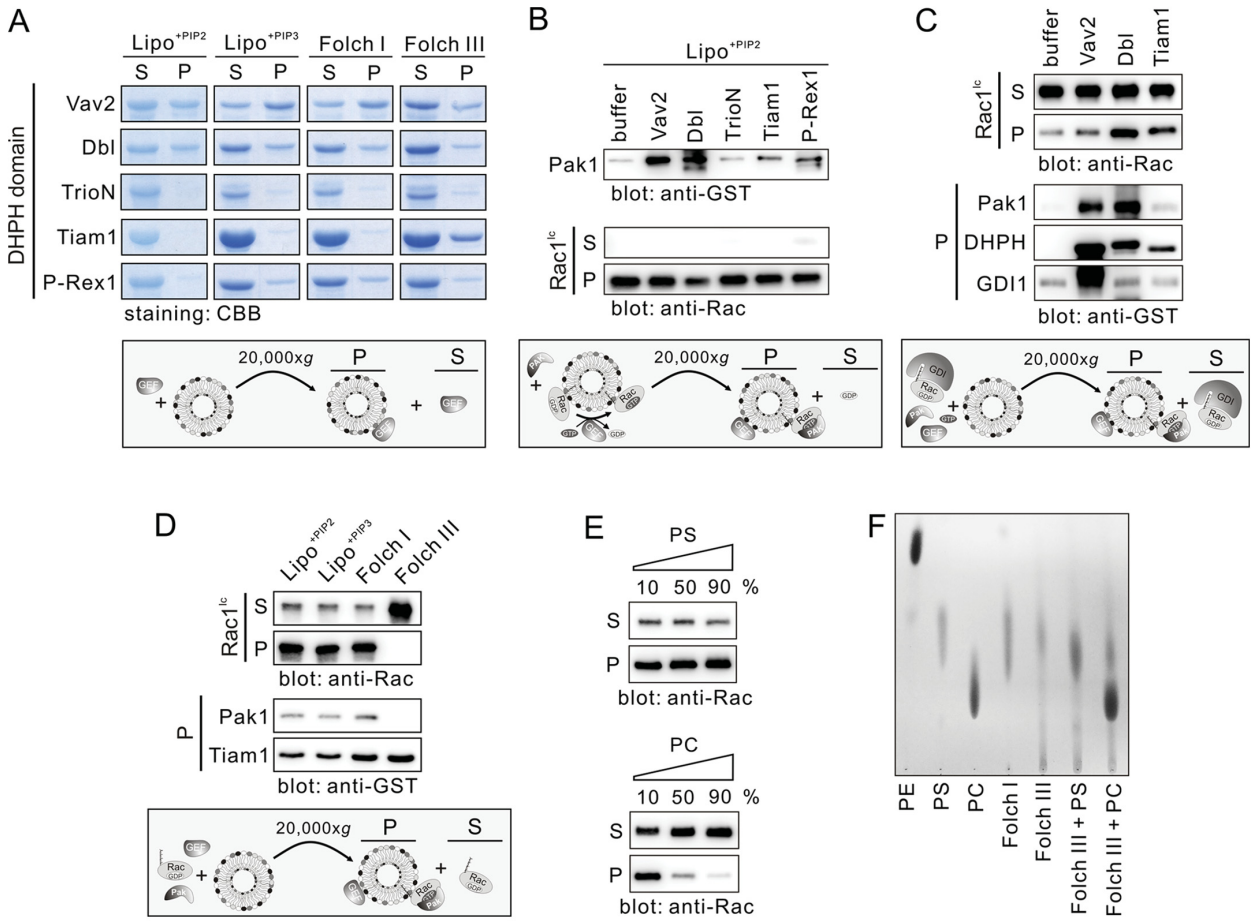

Figure 4. Rac1^{Ic} activation on liposomes by different Dbl family proteins and association with Pak1. (**A**) Differential binding of Vav2, Dbl, TrioN, Tiam1 and P-Rex1 to various liposomes. Lipo^{+PIP2} is composed of PE, PC, PS, SM and PIP2. In Lipo^{+PIP3}, PIP2 is replaced by PIP3. (**B**) Efficient Rac1 activation by Dbl and Vav2 on Lipo^{+PIP2}. (**C**) Displacement from the GDI1 complex, activation by GEFs and association of Rac1^{Ic} with liposomes and Pak1. (**D**) Tiam1 but not Rac1^{Ic} binding to Folch III. Rac1GDP, Pak1, Tiam1, GppNHp and different liposomes were preincubated, afterwards the liposome sedimentation assay was conducted. Rac1, PAKα and Tiam1 from the liposome pellet were detected by GST antibody. (**E**) Rac1^{Ic} repulsion by PC but not PS. Liposomes (PS and PE or PC and PE) at increasing amounts of PS and PC were sedimented after incubation with Rac1^{Ic}. (F) Thin layer chromatography of Folch I and Folch III liposomes. Relative lipid content of Folch I and Folch III liposomes was analyzed by thin layer chromatography. PE, PS and PC as well as Folch III containing PS and PS were used as controls. CBB, coomassie brilliant blue; *Ec*, *E. coli*; Ic, insect cells; P, liposome pellet; S, supernatant.
doi:10.1371/journal.pone.0102425.g004

The capacity of the five Rac-specific Dbl proteins in the Rac1^{Ic} activation on the Lipo^{+PIP2} was next determined under the same conditions as described above (Figs. 3C and 3D). Consistent with their liposome binding pattern Vav2 and Dbl revealed the highest RacGEF activities shown as largest amount of Pak1 sedimented with activated, GppNHp-bound Rac1^{Ic} (Fig. 4B). P-Rex1, Tiam1 and TrioN activated Rac1^{Ic} to a lower extent (Fig. 4B), particularly TrioN, corresponding to their liposome binding capabilities (Fig. 4A). These data suggest that as stronger the respective Dbl protein interact with the liposomes as higher is its accessibility to Rac1. We next examined the capability of Vav2 and Dbl in displacing and activating Rac1^{Ic} from its complex with GDI1. Therefore, we mixed Rac1^{Ic}-GDP-GDI1 with PIP2-containing liposomes, Pak1, GppNHp and the DHPH domains of Vav2, Dbl or Tiam1, respectively, and conducted liposome sedimentation. Dbl DHPH displaced and activated Rac1^{Ic} most efficiently as compared to Tiam1 and Vav2, which is visualized by a significant amount of Rac1^{Ic}-GppNHp-Pak1 complex on the liposomes (Fig. 4C). Unexpectedly, this observation was not confirmed for Vav2, although a considerable amount of DHPH and Pak1 was sedimented with the liposomes (Fig. 4C). This result suggests that Dbl and Tiam1, but however not Vav2, contribute to displacement of Rac1 from the GDI complex by shifting the reaction towards active, GTP-bound Rac1 that is prepared for effector interaction and thus downstream signaling.

Tight Tiam1-binding to Folch III liposomes (Fig. 4A) prompted us to determine Tiam1 GEF activity on all four types of liposomes as we expected by far the highest Rac1^{Ic} activation on Folch III liposomes. Suprisingly, we obtained contrary results. In contrast to the other liposomes, on which Rac1^{Ic} was modestly activated by Tiam1, Folch III did not bind Rac1^{Ic} at all (Fig. 4D). As a consequence, Pak1 sedimentation could not be detected, although Tiam1 was presented on the Folch III liposomes (Fig. 4D). Folch III has been described to contain mainly PS (80%), and minor contents of PE (10%), cerebrosides (5%), and other unidentified membrane lipids (5%) [46]. In fact, we expected Rac1^{Ic}, due to the positive electrostatics, immediately upstream of the prenylated cysteine 189 at its very C-terminus (^{183}KKRKRKCLLL^{192}), to

bind tightly to the abundant, negatively charged PS moiety present in Folch III. However, synthetic liposomes and liposomes composed of Folch I also contain 50% PS (see Materials and Methods). Thus, we tested the effect of increasing PS concentrations in synthetic liposomes on the $Rac1^{Ic}$ binding and used PC as a control. Interestingly, not increasing PS concentrations but PC repelled $Rac1^{Ic}$ from associating with the liposomes (Fig. 4E) clearly supporting the existence of both an electrostatic attraction in the effective potential between $Rac1^{Ic}$ and PS-containing liposomes and an electrostatic repulsion in the case of PC-containing liposomes. These data also suggest that Folch III may contain a different material that repel $Rac1^{Ic}$ from the liposomes, which cannot be PS. Therefore, we analyzed the content of our liposomes by conducting a thin layer chromatography. Data shown in Figure 4F revealed Folch III indeed contains PS and not PC. There is a trace of lipids that are less polar than PS, which may be the cause for the $Rac1^{Ic}$ repulsion. These data strongly suggest that Rac1 association with the membranes depends in addition to isoprenylation and accessory proteins also on local lipid composition.

Discussion

The cell membrane is a platform for signal transduction through transmembrane receptors and membrane-associated proteins, including heterotrimeric G proteins and small GTPases of the Ras superfamily. These proteins are essentially dependent on posttranslational modifications by isoprenylation, palmitoylation or myristoylation to achieve their function [57,58,59]. In addition to studies of structural and chemical aspects of the individual proteins and components of signaling pathways, the new challenge is to investigate the influence of the lipid membrane surface environment on the temporal and spatial regulation of signaling events. One approach is the *in vitro* liposome reconstitution using purified proteins and synthetic liposomes. To this end prenylated GTPases are purified from tissues, eukaryotic cells, such as yeast, or they are synthesized by chemical ligation of unmodified GTPases from *E. coli* with a synthetic peptide harboring an isoprenyl moiety [36]. In this study, we used the baculovirus-insect cell expression system to express and purify recombinant human Rac1 in a prenylated form. This system has the advantage to express recombinant genes from any origin and produce considerable amounts of modified proteins [60]. Purification of postranslationally modified GTPases, such as prenylated Rac1, is challenging in a way that its native, nucelotide-bound form needs to be maintained if extracted from the cell membranes. In a comprehensive detergent screen we found that some detergents, *e.g.* CHAPS, quantitatively extracted human Rac1-GDP from the insect cell membranes as monitored by a RhoGDI pull-down assay. Mass spectrometry, liposome- and RhoGDI-binding revealed that human Rac1 purified form insect cells is, in contrast to that purified from *E. coli*, posttranslationally modified.

Similar to our data, GDI1 has been reported previously to bind to and extract both nucleotide-bound forms of Cdc42 from plasma membranes *in vitro* [23,24]. Robbe and colleagues have shown that purified GDP-bound Rac1 from insect cells was dissociated from its complex with RhoGDI and associated with liposomes when the bound GDP was exchanged for GTP by depleting the bound Mg^{2+} by EDTA treatment [27]. Fewer studies were conducted by using prenylated Rac1 protein alone to elucidate its interaction with GDI1 and the liposomes: It has been shown that Rac1 purified from insect cell membrane fractions interact with artificial phagocyte membranes and that GDI1 counteracted this process [61]. This regulatory process is visualized in the present study in a direct way. We showed that GDI1 preferentially associates with the inactive, GDP-bound Rac1 and displaces it from the membrane as reported previously [50]. In addition, we found that a displacement of the active Rac1-GppNHp is also possible in spite of its low affinity for the GDI1. However, this does not take place if a Rac1 effector is in the proximity, as we showed for PAK1.

We have shown above that GDI1 also binds Rac1-GppNHp, consistent with early reports [62], and extracts it from the liposomes, although not as efficiently as Rac1-GDP (Fig. 2). One reason is that only a few residues of the four regions on Rac1 (amino acids or aa 29–42 of switch I, aa 62–68 of switch II, aa 91–108 of α-helix 3 and aa 187–189 at the C-terminus), which are in direct contact with GDI [3], determine the specificity of the interaction of Rac-GDP with GDI [28,63]. Interestingly, conserved residues, such as Val36 and Asp38 of switch I, and Arg68, Tyr66, Leu69 and Leu72 of switch II, do not only contribute to the interaction with the GDI, but also to the interaction with GAPs and effectors. Under this environmental condition on the surface of the plasma membrane GDI does probably not undergo any interaction with Rac1-GTP because it, as long as it is not switched off by GAPs, may preferentially exist in complex with various signal-transducing effectors, such as Pak1 [18,20,64]. This is exactly what we observed in this study when we mixed Rac1-GppNHp bound to liposomes with both GDI1 and Pak1. The latter binds Rac1 and blocks both, the accessibility of GDI1 and consequently Rac1-GppNHp extraction from the liposomes (Fig. 3B). As a downstream effector of Rac1, Pak1 and its GBD specifically and tightly bind to activated Rac1 [53,65,66,67]. Based on these findings, we can propose that RhoGDIs may also displace GTP-bound Rho GTPases from the plasma membrane presuming there are no Rac-specific effectors or GAPs around.

Another issue to be discussed is the interrelationship between GDIs and GEFs in regulating members of the Rho family. Unlike three known human RhoGDIs [15,16], the classical Dbl GEF family consists of 74 members in human [11]. They are characterized by a unique, catalytic DH domain often preceded by a pleckstrin homology (PH) domain indicating an essential and conserved function [11,12,54]. The PH domain has been implicated to serve multiple roles in signaling events anchoring GEFs to the membrane (*e.g. via* phosphoinositides) [54] and directing them towards their interacting GTPases which are already localized to the membrane [12]. In this regard, it is important to note that the bulk of the added GEFs remained in the soluble fraction in the presence of liposomes (Fig. 4A), which most likely is, except for Vav2 and Dbl, due to low binding affinity of the tandem PH domain for the lipid membrane. This clearly suggests that the GEF recruitment to the cell membrane underlays additional concerted mechanisms. One is that accessory binding domains, existing in some GEFs, may be necessary to promote membrane association. This includes an extra PH domain, e.g. in Tiam1 [68], a diacylglycerol binding C1 (protein kinase C conserved region 1) domain, e.g. in Vav proteins [69], or a Sec14 domain, *e.g.* in Dbl [70]. The other membrane-translocating mechanism involves adaptor proteins, such the G protein βγ subunits recruiting P-Rex1 [71] or the Arp2/3 complex recruiting Tiam1 [72,73].

Moreover, we found that dissociation of Rac1-GDP from its complex with GDI1 strongly correlated with two distinct activities of the DHPH of especially Dbl and Tiam1, including PH-mediated association with liposomes and DH-mediated GDP/GppNHp exchange of Rac1 (Figs. 3E and 4C). This and the fact that the binding affinity of the DH domain for the GDP-bound Rho GTPase is in the lower micromolar range (Z. Guo, E. Amin,

R. Dvorsky and M.R. Ahmadian, unpublished data) indicates that the Rho GTPase-GDI complex may not be as tight as it has been suggested previousely [17,24]. However, future investigations will elucidate the displacement of Rac1 from the GDI complex in the presence of liposomes and RacGEFs, both of which participate in the mechanism of specific activation of Rac1 and are required for accurate downstream signaling. This study has just opened a new window into future mechanistic studies of Rac1 regulation and signaling.

Supporting Information

File S1 Contains Table S1, Detergents used in this study. Supporting References to Table S1. Figure S1, Expression of human Rac1 in insect cells. Figure S2, Mass spectra of $Rac1^{Ec}$ (left panel) and $Rac1^{Ic}$ (right panel) after deconvolution. Figure S3, Liposome preparation and sedimentation experiments using human $Rac1^{Ic}$.
(PDF)

Acknowledgments

We thank R. Piekorz, J. Scheller, and the members of the Institute of Biochemistry & Molecular Biology II for discussions and support.

Author Contributions

Conceived and designed the experiments: SCZ LG HH MRA. Performed the experiments: SCZ LG PJ AS EK. Analyzed the data: SCZ LG PJ EK MRA. Contributed reagents/materials/analysis tools: SCZ LG HH PJ AK ICC EK BN MRA. Contributed to the writing of the manuscript: SCZ MRA.

References

1. Hall A (2012) Rho family GTPases. Biochem Soc Trans 40: 1378–1382.
2. Wennerberg K, Der CJ (2004) Rho-family GTPases: it's not only Rac and Rho (and I like it). J Cell Sci 117: 1301–1312.
3. Dvorsky R, Ahmadian MR (2004) Always look on the bright site of Rho: structural implications for a conserved intermolecular interface. Embo Rep 5: 1130–1136.
4. Lam BD, Hordijk PL (2013) The Rac1 hypervariable region in targeting and signaling: a tail of many stories. Small GTPases 4: 78–89.
5. Philips MR, Cox AD (2007) Geranylgeranyltransferase I as a target for anti-cancer drugs. J Clin Invest 117: 1223–1225.
6. Roberts PJ, Mitin N, Keller PJ, Chenette EJ, Madigan JP, et al. (2008) Rho Family GTPase modification and dependence on CAAX motif-signaled posttranslational modification. J Biol Chem 283: 25150–25163.
7. van Hennik PB, ten Klooster JP, Halstead JR, Voermans C, Anthony EC, et al. (2003) The C-terminal domain of Rac1 contains two motifs that control targeting and signaling specificity. J Biol Chem 278: 39166–39175.
8. Chae YC, Kim JH, Kim KL, Kim HW, Lee HY, et al. (2008) Phospholipase D activity regulates integrin-mediated cell spreading and migration by inducing GTP-Rac translocation to the plasma membrane. Mol Biol Cell 19: 3111–3123.
9. Navarro-Lerida I, Sanchez-Perales S, Calvo M, Rentero C, Zheng Y, et al. (2012) A palmitoylation switch mechanism regulates Rac1 function and membrane organization. EMBO J 31: 534–551.
10. Jaiswal M, Fansa EK, Dvorsky R, Ahmadian MR (2013) New insight into the molecular switch mechanism of human Rho family proteins: shifting a paradigm. Biol Chem 394: 89–95.
11. Jaiswal M, Dvorsky R, Ahmadian MR (2013) Deciphering the molecular and functional basis of Dbl family proteins: a novel systematic approach toward classification of selective activation of the Rho family proteins. J Biol Chem 288: 4486–4500.
12. Rossman KL, Der CJ, Sondek J (2005) GEF means go: turning on RHO GTPases with guanine nucleotide-exchange factors. Nat Rev Mol Cell Biol 6: 167–180.
13. Tcherkezian J, Lamarche-Vane N (2007) Current knowledge of the large RhoGAP family of proteins. Biol Cell 99: 67–86.
14. Jaiswal M, Dvorsky R, Amin E, Risse SL, Fansa EK, et al. (2014) Functional crosstalk between Ras and Rho pathways: p120RasGAP competitively inhibits the RhoGAP activity of Deleted in Liver Cancer (DLC) tumor suppressors by masking its catalytic arginine finger. J Biol Chem 289: 6839–6849
15. DerMardirossian C, Bokoch GM (2005) GDIs: central regulatory molecules in Rho GTPase activation. Trends Cell Biol 15: 356–363.
16. Garcia-Mata R, Boulter E, Burridge K (2011) The 'invisible hand': regulation of RHO GTPases by RHOGDIs. Nat Rev Mol Cell Biol 12: 493–504.
17. Tnimov Z, Guo Z, Gambin Y, Nguyen UT, Wu YW, et al. (2012) Quantitative analysis of prenylated RhoA interaction with its chaperone, RhoGDI. J Biol Chem 287: 26549–26562.
18. Bishop AL, Hall A (2000) Rho GTPases and their effector proteins. Biochem J 348 Pt 2: 241–255.
19. Burridge K, Wennerberg K (2004) Rho and Rac take center stage. Cell 116: 167–179.
20. Parrini MC, Matsuda M, de Gunzburg J (2005) Spatiotemporal regulation of the Pak1 kinase. Biochem Soc Trans 33: 646–648.
21. Etienne-Manneville S, Hall A (2002) Rho GTPases in cell biology. Nature 420: 629–635.
22. Heasman SJ, Ridley AJ (2008) Mammalian Rho GTPases: new insights into their functions from in vivo studies. Nat Rev Mol Cell Biol 9: 690–701.
23. Leonard D, Hart MJ, Platko JV, Eva A, Henzel W, et al. (1992) The identification and characterization of a GDP-dissociation inhibitor (GDI) for the CDC42Hs protein. J Biol Chem 267: 22860–22868.
24. Nomanbhoy TK, Erikson JW, Cerione RA (1999) Kinetics of Cdc42 membrane extraction by Rho-GDI monitored by real-time fluorescence resonance energy transfer. Biochemistry 38: 1744–1750.
25. Fuchs A, Dagher MC, Jouan A, Vignais PV (1994) Activation of the O2(-)-generating NADPH oxidase in a semi-recombinant cell-free system. Assessment of the function of Rac in the activation process. Eur J Biochem 226: 587–595.
26. Molnar G, Dagher MC, Geiszt M, Settleman J, Ligeti E (2001) Role of prenylation in the interaction of Rho-family small GTPases with GTPase activating proteins. Biochemistry 40: 10542–10549.
27. Robbe K, Otto-Bruc A, Chardin P, Antonny B (2003) Dissociation of GDP dissociation inhibitor and membrane translocation are required for efficient activation of Rac by the Dbl homology-pleckstrin homology region of Tiam. J Biol Chem 278: 4756–4762.
28. Grizot S, Faure J, Fieschi F, Vignais PV, Dagher MC, et al. (2001) Crystal structure of the Rac1-RhoGDI complex involved in nadph oxidase activation. Biochemistry 40: 10007–10013.
29. Hoffman GR, Nassar N, Cerione RA (2000) Structure of the Rho family GTP-binding protein Cdc42 in complex with the multifunctional regulator RhoGDI. Cell 100: 345–356.
30. Faure J, Vignais PV, Dagher MC (1999) Phosphoinositide-dependent activation of Rho A involves partial opening of the RhoA/Rho-GDI complex. Eur J Biochem 262: 879–889.
31. Ugolev Y, Berdichevsky Y, Weinbaum C, Pick E (2008) Dissociation of Rac1(GDP).RhoGDI complexes by the cooperative action of anionic liposomes containing phosphatidylinositol 3,4,5-trisphosphate, Rac guanine nucleotide exchange factor, and GTP. J Biol Chem 283: 22257–22271.
32. Gureasko J, Galush WJ, Boykevisch S, Sondermann H, Bar-Sagi D, et al. (2008) Membrane-dependent signal integration by the Ras activator Son of sevenless. Nat Struct Mol Biol 15: 452–461.
33. Alexander M, Gerauer M, Pechlivanis M, Popkirova B, Dvorsky R, et al. (2009) Mapping the isoprenoid binding pocket of PDEdelta by a semisynthetic, photoactivatable N-Ras lipoprotein. Chembiochem 10: 98–108.
34. Ismail SA, Chen YX, Rusinova A, Chandra A, Bierbaum M, et al. (2011) Arl2-GTP and Arl3-GTP regulate a GDI-like transport system for farnesylated cargo. Nat Chem Biol 7: 942–949.
35. Weise K, Kapoor S, Werkmuller A, Mobitz S, Zimmermann G, et al. (2012) Dissociation of the K-Ras4B/PDEdelta complex upon contact with lipid membranes: membrane delivery instead of extraction. J Am Chem Soc 134: 11503–11510.
36. Triola G, Waldmann H, Hedberg C (2012) Chemical biology of lipidated proteins. ACS Chemical Biology 7: 87–99.
37. Wu YW, Oesterlin LK, Tan KT, Waldmann H, Alexandrov K, et al. (2010) Membrane targeting mechanism of Rab GTPases elucidated by semisynthetic protein probes. Nat Chem Biol 6: 534–540.
38. Guo Z, Wu YW, Das D, Delon C, Cramer J, et al. (2008) Structures of RabGGTase-substrate/product complexes provide insights into the evolution of protein prenylation. EMBO J 27: 2444–2456.
39. Wu YW, Tan KT, Waldmann H, Goody RS, Alexandrov K (2007) Interaction analysis of prenylated Rab GTPase with Rab escort protein and GDP dissociation inhibitor explains the need for both regulators. Proc Natl Acad Sci U S A 104: 12294–12299.
40. Herbrand U, Ahmadian MR (2006) p190-RhoGAP as an integral component of the Tiam1/Rac1-induced downregulation of Rho. Biol Chem 387: 311–317.
41. Mena JA, Ramirez OT, Palomares LA (2003) Titration of non-occluded baculovirus using a cell viability assay. Biotechniques 34: 260–262, 264.
42. Reed LJ, Muench H (1938) A simple method of estimating fifty per cent endpoint. Am J Hyg 27: 493–497.
43. Fansa EK, Dvorsky R, Zhang SC, Fiegen D, Ahmadian MR (2013) Interaction characteristics of Plexin-B1 with Rho family proteins. Biochem Biophys Res Commun 434: 785–790.

44. Shymanets A, Ahmadian MR, Kossmeier KT, Wetzker R, Harteneck C, et al. (2012) The p101 subunit of PI3Kgamma restores activation by Gbeta mutants deficient in stimulating p110gamma. Biochem J 441: 851–858.
45. Boura E, Hurley JH (2012) Structural basis for membrane targeting by the MVB12-associated beta-prism domain of the human ESCRT-I MVB12 subunit. Proc Natl Acad Sci U S A 109: 1901–1906.
46. Bloom JW, Nesheim ME, Mann KG (1979) Phospholipid-binding properties of bovine factor V and factor Va. Biochemistry 18: 4419–4425.
47. Saci A, Cantley LC, Carpenter CL (2011) Rac1 Regulates the Activity of mTORC1 and mTORC2 and Controls Cellular Size. Mol Cell 42: 50–61.
48. Michaelson D, Silletti J, Murphy G, D'Eustachio P, Rush M, et al. (2001) Differential localization of Rho GTPases in live cells: regulation by hypervariable regions and RhoGDI binding. J Cell Biol 152: 111–126.
49. Hancock JF, Hall A (1993) A Novel Role for Rhogdi as an Inhibitor of Gap Proteins. EMBO J 12: 1915–1921.
50. Moissoglu K, Slepchenko BM, Meller N, Horwitz AF, Schwartz MA (2006) In vivo dynamics of Rac-membrane interactions. Mol Biol Cell 17: 2770–2779.
51. Morreale A, Venkatesan M, Mott HR, Owen D, Nietlispach D, et al. (2000) Structure of Cdc42 bound to the GTPase binding domain of PAK. Nat Struct Biol 7: 384–388.
52. Gizachew D, Guo W, Chohan KK, Sutcliffe MJ, Oswald RE (2000) Structure of the complex of Cdc42Hs with a peptide derived from P-21 activated kinase. Biochemistry 39: 3963–3971.
53. Haeusler LC, Blumenstein L, Stege P, Dvorsky R, Ahmadian MR (2003) Comparative functional analysis of the Rac GTPases. FEBS Letters 555: 556–560.
54. Viaud J, Gaits-Iacovoni F, Payrastre B (2012) Regulation of the DH-PH tandem of guanine nucleotide exchange factor for Rho GTPases by phosphoinositides. Adv Biol Regul 52: 303–314.
55. Mertens AE, Roovers RC, Collard JG (2003) Regulation of Tiam1-Rac signalling. FEBS Letters 546: 11–16.
56. Boissier P, Huynh-Do U (2014) The guanine nucleotide exchange factor Tiam1: A Janus-faced molecule in cellular signaling. Cell Signal 26: 483–491.
57. Marrari Y, Crouthamel M, Irannejad R, Wedegaertner PB (2007) Assembly and trafficking of heterotrimeric G proteins. Biochemistry 46: 7665–7677.
58. Konstantinopoulos PA, Karamouzis MV, Papavassiliou AG (2007) Post-translational modifications and regulation of the RAS superfamily of GTPases as anticancer targets. Nat Rev Drug Discov 6: 541–555.
59. Brunsveld L, Waldmann H, Huster D (2009) Membrane binding of lipidated Ras peptides and proteins—the structural point of view. Biochim Biophys Acta 1788: 273–288.
60. Contreras-Gomez A, Sanchez-Miron A, Garcia-Camacho F, Chisti Y, Molina-Grima E (2013) Protein production using the baculovirus-insect cell expression system. Biotechnol Prog.
61. Gorzalczany Y, Sigal N, Itan M, Lotan O, Pick E (2000) Targeting of Rac1 to the phagocyte membrane is sufficient for the induction of NADPH oxidase assembly. J Biol Chem 275: 40073–40081.
62. Sasaki T, Kato M, Takai Y (1993) Consequences of weak interaction of rho GDI with the GTP-bound forms of rho p21 and rac p21. J Biol Chem 268: 23959–23963.
63. Scheffzek K, Stephan I, Jensen ON, Illenberger D, Gierschik P (2000) The Rac-RhoGDI complex and the structural basis for the regulation of Rho proteins by RhoGDI. Nat Struct Biol 7: 122–126.
64. Parrini MC, Matsuda M, de Gunzburg J (2005) Spatiotemporal regulation of the Pak1 kinase. Biochem Soc Trans 33: 646–648.
65. Zhang B, Chernoff J, Zheng Y (1998) Interaction of Rac1 with GTPase-activating proteins and putative effectors. A comparison with Cdc42 and RhoA. J Biol Chem 273: 8776–8782.
66. Parrini MC, Lei M, Harrison SC, Mayer BJ (2002) Pak1 kinase homodimers are autoinhibited in trans and dissociated upon activation by Cdc42 and Rac1. Mol Cell 9: 73–83.
67. Hemsath L, Dvorsky R, Fiegen D, Carlier MF, Ahmadian MR (2005) An electrostatic steering mechanism of Cdc42 recognition by Wiskott-Aldrich syndrome proteins. Mol Cell 20: 313–324.
68. Michiels F, Stam JC, Hordijk PL, van der Kammen RA, Ruuls-Van Stalle L, et al. (1997) Regulated membrane localization of Tiam1, mediated by the NH2-terminal pleckstrin homology domain, is required for Rac-dependent membrane ruffling and C-Jun NH2-terminal kinase activation. J Cell Biol 137: 387–398.
69. Rapley J, Tybulewicz VL, Rittinger K (2008) Crucial structural role for the PH and C1 domains of the Vav1 exchange factor. Embo Reports 9: 655–661.
70. Ognibene M, Vanni C, Blengio F, Segalerba D, Mancini P, et al. (2014) Identification of a novel mouse Dbl proto-oncogene splice variant: evidence that SEC14 domain is involved in GEF activity regulation. Gene 537: 220–229.
71. Barber MA, Donald S, Thelen S, Anderson KE, Thelen M, et al. (2007) Membrane translocation of P-Rex1 is mediated by G protein betagamma subunits and phosphoinositide 3-kinase. J Biol Chem 282: 29967–29976.
72. Boissier P, Chen J, Huynh-Do U (2013) EphA2 signaling following endocytosis: role of Tiam1. Traffic 14: 1255–1271.
73. Ten Klooster JP, Evers EE, Janssen L, Machesky LM, Michiels F, et al. (2006) Interaction between Tiam1 and the Arp2/3 complex links activation of Rac to actin polymerization. Biochem J 397: 39–45.

Supporting Information

Liposome reconstitution and modulation of recombinant prenylated human Rac1 by GEFs, GDI1 and Pak1

Si-Cai Zhang, Lothar Gremer, Henrike Heise, Petra Janning, Aliaksei Shymanets, Ion C. Cirstea, Eberhard Krause, Bernd Nürnberg, and Mohammad Reza Ahmadian
Institute of Biochemistry and Molecular Biology II, Medical Faculty of the Heinrich-Heine University, Düsseldorf, Germany.

Table S1. Detergents used in this study.

Detergent	MW(Da)	CMC[a]	Used concentration[b]	
Cholate	430	14 mM (0.6%)	11.6 mM (0.5%)	23.3 mM (1%)
Triton X-100	625	0.24 mM (0.015%)	8 mM (0.5%)	16 mM (1%)
Triton X-114	537	0.2 mM (0.011%)	9.3 mM (0.5%)	18.6 mM (1%)
Igepal CA 630	648	0.083 mM (0.0053%)	7.7 mM (0.5%)	15.4 mM (1%)
Tween 20	1228	0.06 mM (0.0073%)	4 mM (0.5%)	8.1 mM (1%)
CHAPS	615	6-10 mM (0.37-0.61%)	8.1 mM (0.5%)	16.2 mM (1%)
n-hexyl-β-D-glucopyranoside	264	250 mM (6.6%)	18.9 mM (0.5%)	37.8 mM (1%)
n-heptyl-β-D-glucopyranoside	278	79 mM (2.2%)	18 mM (0.5%)	36 mM (1%)
n-octyl-β-D-glucopyranoside	292	20-25 mM (0.58-0.73%)	17.1 mM (0.5%)	34.2 mM (1%)
n-nonyl-β-D-glucopyranoside	306	6.5 mM (0.2%)	16.3 mM (0.5%)	32.6 mM (1%)
n-octyl-β-D-thioglucopyranoside	308	9 mM (0.28%)	12.5 mM (0.39%)	25 mM (0.77%)
n-dodecyl-β-D-maltoside	511	0.1-0.6 mM (0.005-0.03%)	10 mM (0.51%)	20 mM (1.02%)
Zwittergent 3-08	280	330 mM (9.22%)	17.9 mM (0.5%)	35.8 mM (1%)
Zwittergent 3-10	308	25-40 mM (0.77-1.23%)	16.3 mM (0.5%)	32.5 mM (1%)
Zwittergent 3-12	336	2-4 mM (0.067-0.134%)	14.9 mM (0.5%)	29.8 mM (1%)
Zwittergent 3-14	392	0.1-0.4 mM (0.004-0.016%)	12.8 mM (0.5%)	25.5 mM (1%)
Zwittergent 3-16	392	0.01-0.06 mM (0.0004-0.002%)	12.8 mM (0.5%)	25.5 mM (1%)
Deoxycholate	415	2-6 mM (0.082%-0.25%)	12.1 mM (0.5%)	24.2 mM (1%)

[a] Critical micelle concentration; [b] detergent concentration used in this study has been reported previously [Supporting References 1-4].

Supporting References to Table S1

1. Bramley, P. M. & Taylor, R. F. (1985) The Solubilization of Carotenogenic Enzymes of Phycomyces-Blakesleeanus, *Biochim Biophys Acta.* **839**, 155-160.
2. Collins, R. F., Ford, R. C., Kitmitto, A., Olsen, R. O., Tonjum, T. & Derrick, J. P. (2003) Three-dimensional structure of the Neisseria meningitidis secretin PilQ determined from negative-stain transmission electron microscopy, *J Bacteriol.* **185**, 2611-2617.
3. Linke, D. (2009) Detergents: an overview, *Methods Enzymol.* **463**, 603-617.
4. Miskevich, F., Davis, A., Leeprapaiwong, P., Giganti, V., Kostic, N. M. & Angel, L. A. (2011) Metal complexes as artificial proteases in proteomics: A palladium(II) complex cleaves various proteins in solutions containing detergents, *J Inorg Biochem.* **105**, 675-683.

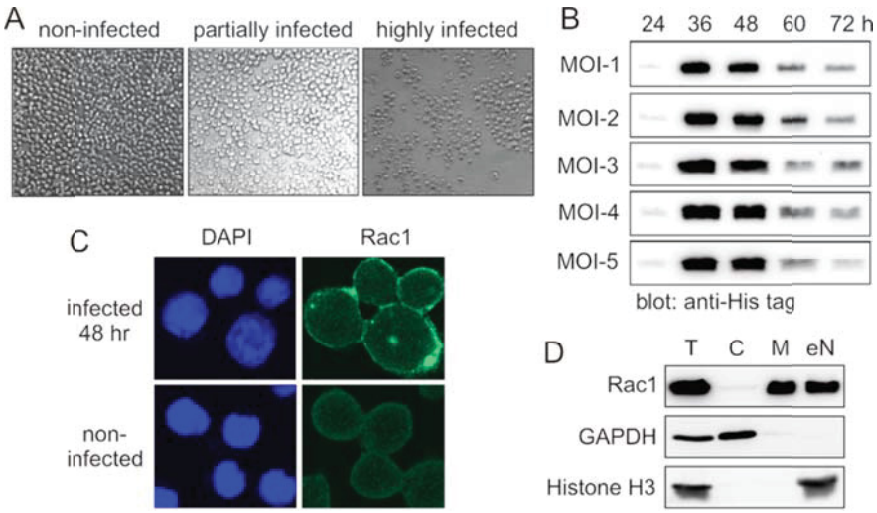

Figure S1. Expression of human Rac1 in insect cells. (**A**) The baculovirus cytopathic effects in *Sf*9 cells. Baculovirus-infected *Sf*9 cells are characterized by reduced cell numbers due to virus replication and subsequent cell death. (**B**) Rac1 expression in *Sf*9 cells. Insect cells are inoculated at different MOI (1 to 5) and harvested at different time points (24 to 72 h). Samples were analyzed by SDS-PAGE and immunoblotting using an anti-His tag antibody. (**C**) Rac1 localization at the plasma membrane of the *Sf*9 cells. Confocal laser scanning microscopy images of the insect cells depicting overexpressed Rac1 using anti-Rac1 antibody and nuclear staining using DAPI. Non-infected cells were used as control. (**D**) Subcellular fractionation of Rac1. *Sf*9 cells were fractionated by differential centrifugation into cytoplasmic (C), membrane (M) and enriched nuclear (eN) fractions. Total cell lysate (T) was used as control. Rac1 as well as GAPDH and histone H3 as markers were analyzed by SDS-PAGE and immunoblot analysis.

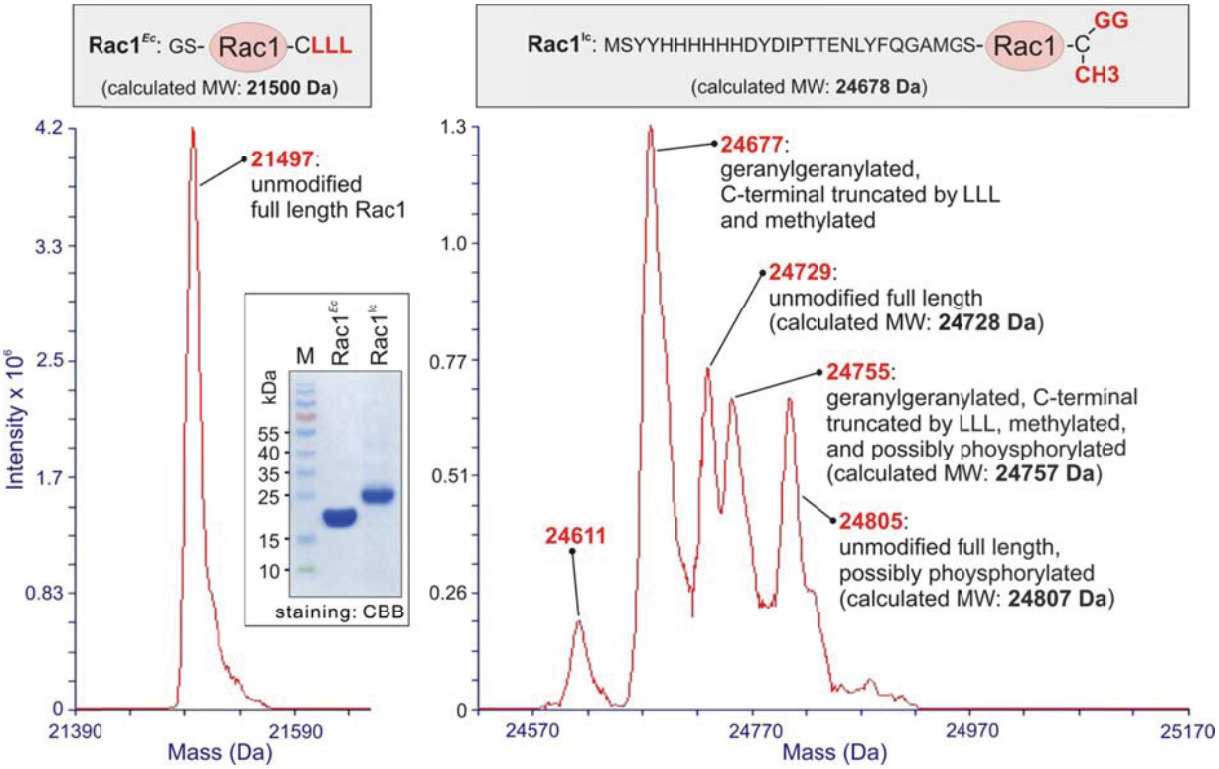

Figure S2. Mass spectra of Rac1^{Ec} (left panel) and Rac1^{IC} (right panel) after deconvolution. Five mg/ml full length Rac1 proteins from *E. coli* and Rac1 from *Sf*9 insect cells were dissolved in 50% (v/v) acetonitrile and 0.2% (v/v) formic acid. Proteins were subjected to a C4 HPLC column (Jupiter C4, 5 µm, 300 Å, 150 mm x 2 mm, Phenomenex, Aschaffenburg, Germany) equilibrated with 20 % (v/v) acetonitrile and 0.1 % (v/v) formic acid. For HPLC separation following conditions were used: HPLC-system 1100 serie (Agilent Technology, Waldbronn, Germany), a flow rate of 200 µl/min, eluent A: 0.1 % (v/v) formic acid in water, eluent B: 0.1 % (v/v) formic acid in acetonitrile, gradient condition: 20 % B for 2 min, linear gradient up to 50 % B in 23 min, linear gradient up to 90 % B in 15 min, 90 % B for 10 min, reequilibration of the column. The HPLC-system was coupled on-line to an ion trap mass spectrometer (LTQ, Thermo Fisher Scientific, Germany) equipped with an electrospray ionization source. Full spectra were acquired using a mass-to-charge range of 700 to 2000. Obtained spectra were deconvoluted using the program package Promass (Thermo Fisher Scientific, Germany). Masses obtained from the respective spectra are described with respect to calculated molecular weights (MW). Note that Rac1^{IC} contains at its N-terminus a 6xHis tag and a thrombin cleavage site. The sodium dodecyl sulfate polyacrylamide gel electrophoresis (SDS-PAGE) in the inset shows the purity of the two analyzed Rac1 protein. CBB, coomassie brilliant blue; CH3, methyl group; Da, Dalton; *Ec*, *E. coli*; Ic, insect cells; GG, geranylgeranyl moiety; LLL, the very C-terminal three leucines of human Rac1; M, molecular weight marker.

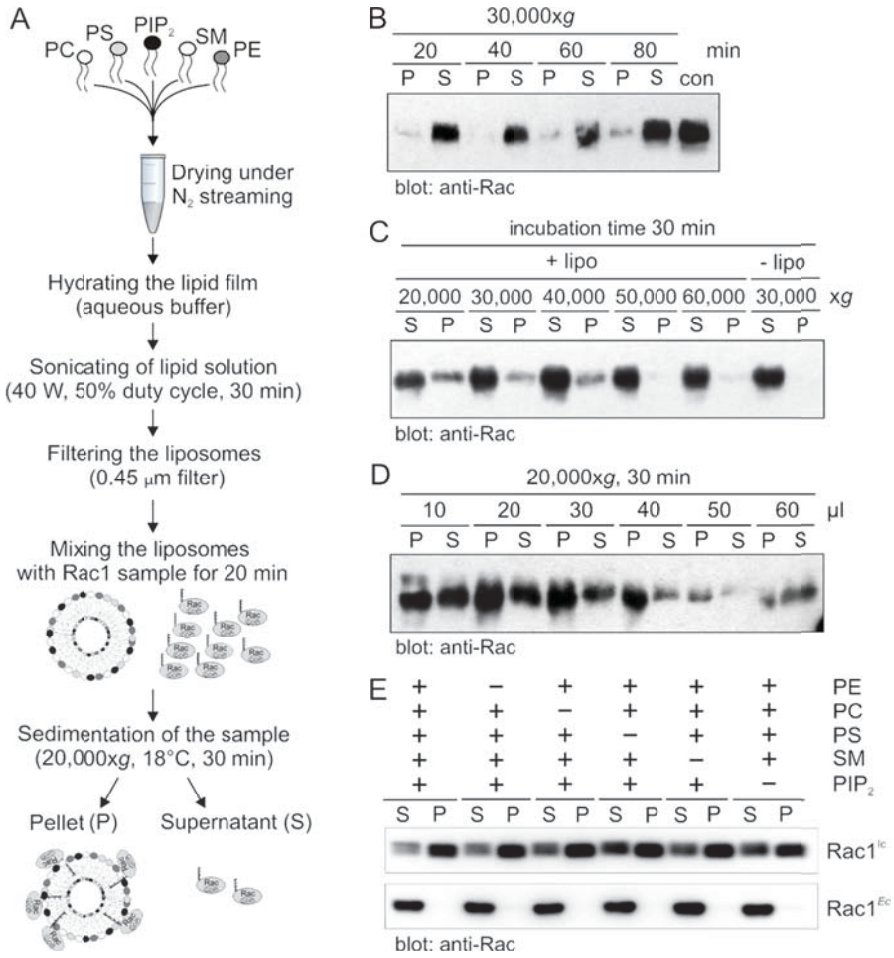

Figure S3. Liposome preparation and sedimentation experiments using human Rac1^{Ic}. (**A**) Schematic workflow of liposome formation using five different lipids, including phosphatidylcholine (PC), phosphatidylserine (PS), phosphatidylinositol 4,5-bisphosphate (PIP_2), sphingomyelin (SM), and phosphatidylethanolamine (PE). (**B**) The effect of different incubation time (20, 40, 60 and 80 min), (**C**) various centrifugation speeds (20,000, 30,000, 40,000, 50,000 and 60,000xg), (**D**) different amounts of liposomes (10, 20, 30, 40, 50 and 60 µl) and (**E**) distinct liposome composition on the association of Rac1^{Ic} (1.5 µg) with liposomes was analyzed using a liposome sedimentation assay. All samples were analyzed by immunoblotting using anti-Rac1 antibody. For the validation of specific interaction of Rac1^{Ic} with the liposomes, full length Rac1 purified from *E. coli* (Rac1^{Ec}) was used as control. Con, control; *Ec*, *E. coli*; Ic, insect cells; lipo; liposomes; P, liposome pellet; S, supernatant.

Biochemical and Biophysical Research Communications 434 (2013) 785–790

Contents lists available at SciVerse ScienceDirect

Biochemical and Biophysical Research Communications

journal homepage: www.elsevier.com/locate/ybbrc

Interaction characteristics of Plexin-B1 with Rho family proteins

Eyad Kalawy Fansa, Radovan Dvorsky, Si-Cai Zhang, Dennis Fiegen [1], Mohammad Reza Ahmadian *

Institut für Biochemie und Molekularbiologie II, Medizinische Fakultät der Heinrich-Heine-Universität, 40225 Düsseldorf, Germany

ARTICLE INFO

Article history:
Received 7 April 2013
Available online 17 April 2013

Keywords:
Interaction selectivity
Plexin-B1
Rho GTPases
Competitive interaction

ABSTRACT

Plexin-B1 regulates various cellular processes interacting directly with several Rho proteins. Molecular details of these interactions are, however, not well understood. In this study, we examined *in vitro* and *in silico* the interaction of the Rho binding domain (B1RBD) of human Plexin-B1 with 11 different Rho proteins. We show that B1RBD binds in a GTP-dependent manner to Rac1, Rac2, Rac3, Rnd1, Rnd2, Rnd3, and RhoD, but not to RhoA, Cdc42, RhoG, or Rif. Interestingly, Rnd1 competitively displaces the Rac1 from B1RBD but not *vice versa*. Structure–function analysis revealed a negatively charged loop region, called B1L^{31}, which may facilitate a selective B1RBD interaction with Rho proteins.

1. Introduction

The semaphorin transmembrane receptor Plexin-B1 is involved in the regulation of several cellular processes including axonal guidance in the developing nervous system [1], cellular migration, immune response [2,3], and angiogenesis [4]. Binding of the specific ligand semaphorin-4D to the extracellular domain of Plexin-B1 induces a variety of signaling processes on the intracellular side, for which proteins of Rho family are known to be important components [1,5]. Members of the Rho family have been shown to directly associate with the Rho binding domain of Plexin-B1 (B1RBD), such as Rnd1, Rac1 and RhoD [6–10]. Structural analysis of B1RBD in complex with Rho proteins has suggested that B1RBD binds to similar regions of Rnd1 and Rac1 [9,11,12]. However, how the selectivity of the Rho protein interactions with B1RBD is determined and how Plexin-B1 discriminates between Rac1 and Rnd1, are still important open questions.

In this study, we have investigated the structure–function relationships of the interaction between B1RBD and 11 different members of the Rho family. B1RBD revealed interaction with the active forms of Rnd and Rac isoforms as well as with RhoD but not with other members of the Rho family, including RhoA, Cdc42, RhoG and Rif. We further demonstrate that Rnd1 displaces Rac1 from B1RBD. Our efforts to elucidate the selectivity-determining residues in B1RBD-Rho proteins interactions led us to focus on a loop region consisting of 31 residues (amino acids 1854–1885) in B1RBD (hereafter referred to as B1L^{31}), which may facilitate the B1RBD interactions with certain Rho proteins at the plasma membrane.

2. Materials and methods

2.1. Constructs

Human Plexin-B1RBD (amino acids or aa 1724–1903), B1RBD variant L1849G/V1850G/P1851A (B1RBD^{GGA}), B1RBD variant E1868A/E1874A/D1875A/D1877A (B1RBD^{AAAA}), as well as human Rho-related genes, i.e. full-length Rac1^{wt}, C-terminal truncated Rac1ΔC (aa 1-179), Rac1^{A95E}, RhoA^{E97A}, Rac2, Rac3, Rnd1, Rnd2ΔNΔC (aa 26-184), Rnd3, RhoA^{wt}, Cdc42ΔC (aa 1-178), RifΔC (aa 1-195) and RhoGΔC (aa 1-184), and mouse RhoDΔC (aa 2-193) were cloned in pGEX vectors.

2.2. Proteins

All proteins were isolated and prepared as previously described [13].

2.3. Isothermal titration calorimetry (ITC)

All measurements were performed using an isothermal titration calorimeter (VP-ITC) at 20 °C as described [14].

2.4. Analytical size exclusion chromatography (aSEC)

Experiments were carried out at 4 °C on a Superdex75 10/300 GL column (GE Healthcare).

* Corresponding author. Address: Institut für Biochemie und Molekularbiologie II, Medizinische Fakultät der Heinrich-Heine-Universität, Universitätsstr. 1, Gebäude 22.03, 40255 Düsseldorf, Germany. Fax: +49 211 811 2726.
E-mail address: reza.ahmadian@uni-duesseldorf.de (M.R. Ahmadian).
[1] Birkendorfer Straße 65, 88397 Biberach an der Riss, Germany.

0006-291X/$ - see front matter © 2013 Elsevier Inc. All rights reserved.
http://dx.doi.org/10.1016/j.bbrc.2013.04.012

2.5. Nucleotide quantification by high pressure liquid chromatography (HPLC)

The type and concentration of guanine nucleotides were analyzed on a reversed-phase (RP-) HPLC as described [13].

2.6. Structural analysis and molecular modeling

Modeling of the human Plexin-B1 region (aa 1854–1885) was performed, based on the crystal structure of cytoplasmic domain of Plexin-B1 in complex with Rac1 (Protein Data Bank code 3SUA), using MODELLER [15]. Structural analysis was done and electrostatic potential maps were obtained using PyMOL (Molecular Graphics System, version 1.5.0.4 Schrödinger, LLC) and APBS [16], respectively.

3. Results and discussion

3.1. B1RBD binds among the Rho family proteins selectively to Rnd and Rac isoforms as well as to RhoD in vitro

Previous reports have shown that B1RBD interacts with Rnd1, Rac1 and RhoD [6,7,10–12]. Here, we set out to investigate the interaction of B1RBD with 11 representative members of the Rho family proteins (i.e. Rac1, Rac2, Rac3, RhoG, Rnd1, Rnd2, Rnd3, RhoA, Cdc42, RhoD and Rif), using ITC. Fig. S1A shows that B1RBD binds selectively to the active (GppNHp-bound) Rac1 with an affinity in the low micromolar range (K_d = 6.6 μM) but not to the inactive (GDP-bound) Rac1. To confirm this interaction, analytical size exclusion chromatography (aSEC) was carried out. It is important to note that B1RBD eluted as a dimer in the absence and in the presence of interacting Rho protein. As shown in Fig. S1B, B1RBD co-eluted with Rac1 GppNHp, but not with Rac1 GDP.

Notably, among the Rac isoforms, Rac1 displayed the highest affinity of B1RBD considering the unprecedented K_d values of 11.0 and 30.3 μM for GppNHp-bound Rac2 and Rac3, respectively (Figs. S2 and S3; Table S1). Like Rac1 GDP, GDP-bound forms of Rac2 and Rac3 showed no interaction with B1RBD (data not shown). The reason for the lower affinity of Rac2 and particularly Rac3 as compared to Rac1 could not be linked to the B1RBD binding amino acids as analyzed below. It is rather likely that the overall dynamics of these isoforms is responsible for their functional specificities as discussed previously [17]. Several studies have shown that Rac1 binding to Plexin-B1 sequesters it from its downstream signaling [18], which in turn results in Rho activation and in the assembly of contractile stress fibers [7].

The interaction of Rnd isoforms with B1RBD was measured in the GTP-bound state, because they do not hydrolyze GTP [13]. As shown in Fig. S2 and summarized in Table S1, Rnd1 and Rnd2 bind to B1RBD with K_d values of 3.2 μM and 4.6 μM, respectively. In this study we further measured the interaction between Rnd3 and B1RBD and showed that also Rnd3, similarly to Rnd1 and Rnd2, is able to bind B1RBD with an affinity of 8.5 μM (Figs. S2 and S3; Table S1). A detailed sequence and structural analysis, using the B1RBD Rnd1 complex (PDB code 2REX) [19], showed that all three Rnd isoforms are likely to interact in a comparable manner with B1RBD. As shown in Fig. 1A, almost all B1RBD contacting residues are identical among the Rnd proteins. Deviations at two different positions, C81 in Rnd1 (A75 in Rnd2, S91 in Rnd3) and Y114 in Rnd1 (F108 in Rnd2 and F124 in Rnd3) does not seem to play a critical role in B1RBD binding as their binding affinities are in a similar range. This suggests that the association of Rnd proteins with Plexin-B1 is most likely mediated via the same mechanism that may

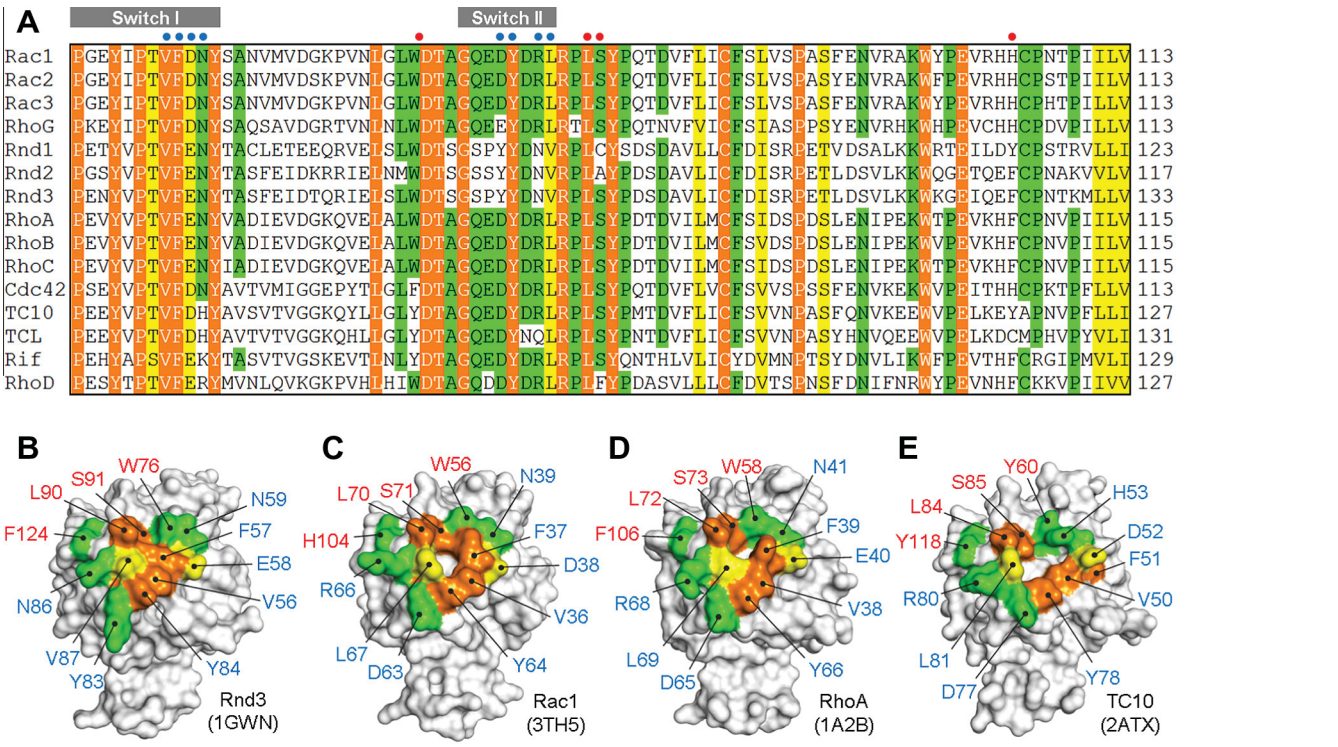

Fig. 1. Conserved B1RBD contact regions on Rnd1 and Rac1. (A) Rho protein sequences were aligned using the ClustalW program and the alignment was edited by GeneDoc. Highlighted are conserved residues in yellow, identical residues in white and orange background, and identical residues in at least 11 proteins in green. Dots indicate B1RBD binding residues of Rnd1 and Rac1, inside the switch regions in blue and outside switch regions in red. (B–E) Surface representation of 3D structures of major representatives of Rho proteins subgroups in their active forms, including Rnd3 [28], Rac1 [27], RhoA [29] and TC10 [30], highlighted are the conserved B1RBD binding residues of Rnd1 and Rac1. The color code of surface patches and amino acid labels correspond to A. (For interpretation of the references to colour in this figure legend, the reader is referred to the web version of this article.)

have different cellular effects, including inactivation of R-Ras [20], and sequestration of Rnd proteins as a modulators of actin Dynamics [21,22]. Rnd2 binding to Plexin-D1 has been shown to inhibit axon outgrowth of cortical neurons and down-regulation of R-Ras activity [23].

Our interaction analysis revealed that yet RhoD was able to bind B1RBD in its active form (K_d = 14.4 μM), but not other members of the Rho family, i.e. RhoA, Cdc42, RhoG, and Rif (Fig. S2; Table S1). RhoD has been shown to exhibit repulsive effects on axons by interfering with the Rnd1 binding to Plexin-A1 [24]. Nevertheless, it is interesting and surprising that B1RBD binds RhoD but not, for example, RhoG which shares the highest sequence homology with Rac isoforms [13].

3.2. Rnd1 displaces Rac1 from its complex with B1RBD

The fact that B1RBD binds to functionally distinct groups of Rho proteins raises the question, whether these interactions control different processes or are rather reciprocal. Data from crystal structures of Plexin-B1 complexes with Rac1 and Rnd1 (PDB codes 3SU8 and 2REX) [9,19] have suggested that Rac1 and Rnd1 share the same binding site on B1RBD. To examine whether and how Rac1 and Rnd1 compete for the same interacting surface on B1RBD, we performed a combination of ITC measurements along with aSEC analysis. First, we successively combined two ITC experiments in row. In the first step, we titrated in two separate experiments Rac1 GppNHp and Rnd1 GTP on B1RBD, which resulted in the respective formation of the expected complexes (Fig. 2A and C, left panels). In the second step, we subsequently titrated to the formed complexes Rnd1 GTP and Rac1 GppNHp, respectively. As shown in the right panels of Fig. 2A and C, addition of Rnd1 to Rac1 GppNHp B1RBD resulted in an additional complex formation that was not observed when Rac1 GppNHp was added to Rnd1 GTP B1RBD. The differences in heat capacity confirm that Rnd1 and Rac1 in fact compete for an overlapping binding site on B1RBD and that Rnd1 displaces Rac1 from its complex with B1RBD but not *vice versa*.

To further confirm this result we monitored the complex formation of B1RBD with Rac1 or/and Rnd1 by aSEC followed by RP-HPLC. Fig. 2B clearly shows that loading a mixture of Rnd1 GTP and Rac1 GppNHp B1RBD complex on Superdex 75 (10/300)

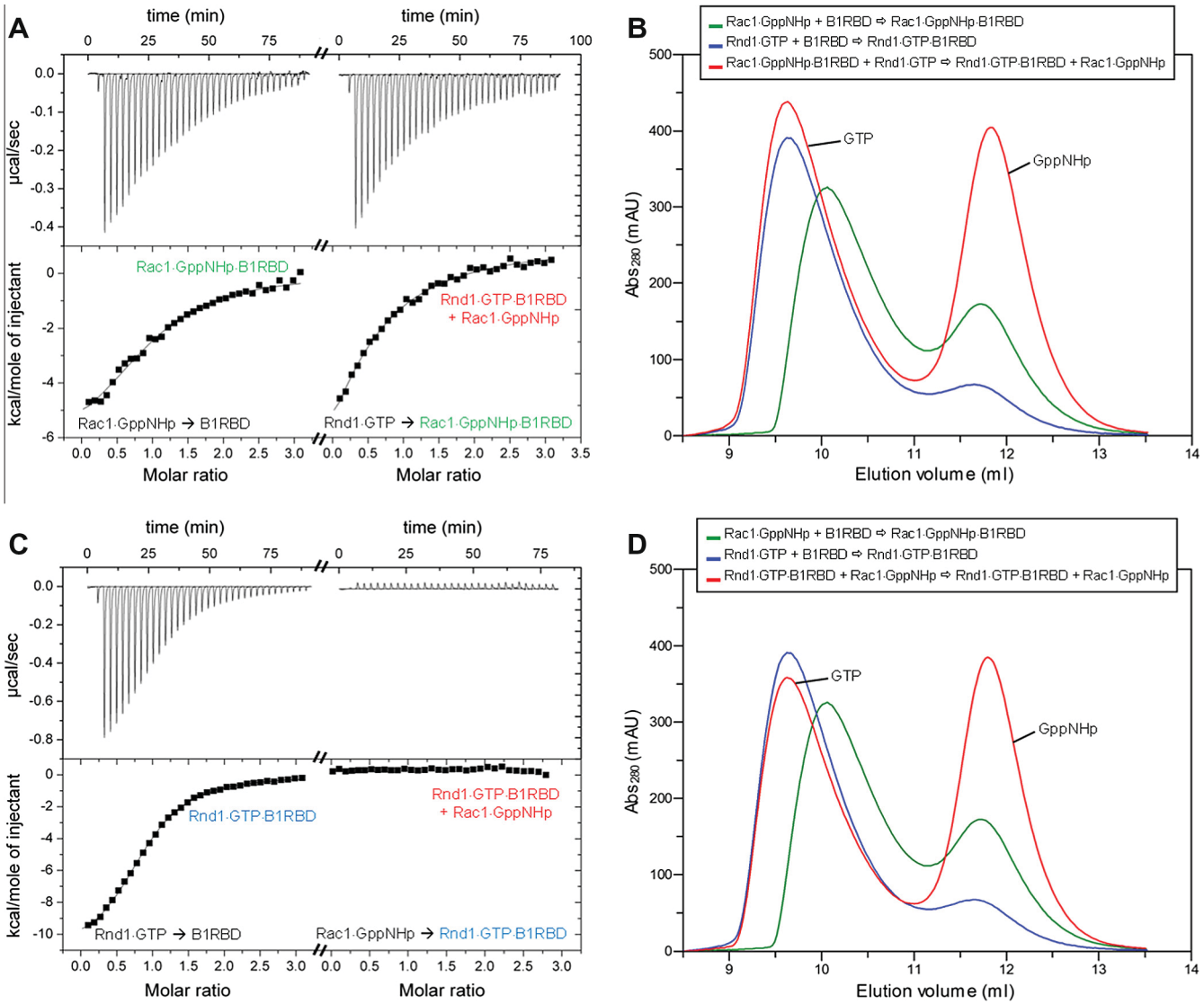

Fig. 2. Displacement of Rac1 from its complex with B1RBD by Rnd1. (A and B) Successive ITC measurements were performed by first titrating Rac1 (300 μM) to B1RBD (20 μM) and second Rnd1 (300 μM) to the Rac1-B1RBD complex. aSEC profiles of various protein complexes are shown in B, in which equivalent amount of Rnd1 GTP displaced Rac1 GppNHp from its complex with B1RBD after incubation for 5 min on ice before loading on the aSEC column. (C and D) In contrast, Rac1 is not able to displace Rnd1 from its complex with B1RBD. Comparable conditions and protein concentrations were used as in A and B. For (B) and (D) peak fractions were analyzed by RP-HPLC for detecting the nucleotide-bound state.

column resulted in co-elution of the Rnd1 GTP B1RBD complex and the release of Rac1 GppNHp. To distinguish between Rnd1- and Rac1-containing fractions, we quantified the peak fractions on a RP-HPLC system regarding the bound nucleotide, e.g. GTP or GppNHp. In contrast, a gel filtration of Rac1 GppNHp mixed with the Rnd1 GTP B1RBD complex did not displace Rnd1 from the complex (Fig. 2D). These data strongly support the notion that Rnd1 facilitates Rac1 release from B1RBD and thus may antagonize its cellular activity.

An important question to be addressed is whether the displacement of Rac1 from B1RBD by Rnd1 releases Rac1 for signaling *via* other effectors or dislodges Rac1 from its signal transduction. A previous study by Negishi and coworkers demonstrated that Rac1 activity is required for the Rnd1-induced neurite formation and that Rac1 is an integral element of the signaling pathway downstream of Rnd1 [25].

3.3. Illuminating the B1RBD selectivity for Rho proteins

One major interest of this study was to explore the selectivity of the interaction between B1RBD and Rho proteins. Importantly, our data showed that B1RBD binds to the active GTP-bound forms of Rho proteins. This clearly demonstrates that B1RBD contacts the switch regions of Rho proteins, which are known to be involved in the recognition of and interaction with various binding partners [26]. In this regard, we investigated sequence–structure–function relationships between the Rho family proteins and B1RBD (Fig. 1). Multiple sequence alignment (Fig. 1A) did not reveal any significant differences in the B1RBD interacting amino acids within the switch regions of Rho proteins. Moreover, analysis of the key amino acids in the binding interface of B1ICDRac1 and B1RBDRnd1 complexes (PDB codes 3SU8 and 2REX, respectively) [9,19] showed that the amino acids responsible for the binding of Rac1 and Rnd1 to B1RBD are remarkably conserved in all Rho proteins (Fig. 1A, dots). To further analyze the overall location and orientation of the B1RBD interacting amino acids, we used crystal structures of Rnd3, Rac1, RhoA, and TC10 (PDB codes 1GWN, 3TH5, 1A2B and 2ATX, respectively) [27–30]. There is currently no structure of Cdc42 in its active form available (see Table S1 in [13]). Therefore, we used in this study the structure of Cdc42-like TC10 [30]. Fig. 1B–E illustrate that all B1RBD binding residues are accessible and arranged in similar positions on the surface of Rac1 and Rnd3 as well as RhoA and TC10, which do not bind B1RBD. A detailed comparison of Rac1 and Rnd1 (Fig. 1B and C) revealed obvious differences regarding the shape and relative orientation of some B1RBD interacting amino acids when compared to the equivalent residues in RhoA and TC10 (Fig. 1D and E). However, these differences in the switch regions cannot account for the disability of RhoA and Cdc42-like TC10 in binding B1RBD because these regions are highly flexible and can adopt specific ordered conformations upon interaction with downstream effectors [31]. This analysis strongly suggests that the differences in B1RBD interacting amino acids may not *per se* determine the selectivity of the B1RBD-Rho protein interactions.

The comparison of the structures available for Rho proteins in complex with various regulators and effectors has revealed common characteristics of the interactions between Rho proteins and their binding partners [26]. Accordingly, the switch regions are most likely the recognition sites and different binding partners contact other regions that are specific to their function [26]. In this context, B1RBD may utilize other contact sites on the guanine nucleotide binding (G) domain of Rho proteins and also in the C-terminal hypervariable region (HVR). Accordingly, a C-terminal truncated Rac1 exhibited a significant reduction in the binding affinity for B1RBD (Table S1, Figs. S2 and S3). This is particularly interesting because HVR is a juxtamembrane region of prenylated Rho proteins and may be a significant contact site for transmembrane proteins, including Plexins.

3.4. Structural and functional insights into $B1L^{31}$, a non-structured region in B1RBD

We next addressed the question which regions of B1RBD determine the selective binding to Rac, Rnd, and RhoD proteins, but not to RhoA, Cdc42, Rif, or RhoG. An interesting B1RBD variant is the $B1RBD^{GGA}$ (L1849G, V1850G, and P1851A), which was shown to be defective in Rac1 and Rnd1 binding in cell-based experiments [6,32]. Here, we investigated the $B1RBD^{GGA}$ variant in detail *in vitro*. Interestingly, experiments under the same conditions as in Fig. S1 showed that $B1RBD^{GGA}$ is disabled in associating with Rac1 GppNHp and Rnd1 GTP using ITC and aSEC/RP-HPLC (data not shown). Additionally, CD measurements of $B1RBD^{wt}$ and $B1RBD^{GGA}$ showed that both proteins exhibit almost identical secondary structure elements (data not shown). Structural analysis of B1RBD complexes with Rnd1 and Rac1 (PDB codes 2REX and 3SU8) [9,19] showed that the region containing the ^{1849}LVP^{1851} sequence is not in direct contact with Rho proteins. Notably, these residues are directly followed by a disordered region (amino acids 1854–1885), which is not visible in any B1RBD-related crystal structures. This raises an important question to what extent this region contributes to a selective interaction of B1RBD with the Rho proteins.

On the basis of the B1ICD-Rac1 complex structure (PDB code 3SU8) [9], we modeled different conformations of this region consisting of 31 residues (referred to as $B1L^{31}$). We visually analyzed all obtained models using the PyMOL program and selected those conformations that could potentially interact with Rac1 (Fig. 3A). In this way, we identified a patch of negatively charged amino acids (E1868, E1874, D1875 and D1877) in $B1L^{31}$ (Fig. 3A). Such prevalence of negative charges causes significant negative electrostatic potentials around the $B1RBD^{wt}$, as can be seen from electrostatics map calculated for one conformation of $B1L^{31}$ (Fig. 3B, left panel). For a comparison, a model of the $B1RBD^{AAAA}$ variant lacking these four negative residues, does not exhibit such a pronounced negative potential (Fig. 3B, right panel). Strikingly, A95 in Rac isoforms, located in a very close proximity of $B1L^{31}$, is variable among the members of the Rho family (Fig. 3A, magnified view and C). Interestingly, Rnd proteins contain a lysine and most of the other Rho proteins a glutamic acid at the corresponding position. We thus proposed that replacement of Ala95 in Rac1 with glutamic acid or the negatively charged residues of $B1L^{31}$ with alanine, may impair B1RBD-Rac1 interaction. To examine this idea, $B1RBD^{AAAA}$ lacking the four negative residues (E1868, E1874, D1875 and D1877; Fig. 3B, right panel) along with $Rac1^{A95E}$ and as control $RhoA^{E97A}$ were generated and tested using ITC. As shown in Fig. 3D, the association constant for the interaction of $Rac1^{wt}$ with B1RBD was slightly changed when the negative residues were substituted by alanine ($B1RBD^{AAAA}$). However, $Rac1^{A95E}$ binding to $B1RBD^{wt}$ was reduced by 2.5-fold as compared to that of $Rac1^{wt}$. On the other hand, no difference was observed for the binding of $Rnd1^{wt}$ and $RhoA^{E97A}$ to $B1RBD^{AAAA}$ compared to $B1RBD^{wt}$ (Table S2). Closer look at the B1ICD-Rac1 complex structure (PDB code 3SU8) [9] further revealed that the C-terminal HVR of the B1RBD binding Rho proteins contains a set of positively charged residues, which can in principle bind to $B1L^{31}$. To investigate this idea, we next measured the interaction between $B1RBD^{AAAA}$ and Rac1ΔC. Fig. 3D shows clearly that Rac1 HVR does not undergo any interaction with $B1L^{31}$ of B1RBD. All ITC data of the $B1RBD^{AAAA}$ variant are summarized in Table S2. Taken together, our data support the notion that $B1L^{31}$ facilitates to some extent the B1RBD-Rho proteins interaction and thereby might slightly influence the selectivity for distinct Rho protein. This loop region that very likely resides in a close proximity of the lipid membrane and Rac1

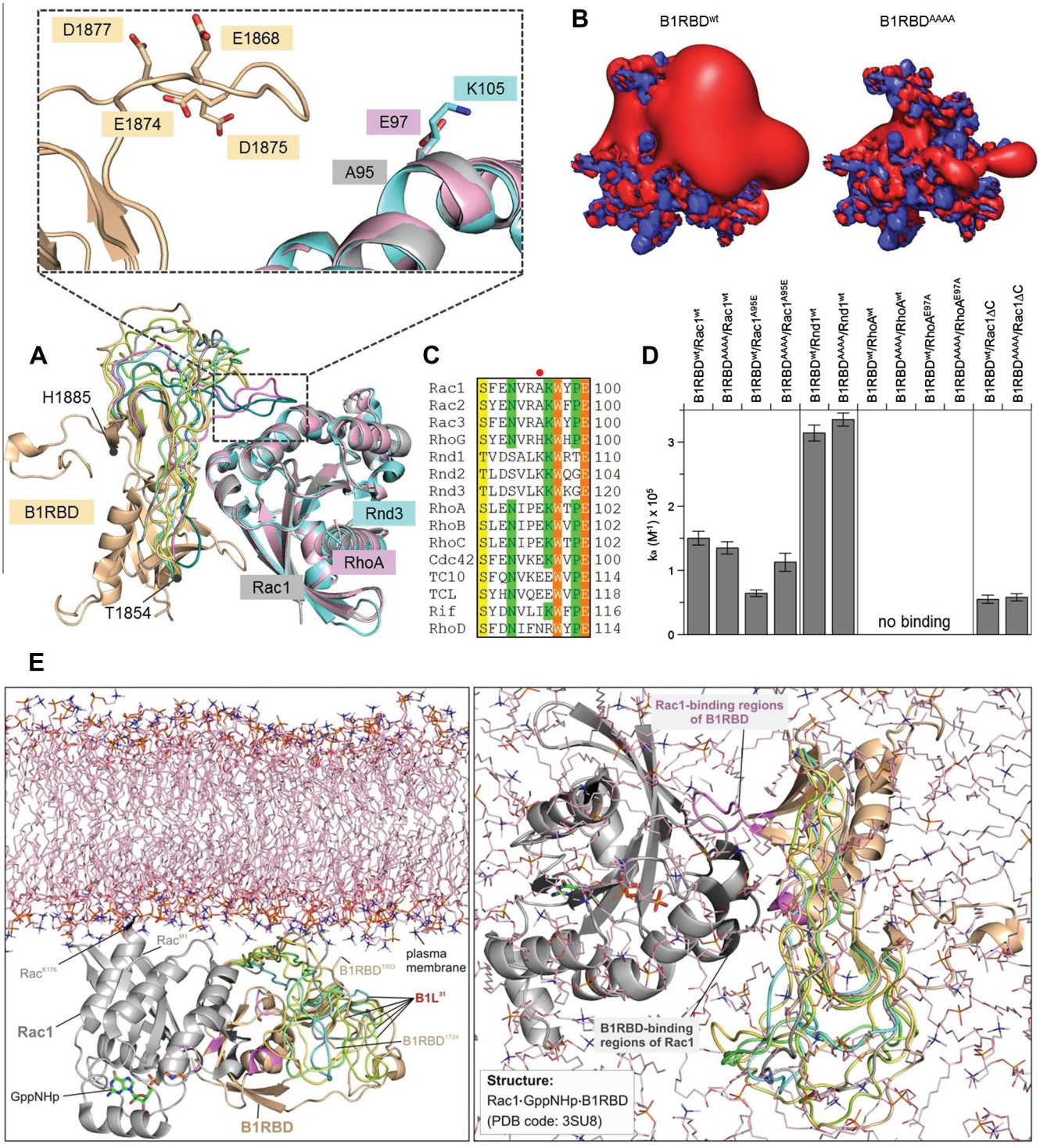

Fig. 3. Impact of modeled B1L^{31} on the B1RBD interaction with Rac1 and the plasma membrane. (A) Visualization of the B1L^{31} region (residues 1854–1885) of Plexin-B1 modeled on the basis of previous structure [9-11]. RhoA and Rnd3 crystal structures [29,30] were superimposed with Rac1 in the complex with B1ICD. Chosen conformation of modeled loop (magnified view) shows a detailed view of negatively charged B1L^{31} region that is in a close vicinity to potential interacting residues, such as Ala95 in Rac1 and Lys105 in Rnd1, which are located at the equivalent position to Glu97 in RhoA. (B) B1L^{31} with an isosurface of negative electrostatic potential. Electrostatic potential maps of B1RBD^{wt} and B1RBD^{AAAA} are represented by their isosurfaces at $-3k_bT/e_c$ (red) or $+3k_bT/e_c$ (blue) (C) Multiple sequence alignment of Rho proteins. Red dot represents the position of A95 of Rac1, Lys105 in Rnd1, and Glu97 in RhoA. (D) B1L^{31} as a potential Rho proteins contact region. ITC measurements of wild-type and variants of B1RBD, Rac1, Rnd1 and RhoA were performed to examine the impact of the B1L^{31} of B1RBD on a selective interaction with Rho proteins. For more clarity K_a values are shown (calculated K_d values are summarized in Table S2). (E) Illustrative positioning of B1RBD-Rac1 complex structure [9] at the plasma membrane with respect to Rac1 C-terminus, which associates with lipid bilayer via posttranslational modification (side view left and top view right). Six different conformations of B1L^{31} (aa 1854–1885) are shown that may approach the lipid membrane and are in the proximity of Rac1 are shown. (For interpretation of the references to colour in this figure legend, the reader is referred to the web version of this article.)

(Fig. 3E), may provide a supportive mechanism to regulate the activity of Plexin-B1 in the cellular context.

Acknowledgments

We thank Christian Hermann and Roland Piekorz for support and discussions and Wolfgang Hoyer for helping to perform the CD measurements. This work was supported by the International NRW research school Biostruct and the Federal Ministry of Education and Research (BMBF) as part of the NGFNplus program (Grant No. 01GS08100).

Appendix A. Supplementary data

Supplementary data associated with this article can be found, in the online version, at http://dx.doi.org/10.1016/j.bbrc.2013.04.012.

References

[1] M. Negishi, I. Oinuma, H. Katoh, Plexins: axon guidance and signal transduction, Cellular and Molecular Life Sciences: CMLS 62 (2005) 1363–1371.
[2] T. Worzfeld, J.M. Swiercz, M. Looso, B.K. Straub, K.K. Sivaraj, S. Offermanns, ErbB-2 signals through Plexin-B1 to promote breast cancer metastasis, The Journal of Clinical Investigation 122 (2012) 1296–1305.
[3] T. Okuno, Y. Nakatsuji, M. Moriya, H. Takamatsu, S. Nojima, N. Takegahara, T. Toyofuku, Y. Nakagawa, S. Kang, R.H. Friedel, S. Sakoda, H. Kikutani, A. Kumanogoh, Roles of Sema4D-plexin-B1 interactions in the central nervous system for pathogenesis of experimental autoimmune encephalomyelitis, Journal of Immunology 184 (2010) 1499–1506.
[4] H. Zhou, N.O. Binmadi, Y.H. Yang, P. Proia, J.R. Basile, Semaphorin 4D cooperates with VEGF to promote angiogenesis and tumor progression, Angiogenesis 15 (2012) 391–407.
[5] A.W. Puschel, GTPases in semaphorin signaling, Advances in Experimental Medicine and Biology 600 (2007) 12–23.
[6] H.G. Vikis, W. Li, Z. He, K.L. Guan, The semaphorin receptor plexin-B1 specifically interacts with active Rac in a ligand-dependent manner, Proceedings of the National Academy of Sciences of the United States of America 97 (2000) 12457–12462.
[7] M.H. Driessens, H. Hu, C.D. Nobes, A. Self, I. Jordens, C.S. Goodman, A. Hall, Plexin-B semaphorin receptors interact directly with active Rac and regulate the actin cytoskeleton by activating Rho, Current Biology: CB 11 (2001) 339–344.
[8] Y. Tong, P.K. Hota, M.B. Hamaneh, M. Buck, Insights into oncogenic mutations of plexin-B1 based on the solution structure of the Rho GTPase binding domain, Structure 16 (2008) 246–258.
[9] C.H. Bell, A.R. Aricescu, E.Y. Jones, C. Siebold, A dual binding mode for RhoGTPases in plexin signalling, PLoS Biology 9 (2011) e1001134.
[10] Y. Tong, P. Chugha, P.K. Hota, R.S. Alviani, M. Li, W. Tempel, L. Shen, H.W. Park, M. Buck, Binding of Rac1, Rnd1, and RhoD to a novel Rho GTPase interaction motif destabilizes dimerization of the plexin-B1 effector domain, The Journal of Biological Chemistry 282 (2007) 37215–37224.
[11] P.K. Hota, M. Buck, Thermodynamic characterization of two homologous protein complexes: associations of the semaphorin receptor plexin-B1 RhoGTPase binding domain with Rnd1 and active Rac1, Protein Science: A Publication of the Protein Society 18 (2009) 1060–1071.
[12] H. Wang, P.K. Hota, Y. Tong, B. Li, L. Shen, L. Nedyalkova, S. Borthakur, S. Kim, W. Tempel, M. Buck, H.W. Park, Structural basis of Rnd1 binding to plexin Rho GTPase binding domains (RBDs), The Journal of Biological Chemistry 286 (2011) 26093–26106.
[13] M. Jaiswal, E.K. Fansa, R. Dvorsky, M.R. Ahmadian, New insight into the molecular switch mechanism of human Rho family proteins: shifting a paradig, Biological Chemistry 394 (2013) 89–95.
[14] S.L. Risse, B. Vaz, M.F. Burton, P. Aspenstrom, R.P. Piekorz, L. Brunsveld, M.R. Ahmadian, SH3-mediated targeting of Wrch1/RhoU by multiple adaptor proteins, Biological Chemistry 394 (2013) 421–432.
[15] A. Sali, L. Potterton, F. Yuan, H. van Vlijmen, M. Karplus, Evaluation of comparative protein modeling by MODELLER, Proteins 23 (1995) 318–326.
[16] N.A. Baker, D. Sept, S. Joseph, M.J. Holst, J.A. McCammon, Electrostatics of nanosystems: application to microtubules and the ribosome, Proceedings of the National Academy of Sciences of the United States of America 98 (2001) 10037–10041.
[17] L.C. Haeusler, L. Blumenstein, P. Stege, R. Dvorsky, M.R. Ahmadian, Comparative functional analysis of the Rac GTPases, FEBS Letters 555 (2003) 556–560.
[18] H.G. Vikis, W. Li, K.L. Guan, The plexin-B1/Rac interaction inhibits PAK activation and enhances Sema4D ligand binding, Genes & Development 16 (2002) 836–845.
[19] Y. Tong, P.K. Hota, J.Y. Penachioni, M.B. Hamaneh, S. Kim, R.S. Alviani, L. Shen, H. He, W. Tempel, L. Tamagnone, H.W. Park, M. Buck, Structure and function of the intracellular region of the plexin-b1 transmembrane receptor, The Journal of Biological Chemistry 284 (2009) 35962–35972.
[20] I. Oinuma, Y. Ishikawa, H. Katoh, M. Negishi, The Semaphorin 4D receptor Plexin-B1 is a GTPase activating protein for R-Ras, Science 305 (2004) 862–865.
[21] P.K. Hota, M. Buck, Plexin structures are coming: opportunities for multilevel investigations of semaphorin guidance receptors, their cell signaling mechanisms, and functions, Cellular and Molecular Life Sciences: CMLS 69 (2012) 3765–3805.
[22] P. Riou, P. Villalonga, A.J. Ridley, Rnd proteins: multifunctional regulators of the cytoskeleton and cell cycle progression, BioEssays: News and Reviews in Molecular, Cellular and Developmental Biology 32 (2010) 986–992.
[23] K. Uesugi, I. Oinuma, H. Katoh, M. Negishi, Different requirement for Rnd GTPases of R-Ras GAP activity of Plexin-C1 and Plexin-D1, The Journal of Biological Chemistry 284 (2009) 6743–6751.
[24] S.M. Zanata, I. Hovatta, B. Rohm, A.W. Puschel, Antagonistic effects of Rnd1 and RhoD GTPases regulate receptor activity in Semaphorin 3A-induced cytoskeletal collapse, The Journal of Neuroscience: The Official Journal of the Society for Neuroscience 22 (2002) 471–477.
[25] J. Aoki, H. Katoh, K. Mori, M. Negishi, Rnd1, a novel rho family GTPase, induces the formation of neuritic processes in PC12 cells, Biochemical and Biophysical Research Communications 278 (2000) 604–608.
[26] R. Dvorsky, M.R. Ahmadian, Always look on the bright site of Rho: structural implications for a conserved intermolecular interface, EMBO Reports 5 (2004) 1130–1136.
[27] M. Krauthammer, Y. Kong, B.H. Ha, P. Evans, A. Bacchiocchi, J.P. McCusker, E. Cheng, M.J. Davis, G. Goh, M. Choi, S. Ariyan, D. Narayan, K. Dutton-Regester, A. Capatana, E.C. Holman, M. Bosenberg, M. Sznol, H.M. Kluger, D.E. Brash, D.F. Stern, M.A. Materin, R.S. Lo, S. Mane, S. Ma, K.K. Kidd, N.K. Hayward, R.P. Lifton, J. Schlessinger, T.J. Boggon, R. Halaban, Exome sequencing identifies recurrent somatic RAC1 mutations in melanoma, Nature Genetics 44 (2012) 1006–1014.
[28] H. Garavini, K. Riento, J.P. Phelan, M.S. McAlister, A.J. Ridley, N.H. Keep, Crystal structure of the core domain of RhoE/Rnd3: a constitutively activated small G protein, Biochemistry 41 (2002) 6303–6310.
[29] K. Ihara, S. Muraguchi, M. Kato, T. Shimizu, M. Shirakawa, S. Kuroda, K. Kaibuchi, T. Hakoshima, Crystal structure of human RhoA in a dominantly active form complexed with a GTP analogue, The Journal of Biological Chemistry 273 (1998) 9656–9666.
[30] L. Hemsath, R. Dvorsky, D. Fiegen, M.F. Carlier, M.R. Ahmadian, An electrostatic steering mechanism of Cdc42 recognition by Wiskott-Aldrich syndrome proteins, Molecular Cell 20 (2005) 313–324.
[31] I.R. Vetter, A. Wittinghofer, The guanine nucleotide-binding switch in three dimensions, Science 294 (2001) 1299–1304.
[32] I. Oinuma, H. Katoh, A. Harada, M. Negishi, Direct interaction of Rnd1 with Plexin-B1 regulates PDZ-RhoGEF-mediated Rho activation by Plexin-B1 and induces cell contraction in COS-7 cells, The Journal of Biological Chemistry 278 (2003) 25671–25677.

Human Molecular Genetics, 2013, Vol. 22, No. 2 **262–270**
doi:10.1093/hmg/dds426
Advance Access published on October 11, 2012

Diverging gain-of-function mechanisms of two novel KRAS mutations associated with Noonan and cardio-facio-cutaneous syndromes

Ion C. Cirstea[1,2], Lothar Gremer[1,†], Radovan Dvorsky[1], Si-Cai Zhang[1], Roland P. Piekorz[1], Martin Zenker[3] and Mohammad Reza Ahmadian[1,*]

[1]Institute of Biochemistry & Molecular Biology II, Heinrich-Heine University, Düsseldorf 40225, Germany, [2]Leibniz Institute for Age Research, Beutenberg Str. 11, 07745 Jena, Germany and [3]Institute of Human Genetics, University Hospital Magdeburg, Magdeburg 39120, Germany

Received August 28, 2012; Revised August 28, 2012; Accepted October 4, 2012

Activating somatic and germline mutations of closely related *RAS* genes (H, K, N) have been found in various types of cancer and in patients with developmental disorders, respectively. The involvement of the RAS signalling pathways in developmental disorders has recently emerged as one of the most important drivers in RAS research. In the present study, we investigated the biochemical and cell biological properties of two novel missense *KRAS* mutations (Y71H and K147E). Both mutations affect residues that are highly conserved within the RAS family. KRAS^{Y71H} showed no clear differences to KRAS^{wt}, except for an increased binding affinity for its major effector, the RAF1 kinase. Consistent with this finding, even though we detected similar levels of active KRAS^{Y71H} when compared with wild-type protein, we observed an increased activation of MEK1/2, irrespective of the stimulation conditions. In contrast, KRAS^{K147E} exhibited a tremendous increase in nucleotide dissociation generating a self-activating RAS protein that can act independently of upstream signals. As a consequence, levels of active KRAS^{K147E} were strongly increased regardless of serum stimulation and similar to the oncogenic KRAS^{G12V}. In spite of this, KRAS^{K147E} downstream signalling did not reach the level triggered by oncogenic KRAS^{G12V}, especially because KRAS^{K147E} was downregulated by RASGAP and moreover exhibited a 2-fold lower affinity for RAF kinase. Here, our findings clearly emphasize that individual RAS mutations, despite being associated with comparable phenotypes of developmental disorders in patients, can cause remarkably diverse biochemical effects with a common outcome, namely a rather moderate gain-of-function.

INTRODUCTION

The RAS-mitogen-activated protein kinase (MAPK) pathway is a kinase cascade pathway leading to cell proliferation and differentiation and was intensively studied due to its importance in cancer development. In the past decade, a new group of genetic developmental diseases determined by germline mutations related to the RAS/MAPK pathway components were identified and intensively studied. This group of RAS-MAPK-related disorders include Noonan syndrome (NS; MIM#163950), Costello syndrome (CS; MIM#218040) and cardio-facio-cutaneous syndrome (CFCS; MIM#115150). Typical clinical features of these disorders are short stature, facial dysmorphism, skin abnormalities and cardiac defects (1,2).

RAS proteins (HRAS, KRAS-A, KRAS-B and NRAS) act as molecular switches and cycle between an inactive, guanosine diphosphate (GDP) bound and active, guanosine triphosphate (GTP) bound state (3). The intrinsic functions of RAS proteins, their GDP/GTP exchange and GTP-hydrolysis are extremely slow. Guanine nucleotide exchange factors (GEFs) accelerate the exchange of bound GDP for the cellular abundant GTP (4), whereas GTPase-activating proteins (GAPs) terminate their signal transduction by stimulating the GTP-hydrolysis reaction (5). In their GTP-bound forms, RAS proteins interact

*To whom correspondence should be addressed at: Institute of Biochemistry & Molecular Biology II, Heinrich Heine University Medical Center, Universitätsstr. 1, Düsseldorf 40225, Germany. Tel: +49 2118112384; Fax: +49 211811 2726; Email: reza.ahmadian@uni-duesseldorf.de
†Present address: Forschungszentrum Jülich, Institute of Complex Systems (ICS-6), Wilhelm-Johnen-Strasse, 52425 Jülich, Germany.

with and regulate a spectrum of functionally diverse downstream effectors, including RAF kinases, phosphatidylinositol 3-kinase (PI3K) and RALGDS (6).

Somatic mutations of RAS proteins are involved in 32% of human cancers with *KRAS* as the most frequently mutated gene (85%), followed by *NRAS* (12%) and *HRAS* (3%) (7–9). The hot spots for cancer mutations are codons 12, 13 and 61, encoding amino acids that are fundamental for the GTP-hydrolysis reaction. In most cases, a GAP insensitivity of the mutants leads to a persistent downstream signalling. As in cases of cancer, KRAS-B is the predominantly affected isoform in RAS germline mutations associated with NS and CFCS (1,10–17). HRAS is the only gene associated with CS (18,19), and NRAS mutations were found in very rare cases of NS (20).

Recently, we have described in detail the functional properties of a spectrum of KRAS-B and NRAS mutations related to NS (17,20). Overall, our studies revealed several new mechanisms by which germline *KRAS* mutations contribute to human disease and lead to disturbed embryonic development. Two aspects are of high importance for the understanding of RAS function(s): (i) we showed that the mild gain-of-function in the case of KRAS mutations at positions 34 and 60 is due to a mechanism counterbalancing GAP resistance by a reduced RAF1 interaction and (ii) NRAS substitution of Thr50 to isoleucine possibly leads to an impaired interaction between RAS and the plasma membrane. The latter sheds light on the role of the plasma membrane in modulating RAS signalling (20,21).

RAS can exert a direct control on other signalling pathways either via their multitude of effectors or indirectly via MAPK and PI3K/AKT pathways. Briefly, PI3K activation by RAS leads to the production of phosphatidylinositol 3,4,5-trisphosphate, activation of phosphoinositide-dependent kinase-1 that leads in turn to AKT-activating phosphorylation at threonine 308 (22). Another AKT-activating event is the phosphorylation at serine 473 by mammalian/mechanistic target of rapamycin (mTOR) complex 2 (mTORC2), a protein complex which can be activated by RAS-MAPK via ERK1/2 (23).

In the present study, we characterized biochemically two new KRAS-B mutations (termed further as KRAS) that were recently found to be associated with NS and CFCS. The patients displayed mutations at the codon p.Y71H and p.K147E, respectively. The first was found as a *de novo* mutation in a child with NS, whereas the second was identified in a mother and her son with a CFCS phenotype (24). Both mutations in KRAS affect highly conserved residues within the RAS isoforms. Functional characterization using structural, biophysical and cellular biochemistry clearly shows comparable gain-of-function phenotypes of these two KRAS mutants that, however, display rather different biochemical characteristics.

RESULTS

For practical reasons (see Materials and Methods), we generated the *KRAS* mutations in the context of both the *HRAS* gene in the *Escherichia coli* expression system and in the *KRAS* gene in the eukaryotic expression system. Purified mutant RAS proteins were comprehensively characterized using advanced physical and cellular biochemistry. As controls, we used wild-type RAS (RAS^{wt}) and a GTPase deficient mutant (RAS^{G12V}).

Activation and downstream signalling of $KRAS^{Y71H}$ and $KRAS^{K147E}$

To gain insights into the regulatory cycle of the RAS mutants in cells, we transiently transfected COS-7 cells with plasmids expressing $KRAS^{wt}$ or the KRAS mutants G12V, Y71H and K147E. The amount of active, GTP-bound RAS in the presence of serum was determined using glutathione S-transferase (GST)-fusion proteins of the RAS-binding domain (RBD) of RAF1 (GST-RAF1-RBD) immobilized on glutathione sepharose. Interestingly, the two investigated KRAS mutants in this study exhibited quite different amounts of activated, GTP-bound states in the presence of serum. The level of activated RAS^{Y71H} was rather comparable to RAS^{wt}, whereas the level of activated $KRAS^{K147E}$ was comparable to the level of the oncogenic mutant $KRAS^{G12V}$ (Fig. 1A). To uncouple KRAS activation from stimulation with growth factors present in the serum, we next performed these experiments under serum-starved conditions. Interestingly, we obtained comparable levels of the GTP-bound states as in the presence of serum, i.e. a very low level for $KRAS^{Y71H}$ like in the wild type and a very high level in the case of $KRAS^{K147E}$ comparable to $KRAS^{G12V}$ (Fig. 1B).

The immense accumulation of $KRAS^{K147E}$ in a GTP-bound active state may have various reasons, e.g. an increased GDP/GTP exchange or an impaired intrinsic or/and GAP-stimulated GTP-hydrolysis rate. Therefore, we investigated the GAP sensitivity of these RAS mutants by repeating the GST pull-down assays under the same conditions as before, but including the catalytic GAP domain of neurofibromin (NF1-333) to the assays (25), which was added as purified protein to the cleared cell lysates (Fig. 1B). The results clearly indicate that both mutants, $KRAS^{K147E}$ and $KRAS^{Y71H}$, are GAP sensitive comparable to RAS^{wt} and in clear contrast to the GAP-insensitive $KRAS^{G12V}$.

The fact that the KRAS mutants exist in different states of activation due to differences in their regulatory cycle indicates that they may also cause considerable differences in their downstream signalling pathways. This was demonstrated, e.g. for CFCS-related KRAS mutants with alterations at positions Pro34 and Gly60 (17). Therefore, we investigated the activation of the major RAS effector pathways, the RAF kinase and PI3-kinase (PI3K) signalling cascades. The phosphorylation of MEK1/2, ERK 1/2 and AKT was analyzed in COS-7 cells transiently transfected with the indicated RAS mutants and grown under serum-containing (Fig. 1C) or serum-starved (Fig. 1D) conditions. Although the expression of $KRAS^{K147E}$ resulted in a massive accumulation of the GTP-bound active form (Fig. 1A) and subsequent clearly elevated the activation of MEK1/2 in the presence of serum (Fig. 1C), the activation of ERK1/2 was rather moderate in comparison to $KRAS^{G12V}$ (Fig. 1C). Under serum-free conditions, we detected a hyperactivated $KRAS^{K147E}$ (Fig. 1B), a moderate MEK1/2 activation and only slightly elevated pERK1/2 levels (Fig. 1D), the latter ones clearly differing from the massive effect of expressed oncogenic $KRAS^{G12V}$

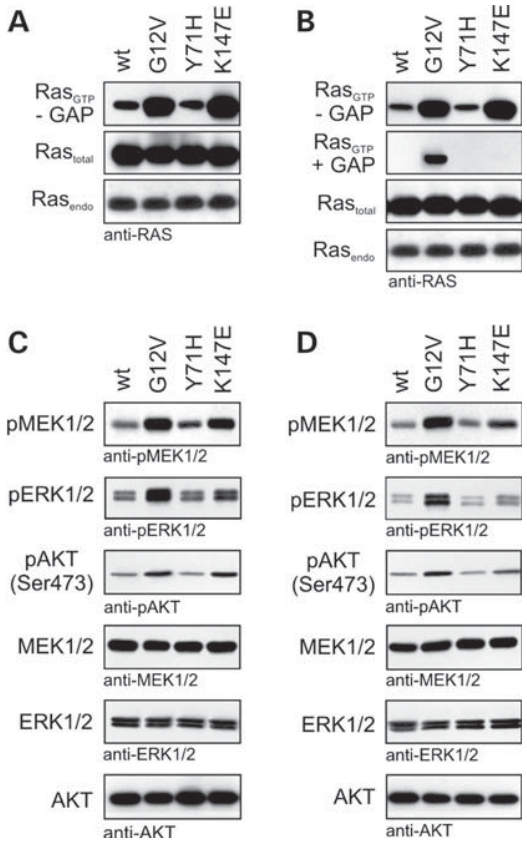

Figure 1. $KRAS^{Y71H}$ and $KRAS^{K147E}$ signalling activities in cells. Cleared lysates of COS-7 cells transiently expressing either $KRAS^{wt}$, the constitutive active $KRAS^{G12V}$ or germline KRAS mutants in the presence (**A**, **C**) and in the absence of serum (**B**, **D**) were used to analyze cellular levels of the components of the RAS-RAF1 and RAS-PI3K cascades. (A) Pull-down experiments of active, GTP-bound KRAS proteins (RAS^{GTP}) showed strong accumulation of $KRAS^{K147E}$ comparable to $KRAS^{G12V}$, whereas $KRAS^{Y71H}$ was in this regard similar to $KRAS^{wt}$. (B) Purified RASGAP, added to the cleared cell lysates, proved the GAP sensitivity for all mutants when compared with the GAP-insensitive oncogenic $KRAS^{G12V}$. The same lysates were analyzed for the phosphorylation level of MEK1/2 (pMEK1/2), ERK1/2 (pERK1/2) and AKT (pAKT) under serum-induced (C) and serum-free culture conditions (D). Despite high GTP-bound levels, $KRAS^{K147E}$ does not lead to strong downstream signalling when compared with $KRAS^{G12V}$, under the given conditions. The amounts of total RAS, MEK1/2, ERK1/2 and AKT in the cleared cell lysates and RAS^{wt}, RAS^{G12V} were included as controls.

(Fig. 1D). Taken together, these data indicate that $KRAS^{K147E}$, regardless of its strong activation, leads to a milder gain-of-function in downstream signalling when compared with the $KRAS^{G12V}$ oncogenic mutation.

There are two intriguing aspects coming out from $KRAS^{Y71H}$ mutant expression in COS-7 cells. First, $KRAS^{Y71H}$ expression showed, under serum induction and in comparison to the wild type, a slight increase in pMEK1/2 levels (Fig. 1C), despite of comparable levels of the GTP-bound active form in $KRAS^{wt}$ and $KRAS^{Y71H}$ mutant, respectively (Fig. 1A). Second, the increased pMEK1/2 level did not lead to stronger ERK1/2 activation when compared with wild-type protein (Fig. 1A). Under serum-free conditions, we detected only a slight increase in MEK1/2 activation when compared with $KRAS^{wt}$ (Fig. 1D), but this was now followed by a concomitant slight decrease in ERK1/2 activation (Fig. 1D). Thus, the effects observed with $KRAS^{Y71H}$ are more subtle than expected. In addition to MEK1/2 and ERK1/2 activation, we investigated AKT-activating phosphorylation at Ser 473. We observed that $KRAS^{Y71H}$ leads to similar levels of phosphorylated AKT as $KRAS^{wt}$, irrespective of serum conditions (Fig. 1C and D). $KRAS^{K147E}$ in the presence of serum displays similar levels of phosphorylated AKT as $KRAS^{G12V}$ in the presence of serum (Fig. 1C), but in the absence of serum, the amount of phosphorylated AKT was reduced (Fig. 1D).

Next, analysis of the downstream activities of both KRAS mutants was performed under well-defined and controlled conditions, using epidermal growth factor (EGF) stimulation in a time-dependent manner (Fig. 2). EGF-induced activation of $KRAS^{Y71H}$ revealed a significantly different picture (Fig. 2) when compared with our observations under serum-stimulated conditions (Fig. 1C). Its activity toward MEK1/2 is slightly higher than $KRAS^{wt}$. This rather correlates with elevated levels of pMEK1/2 in the presence of 10% serum (Fig. 1C). However, following serum starvation and EGF treatment, the ERK1/2 phosphorylation levels by $KRAS^{Y71H}$ were clearly and surprisingly higher than those for $KRAS^{wt}$ and almost comparable to $KRAS^{G12V}$ (Fig. 2). For the time-dependent $KRAS^{K147E}$-mediated ERK activation, surprisingly EGF seems to lead to higher MEK1/2 activation when compared with $KRAS^{G12V}$, but in turn similar ERK1/2 activation when compared with $KRAS^{G12V}$ (Fig. 2). A different and very interesting scenario is $KRAS^{K147E}$ that increased significantly the level of both pAKT (Ser473) and pAKT (Thr308), comparable to KRASG12V (Fig. 1C and D). These effects are quite consistent with the germline KRAS mutations Q22E and F156L, as demonstrated recently (17). Hence, an important question arises as to whether KRAS mutants, identified in patients with developmental disorders, mediate exclusively activation of the RAS-MAPK pathway or whether they also differentially influence other key signalling pathways, including PI3K/AKT.

To address this issue in more detail, we studied the AKT activation via two different pathways, including ERK/mTORC2 leading to AKT phosphorylation at Ser473 and PI3K/PDK1 leading to AKT phosphorylation at Thr308 (Fig. 2). We detected that under basal conditions (prior to EGF stimulation), $KRAS^{Y71H}$ caused a weaker activation of AKT when compared with the effect of $KRAS^{K147E}$. On treatment with EGF for 30 s, activation of the Y71H mutant led to higher levels of pAKT when compared with $KRAS^{wt}$ with an earlier activation, which can be attributed to the $KRAS^{Y71H}$ in the absence of EGF (time point zero). The highest and most robust AKT phosphorylation at Ser473 was observed for $KRAS^{K147E}$ that is apparently even higher than in the presence of $KRAS^{G12V}$ (Fig. 2), despite of their similar GTP-bound levels (Fig. 1A and B). The difference between these two mutants is that $KRAS^{K147E}$ is sensitive to RASGAPs, whereas $KRAS^{G12V}$ is RASGAP insensitive (Fig. 1B). The same tendency was also observed for the phosphorylation of ERK1/2 by the KRAS mutants. Contrary to the AKT phosphorylation at Ser473, no obvious difference was detectable for Thr308 phosphorylation. K147E mutant appeared to be more active than Y71H mutant (Fig. 2). Taken together, these data support the notion that the

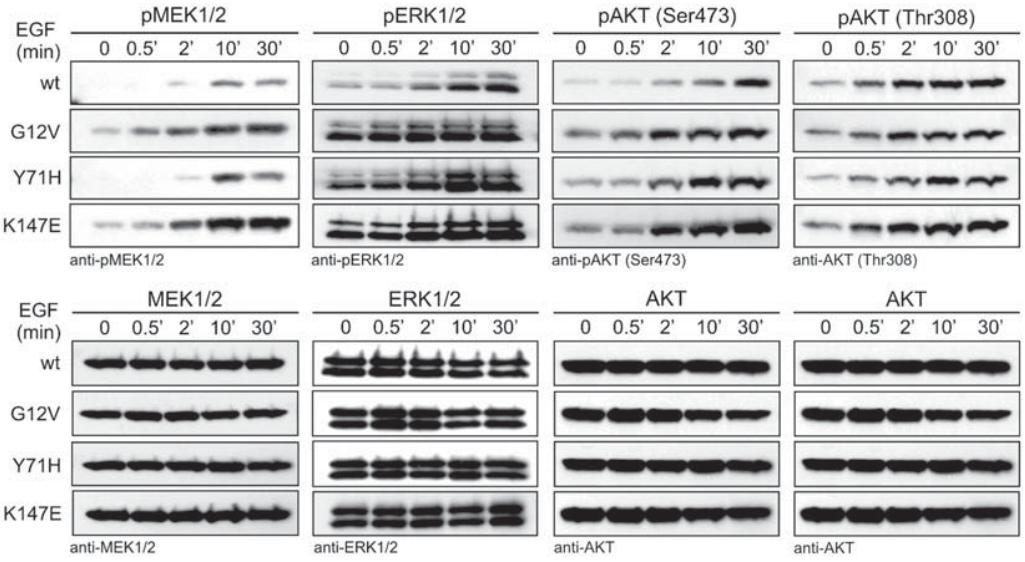

Figure 2. EGF-induced effects on downstream signalling on expression of $KRAS^{Y71H}$ and $KRAS^{K147E}$. COS-7 cells were stimulated with 20 ng/ml EGF and harvested at the indicated time points. Cleared cell lysates were analyzed for phosphorylated MEK1/2, ERK1/2 and AKT (Ser473 by ERK/mTORC2 and Thr308 by PI3K/PDK1), respectively (upper panels). The lower panels represent the total MEK1/2, ERK1/2 and AKT loading controls.

RAS-MAPK pathway is a specific determinant of developmental disorders, obviously in contrast to the RAS-AKT pathway. The effects of these and other KRAS effectors on the perturbation of embryonic development remain to be determined.

Functional characteristics of $KRAS^{Y71H}$ and $KRAS^{K147E}$

To analyze how the observed biochemical effects in cells are related to the molecular properties of the investigated KRAS mutants, we characterized them under *in vitro* conditions and analyzed the possible impact of the mutations at the structural level. Purified proteins were comprehensively studied for their intrinsic and SOS1-catalyzed nucleotide dissociation, intrinsic and neurofibromin (NF1)-stimulated GTP hydrolysis and interaction with the RAF1 effector protein. Data are summarized in Figure 3 and are shown in detail in Supplementary Material, Figure S1.

The cellular activation of RAS is generally achieved by a nucleotide exchange of bound GDP with cellular abundant GTP, which starts with the release of the bound nucleotide. Therefore, the first experiment related to RAS activation was the determination of the intrinsic nucleotide dissociation rate constants, i.e. in the absence of a GEF. We observed that RAS^{Y71H} exhibits an exchange reaction comparable to RAS^{wt} (Fig. 3A). This is in agreement with the structural localization of the Tyr71 residue that is surface exposed and remote from the nucleotide binding side (Fig. 4A and B). In addition, the *in vitro* exchange reaction of RAS^{Y71H} is consistent with the levels of activated RAS^{Y71H} in transfected COS-7 cells, especially in the absence of serum (Fig. 1B).

In contrast, the exchange reaction of RAS^{K147E} was strongly increased (150-fold) when compared with RAS^{wt} and RAS^{Y71H} (Fig. 3A). Because Lys147 is part of the nucleotide base binding ^{145}SAK^{147} motif (Fig. 4A and B), it is likely that its mutation to an inversely charged glutamate residue interferes with and weakens guanine nucleotide binding (Fig. 4D). It is also obvious that the dramatically increased nucleotide exchange of RAS^{K147E} is the cause for the strongly increased level of the activated GTP-bound state in transfected COS-7 cells, especially in the absence of serum (Fig. 1B), i.e. in the absence of external stimuli and thus in the absence of upstream-activating GEFs. In summary, the 150-fold increased nucleotide exchange reaction enables the RAS^{K147E} mutant to act as a real self-activating mutant without the requirement of GEFs.

This finding is also in agreement with the observation that highly elevated intrinsic nucleotide exchange level of RAS^{K147E} cannot be further activated in the presence of RASGEF SOS1 as typically observed for RAS^{wt} under identical conditions (Fig. 3B). Fold activation calculated from the SOS1-catalyzed reaction rates (Fig. 3B) divided by the k_{obs} values of the intrinsic GTP hydrolysis reactions (Fig. 3A) is 536-fold for RAS^{wt}, 183-fold for RAS^{Y71H} and strikingly only 1.4-fold for RAS^{K147E}, respectively. The fact that the GEF-stimulated activation of RAS^{Y71H} was reduced when compared with RAS^{wt} (Fig. 3B) indicates that the substitution of Tyr71 to histidine may slightly interfere with RAS–GEF complex formation and/or GEF-mediated catalysis (Fig. 3B).

The key properties of RAS in the active, GTP-bound state are the interaction with and subsequent activation of effectors for downstream signalling. The activated status is then terminated by an inactivating hydrolysis of GTP that is stimulated by RASGAPs. These properties are for both novel KRAS mutants only slightly altered as compared to RAS^{wt} (Fig. 3C and D), indicating that both complex formation with GAPs and effectors as well as GAP-mediated catalysis are functional. Under the conditions applied, the addition of NF1-stimulated the GTP-hydrolysis reaction for all three RAS proteins by more than three orders of magnitude. Notably, RAS^{Y71H} exhibited even a 2-fold increased intrinsic and NF1-stimulated

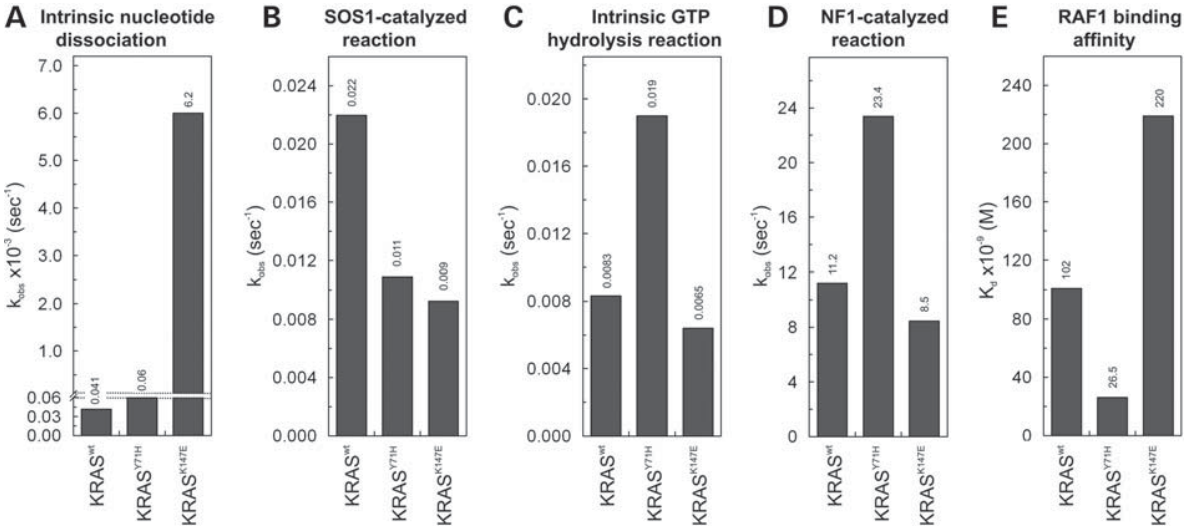

Figure 3. Comparative, quantitative *in vitro* analyses of the functional properties of KRAS^{Y71H} and KRAS^{K147E}. (**A**) Dissociation of mant-GDP from the RAS proteins, measured in the presence of excess, free GDP, showed the breakdown of the nucleotide binding of the K147E mutant. (**B**) The GEF activity of SOS1 toward KRAS^{Y71H} is reduced, and KRAS^{K147E} is almost abrogated. (**C**) The intrinsic hydrolysis of GTP is faster in the case of KRAS^{Y71H}. The GTP hydrolysis rate of KRAS^{K147E} is slightly slower than the rate of the intrinsic nucleotide dissociation, which explains its accumulation in the GTP-bound state in cells (Fig. 1). (**D**) KRAS^{Y71H} also revealed higher GTP hydrolysis rate in the presence of the RASGAP neurofibromin (NF1). (**E**) Diverging effects of the KRAS mutations on the RAF1-RBD dissociation constants (K_d) elevated in the case of Y71H and diminished in the case of K147E. The underlying measurements and analyses are shown and described in Supplementary Material, Figure S1.

GTP-hydrolysis (Fig. 3C and D) and a higher affinity for RAF1-RBD with a dissociation constant (K_d) of 26.5 nM. This corresponds to a 4-fold higher affinity of the effector as compared to that of RAS^{wt} ($K_d = 102$ nM) (Fig. 3E). These data indicate that the surface-exposed Tyr71 when replaced by histidine (Fig. 4A) contributes to the interaction with effectors and to the catalysis by GAPs. These results are in agreement with the moderately increased pMEK signal of RAS^{Y71H} (Figs 1B and 2), which is typical for a moderate increased downstream signalling via RAF1 when compared with RAS^{wt}. A 2-fold lower RAF1 binding affinity of RAS^{K147E} (Fig. 3D) slightly compensates the high rates of the intrinsic nucleotide exchange (Fig. 3A) and the high levels of the GTP-bound state (Fig. 1A) and explains the lower MEK1/2 phosphorylation when compared with KRAS^{G12V}, especially under serum-starved conditions (Fig. 1B).

Structural characteristics of KRAS^{Y71H} and KRAS^{K147E}

To understand and visualize the structural and functional effects caused by KRAS mutations, we inspected more than 50 RAS structures available in the protein database (see Supplementary Information in (17)). Overall, the location, spatial orientation and accessibility of the Tyr71 and Lys147 side chains were analyzed with respect to nucleotide binding and hydrolysis, interaction and regulation by GEFs and GAPs and the specificity of effector binding.

Tyr71 is localized at the end of the switch II region of RAS proteins (Fig. 4A). It is involved in conformational changes on GDP/GTP exchange, and its side chain, thus, faces different protein environments in the active and inactive state. However, the substitution of Tyr71 to histidine appears not to cause steric clashes with the neighboring residues. Despite the large conformational changes, Tyr71 is rather accessible and available for the interaction with regulatory proteins or effectors. The latter could be even more significant, given that an alternative conformation of Tyr71 is found in the complex structure with RAF1-RBD, where Tyr71 points outside of the protein (26). Notably, Tyr71 and its substitute His71 are not in direct contact with the GAP or the effector proteins, but in close proximity (7–9 Å). Thus, the observed increase in the binding affinity for RAF1 and subsequent MEK1/2 phosphorylation cannot be attributed to direct physical changes of the RAS–RAF1 interface, but rather to the overall indirect structural effects. As highlighted in Figure 4B, these effects can be mediated through stabilization of Glu37, which is sandwiched between Tyr71 and a critical arginine in RAF1 (Arg59). Mutations of Arg59 in RAF1 or Glu37 in HRAS have been shown to impair both their complex formation and subsequent downstream signalling (27,28). Thus, RAF1 binding to the switch I region appears to sense also the switch II conformation via indirect interaction with Tyr71 (Fig. 4B). Thus, we hypothesize that KRAS^{Y71H} undergoes a stronger binding to the RAF1-RBD because His71 may provide an additional hydrogen bond to contact Glu37 when compared with Tyr71. A similar scenario could be applied for the KRAS^{Y71H} interaction with the RASGAP as the GAP-stimulated reaction was 2-fold increased. Glu37 is also a critical RASGAP binding residue (29).

The residue Lys147 is an integral part of the conserved ^{145}SAK^{147} motif that is important for guanine base binding (Fig. 4A and C). Lys147 does not change its position on the nucleotide-dependent conformational switch of RAS. It is located in close vicinity, but does not directly bind to the guanine base of the bound nucleotide. Lys147 exhibits two major interactions and, thus, contributes indirectly to high-affinity guanine nucleotide binding (Fig. 4C). It makes

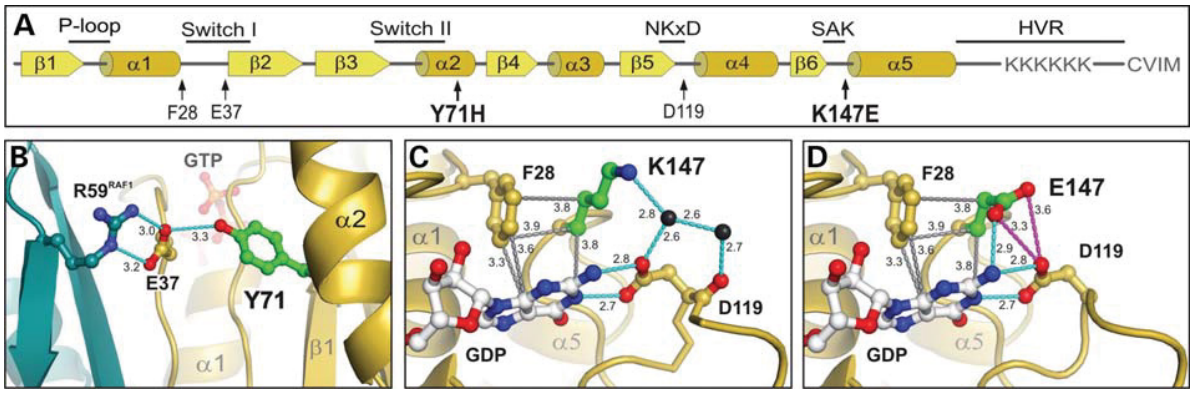

Figure 4. Structural impact of KRAS^{Y71H} and KRAS^{K147E}. (**A**) The relative position of the studied mutants (bold letters and bold arrows ↑) in the context of secondary structure elements (α-helices/β-strands as cylinders/arrows) and conserved motifs (bold lines), including the hypervariable region and the isoprenylation motif of KRAS at the C-terminus. (**B**) The role of Tyr71 in the RAS-effector interaction. Tyr71 stabilizes the orientation and the interaction of Glu37 with Arg59 of RAF1 (dark green). Y71H mutation is proposed to potentiate the overall affinity of KRAS for RAF1 by providing additional attractive contact with E37. (**C**) The interaction networks of Lys147. Lys147 largely contribute to the nucleotide binding indirectly by positioning both Phe28 through hydrophobic interaction (gray dashed lines) and D119 through the polar interactions (cyan dashed lines) with water molecules (black spheres). (**D**) K147E mutation strongly affects the high affinity binding of the nucleotides through repulsive effects on Asp119 (magenta dashed lines). Protein structures are shown as ribbons, crucial residues and nucleotides as ball and sticks. Nitrogen atoms are colored blue, oxygen atoms red, phosphorus atoms orange and the side chains of the studied residues 71 and 147 in green.

strong aliphatic interaction with Phe28 and, thus, orientates this residue that directly contacts the guanine base. The amino group of Lys147 is in contact with the conserved Asp119 via two water molecules stabilizing its interaction with the guanine base by two hydrogen bonds (Fig. 4C). Mutations of both residues have been shown to dramatically change nucleotide binding properties of HRAS. HRAS^{F28L} exhibits an increased nucleotide dissociation rate (30). HRAS^{D119N} revealed a shift in its specificity from guanosine to xanthosine nucleotides (31) and acts as a strong dominant-negative mutant in cells (32).

Lys147 is a conserved amino acid within the RAS family proteins suggesting that its interactions are of structural and functional importance. Disturbing these interactions by the substitution of Lys147 to an acidic glutamic acid has, thus, a massive impact on the affinity of KRAS for guanine nucleotides (Fig. 2A). K147E mutation obviously causes three cumulative effects (Fig. 4D). First, Glu147 apparently stabilizes Phe28 for guanine base binding as effectively as Lys147 does. Second, the acidic side chain of Glu147 causes an electrostatic repulsion with the Asp119 and consequently a strong increase in the nucleotide dissociation rate of this mutant. Third, Glu147 partially replaces the loss of Asp119 function by directly contacting the guanine base itself. We think that without the latter protective effect, HRAS^{K147E} may behave as a strong dominant-negative mutant that is described to have a high affinity for the RASGEFs and to inhibit RAS activation (32).

DISCUSSION

One of the most exciting recent developments in human genetics has been the identification of heterozygous germline mutations in key components of the highly conserved RAS-MAPK pathway as the cause of developmental disorders (33–35). An overall increase in activation of the RAS-MAPK pathway is thought to be the common pathophysiologic denominator for clinically overlapping syndromes, including NS, CFCS and CS (2). A large number of germline RAS mutations have been identified in the last 5 years. KRAS and NRAS mutations are causally related with NS (1,12,16,17,20,36), some KRAS mutations with CFCS (12,17,37) and HRAS mutations with CS (18,19,38–40). Functional effects caused by the majority of these mutations, which are markedly different from RAS mutations found in human cancer, are diverse and can be grouped into different classes according to their pattern of functional alterations (17). The two KRAS variants characterized in this study clearly demonstrate how different (non-overlapping) and diverse the structural and functional effects can be to cause a mild, non-lethal gain-of-function phenotype (24). To visualize these effects, we analyzed the structure–property–function relationship of these new variants *in vivo*, *in vitro* and *in silico*, in direct comparison to KRAS^{wt} and KRAS^{G12V}.

RAS^{Y71H} did not show any obvious differences to RAS^{wt} regarding its activation, but revealed a lower basal GTP level in the absence of stimuli, like EGF. Moreover, a slight but significant increase in RAF1 effector binding and consequently increased activation of MEK1/2 and ERK1/2 kinases were observed. These effects are most obvious in the time course of EGF stimulation (Fig. 2). Substitution of lysine at position 147 by glutamic acid very likely disturbs the guanine base coordination (Fig. 4D) and thus weakens the overall nucleotide binding. This leads due to the abundant cellular GTP to elevated active KRAS^{K147E} mutant, irrespective of stimulation conditions and GEF activity. In contrast to oncogenic KRAS^{G12V}, where the activated state stays persistent due to an impaired GAP-catalyzed GTP hydrolysis, the RAS^{K147E} mutant can be still inactivated by the GAP function as efficiently as activated KRAS^{wt}. Moreover, and characteristically for a NS and CFCS variant, the elevated signal of active KRAS^{K147E} is not transmitted as efficiently through the MAPK pathway as seen for the strong KRAS^{G12V}. This can be partially caused by a lower binding affinity for the downstream effector, i.e. RAF1.

Intriguingly enough, $KRAS^{Y71H}$, despite stronger affinity to RAF and stronger activation of MEK1/2, did not lead to a similar increase in ERK1/2 activation when compared with the wild type. It is not surprising that MEK1/2 does not show strong activation because even in cancer cell lines with endogenous oncogenic RAS isoforms, the activation of downstream signalling was not evident, as observed in pancreatic cell lines, leukemia cells and mouse embryonic fibroblasts from a mouse model expressing oncogenic KRAS (41–44).

Taking into account the overall properties of KRAS mutants from the present study, we add them into the classification of KRAS mutants leading to developmental disorders (17). Because the properties of $KRAS^{Y71H}$ are similar to the wild type, with the exception of the higher effector affinity, it belongs to class A of mutations. $KRAS^{K147E}$ based on its fast intrinsic dissociation (faster than the previously studied $KRAS^{F156L}$), abrogated SOS1-catalyzed nucleotide exchange and slight reduction in effector binding can be placed in class D of mutations.

Another interesting aspect to be mentioned is the posttranslational modification of KRAS at Lys147 and probably also at Tyr71. Recent studies have shown that RAS proteins are ubiquitinated at the Lys 147, which leads to increased RAS activation by GEF proteins (45). A small fraction of the total RAS is ubiquitinated, which seems to represent an important amount of the PI3K- or RAF-bound active RAS (45). Therefore, Lys147 substitution to glutamate will possibly hinder ubiquitination and, in spite of the considerable amount of active $KRAS^{K147E}$ accumulated in the cells, the number of RAS molecules bound to their effector proteins is reduced. Moreover, $KRAS^{G12V/K147L}$ showed that in the absence of ubiquitination, the tumors are smaller than the control $KRAS^{G12V}$ (45). This may be another explanation why $KRAS^{K147E}$ despite immense accumulation in its active state exhibits only mild gain-of-function effects. Interestingly, Ser71, an equivalent residue in RAC1, has been shown to be a target of serine/threonine kinases, which if phosphorylated diminishes microbial pathogenesis by blocking RAC1 glucosylation by bacterial toxins (46). Taking the high structural identity of RAS and RAC1 into account, it is tempting to speculate that Tyr71 phosphorylation of KRAS by tyrosine kinases may likewise contribute negatively to RAS signalling, a scenario that would be perturbed in the case of $KRAS^{Y71H}$.

It seems that RAS mutations leading to developmental disorders might be the sum of all effects of RAS effector proteins. The phenotype/pathology observed in patients can be correlated with the biological functions derived from disturbed signalling of the wide variety of RAS effector proteins. In addition to the complexity brought by the wide variety of RAS effectors, not only the RAS/RAF/MEK/ERK axis may well be affected by RAS mutations. Using either MEK 1/2 inhibitors or siRNA against MEK1/2, one may monitor both RAF activity on other substrates and the ERK1/2 activation by other pathways. For example, eukaryotic translation elongation factor 1A, apoptosis-linked gene-2, Bcl-2-associated death promoter and their phosphorylation by RAF appear to have prosurvival functions (47–49) and might influence embryonic development. In addition, using MEK inhibitors or MEK siRNA, one can shed light as well in the ERK1/2 activation from p21-activated kinase 1 (PAK1), a mechanism important in lamellopodial dynamics (50). Posttranslational modification, including phosphorylation and ubiquitination, adds an additional degree in modulating RAS signalling that needs further attention.

A remarkable issue that should be mentioned at this point is the substitution of the highly conserved, positively charged lysine 147 for a negatively charged glutamic acid in the case of $KRAS^{K147E}$. Such substitutions often cause drastic changes in the attractive and/or repulsive interactions between adjacent amino acid residues. Interestingly, K147E mutation in KRAS is not as drastic as it seemed at first view. A comparison of Figure 4C and D shows that the interaction with Asp119 is basically affected. Such an effect is sufficient to cause a 150-fold increase in the GDP dissociation from $KRAS^{K147E}$ (Fig. 3A). However, all other contacts of the Lys147 side chain with both the nucleotide and particularly Phe28 are preserved by the Glu147 side chain. We hypothesize that a germline mutation causing a substitution of Lys147 with a smaller side chain such as alanine or glycine is highly likely lethal. Such a KRAS protein may function as a strong dominant-negative mutant and inhibit RAS signalling in cell during development. We conclude that most mutations associated with developmental disorders, including $KRAS^{K147E}$, are permissive mutations and are, thus, tolerated in the germline. Therefore, it is of major importance to look attentively at substituting amino acid, too.

MATERIALS AND METHODS

Plasmids and proteins

All constructs were produced and purified as described (19,20,25,51). Fluorescent nucleotide-loaded RAS proteins were prepared as described previously (52).

Kinetics of nucleotide dissociation and GEF-catalyzed nucleotide dissociation

Intrinsic dissociation of mant-GDP was quantified using a LS 50 B fluorescence spectrophotometer (Perkin Elmer) (19,53), and GEF-catalyzed mant-GDP dissociation from RAS proteins was studied using an Hightech stopped-flow apparatus as described (19,20,52,54). Observed rate constants (k_{obs}) were obtained by single exponential fitting of the data.

Intrinsic and GAP-stimulated GTP hydrolysis

Intrinsic and GAP-stimulated GTP hydrolysis of the RAS proteins was performed as described (25,52,54).

RAS/RAF1-RBD binding measurements

Interaction of RAS with RAF1-RBD was determined by isothermal titration calorimetry (ITC) using a VP-ITC-Isothermal Titration Calorimeter (Microcal, GE Healthcare) in 30 mM Tris–HCl, pH 7.6, 50 mM NaCl, 5 mM $MgCl_2$ at 25°C. GppNHp-loaded RAS proteins were filled into the sample cell and titrated with RAF-RBD. General instrument settings were as follows: 25°C, initiation delay 240 s, spacing 240 s, 11–13 μCal/sec reference power, 5–6 μl injection volume.

Cell-based assays

All cell-based experiments were performed as described (17,20). The EGF experiments were performed at a final concentration of 20 ng EFG (Sigma) per milliliter of culture medium. Antibodies for immunoblotting against RAS were obtained from Millipore™. Antibodies against MEK1/2, ERK1/2, AKT, phospho-MEK1/2 (Ser217/221), phospho-ERK1/2 (Thr202/Tyr204) and phospho-AKT (Ser473 or Thr308) were from Cell Signalling Technology.

Structural methods

Because no $KRAS^{wt}$ structure is available to date, the structures of HRAS were used in our study. The G-domains of HRAS and KRAS share 97% identity and are generally accepted to be structurally very similar, if not identical (25). The differences between the active and inactive state of RAS were analyzed by comparison of the GDP-bound (55) Protein Data Bank code [4Q21] and GTP-bound (56) [1CTQ] HRAS structure, respectively. These structures were selected because they represent wild-type RAS (RAS^{wt}) protein and have high resolutions among GDP- or GTP-bound structures. The interactions of RAS with its binding partners were analyzed on the basis of the structures of HRAS in complexes with $p120^{RASGAP}$ (29) [1WQ1], the GEF SOS1 (57) [1NVV] and the downstream effectors, RAF1-RBD (26) [1C1Y], PI3Kγ (58) [1HE8], BYR2-RBD (59) [1K8R], RALGDS (60) [1LFD] and PLCε (61) [2C5L].

SUPPLEMENTARY MATERIAL

Supplementary Material is available at *HMG* online.

Conflict of Interest statement. The authors have no conflicting interests.

FUNDING

This work was supported by the grants of E–Rare (NsEuroNet) to M.R.A. and M.Z.; Bundesministerium für Bildung und Forschung/Nationalen Genomforschungsnetzes Plus (grant number 01GS08100) to L.G.; Forschungskommission der Medizinischen Fakultät der Heinrich-Heine-Universität Düsseldorf (grant number 9772402) to S.C.Z.; and Deutsche Forschung Gemeinschaft (Sonderforschungbereich 974) to M.R.A. and I.C.C.

REFERENCES

1. Kratz, C.P., Schubbert, S., Bollag, G., Niemeyer, C.M., Shannon, K.M. and Zenker, M. (2006) Germline mutations in components of the Ras signalling pathway in Noonan syndrome and related disorders. *Cell Cycle*, **5**, 1607–1611.
2. Zenker, M. (2011) Clinical manifestations of mutations in Ras and related intracellular signal transduction factors. *Curr. Opin. Pediatr.*, **23**, 443–451.
3. Vetter, I.R. and Wittinghofer, A. (2001) Signal transduction–the guanine nucleotide-binding switch in three dimensions. *Science*, **294**, 1299–1304.
4. Guo, Z., Ahmadian, M.R. and Goody, R.S. (2005) Guanine nucleotide exchange factors operate by a simple allosteric competitive mechanism. *Biochemistry (Mosc)*, **44**, 15423–15429.
5. Scheffzek, K. and Ahmadian, M.R. (2005) GTPase activating proteins: structural and functional insights 18 years after discovery. *Cell Mol. Life Sci.*, **62**, 3014–3038.
6. Herrmann, C. (2003) Ras effector interactions: after one decade. *Curr. Opin. Struct. Biol.*, **13**, 122–129.
7. Karnoub, A.E. and Weinberg, R.A. (2008) Ras oncogenes: split personalities. *Nat. Rev. Mol Cell Biol.*, **9**, 517–531.
8. Harris, T.J.R. and McCormick, F. (2010) The molecular pathology of cancer. *Nat. Rev. Clin. Oncol.*, **7**, 251–265.
9. Pylayeva-Gupta, Y., Grabocka, E. and Bar-Sagi, D. (2011) Ras oncogenes: weaving a tumorigenic web. *Nat. Rev. Cancer*, **11**, 761–774.
10. Lo, F.S., Lin, J.L., Kuo, M.T., Chiu, P.C., Shu, S.G., Chao, M.C., Lee, Y.J. and Lin, S.P. (2009) Noonan syndrome caused by germline *KRAS* mutation in Taiwan: report of two patients and a review of the literature. *Eur. J. Pediatr.*, **168**, 919–923.
11. Carta, C., Pantaleoni, F., Bocchinfuso, G., Stella, L., Vasta, I., Sarkozy, A., Digilio, C., Palleschi, A., Pizzuti, A., Grammatico, P. *et al.* (2006) Germline missense mutations affecting KRAS isoform B are associated with a severe Noonan syndrome phenotype. *Am. J. Hum. Genet.*, **79**, 129–135.
12. Schubbert, S., Zenker, M., Rowe, S.L., Boll, S.B., Klein, C., Bollag, G., van der Burgt, I., Musante, L., Kalscheuer, V., Wehner, L.E. *et al.* (2006) Germline KRAS mutations cause Noonan syndrome. *Nat. Genet.*, **38**, 331–336.
13. Niihori, T., Aoki, Y., Narumi, Y., Neri, G., Cave, H., Verloes, A., Okamoto, N., Hennekam, R.C.M., Gillessen-Kaesbach, G., Wieczorek, D. *et al.* (2006) Germline KRAS and BRAF mutations in cardio-facio-cutaneous syndrome. *Nat. Genet.*, **38**, 294–296.
14. Nava, C., Hanna, N., Michot, C., Pereira, S., Pouvreau, N., Niihori, T., Aoki, Y., Matsubara, Y., Arveiler, B., Lacombe, D. *et al.* (2007) Cardio-facio-cutaneous and Noonan syndromes due to mutations in the RAS/MAPK signalling pathway: genotype-phenotype relationships and overlap with Costello syndrome. *J. Med. Genet.*, **44**, 763–771.
15. Kratz, C.P., Niemeyer, C.M. and Zenker, M. (2007) An unexpected new role of mutant Ras: perturbation of human embryonic development. *J. Mol. Med.*, **85**, 223–231.
16. Zenker, M., Lehmann, K., Schulz, A.L., Barth, H., Hansmann, D., Koenig, R., Korinthenberg, R., Kreiss-Nachtsheim, M., Meinecke, P., Morlot, S. *et al.* (2007) Expansion of the genotypic and phenotypic spectrum in patients with KRAS germline mutations. *J. Med. Genet.*, **44**, 131–135.
17. Gremer, L., Merbitz-Zahradnik, T., Dvorsky, R., Cirstea, I.C., Kratz, C.P., Zenker, M., Wittinghofer, A. and Ahmadian, M.R. (2011) Germline KRAS mutations cause aberrant biochemical and physical properties leading to developmental disorders. *Hum. Mutat.*, **32**, 33–43.
18. Aoki, Y., Niihori, T., Kawame, H., Kurosawa, K., Ohashi, H., Tanaka, Y., Filocamo, M., Kato, K., Suzuki, Y., Kure, S. and Matsubara, Y. (2005) Germline mutations in HRAS proto-oncogene cause Costello syndrome. *Nat. Genet.*, **37**, 1038–1040.
19. Gremer, L., De Luca, A., Merbitz-Zahradnik, T., Dallapiccola, B., Morlot, S., Tartaglia, M., Kutsche, K., Ahmadian, M.R. and Rosenberger, G. (2010) Duplication of Glu37 in the switch I region of HRAS impairs effector/GAP binding and underlies Costello syndrome by promoting enhanced growth factor-dependent MAPK and AKT activation. *Hum. Mol. Genet.*, **19**, 790–802.
20. Cirstea, I.C., Kutsche, K., Dvorsky, R., Gremer, L., Carta, C., Horn, D., Roberts, A.E., Lepri, F., Merbitz-Zahradnik, T., Konig, R. *et al.* (2010) A restricted spectrum of NRAS mutations causes Noonan syndrome. *Nat. Genet.*, **42**, 27–29.
21. Abankwa, D., Hanzal-Bayer, M., Ariotti, N., Plowman, S.J., Gorfe, A.A., Parton, R.G., McCammon, J.A. and Hancock, J.F. (2008) A novel switch region regulates H-ras membrane orientation and signal output. *EMBO J.*, **27**, 727–735.
22. Castellano, E. and Downward, J. (2011) Ras interaction with PI3K: more than just another effector pathway. *Genes and Cancer*, **2**, 261–274.
23. Merla, R., Ye, Y., Lin, Y., Manickavasagam, S., Huang, M.H., Perez-Polo, R.J., Uretsky, B.F. and Birnbaum, Y. (2007) The central role of adenosine in statin-induced ERK1/2, Akt, and eNOS phosphorylation. *Am. J. Physiol. Heart Circ. Physiol.*, **293**, H1918–H1928.
24. Stark, Z., Gillessen-Kaesbach, G., Ryan, M.M., Cirstea, I.C., Gremer, L., Ahmadian, M.R., Savarirayan, R. and Zenker, M. (2011) Two novel

germline KRAS mutations: expanding the molecular and clinical phenotype. *Clin. Genet.*, **81**, 590–594.
25. Ahmadian, M.R., Hoffmann, U., Goody, R.S. and Wittinghofer, A. (1997) Individual rate constants for the interaction of Ras proteins with GTPase-activating proteins determined by fluorescence spectroscopy. *Biochemistry*, **36**, 4535–4541.
26. Nassar, N., Horn, G., Herrmann, C., Scherer, A., McCormick, F. and Wittinghofer, A. (1995) The 2.2 A crystal structure of the Ras-binding domain of the serine/threonine kinase c-Raf1 in complex with RaplA and a GTP analogue. *Nature*, **375**, 554–560.
27. Jaitner, B.K., Becker, J., Linnemann, T., Herrmann, C., Wittinghofer, A. and Block, C. (1997) Discrimination of amino acids mediating RAS binding from noninteracting residues affecting Raf activation by double mutant analysis. *J. Biol. Chem.*, **272**, 29927–29933.
28. Weber, K.C., Slupsky, J.R., Herrmann, C., Schuler, M., Rapp, U.R. and Block, C. (2000) Mitogenic signalling of Ras is regulated by differential interaction with Raf isozymes. *Oncogene*, **19**, 169–176.
29. Scheffzek, K., Ahmadian, M.R., Kabsch, W., Wiesmuller, L., Lautwein, A., Schmitz, F. and Wittinghofer, A. (1997) The Ras-RasGAP complex: structural basis for GTPase activation and its loss in oncogenic Ras mutants. *Science*, **277**, 333–338.
30. Reinstein, J., Schlichting, I., Frech, M., Goody, R.S. and Wittinghofer, A. (1991) p21 with a phenylalanine 28–leucine mutation reacts normally with the GTPase activating protein GAP but nevertheless has transforming properties. *J. Biol. Chem.*, **266**, 17700–17706.
31. Schmidt, G., Lenzen, C., Simon, I., Deuter, R., Cool, R., Goody, R. and Wittinghofer, A. (1996) Biochemical and biological consequences of changing the specificity of p21Ras from guanosine to xanthosine nucleotides. *Oncogene*, **12**, 87–96.
32. Cool, R.H., Schmidt, G., Lenzen, C.U., Prinz, H., Vogt, D. and Wittinghofer, A. (1999) The Ras mutant D119N is both dominant negative and activated. *Mol. Cell. Biol.*, **19**, 6297–6305.
33. Aoki, Y., Niihori, T., Narumi, Y., Kure, S. and Matsubara, Y. (2008) The RAS/MAPK syndromes: novel roles of the RAS pathway in human genetic disorders. *Hum. Mutat.*, **29**, 992–1006.
34. Tidyman, W.E. and Rauen, K.A. (2008) Noonan, Costello and cardio-facio-cutaneous syndromes: dysregulation of the Ras-MAPK pathway. *Expert Rev. Mol. Med.*, **10**, e37.
35. Tartaglia, M., Gelb, B.D. and Zenker, M. (2011) Noonan syndrome and clinically related disorders. *Best Pract. Res. Clin. Endocrinol. Metab.*, **25**, 161–179.
36. Noonan, J.A. (2006) Noonan syndrome and related disorders: alterations in growth and puberty. *Rev. Endocr. Metab. Dis.*, **7**, 251–255.
37. Schubbert, S., Bollag, G., Lyubynska, N., Nguyen, H., Kratz, C.P., Zenker, M., Niemeyer, C.M., Molven, A. and Shannon, K. (2007) Biochemical and functional characterization of germ line KRAS mutations. *Mol. Cell. Biol.*, **27**, 7765–7770.
38. Gripp, K.W., Stabley, D.L., Nicholson, L., Hoffman, J.D. and Sol-Church, K. (2006) Somatic mosaicism for an HRAS mutation causes Costello syndrome. *Am. J. Med. Genet. A*, **140**, 2163–2169.
39. Rauen, K.A. (2007) HRAS and the Costello syndrome. *Clin. Genet.*, **71**, 101–108.
40. Gripp, K.W., Innes, A.M., Axelrad, M.E., Gillan, T.L., Parboosingh, J.S., Davies, C., Leonard, N.J., Lapointe, M., Doyle, D., Catalano, S. *et al.* (2008) Costello syndrome associated with novel germline HRAS mutations: an attenuated phenotype? *Am. J. Med. Genet. A,* **146A**, 683–690.
41. Yip-Schneider, M.T., Lin, A., Barnard, D., Sweeney, C.J. and Marshall, M.S. (1999) Lack of elevated MAP kinase (Erk) activity in pancreatic carcinomas despite oncogenic K-ras expression. *Int. J. Oncol.*, **15**, 271–279.
42. Giehl, K., Skripczynski, B., Mansard, A., Menke, A. and Gierschik, P. (2000) Growth factor-dependent activation of the Ras-Raf-MEK-MAPK pathway in the human pancreatic carcinoma cell line PANC-1 carrying activated K-ras: implications for cell proliferation and cell migration. *Oncogene*, **19**, 2930–2942.
43. Tuveson, D.A., Shaw, A.T., Willis, N.A., Silver, D.P., Jackson, E.L. and Chang, S. (2004) Endogenous oncogenic K-ras(G12D) stimulates proliferation and widespread neoplastic and developmental defects. *Cancer Cell*, **5**, 375–387.
44. Omerovic, J., Hammond, D.E., Clague, M.J. and Prior, I.A. (2007) Ras isoform abundance and signalling in human cancer cell lines. *Oncogene*, **27**, 2754–2762.
45. Sasaki, A.T., Carracedo, A., Locasale, J.W., Anastasiou, D., Takeuchi, K., Kahoud, E.R., Haviv, S., Asara, J.M., Pandolfi, P.P. and Cantley, L.C. (2011) Ubiquitination of K-ras enhances activation and facilitates binding to select downstream effectors. *Sci. Signal.*, **4**, ra13.
46. Schoentaube, J., Olling, A., Tatge, H., Just, I. and Gerhard, R. (2009) Serine-71 phosphorylation of Rac1/Cdc42 diminishes the pathogenic effect of *Clostridium difficile* toxin A. *Cell. Microbiol.*, **11**, 1816–1826.
47. Chen, C. and Sytkowski, A.J. (2005) Apoptosis-linked gene-2 connects the Raf-1 and ASK1 signallings. *Biochem. Biophys. Res. Commun.*, **333**, 51–57.
48. Ye, D.Z., Jin, S., Zhuo, Y. and Field, J. (2011) p21-Activated kinase 1 (Pak1) phosphorylates BAD directly at Serine 111 in vitro and indirectly through Raf-1 at Serine 112. *PLoS One*, 6, e27637.
49. Sanges, C., Scheuermann, C., Zahedi, R.P., Sickmann, A., Lamberti, A., Migliaccio, N., Baljuls, A., Marra, M., Zappavigna, S., Rapp, U. *et al.* (2012) Raf kinases mediate the phosphorylation of eukaryotic translation elongation factor 1A and regulate its stability in eukaryotic cells. *Cell Death Dis.*, **3**, e276.
50. Smith, S.D., Jaffer, Z.M., Chernoff, J. and Ridley, A.J. (2008) PAK1-mediated activation of ERK1/2 regulates lamellipodial dynamics. *J. Cell Sci.*, **121**, 3729–3736.
51. Hemsath, L. and Ahmadian, M.R. (2005) Fluorescence approaches for monitoring interactions of Rho GTPases with nucleotides, regulators, and effectors. *Methods*, **37**, 173–182.
52. Gremer, L., Gilsbach, B., Ahmadian, M.R. and Wittinghofer, A. (2008) Fluoride complexes of oncogenic Ras mutants to study the Ras-RasGAP interaction. *Biol. Chem.*, **389**, 1163–1171.
53. Eberth, A., Lundmark, R., Gremer, L., Dvorsky, R., Koessmeier, K.T., McMahon, H.T. and Ahmadian, M.R. (2009) A BAR domain-mediated autoinhibitory mechanism for RhoGAPs of the GRAF family. *Biochem. J.*, **417**, 371–377.
54. Eberth, A. and Ahmadian, M.R. (2009) *Current Protocols in Cell Biology*, **43**, 14.9.1–14.9.25. John Wiley & Sons, USA, Chapter 14:Unit 14.9.
55. Milburn, M.V., Tong, L., deVos, A.M., Brunger, A., Yamaizumi, Z., Nishimura, S. and Kim, S.H. (1990) Molecular switch for signal transduction: structural differences between active and inactive forms of protooncogenic Ras proteins. *Science*, **247**, 939–945.
56. Pai, E.F., Krengel, U., Petsko, G.A., Goody, R.S., Kabsch, W. and Wittinghofer, A. (1990) Refined crystal structure of the triphosphate conformation of H-ras p21 at 1.35 A resolution: implications for the mechanism of GTP hydrolysis. *EMBO J.*, **9**, 2351–2359.
57. Margarit, S.M., Sondermann, H., Hall, B.E., Nagar, B., Hoelz, A., Pirruccello, M., Bar-Sagi, D. and Kuriyan, J. (2003) Structural evidence for feedback activation by Ras.GTP of the Ras-specific nucleotide exchange factor SOS. *Cell*, **112**, 685–695.
58. Pacold, M.E., Suire, S., Perisic, O., Lara-Gonzalez, S., Davis, C.T., Walker, E.H., Hawkins, P.T., Stephens, L., Eccleston, J.F. and Williams, R.L. (2000) Crystal structure and functional analysis of Ras binding to its effector phosphoinositide 3-kinase gamma. *Cell*, **103**, 931–943.
59. Scheffzek, K., Grunewald, P., Wohlgemuth, S., Kabsch, W., Tu, H., Wigler, M., Wittinghofer, A. and Herrmann, C. (2001) The Ras-Byr2RBD complex: structural basis for RAS effector recognition in yeast. *Structure (Camb.)*, **9**, 1043–1050.
60. Huang, L., Hofer, F., Martin, G.S. and Kim, S.H. (1998) Structural basis for the interaction of RAS with RalGDS. *Nat. Struct. Biol.*, **5**, 422–426.
61. Bunney, T.D., Harris, R., Gandarillas, N.L., Josephs, M.B., Roe, S.M., Sorli, S.C., Paterson, H.F., Rodrigues-Lima, F., Esposito, D., Ponting, C.P. *et al.* (2006) Structural and mechanistic insights into ras association domains of phospholipase C epsilon. *Mol. Cell*, **21**, 495–507.

THE JOURNAL OF BIOLOGICAL CHEMISTRY VOL. 289, NO. 10, pp. 6839–6849, March 7, 2014

Functional Cross-talk between Ras and Rho Pathways

A Ras-SPECIFIC GTPase-ACTIVATING PROTEIN (p120RasGAP) COMPETITIVELY INHIBITS THE RhoGAP ACTIVITY OF DELETED IN LIVER CANCER (DLC) TUMOR SUPPRESSOR BY MASKING THE CATALYTIC ARGININE FINGER[*]

Received for publication, October 16, 2013, and in revised form, December 18, 2013 Published, JBC Papers in Press, January 17, 2014, DOI 10.1074/jbc.M113.527655

Mamta Jaiswal[‡1], Radovan Dvorsky[‡], Ehsan Amin[‡], Sarah L. Risse[‡], Eyad K. Fansa[‡], Si-Cai Zhang[‡], Mohamed S. Taha[‡], Aziz R. Gauhar[‡2], Saeideh Nakhaei-Rad[‡], Claus Kordes[§], Katja T. Koessmeier[‡], Ion C. Cirstea[‡¶], Monilola A. Olayioye[‖3], Dieter Häussinger[§], and Mohammad R. Ahmadian[‡4]

From the [‡]Institute of Biochemistry and Molecular Biology II and [§]Clinic for Gastroenterology, Hepatology and Infectiology, Medical Faculty, Heinrich Heine University, 40225 Düsseldorf, [¶]Leibniz Institute for Age Research, 07745 Jena, and [‖]Institute of Cell Biology and Immunology, University of Stuttgart, 70569 Stuttgart, Germany

Background: The regulatory mechanism of the DLC1 tumor suppressor protein is unclear.
Results: Structure-function analysis revealed determinants for the selectivity, activity, and inhibition of DLC1 RhoGAP function.
Conclusion: p120RasGAP competitively and selectively inhibits DLC1 by targeting its catalytic arginine finger.
Significance: This mechanistic study emphasizes the importance of the functional inter-relationships of GTPase-activating proteins mediating cross-talk between the Ras and Rho pathways.

The three deleted in liver cancer genes (DLC1–3) encode Rho-specific GTPase-activating proteins (RhoGAPs). Their expression is frequently silenced in a variety of cancers. The RhoGAP activity, which is required for full DLC-dependent tumor suppressor activity, can be inhibited by the Src homology 3 (SH3) domain of a Ras-specific GAP (p120RasGAP). Here, we comprehensively investigated the molecular mechanism underlying cross-talk between two distinct regulators of small GTP-binding proteins using structural and biochemical methods. We demonstrate that only the SH3 domain of p120 selectively inhibits the RhoGAP activity of all three DLC isoforms as compared with a large set of other representative SH3 or RhoGAP proteins. Structural and mutational analyses provide new insights into a putative interaction mode of the p120 SH3 domain with the DLC1 RhoGAP domain that is atypical and does not follow the classical P*XX*P-directed interaction. Hence, p120 associates with the DLC1 RhoGAP domain by targeting the catalytic arginine finger and thus by competitively and very potently inhibiting RhoGAP activity. The novel findings of this study shed light on the molecular mechanisms underlying the DLC inhibitory effects of p120 and suggest a functional cross-talk between Ras and Rho proteins at the level of regulatory proteins.

The Ras and Rho families of small GTP-binding proteins are key transducers of a variety of cellular processes ranging from reorganization of the cytoskeleton to transcriptional regulation and control of cell growth and survival (1). Loss of the control mechanisms and aberrant activation of Ras and Rho proteins are one of the most common molecular alterations found in cancer cells promoting tumor growth and metastasis (2–5). Ras signaling stimulates diverse pathways and signals toward Rho proteins, which are known to be required for cell transformation by oncogenic Ras (6–8). Emerging evidence suggests that the GTPase-activating proteins (GAPs),[5] in particular p120RasGAP (also known as RAS p21 protein activator 1 or RASA1; here called p120) and the Rho-specific p190ARhoGAP (also known as ARHGAP35; here called p190), p200RhoGAP (also known as ARHGAP32, p250GAP, GC-GAP, Rics, or Grit) and deleted in liver cancer 1 (DLC1; also known as ARHGAP7, p122RhoGAP, or STARD12), act as a linker between Ras and Rho signaling pathways (9–11). GAPs are multifaceted and multifunctional molecules (12, 13) and are the principal inactivators of Ras and Rho signaling. They utilize a catalytic "arginine finger" to stimulate the inefficient intrinsic GTP hydrolysis reaction of these small GTP-binding proteins by several orders of magnitude (14).

* This work was supported in part by the German Research Foundation (Deutsche Forschungsgemeinschaft (DFG)) through the Collaborative Research Center 974 (SFB 974) "Communication and Systems Relevance during Liver Injury and Regeneration," the International Research Training Group 1902 (IRGT1902), and Project Grant AH 92/5-1; the National Genome Research Network Plus program of the German Ministry of Science and Education (Bundesministerium für Bildung und Forschung Grant 01GS08100); and the International North Rhine-Westphalia Research School BioStruct granted by the Ministry of Innovation, Science and Research of the State North Rhine-Westphalia, the Heinrich Heine University of Düsseldorf, and the Entrepreneur Foundation at the Heinrich Heine University of Düsseldorf.
[1] Present address: Structural Biology Group, Max Planck Inst. for Molecular Physiology, Otto-Hahn-Strasse 11, 44227 Dortmund, Germany.
[2] Present address: Inst. of Physical Biology, Heinrich Heine University, 40255 Düsseldorf, Germany.
[3] Supported by the DFG Heisenberg program.
[4] To whom correspondence should be addressed: Inst. für Biochemie und Molekularbiologie II, Medizinische Fakultät der Heinrich-Heine-Universität, Universitätsstrasse 1, Gebäude 22.03, 40255 Düsseldorf, Germany. Tel.: 49-211-811-2384; Fax: 49-211-811-2726; E-mail: reza.ahmadian@uni-duesseldorf.de.

[5] The abbreviations used are: GAP, GTPase-activating protein; DLC, deleted in liver cancer; SH, Src homology; SAM, sterile α motif; START, steroidogenic acute regulatory related lipid transfer; aa, amino acids; tamra, tetramethylrhodamine; aSEC, analytical size exclusion chromatography; ITC, isothermal titration calorimetry.

Frequent loss of *DLC1* gene expression was first described in liver cancer (15) and later in breast, colon, gastric, prostate, cervical, esophageal, and other cancers (16–18). DLC1 RhoGAP function is required for the maintenance of cell morphology and the coordination of cell migration (11, 19–21). DLC1 and its isoforms DLC2 (also known as ARHGAP37 or STARD13) and DLC3 (also known as ARHGAP38 or STARD8) consist of an N-terminal sterile α motif (SAM) domain, a central phosphorylation region followed by the catalytic RhoGAP domain, and a C-terminal steroidogenic acute regulatory related lipid transfer (START) domain (see Fig. 1*A*) (22, 23). The SAM and GAP domains are linked by a serine-containing region, which contains a recognition motif for the phosphoserine/phosphothreonine-binding 14-3-3 adaptor proteins (22). DLC1 has been reported to interact with tensin, talin, focal adhesion kinase, and α-catenin (22, 24–29) and with lipids (30). However, the precise mechanism of DLC1 regulation remains unclear.

An emerging theme is that RhoGAPs, such as the OPHN1 and GRAF1 (31, 32) and p50RhoGAP (33–36), require activation through the relief of autoinhibitory elements. These elements are collectively membrane-binding modules, including BAR (Bin/Amphiphysin/Rvs), PH (pleckstrin homology), C1, and Sec14 domains (31–33, 36). The SAM domain of DLC1 has been suggested to act as an autoinhibitory domain of DLC1 RhoGAP activity *in vitro* and *in vivo*. SAM domain-deleted DLC1 displayed enhanced catalytic activity for RhoA (20). However, it is still unclear how such an autoregulatory mechanism of DLC1 may operate.

p120 contains multiple domains with different functions (see Fig. 1*B*) (37). Whereas the C terminus of p120 with the catalytic GAP activity is responsible for Ras inactivation (38–40), its N-terminal Src homology 2 and 3 (SH2 and SH3) domains have been suggested to possess an effector function (41–44). p120 functionally modulates Rho signaling by direct binding to two Rho-specific GAPs, p190 and DLC1 (9, 11, 45). The association of p120 with the tyrosine phosphorylated p190 via its SH2 domain promotes Rho inactivation (45–47). Thus, p120 positively regulates the RhoGAP function of p190. Another mechanism, which connects the Ras and Rho pathways and regulates the actin cytoskeleton, is dependent on the p120 SH3 domain and controls Rho activation (41). This mechanism was later revealed to involve DLC1 but not p190 (11). Here, the p120 SH3 domain (called $p120^{SH3}$) binds to the RhoGAP domain of DLC1 (called $DLC1^{GAP}$) and inhibits the DLC1-dependent Rho inactivation (11). Hereby, p120 acts as a negative regulator not only for Ras but also for the GAP activity of DLC1. However, the molecular mechanisms underlying these cross-talk phenomena have not yet been elucidated.

In this study, we have explored the regulatory mechanism of DLC1 at the molecular level, in particular its *trans*-inhibition by $p120^{SH3}$. We have characterized the selectivity of the interaction between the $DLC1^{GAP}$ and $p120^{SH3}$ using a large number of purified SH3 and RhoGAP proteins and identified structural and functional determinants for the DLC1-p120 interaction. This study provides deep insights into the underlying regulatory cross-talk between the Rho and Ras family of small GTP-binding proteins.

EXPERIMENTAL PROCEDURES

Constructs—Human Abr^{GAP} (aa 559–822), $DLC1^{fl}$ (aa 1–1091), $DLC1^{GAP}$ (aa 609–878), $DLC1^{SAM}$ (aa 1–96), $DLC1^{START}$ (aa 880–1079), $DLC2^{GAP}$ (aa 644–916), $DLC3^{GAP}$ (aa 620–890), $GRAF1^{GAP}$ (aa 383–583), $MgcRac^{GAP}$ (aa 343–620), $Nadrin^{GAP}$ (aa 245–499), $OPHN1^{GAP}$ (aa 375–583), $p50^{GAP}$ (aa 198–439), $p190^{GAP}$ (aa 1250–1513), N-terminal truncated $p120^{\Delta n128}$ (aa 129–1047); SH2-SH3-SH2-encoding $p120^{SH2\text{-}3\text{-}2}$ (aa 129–447), $p120^{SH3}$ (aa 275–350), Src^{SH3} (aa 77–140), and human RhoA (aa 1–181), Cdc42 (aa 1–178), and Rac1 (aa 1–184) were amplified by standard PCR and cloned in pGEX-4T1 and pGEX-4T1-NTEV, respectively. Constructs of SH3 domain of $Crk1^{SH3}$ (aa 131–191), $Grb2^{SH3\text{-}1}$ (aa 1–55), $Grb2^{SH3\text{-}2}$ (aa 159–217), $Nck1^{SH3\text{-}1}$ (aa 5–60), $Nck1^{SH3\text{-}2}$ (aa 109–163), and $Nck1^{SH3\text{-}3}$ (aa 173–262) were created as described previously (48).

Site-directed Mutagenesis—Point mutations N311R; L313A; W319G; and N311R,L313A,W319G in $p120^{SH3}$ and R677A in $DLC1^{GAP}$ were generated using the QuikChange™ site-directed mutagenesis kit (Stratagene) and confirmed by DNA sequencing.

Proteins—Escherichia coli BL21(DE3) pLysS, BL21(DE3) CodonPlus-RIL, and Rosetta(DE3) strains containing the respective plasmids (see constructs) were grown to an A_{600} of 0.7 (37 °C at 140 rpm) and induced with 0.1 mM isopropyl β-D-thiogalactopyranoside overnight at 25 °C as described before (49, 50). All proteins were isolated in a first step as glutathione *S*-transferase (GST) fusion proteins by affinity chromatography on a GSH-agarose column and in a second step by size exclusion chromatography (Superdex S75 or S200) after proteolytic cleavage of GST. GTP-binding proteins without nucleotide (nucleotide-free form) or with tetramethylrhodamine-conjugated GTP (tamraGTP) were prepared as described before (49, 50). Concentrations of proteins were determined by Bradford assay or absorbance at 280 nm using the extinction coefficient deduced from the protein sequence. Purified proteins were snap frozen in liquid nitrogen and stored at −80 °C.

Analytical Size Exclusion Chromatography (aSEC)—aSEC for the detection of complex formation was performed for $DLC1^{GAP}$ and $p120^{SH3}$ on a Superdex 75 column (10/300) using buffer containing 30 mM HEPES, pH 7.6, 5 mM $MgCl_2$, 150 mM NaCl, and 3 mM DTT. 10 μM $DLC1^{GAP}$ was incubated with 15 μM $p120^{SH3}$ for 5 min at 4 °C in the same buffer in a total volume of 150 μl. Before loading to an aSEC column, samples were spun at 13,000 rpm at 4 °C to remove any particulate impurities. The flow rate was maintained at 0.5 ml/min, and 500-μl fractions were collected. Peak fractions were visualized by 15% SDS-PAGE and subsequent Coomassie Blue staining.

Kinetics Measurements—All fluorescence measurements were performed at 25 °C in a buffer containing 30 mM Tris-HCl, pH 7.5, 10 mM K_2HPO_4/KH_2PO_4, pH 7.4, 10 mM $MgCl_2$, and 3 mM DTT. The tamraGTP hydrolysis of Rho proteins (0.2 μM) was measured in the absence and presence of different amounts of respective GAP proteins as described previously (49, 52). Fast kinetics (<1000 s) were performed with a Hi-Tech Scientific SF-61 stopped-flow instrument with a mercury xenon light source and TgK Scientific Kinetic Studio software (version

2.19). An excitation wavelength of 545 nm was used for tamra. Emission was detected through a cutoff filter of 570 nm. Slow kinetics (>1000 s) were measured on a PerkinElmer Life Sciences spectrofluorometer (LS50B) using an excitation wavelength of 545 nm and an emission wavelength of 583 nm. Data were evaluated by single exponential fitting with the GraFit program to obtain the observed rate constant (k_{obs}) for the respective reaction as described before (49, 52).

Isothermal Titration Calorimetry (ITC) Measurements—The interaction of $DLC1^{GAP}$ and $p120^{SH3}$ and analysis of $DLC1^{GAP}$ variant and different $p120^{SH3}$ variants were studied by ITC (MicroCal™ VP-ITC microcalorimeter) as described (48). All measurements were carried out in 30 mM Tris-HCl, pH 7.5, 150 mM NaCl, 5 mM $MgCl_2$, and 1 mM tris(2-carboxyethyl)phosphine hydrochloride. The data were analyzed using Origin 7.0 software provided by the manufacturer.

Structural Analysis—To obtain insight into the residues responsible for the binding of the SH3 domain of p120 and RhoGAP domain of DLC1, docking of their corresponding structures (Protein Data Bank code 2J05 (53) and Protein Data Bank code 3KUQ, respectively), was performed with the program PatchDock (54). From the 20 best scored models, we selected the lowest energy model, which also has the Arg finger Arg-677 at the interface, and used it for further refinement with the program CHARMM (55). As the arginine finger is assumed to be crucial for the formation of the complex, we thoroughly explored its conformation in the course of refinement. Torsion angles of its side chain were additionally set up according to the Dynameomics rotamer library (56), and the energy of each complex was minimized by 2000 steps using the adapted basis Newton-Raphson method.

RESULTS

Low GAP Activities of the DLC Isoforms—Real time kinetic measurements of the RhoGAP activities of the DLC isoforms toward Cdc42, Rac1, and RhoA were performed using purified RhoGAP domains of the DLC proteins (Fig. 1) and fluorescent tamraGTP. This GTP analog is sensitive toward conformational changes induced by GTP hydrolysis (52). As shown in Fig. 2*A*, the very slow intrinsic tamraGTP hydrolysis of Cdc42 (*inset*) was markedly increased in the presence of the RhoGAP domain of DLC1 ($DLC1^{GAP}$). Similar experiments were performed under the same conditions with Rac1 and RhoA (Fig. 2*B*). Observed rate constants (k_{obs}) of respective $DLC1^{GAP}$ activities are presented in comparison with intrinsic hydrolysis rates as *bars* in Fig. 2*B*. $DLC1^{GAP}$ exhibited the highest activity for RhoA (1,650-fold) and Cdc42 (332-fold) and the lowest activity for Rac1 (75-fold). We next focused on the differences among the DLC isoforms and measured the activities of DLC2 and DLC3 for Cdc42 (Fig. 2*C*). Obtained data show that DLC2 and DLC3 exhibit 78- and 11-fold lower GAP activities, respectively, as compared with that of DLC1. Our results indicate that the DLC family members are inefficient GAPs, at least *in vitro*, with catalytic activities that are several orders of magnitude lower than the activities of the RhoGAPs p50 and p190 (Fig. 2*C*) or other highly efficient RhoGAPs, such as GRAF1 or OPHN1 (32).

A comparison of the obtained data on the DLC isoforms with those of other RhoGAP family members raised the question of whether the extremely low GAP activities of DLC proteins stem from effects on either binding affinity (K_d) or catalytic activity (k_{cat}). Therefore, we measured the kinetics of tamraGTP hydrolysis of Cdc42 at increasing concentrations of $DLC1^{GAP}$ and $GRAF1^{GAP}$. The rate constants (k_{obs}) of the fitted single exponential decays increased in a hyperbolic manner as a function of GAP concentrations as described previously (52, 57). We used Cdc42 in most experiments because of a large change in fluorescence upon tamraGTP hydrolysis as compared with Rac1 and RhoA. Fitting a hyperbolic curve to the points according to Equation 1 led to the corresponding kinetic parameters K_d and k_{cat} (Fig. 2*D*).

$$k_{obs} = \frac{k_{cat}}{1 + \frac{K_d}{[DLC1]}} \quad \text{(Eq. 1)}$$

Unlike the relatively similar K_d values, there was a large difference in the k_{cat} values for the GTP hydrolysis reaction: 6.26 s^{-1} for $DLC1^{GAP}$compared with 289 s^{-1} for the highly efficient $GRAF1^{GAP}$. These data clearly indicate that the very low GAP activity of the DLC proteins relies more on the catalytic activity than on the binding affinity to Cdc42.

Insights into cis-Regulatory Modules of DLC1 Function—To examine the influence of other domains of DLC1 (Fig. 1*A*) on its GAP activity, we further measured tamraGTP hydrolysis of Cdc42 stimulated by full-length DLC1 ($DLC1^{fl}$). As shown in Fig. 3*A*, $DLC1^{fl}$ exhibited a strongly reduced GAP activity as compared with the isolated $DLC1^{GAP}$. The k_{obs} values obtained from single turnover kinetic data were 0.02 and 0.47 s^{-1}, respectively, and reveal that the $DLC1^{fl}$ activity was 23.5-fold lower than that of $DLC1^{GAP}$ (Fig. 3*B*). This result strongly supports the previous notion that other regions of DLC1, such as the SAM domain (20), may undergo an intramolecular interaction with the GAP domain and thus contribute to its autoinhibition in a *cis*-inhibitory manner.

To analyze whether the autoinhibitory effect is caused by N- and C-terminal SAM and/or START domains of DLC1 (Fig. 1*A*), we purified these domains and measured their effects on the $DLC1^{GAP}$ activity *in vitro*. Using high concentrations of SAM, START, or both (up to a 100-fold molar excess above the GAP domain), we did not observe any significant inhibition of the $DLC1^{GAP}$ activity using tamraGTP hydrolysis of Cdc42 (Fig. 3*C*). The fact that the isolated SAM and START domains did not reveal any GAP-inhibitory activity strongly suggests that the autoinhibitory mechanism of DLC1 may require additional regions of the full-length protein. One possibility is the serine-rich 14-3-3 binding region between the SAM and the GAP domains (Fig. 1*A*).

p120 SH3 as a Potent trans-Inhibitory Factor of the $DLC1^{GAP}$ Activity—The SH3 domain of p120 has been reported as a novel binding partner of DLC1 with GAP-inhibitory and growth suppression activity (11). To monitor this effect in real time, $DLC1^{GAP}$ activity was measured in the absence and presence of purified $p120^{SH3}$ under the same conditions as in the experiments described above (Fig. 2). As shown in Fig. 4*A*, $DLC1^{GAP}$-

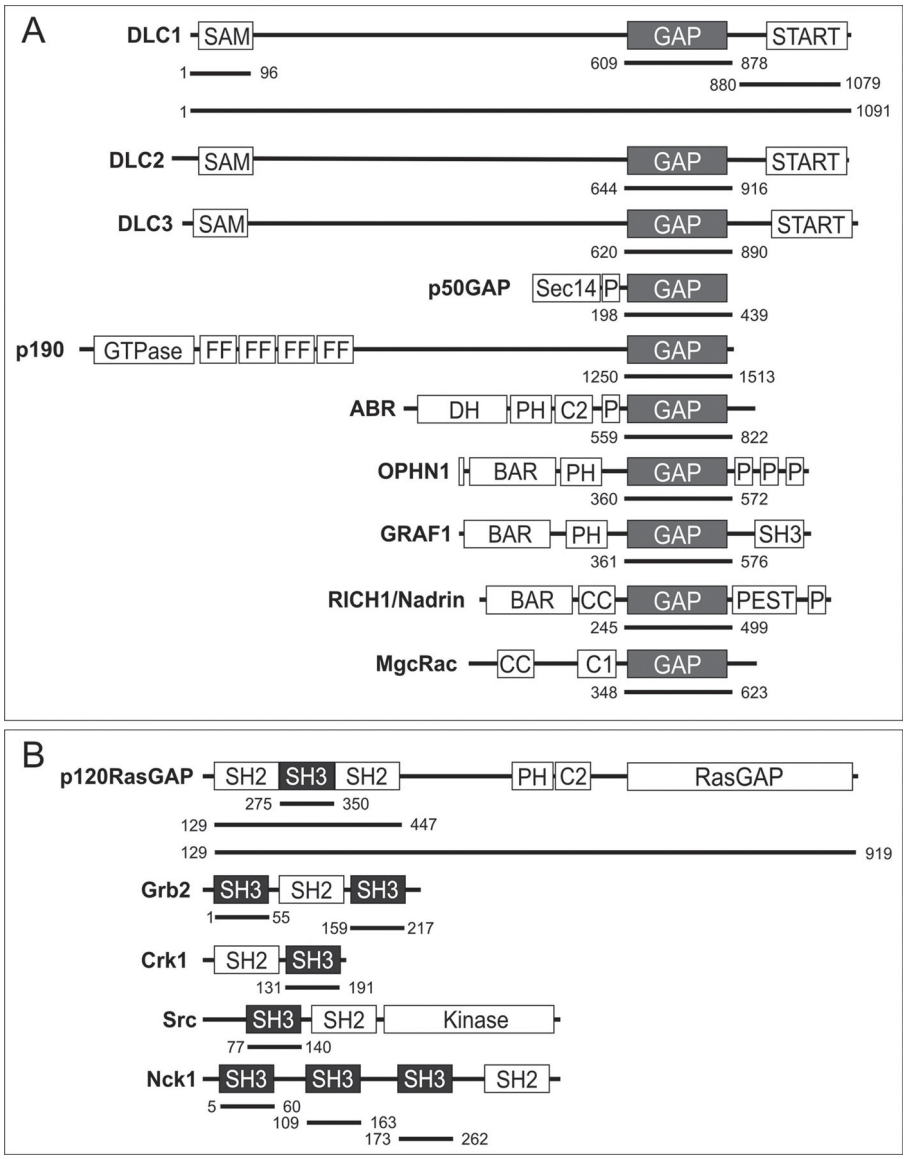

FIGURE 1. **Schematic representation of domain organization and designed fragments of GAP (*A*) and SH3 domain-containing proteins (*B*) used in this study.** The *numbers* indicate the N and C termini of the amino acids of the respective fragments. *BAR*, Bin/Amphiphysin/Rvs; *C1*, cysteine-rich region; *CC*, coiled coil; *DH*, Dbl homology domain; *FF*, double phenylalanine; *P*, proline-rich; *PH*, pleckstrin homology; *PSET*, proline, serine, glutamic acid, and threonine; *RGS*, regulator of G-protein signaling; *Sec14*, secretion and cell surface growth 14.

stimulated tamraGTP hydrolysis of Cdc42 was drastically reduced using a 10-fold excess of $p120^{SH3}$ over the $DLC1^{GAP}$ concentration. The respective k_{obs} value of 0.63 for $DLC1^{GAP}$ activity was reduced by 83-fold in the presence of $p120^{SH3}$ to 0.0076 s^{-1} (Fig. 4*B*), which is close to the intrinsic tamraGTP hydrolysis of Cdc42 (0.02 s^{-1}). These measurements were also performed for RhoA and Rac1 using the same conditions as for Cdc42 (Fig. 4*B*). Similarly, 247- and 15.5-fold reductions of the $DLC1^{GAP}$ activity for RhoA and Rac1, respectively, were determined in the presence of a 10-fold molar excess of $p120^{SH3}$. An explanation for this large variation may be the significant differences in $DLC1^{GAP}$ binding affinity for the three members of the Rho family.

In the next step, we analyzed the inhibitory effect of $p120^{SH3}$ on the GAP activity of DLC2 and DLC3 toward Cdc42. Fig. 4*C* shows that the catalytic GAP activity of purified $DLC2^{GAP}$ and $DLC3^{GAP}$ was also inhibited in the presence of $p120^{SH3}$ but not as drastically as in the case of $DLC1^{GAP}$. The next question we addressed was whether the SH3 domain is freely accessible to exert its inhibitory effect or whether other domains of p120 also play a role in the inhibition of DLC GAP activity (Fig. 1). Therefore, we purified the SH2-SH3-SH2-encompassing $p120^{SH2\text{-}3\text{-}2}$ and N-terminal truncated $p120^{\Delta n128}$ proteins and analyzed their $DLC1^{GAP}$ inhibitory effects in direct comparison with isolated $p120^{SH3}$. Larger p120 fragments inhibited the $DLC1^{GAP}$ activity but to a 19- and 10-fold lower extent than $p120^{SH3}$ (Fig. 4*D*).

Taken together, our *in vitro* data demonstrate that (i) $p120^{SH3}$ acts as a potent *trans*-inhibitory factor of the GAP activity of the DLC isoforms and (ii) the SH3 domain of p120 is not completely unmasked (freely accessible) in the presence of other p120 domains, especially the adjacent SH2 domains. Whether the N-terminal 128 amino acids play a role in this regard remains unclear. Full-length p120 could not be purified due to its instability.

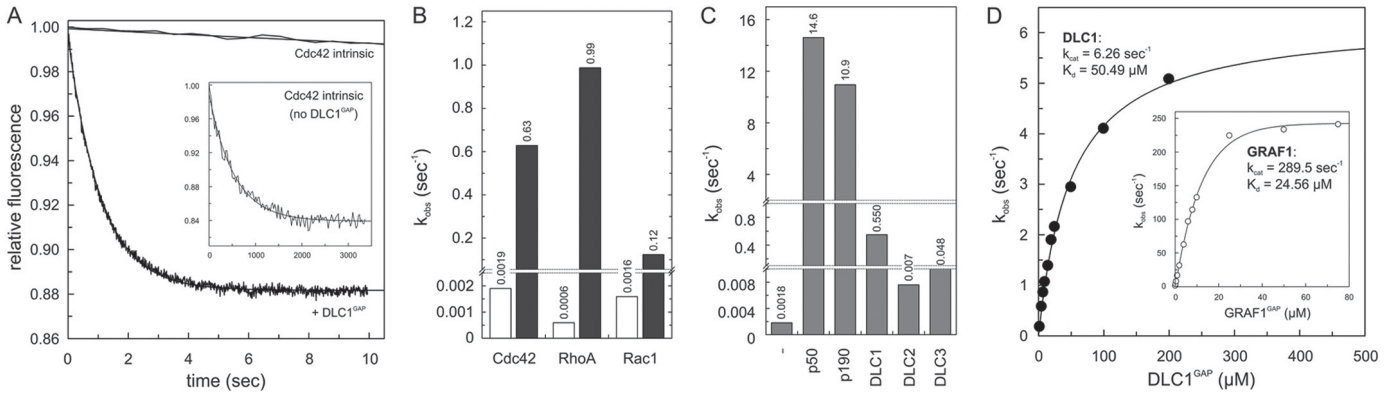

FIGURE 2. **Inefficient GAP activities of the DLC isoforms.** *A*, Cdc42-tamraGTP (0.2 μM) was rapidly mixed with 5 μM DLC1^{GAP} to monitor the GAP-stimulated tamraGTP hydrolysis reaction of Cdc42 in real time. Note the very slow intrinsic GTPase reaction of Cdc42 (*inset*) that was measured in the absence of GAP. Rate constants (k_{obs}) were obtained by single exponential fitting of the data. *B*, the k_{obs} values of GTP hydrolysis of Rho proteins (0.2 μM) measured in the presence of DLC1^{GAP} (5 μM) are represented as a column chart. Calculated -fold activation values were obtained by dividing the k_{obs} values of GAP-stimulated reactions by the k_{obs} values of the intrinsic reactions of respective GTPases. For convenience, the k_{obs} values are given above the *bar charts*. *C*, measured GAP activities of DLC1, DLC2, and DLC3 (5 μM, respectively) toward Cdc42 (0.2 μM) were very low as compared with p150 and p190. *D*, the GTP hydrolysis of Cdc42 (0.2 μM) was measured in the presence of increasing concentrations of the respective GAP domains of DLC1 and GRAF1 (*inset*). The dependence of the k_{obs} values of the GAP-stimulated GTP hydrolysis plotted on the concentrations of DLC1^{GAP} and GRAF1 was fitted by a hyperbolic curve to obtain the kinetic parameters (k_{cat} and K_d).

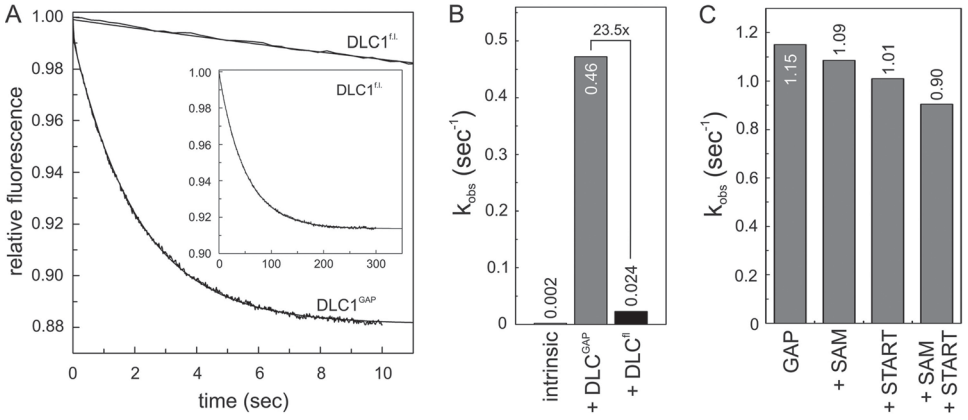

FIGURE 3. ***cis*-Acting regulation of DLC1^{GAP} activity.** *A*, kinetics of the tamraGTP hydrolysis reaction of Cdc42 (0.2 μM) stimulated by DLC1^{fl} (5 μM) was much slower (*inset*) than that stimulated by DLC^{GAP} (5 μM). *B*, the k_{obs} values, illustrated as a bar chart, showed that the GAP activity of DLC1^{fl} is reduced by 23.5-fold as compared with that of the DLC1^{GAP} but not completely inhibited as compared with the intrinsic GTPase reaction. For convenience, the k_{obs} values are given above the *bar charts*. *C*, the activity of DLC1^{GAP} (10 μM) on tamraGTP hydrolysis of Cdc42 (0.2 μM) was not significantly changed in the presence of a 100-fold excess of SAM, START, or both domains (1 mM, respectively).

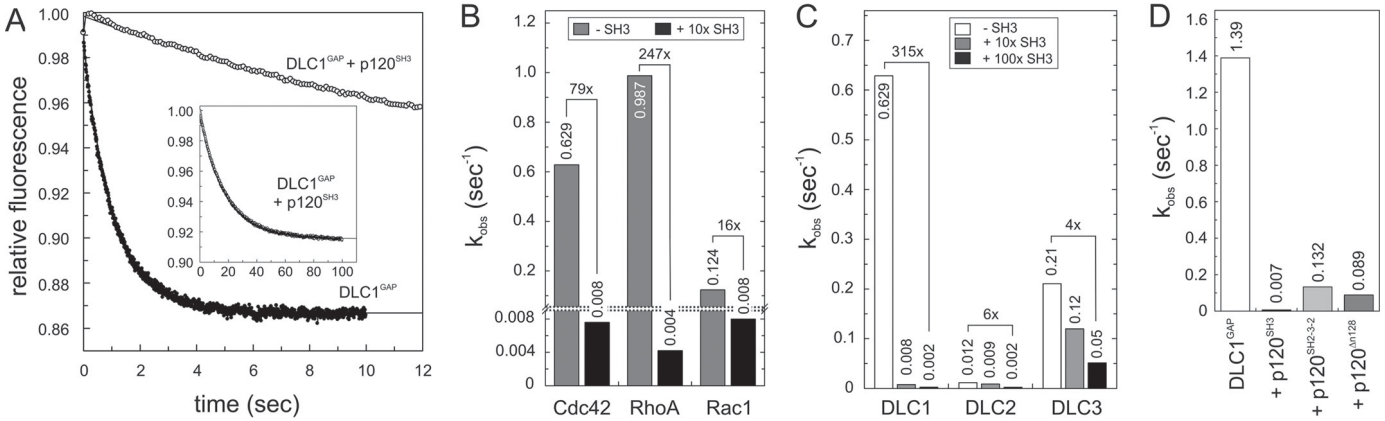

FIGURE 4. **p120^{SH3} as a potent inhibitor of the DLC GAP function.** *A*, kinetics of the tamraGTP hydrolysis reaction of Cdc42 (0.2 μM) stimulated by DLC1^{GAP} (5 μM) was reduced in the presence of a 10-fold excess of p120^{SH3} (50 μM). The complete reaction is shown in the *inset*. *B*, DLC1^{GAP} activities toward Cdc42, RhoA, and Rac1, measured under the same conditions as in *A*, are strongly inhibited by p120^{SH3}. For convenience, the k_{obs} values are given above the *bar charts*. *C*, DLC3^{GAP} (5 μM) was not inhibited by p120^{SH3} (50 and 500 μM) as efficiently as DLC1^{GAP} and DLC2^{GAP} (5 μM, respectively). *D*, p120$^{SH2\text{-}3\text{-}2}$ and p120$^{\Delta n128}$ (40 μM) inhibited the activity of DLC^{GAP} (10 μM) but not as efficiently as p120^{SH3} (40 μM).

Highly Selective Interaction between p120^{SH3} and DLC1^{GAP}—The next issue we addressed was the selectivity of the p120^{SH3} toward DLC1^{GAP}. Therefore, we purified seven additional RhoGAP and SH3 domains of other proteins (Fig. 1). We measured the effect of p120^{SH3} on the GAP activity of Abr, GRAF1, MgcRacGAP, Nadrin, OPHN1, p50, and p190 on the one hand

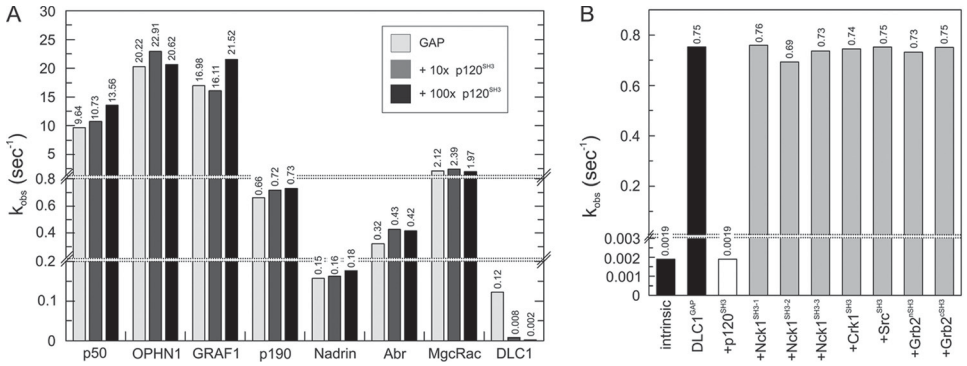

FIGURE 5. **Highly selective interaction between p120^{SH3} and DLC1^{GAP}.** *A*, p120^{SH3}-inhibiting effect on seven additional RhoGAPs (2 μM, respectively) was measured using the tamraGTP hydrolysis reaction of Cdc42 (0.2 μM) and p120^{SH3} (20 and 200 μM, respectively). p120^{SH3} inhibited only DLC1^{GAP} but not the other RhoGAPs. For convenience, the k_{obs} values are given above the *bar charts*. *B*, the effect of seven additional SH3 proteins (100 μM, respectively) on inhibiting DLC1^{GAP} (10 μM) was measured. Only p120^{SH3} inhibited DLC1^{GAP} but not the other SH3 domains.

and the effects of the SH3 domains of Crk1, c-Src, Grb2 (N- and C-terminal SH3 domains), and Nck1 (all three SH3 domains) on the DLC1^{GAP} activity on the other hand. As summarized in Fig. 5, neither did p120^{SH3} inhibit the activity of other GAPs of the Rho family (Fig. 5*A*) nor was the DLC1^{GAP} activity affected by the presence of other SH3 domains (Fig. 5*B*). These data clearly demonstrate that the p120^{SH3}-mediated *trans*-inhibition of DLC isoforms is highly selective.

Potent DLC1 Inhibition Due to High Affinity p120^{SH3}-DLC1^{GAP} Complex Formation—In the next step, we characterized in more detail the interaction between p120^{SH3} and DLC1^{GAP} as well as the inhibition of the DLC1^{GAP} activity induced by p120^{SH3} using different qualitative and quantitative biophysical and biochemical methods. aSEC is an accurate and simple method to visualize high affinity protein-protein interactions. p120^{SH3} (9 kDa) and DLC1^{GAP} (31 kDa) alone and a mixture of both proteins were loaded on a Superdex 75 (10/300) column, and eluted peak fractions were analyzed by SDS-PAGE. Data summarized in Fig. 6*A* clearly illustrate that a mixture of p120^{SH3} and DLC1^{GAP} shift the elution profile of the respective protein domains to an elution volume of 10.5 ml, indicating the formation of a complex between both proteins. We next determined the inhibitory potency of p120^{SH3} by measuring DLC1^{GAP} activity at increasing concentrations of p120^{SH3}. An inhibitory constant (K_i) of 0.61 μM was calculated by fitting the Morrison equation for a tight binding inhibitor (58) to individual k_{obs} values plotted against different p120^{SH3} concentrations (Fig. 6*B*). Furthermore, we measured the dissociation constant of the p120^{SH3}-DLC1^{GAP} interaction using ITC. The results shown in Fig. 6*C* allowed the determination of a stoichiometry of 1:1 and a dissociation constant (K_d) of 0.6 μM for the binding of p120^{SH3} to DLC1^{GAP} (Fig. 6*C*); this value nicely resembles the K_i value obtained from inhibition kinetics (Fig. 6*B*). This binding affinity is remarkably high and unexpected considering the low micromolar range affinities of SH3 domains for their P*XX*P-containing proteins (59). Taken together, these data strongly suggest that the mode of the p120^{SH3}-DLC1^{GAP} interaction most likely differs from the conventional SH3 interaction with P*XX*P loop motifs as recently published (48).

Structural Insight into a Putative Binding Mode between p120^{SH3} and DLC1^{GAP}—The high nanomolar affinity of p120^{SH3} for DLC1^{GAP} and the absence of a P*XX*P motif in DLC1^{GAP} strongly support the notion that the p120^{SH3}-DLC1^{GAP} interaction is mediated via a novel binding mechanism. To gain insight into the structural basis of this interaction, we first performed protein-protein docking of available crystal structures of p120^{SH3} (Protein Data Bank code 2J05) (53) and DLC1^{GAP} (Protein Data Bank code 3KUQ) using the PatchDock program (54). The model of the complex ranked as the first among 20 resulting models fulfilled the criteria for a close proximity of p120^{SH3} to the catalytic arginine finger (Arg-677) of the DLC1^{GAP} domain and was thus selected for refinement by molecular modeling methods. Inspecting the refined model, we identified three potential DLC1^{GAP} binding residues of p120^{SH3} (Asn-311, Leu-313, and Trp-319) that were closest to the catalytic Arg-677 of DLC1^{GAP} (Fig. 7*A*). We proposed that mutation of these residues may impair binding of the SH3 domain, which otherwise masks the arginine finger of DLC1^{GAP}. Catalytic arginine is known to stabilize the transition intermediate state of the hydrolysis reaction in the active center of Rho proteins (Fig. 7*B*) (14, 60). This assumption also suggests that p120 competitively inhibits DLC1 GAP function.

To validate our assumption, we performed mutational analysis of the above mentioned key residues at the p120^{SH3}-DLC1^{GAP} interface: N311R, L313A, and W319G in p120^{SH3} (single, double, and triple single point mutations) and R677A in DLC1^{GAP}. Expectedly, DLC1^{GAP} with the catalytic arginine finger substituted to alanine was deficient in stimulating tamraGTP hydrolysis of Cdc42 (data not shown) and most remarkably in associating with p120^{SH3} (Fig. 8, *A* and *B*). The latter was examined using two independent methods, ITC and aSEC. Reciprocally, p120$^{SH3(N311R,L313A,W319G)}$ was almost disabled in inhibiting DLC1^{GAP} activity (Fig. 8*E*), most probably due to its inability to bind to DLC1^{GAP} (Fig. 8, *C* and *D*). The analysis of the single point mutations revealed that W319G substitution had a minor effect on the association with (data not shown) and on the inhibition of DLC^{GAP} (Fig. 8*E*). p120$^{SH3(N311R,L313A)}$ on the other hand significantly abolished both the inhibitory effect of p120^{SH3} (Fig. 8*E*) and the complex formation with DLC1^{GAP} (data not shown) as compared with wild-type p120^{SH3}. Taken together,

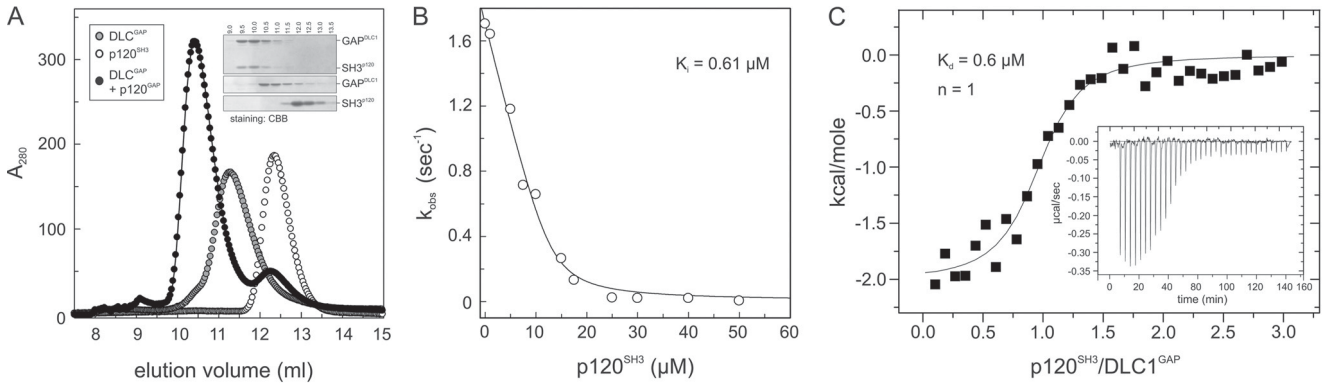

FIGURE 6. **High affinity interaction between p120^{SH3} and DLC1^{GAP}.** *A*, co-elution of a mixture of DLC1^{GAP} (10 μM) and p120^{SH3} (15 μM) (*open circles*) from a Superdex 75 (10/300) as shown by SDS-PAGE (15%) and Coomassie Brilliant Blue (*CBB*) staining (*inset*) indicates their complex formation. *B*, the activity of DLC1^{GAP} (20 μM) toward Cdc42 (0.2 μM) was measured at increasing concentrations of p120^{SH3}, and the obtained k_{obs} values were plotted against increasing concentrations of the inhibitor p120^{SH3}. The K_i value was obtained by non-linear regression based on the Morrison equation for tight binding inhibitors (58). *C*, ITC analysis was performed by titrating DLC1^{GAP} (20 μM) with p120^{SH3} (400 μM). K_d is the dissociation constant, and *n* is the stoichiometry.

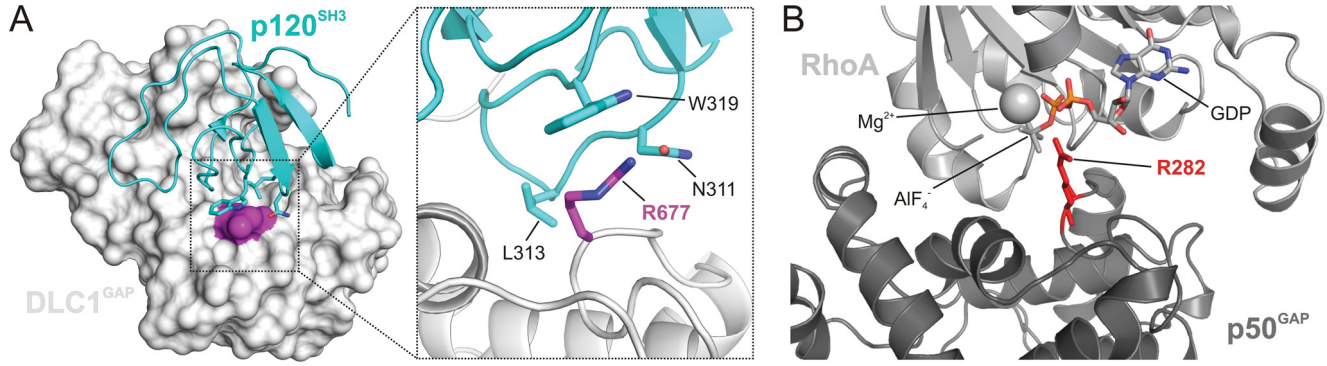

FIGURE 7. **Structural insight into a putative binding mode between p120^{SH3} and DLC1^{GAP}.** *A*, molecular docking analyses were performed between the available crystal structures of p120^{SH3} (Protein Data Bank code 2J05) (53) and DLC1^{GAP} (Protein Data Bank code 3KUQ) using the program PatchDock (54). In the best ranked and refined model, p120^{SH3} was located in close proximity of the catalytic arginine finger (Arg-677; *magenta*) of DLC1^{GAP}. In this model, p120^{SH3} supplied three amino acids (Asn-311, Leu-313, and Trp-319) to directly contact the catalytic core of DLC1^{GAP}, especially Arg-677, and mask its accessibility to the Rho proteins. *B*, p50GAP provides an arginine finger (Arg-282; *red*) in the active site of RhoA to stabilize the transition state of the GTP hydrolysis reaction (Protein Data Bank code 1TX4) (60). GDP-AlF$_4^-$ mimics the transition state of the GTP hydrolysis reaction.

our mutational and biochemical analyses support the *in silico* structural model (Fig. 7*A*) and provide new insight into how p120^{SH3} may bind and inhibit the catalytic activity of DLC1^{GAP}.

DISCUSSION

In this study, we have elucidated the molecular mechanism of how the RasGAP p120 selectively acts as a negative regulator of the RhoGAP activity of DLC1. We have shown that p120^{SH3}, by utilizing a novel binding mode, selectively undergoes a high affinity interaction with the RhoGAP domain of DLC1 and effectively inhibits its GAP activity by targeting its catalytic arginine finger. Interestingly, p120^{SH3} acts on the DLC isoforms but not on seven other representative members of the RhoGAP family. Our data together support the notion of a functional cross-talk between Ras and Rho proteins at the level of regulatory proteins (11, 45).

In contrast to the molecular mechanism of Rho protein inactivation by GAPs, which is well established (14, 61), it is still unclear how GAPs themselves are regulated. Different mechanisms are implicated in the regulation of GAPs, such as regulation by protein phosphorylation, proteolytic degradation, intramolecular autoinhibition, and changes in subcellular localization or protein complex formation (62, 63). "Intramolecular inhibition" (also called "autoinhibition," "*cis*-inhibition," "autoinhibitory loop," "autoregulation," and "bistable switch") of biological molecules is a fundamental control mechanism in nature and is an emerging theme in the regulation of different kinds of proteins, including the regulators of small GTP-binding proteins themselves. Besides the guanine nucleotide exchange factors (64–69), GAPs also have been reported to require activation through the relief of autoinhibitory elements (20, 31–33, 35, 36). Kim *et al.* (20) have shown that DLC1^{fl} has a reduced GAP activity and have proposed that the N-terminal SAM domain may be a *cis*-inhibitory element contributing to DLC1 autoinhibition. Our real time kinetic experiments, however, have shown that neither isolated SAM or START alone nor both domains in combination are directly responsible for the observed DLC1^{fl} autoinhibition in a cell-free system (Fig. 3). Taken together, it rather seems plausible that other regions, probably together with SAM and START domains, are involved in the autoinhibition of DLC1. In addition, it is important to note that release of the autoinhibitory loop of DLC1 is most likely subjected to posttranslational modifications (21, 70) and interactions with other proteins (16, 28, 34) along with changes in subcellular localization (30), collectively contribute to the regulation of DLC1 GAP activity in intact cells. In this context, PKD-mediated phosphorylation (70) and 14-3-3 binding and

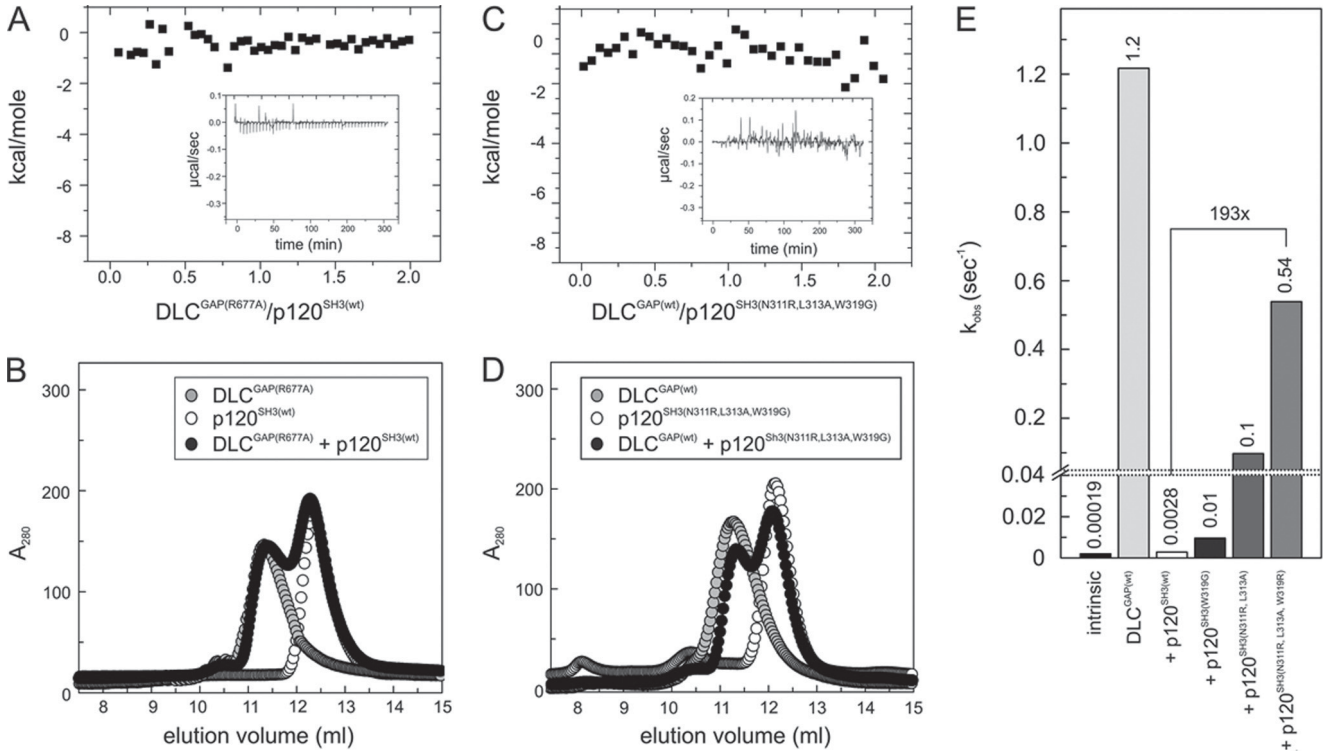

FIGURE 8. **Loss of p120-DLC1 interaction by mutational analysis.** No interaction was observed between DLC1$^{GAP(R677A)}$ and p120$^{SH3(WT)}$ (*A* and *B*) and DLC1$^{GAP(WT)}$ and p120$^{SH3(N311R,L313A,W319G)}$ (*C* and *D*). Loss of interaction and of inhibition was measured by ITC (*A* and *C*) and aSEC (*B* and *D*) as compared with the p120$^{SH3(WT)}$-DLC1$^{GAP(WT)}$ interaction shown in Fig. 6. *E*, the activity of DLC1^{GAP} (25 μM) in stimulating tamraGTP hydrolysis of Cdc42 (0.2 μM) was measured in the presence of p120^{SH3} variants (125 μM), respectively. For convenience, the k_{obs} values are given above the *bar charts*.

cytosolic sequestration (22) are good examples for the regulation DLC1 function.

Functional characterization and structural elucidation of the *trans*-inhibitory mechanism of DLC1 mediated by the Ras-specific GAP p120 protein (11) was the central theme of this study. Our data clearly revealed that the GAP activity of not only DLC1 but also that of DLC2 and DLC3 was almost completely abolished in the presence of the SH3 domain of p120 (Fig. 4). We showed that larger fragments of p120, such as p120$^{SH2\text{-}3\text{-}2}$ and the almost full-length p120$^{\Delta n128}$, inhibit the DLC GAP function but strikingly not to the same extent as seen for the isolated SH3 domain (Fig. 4*D*). These data indicate that only a freely accessible and exposed SH3 domain of p120, most probably following an upstream signal and in a defined subcellular environment (11, 37), is able to potently inhibit DLC proteins. One of the p120 binding partners is p190, which has been proposed to induce a conformational change in p120 by binding to its SH2 domains and exposing the adjacent SH3 domain for additional protein interactions with additional proteins (47), one of which is most likely DLC1.

Several studies have shown that DLC1 is able to inactivate Cdc42 and the Rho isoforms (RhoA, RhoB, and RhoC) but not Rac1 *in vitro* (20, 71–73). DLC1^{GAP} activity toward other members of the Rho family has not yet been published. Our preliminary data showed that the DLC proteins are active *in vitro* on almost all members of the Rho family that are able to hydrolyze GTP.[6]

Chan *et al.* (74) have shown an increased level of RhoA-GTP in DLC2-null mice but not in samples from control mice. Consistently, the overexpression of DLC isoforms has been shown to lead to inactivation of RhoA and to the reduction of actin stress fiber formation (75, 76), suggesting that DLC proteins are Rho-selective GAPs and the role of the DLC *trans*-inhibitory protein p120 is to retain Rho proteins in their active GTP-bound states. Contrary to DLC proteins, p120 binding is part of the p190 activation process that controls inactivation of Rho-type proteins (45, 47, 77). A prerequisite for this interaction is phosphorylation of p190 at tyrosine 1105, which is a target of the p120 SH2 domains (77). In this regard, p120 oppositely controls the activities of two different RhoGAPs and obviously two different Rho/Rho effector systems; one is left activated, and the other is switched off.

SH3 domain-containing cellular signaling proteins mediate interactions via specific proline-containing peptides. The SH3 domain of p120 has been discussed recently to interact with other proteins in a P*XX*P motif-independent manner (48). *In silico* analysis revealed that the GAP domain of DLC1 does not possess a proline-rich region and therefore, unlike classical P*XX*P motif-recognizing SH3 domains, the interaction mode of the p120 SH3 domain is atypical and utilizes different amino acids to bind and mask the catalytic arginine finger of the GAP domain of DLC1. The Ser/Thr kinases Aurora A and Aurora B are other examples in addition to DLC1 for negative modulation of biological processes by p120 (78). The SH3 domain of p120 binds to the catalytic domain of Aurora kinases that inhibits their kinase activity. These interactions also do not involve a

[6] M. Jaiswal, E. Amin, and R. Dvorsky, unpublished data.

proline-rich consensus sequence. Two accessible hydrophobic regions of p120 SH3 have been suggested to function as binding sites for protein interaction (79). Our study supports this notion as we have shown that mutation of three amino acids close to one of these proposed binding sites indeed diminished the $DLC1^{GAP}$ binding and inhibiting ability of p120 SH3.

We demonstrated that the interaction between $p120^{SH3}$ and $DLC1^{GAP}$ displays at least three remarkable characteristics, namely high affinity, high selectively, and a non-canonical binding mode. The high affinity interaction of 0.6 μM is striking because the binding constants of SH3 domains for proline-rich motifs in their target proteins are mostly in the micromolar range (48, 59). The very few examples of high affinity binding of SH3 domains are those between Mona/Gads and SLP-76 (80), C3G and c-Crk (51), and Grb2 and Wrch1 (48).

CONCLUSION

Mechanistic and structural insights into selectivity, activity, and regulation of DLC1 presented in this study shed light on the role of the multifunctional, regulatory signaling molecule p120RasGAP. It is evident that p120 acts in addition to its RasGAP domain, which is required to switch off Ras signal transduction, as an "effector" conversely controlling, via its SH2 domains and a non-canonical SH3 domain, the RhoGAP activities of the DLC and p190 proteins and hence Rho signal transduction. Interestingly, p120 interacts, in addition to DLC1 and p190, with a third RhoGAP, called p200RhoGAP. In contrast to p190 and DLC1, which are downstream of p120, p200RhoGAP has been proposed to bind to the p120 SH3 domain via its very C-terminal proline-rich region and to sequestrate its RasGAP function from inactivating Ras (10). These examples nicely illustrate the interdependence of the Ras and Rho signaling pathways and underline the multifunctional and multifaceted nature of regulatory proteins beyond their critical GAP functions.

Acknowledgments—We thank Linda van Aelst, Katrin Rittinger, Olivier Dorseui, Gerard Gacon, Alan Hall, Tony Pawson, and Jeffrey Settleman for sharing reagents with us that proved indispensable for the work.

REFERENCES

1. Aznar, S., and Lacal, J. C. (2001) Searching new targets for anticancer drug design: the families of Ras and Rho GTPases and their effectors. *Prog. Nucleic Acid Res. Mol. Biol.* **67,** 193–234
2. Fritz, G., Just, I., and Kaina, B. (1999) Rho GTPases are over-expressed in human tumors. *Int. J. Cancer* **81,** 682–687
3. Pruitt, K., and Der, C. J. (2001) Ras and Rho regulation of the cell cycle and oncogenesis. *Cancer Lett.* **171,** 1–10
4. Zondag, G. C., Evers, E. E., ten Klooster, J. P., Janssen, L., van der Kammen, R. A., and Collard, J. G. (2000) Oncogenic Ras downregulates Rac activity, which leads to increased Rho activity and epithelial-mesenchymal transition. *J. Cell Biol.* **149,** 775–782
5. Sahai, E., and Marshall, C. J. (2002) RHO-GTPases and cancer. *Nat. Rev. Cancer* **2,** 133–142
6. Khosravi-Far, R., Campbell, S., Rossman, K. L., and Der, C. J. (1998) Increasing complexity of Ras signal transduction: involvement of Rho family proteins. *Adv. Cancer Res.* **72,** 57–107
7. Coleman, M. L., Marshall, C. J., and Olson, M. F. (2004) RAS and RHO GTPases in G1-phase cell-cycle regulation. *Nat. Rev. Mol. Cell Biol.* **5,** 355–366
8. Karnoub, A. E., and Weinberg, R. A. (2008) Ras oncogenes: split personalities. *Nat. Rev. Mol. Cell Biol.* **9,** 517–531
9. Asnaghi, L., Vass, W. C., Quadri, R., Day, P. M., Qian, X., Braverman, R., Papageorge, A. G., and Lowy, D. R. (2010) E-cadherin negatively regulates neoplastic growth in non-small cell lung cancer: role of Rho GTPases. *Oncogene* **29,** 2760–2771
10. Shang, X., Moon, S. Y., and Zheng, Y. (2007) p200 RhoGAP promotes cell proliferation by mediating cross-talk between Ras and Rho signaling pathways. *J. Biol. Chem.* **282,** 8801–8811
11. Yang, X. Y., Guan, M., Vigil, D., Der, C. J., Lowy, D. R., and Popescu, N. C. (2009) p120Ras-GAP binds the DLC1 Rho-GAP tumor suppressor protein and inhibits its RhoA GTPase and growth-suppressing activities. *Oncogene* **28,** 1401–1409
12. Scheffzek, K., and Ahmadian, M. R. (2005) GTPase activating proteins: structural and functional insights 18 years after discovery. *Cell. Mol. Life Sci.* **62,** 3014–3038
13. Ligeti, E., Welti, S., and Scheffzek, K. (2012) Inhibition and termination of physiological responses by GTPase activating proteins. *Physiol. Rev.* **92,** 237–272
14. Scheffzek, K., Ahmadian, M. R., and Wittinghofer, A. (1998) GTPase-activating proteins: helping hands to complement an active site. *Trends Biochem. Sci.* **23,** 257–262
15. Yuan, B. Z., Miller, M. J., Keck, C. L., Zimonjic, D. B., Thorgeirsson, S. S., and Popescu, N. C. (1998) Cloning, characterization, and chromosomal localization of a gene frequently deleted in human liver cancer (DLC-1) homologous to rat RhoGAP. *Cancer Res.* **58,** 2196–2199
16. Durkin, M. E., Yuan, B. Z., Zhou, X., Zimonjic, D. B., Lowy, D. R., Thorgeirsson, S. S., and Popescu, N. C. (2007) DLC-1: a Rho GTPase-activating protein and tumour suppressor. *J. Cell. Mol. Med.* **11,** 1185–1207
17. Liao, Y. C., and Lo, S. H. (2008) Deleted in liver cancer-1 (DLC-1): a tumor suppressor not just for liver. *Int. J. Biochem. Cell Biol.* **40,** 843–847
18. Zimonjic, D. B., and Popescu, N. C. (2012) Role of DLC1 tumor suppressor gene and MYC oncogene in pathogenesis of human hepatocellular carcinoma: potential prospects for combined targeted therapeutics (review). *Int. J. Oncol.* **41,** 393–406
19. Holeiter, G., Heering, J., Erlmann, P., Schmid, S., Jähne, R., and Olayioye, M. A. (2008) Deleted in liver cancer 1 controls cell migration through a Dia1-dependent signaling pathway. *Cancer Res.* **68,** 8743–8751
20. Kim, T. Y., Healy, K. D., Der, C. J., Sciaky, N., Bang, Y. J., and Juliano, R. L. (2008) Effects of structure of Rho GTPase-activating protein DLC-1 on cell morphology and migration. *J. Biol. Chem.* **283,** 32762–32770
21. Kim, T. Y., Vigil, D., Der, C. J., and Juliano, R. L. (2009) Role of DLC-1, a tumor suppressor protein with RhoGAP activity, in regulation of the cytoskeleton and cell motility. *Cancer Metastasis Rev.* **28,** 77–83
22. Scholz, R. P., Regner, J., Theil, A., Erlmann, P., Holeiter, G., Jähne, R., Schmid, S., Hausser, A., and Olayioye, M. A. (2009) DLC1 interacts with 14-3-3 proteins to inhibit RhoGAP activity and block nucleocytoplasmic shuttling. *J. Cell Sci.* **122,** 92–102
23. Lukasik, D., Wilczek, E., Wasiutynski, A., and Gornicka, B. (2011) Deleted in liver cancer protein family in human malignancies (review). *Oncol. Lett.* **2,** 763–768
24. Yam, J. W., Ko, F. C., Chan, C. Y., Jin, D. Y., and Ng, I. O. (2006) Interaction of deleted in liver cancer 1 with tensin2 in caveolae and implications in tumor suppression. *Cancer Res.* **66,** 8367–8372
25. Liao, Y. C., Si, L., deVere White, R. W., and Lo, S. H. (2007) The phosphotyrosine-independent interaction of DLC-1 and the SH2 domain of cten regulates focal adhesion localization and growth suppression activity of DLC-1. *J. Cell Biol.* **176,** 43–49
26. Qian, X., Li, G., Asmussen, H. K., Asnaghi, L., Vass, W. C., Braverman, R., Yamada, K. M., Popescu, N. C., Papageorge, A. G., and Lowy, D. R. (2007) Oncogenic inhibition by a deleted in liver cancer gene requires cooperation between tensin binding and Rho-specific GTPase-activating protein activities. *Proc. Natl. Acad. Sci. U.S.A.* **104,** 9012–9017
27. Chan, L. K., Ko, F. C., Ng, I. O., and Yam, J. W. (2009) Deleted in liver cancer 1 (DLC1) utilizes a novel binding site for Tensin2 PTB domain interaction and is required for tumor-suppressive function. *PLoS One* **4,** e5572

28. Tripathi, V., Popescu, N. C., and Zimonjic, D. B. (2013) DLC1 induces expression of E-cadherin in prostate cancer cells through Rho pathway and suppresses invasion. *Oncogene* **4,** 1–10
29. Li, G., Du, X., Vass, W. C., Papageorge, A. G., Lowy, D. R., and Qian, X. (2011) Full activity of the deleted in liver cancer 1 (DLC1) tumor suppressor depends on an LD-like motif that binds talin and focal adhesion kinase (FAK). *Proc. Natl. Acad. Sci. U.S.A.* **108,** 17129–17134
30. Erlmann, P., Schmid, S., Horenkamp, F. A., Geyer, M., Pomorski, T. G., and Olayioye, M. A. (2009) DLC1 activation requires lipid interaction through a polybasic region preceding the RhoGAP domain. *Mol. Biol. Cell* **20,** 4400–4411
31. Fauchereau, F., Herbrand, U., Chafey, P., Eberth, A., Koulakoff, A., Vinet, M. C., Ahmadian, M. R., Chelly, J., and Billuart, P. (2003) The RhoGAP activity of OPHN1, a new F-actin-binding protein, is negatively controlled by its amino-terminal domain. *Mol. Cell. Neurosci.* **23,** 574–586
32. Eberth, A., and Ahmadian, M. R. (2009) *In vitro* GEF and GAP assays. *Curr. Protoc. Cell Biol.* **Chapter 14,** Unit 14.19
33. Colón-González, F., Leskow, F. C., and Kazanietz, M. G. (2008) Identification of an autoinhibitory mechanism that restricts C1 domain-mediated activation of the Rac-GAP α2-chimaerin. *J. Biol. Chem.* **283,** 35247–35257
34. Jian, X., Brown, P., Schuck, P., Gruschus, J. M., Balbo, A., Hinshaw, J. E., and Randazzo, P. A. (2009) Autoinhibition of Arf GTPase-activating protein activity by the BAR domain in ASAP1. *J. Biol. Chem.* **284,** 1652–1663
35. Zhou, Y. T., Chew, L. L., Lin, S. C., and Low, B. C. (2010) The BNIP-2 and Cdc42GAP homology (BCH) domain of p50RhoGAP/Cdc42GAP sequesters RhoA from inactivation by the adjacent GTPase-activating protein domain. *Mol. Biol. Cell* **21,** 3232–3246
36. Moskwa, P., Paclet, M. H., Dagher, M. C., and Ligeti, E. (2005) Autoinhibition of p50 Rho GTPase-activating protein (GAP) is released by prenylated small GTPases. *J. Biol. Chem.* **280,** 6716–6720
37. Pamonsinlapatham, P., Hadj-Slimane, R., Lepelletier, Y., Allain, B., Toccafondi, M., Garbay, C., and Raynaud, F. (2009) p120-Ras GTPase activating protein (RasGAP): a multi-interacting protein in downstream signaling. *Biochimie* **91,** 320–328
38. Ahmadian, M. R., Hoffmann, U., Goody, R. S., and Wittinghofer, A. (1997) Individual rate constants for the interaction of Ras proteins with GTPase-activating proteins determined by fluorescence spectroscopy. *Biochemistry* **36,** 4535–4541
39. Ahmadian, M. R., Stege, P., Scheffzek, K., and Wittinghofer, A. (1997) Confirmation of the arginine-finger hypothesis for the GAP-stimulated GTP-hydrolysis reaction of Ras. *Nat. Struct. Biol.* **4,** 686–689
40. Scheffzek, K., Ahmadian, M. R., Kabsch, W., Wiesmüller, L., Lautwein, A., Schmitz, F., and Wittinghofer, A. (1997) The Ras-RasGAP complex: structural basis for GTPase activation and its loss in oncogenic Ras mutants. *Science* **277,** 333–338
41. Leblanc, V., Tocque, B., and Delumeau, I. (1998) Ras-GAP controls Rho-mediated cytoskeletal reorganization through its SH3 domain. *Mol. Cell. Biol.* **18,** 5567–5578
42. Chan, P. C., and Chen, H. C. (2012) p120RasGAP-mediated activation of c-Src is critical for oncogenic Ras to induce tumor invasion. *Cancer Res.* **72,** 2405–2415
43. Clark, G. J., and Der, C. J. (1995) Aberrant function of the Ras signal transduction pathway in human breast cancer. *Breast Cancer Res. Treat.* **35,** 133–144
44. Clark, G. J., Westwick, J. K., and Der, C. J. (1997) p120 GAP modulates Ras activation of Jun kinases and transformation. *J. Biol. Chem.* **272,** 1677–1681
45. Herbrand, U., and Ahmadian, M. R. (2006) p190-RhoGAP as an integral component of the Tiam1/Rac1-induced downregulation of Rho. *Biol. Chem.* **387,** 311–317
46. Wang, Z., Tung, P. S., and Moran, M. F. (1996) Association of p120 ras GAP with endocytic components and colocalization with epidermal growth factor (EGF) receptor in response to EGF stimulation. *Cell Growth Differ.* **7,** 123–133
47. Hu, K. Q., and Settleman, J. (1997) Tandem SH2 binding sites mediate the RasGAP-RhoGAP interaction: a conformational mechanism for SH3 domain regulation. *EMBO J.* **16,** 473–483
48. Risse, S. L., Vaz, B., Burton, M. F., Aspenström, P., Piekorz, R. P., Brunsveld, L., and Ahmadian, M. R. (2013) SH3-mediated targeting of Wrch1/RhoU by multiple adaptor proteins. *Biol. Chem.* **394,** 421–432
49. Jaiswal, M., Dubey, B. N., Koessmeier, K. T., Gremer, L., and Ahmadian, M. R. (2012) Biochemical assays to characterize Rho GTPases. *Methods Mol. Biol.* **827,** 37–58
50. Eberth, A., Lundmark, R., Gremer, L., Dvorsky, R., Koessmeier, K. T., McMahon, H. T., and Ahmadian, M. R. (2009) A BAR domain-mediated autoinhibitory mechanism for RhoGAPs of the GRAF family. *Biochem. J.* **417,** 371–377
51. Wu, X., Knudsen, B., Feller, S. M., Zheng, J., Sali, A., Cowburn, D., Hanafusa, H., and Kuriyan, J. (1995) Structural basis for the specific interaction of lysine-containing proline-rich peptides with the N-terminal SH3 domain of c-Crk. *Structure* **3,** 215–226
52. Eberth, A., Dvorsky, R., Becker, C. F., Beste, A., Goody, R. S., and Ahmadian, M. R. (2005) Monitoring the real-time kinetics of the hydrolysis reaction of guanine nucleotide-binding proteins. *Biol. Chem.* **386,** 1105–1114
53. Ross, B., Kristensen, O., Favre, D., Walicki, J., Kastrup, J. S., Widmann, C., and Gajhede, M. (2007) High resolution crystal structures of the p120 RasGAP SH3 domain. *Biochem. Biophys. Res. Commun.* **353,** 463–468
54. Schneidman-Duhovny, D., Inbar, Y., Nussinov, R., and Wolfson, H. J. (2005) PatchDock and SymmDock: servers for rigid and symmetric docking. *Nucleic Acids Res.* **33,** W363–W367
55. Brooks, B. R., Brooks, C. L., 3rd, Mackerell, A. D., Jr., Nilsson, L., Petrella, R. J., Roux, B., Won, Y., Archontis, G., Bartels, C., Boresch, S., Caflisch, A., Caves, L., Cui, Q., Dinner, A. R., Feig, M., Fischer, S., Gao, J., Hodoscek, M., Im, W., Kuczera, K., Lazaridis, T., Ma, J., Ovchinnikov, V., Paci, E., Pastor, R. W., Post, C. B., Pu, J. Z., Schaefer, M., Tidor, B., Venable, R. M., Woodcock, H. L., Wu, X., Yang, W., York, D. M., and Karplus, M. (2009) CHARMM: the biomolecular simulation program. *J. Comput. Chem.* **30,** 1545–1614
56. Scouras, A. D., and Daggett, V. (2011) The Dynameomics rotamer library: amino acid side chain conformations and dynamics from comprehensive molecular dynamics simulations in water. *Protein Sci.* **20,** 341–352
57. Eccleston, J. F., Moore, K. J., Morgan, L., Skinner, R. H., and Lowe, P. N. (1993) Kinetics of interaction between normal and proline 12 Ras and the GTPase-activating proteins, p120-GAP and neurofibromin. The significance of the intrinsic GTPase rate in determining the transforming ability of *ras*. *J. Biol. Chem.* **268,** 27012–27019
58. Morrison, J. F. (1969) Kinetics of the reversible inhibition of enzyme-catalysed reactions by tight-binding inhibitors. *Biochim. Biophys. Acta* **185,** 269–286
59. Kärkkäinen, S., Hiipakka, M., Wang, J. H., Kleino, I., Vähä-Jaakkola, M., Renkema, G. H., Liss, M., Wagner, R., and Saksela, K. (2006) Identification of preferred protein interactions by phage-display of the human Src homology-3 proteome. *EMBO Rep.* **7,** 186–191
60. Rittinger, K., Walker, P. A., Eccleston, J. F., Smerdon, S. J., and Gamblin, S. J. (1997) Structure at 1.65 Å of RhoA and its GTPase-activating protein in complex with a transition-state analogue. *Nature* **389,** 758–762
61. Dvorsky, R., and Ahmadian, M. R. (2004) Always look on the bright site of Rho: structural implications for a conserved intermolecular interface. *EMBO Rep.* **5,** 1130–1136
62. Moon, S. Y., and Zheng, Y. (2003) Rho GTPase-activating proteins in cell regulation. *Trends Cell Biol.* **13,** 13–22
63. Tcherkezian, J., and Lamarche-Vane, N. (2007) Current knowledge of the large RhoGAP family of proteins. *Biol. Cell* **99,** 67–86
64. Rossman, K. L., Der, C. J., and Sondek, J. (2005) GEF means go: turning on RHO GTPases with guanine nucleotide-exchange factors. *Nat. Rev. Mol. Cell Biol.* **6,** 167–180
65. Aittaleb, M., Boguth, C. A., and Tesmer, J. J. (2010) Structure and function of heterotrimeric G protein-regulated Rho guanine nucleotide exchange factors. *Mol. Pharmacol.* **77,** 111–125
66. DiNitto, J. P., Lee, M. T., Malaby, A. W., and Lambright, D. G. (2010) Specificity and membrane partitioning of Grsp1 signaling complexes with Grp1 family Arf exchange factors. *Biochemistry* **49,** 6083–6092
67. Gureasko, J., Kuchment, O., Makino, D. L., Sondermann, H., Bar-Sagi, D., and Kuriyan, J. (2010) Role of the histone domain in the autoinhibition and activation of the Ras activator Son of Sevenless. *Proc. Natl. Acad. Sci.*

U.S.A. **107,** 3430–3435
68. Jaiswal, M., Gremer, L., Dvorsky, R., Haeusler, L. C., Cirstea, I. C., Uhlenbrock, K., and Ahmadian, M. R. (2011) Mechanistic insights into specificity, activity, and regulatory elements of the regulator of G-protein signaling (RGS)-containing Rho-specific guanine nucleotide exchange factors (GEFs) p115, PDZ-RhoGEF (PRG), and leukemia-associated RhoGEF (LARG). *J. Biol. Chem.* **286,** 18202–18212
69. Mitin, N., Betts, L., Yohe, M. E., Der, C. J., Sondek, J., and Rossman, K. L. (2007) Release of autoinhibition of ASEF by APC leads to CDC42 activation and tumor suppression. *Nat. Struct. Mol. Biol.* **14,** 814–823
70. Scholz, R. P., Gustafsson, J. O., Hoffmann, P., Jaiswal, M., Ahmadian, M. R., Eisler, S. A., Erlmann, P., Schmid, S., Hausser, A., and Olayioye, M. A. (2011) The tumor suppressor protein DLC1 is regulated by PKD-mediated GAP domain phosphorylation. *Exp. Cell Res.* **317,** 496–503
71. Ching, Y. P., Wong, C. M., Chan, S. F., Leung, T. H., Ng, D. C., Jin, D. Y., and Ng, I. O. (2003) Deleted in liver cancer (DLC) 2 encodes a RhoGAP protein with growth suppressor function and is underexpressed in hepatocellular carcinoma. *J. Biol. Chem.* **278,** 10824–10830
72. Wong, C. M., Lee, J. M., Ching, Y. P., Jin, D. Y., and Ng, I. O. (2003) Genetic and epigenetic alterations of DLC-1 gene in hepatocellular carcinoma. *Cancer Res.* **63,** 7646–7651
73. Healy, K. D., Hodgson, L., Kim, T. Y., Shutes, A., Maddileti, S., Juliano, R. L., Hahn, K. M., Harden, T. K., Bang, Y. J., and Der, C. J. (2008) DLC-1 suppresses non-small cell lung cancer growth and invasion by RhoGAP-dependent and independent mechanisms. *Mol. Carcinog.* **47,** 326–337
74. Chan, F. K., Chung, S. S., Ng, I. O., and Chung, S. K. (2012) The RhoA GTPase-activating protein DLC2 modulates RhoA activity and hyperalgesia to noxious thermal and inflammatory stimuli. *Neurosignals* **20,** 112–126
75. Leung, T. H., Ching, Y. P., Yam, J. W., Wong, C. M., Yau, T. O., Jin, D. Y., and Ng, I. O. (2005) Deleted in liver cancer 2 (DLC2) suppresses cell transformation by means of inhibition of RhoA activity. *Proc. Natl. Acad. Sci. U.S.A.* **102,** 15207–15212
76. Kawai, K., Kiyota, M., Seike, J., Deki, Y., and Yagisawa, H. (2007) START-GAP3/DLC3 is a GAP for RhoA and Cdc42 and is localized in focal adhesions regulating cell morphology. *Biochem. Biophys. Res. Commun.* **364,** 783–789
77. Roof, R. W., Haskell, M. D., Dukes, B. D., Sherman, N., Kinter, M., and Parsons, S. J. (1998) Phosphotyrosine (p-Tyr)-dependent and -independent mechanisms of p190 RhoGAP-p120 RasGAP interaction: Tyr 1105 of p190, a substrate for c-Src, is the sole p-Tyr mediator of complex formation. *Mol. Cell. Biol.* **18,** 7052–7063
78. Gigoux, V., L'Hoste, S., Raynaud, F., Camonis, J., and Garbay, C. (2002) Identification of Aurora kinases as RasGAP Src homology 3 domain-binding proteins. *J. Biol. Chem.* **277,** 23742–23746
79. Yang, Y. S., Garbay, C., Duchesne, M., Cornille, F., Jullian, N., Fromage, N., Tocque, B., and Roques, B. P. (1994) Solution structure of GAP SH3 domain by ^{1}H NMR and spatial arrangement of essential Ras signaling-involved sequence. *EMBO J.* **13,** 1270–1279
80. Harkiolaki, M., Lewitzky, M., Gilbert, R. J., Jones, E. Y., Bourette, R. P., Mouchiroud, G., Sondermann, H., Moarefi, I., and Feller, S. M. (2003) Structural basis for SH3 domain-mediated high-affinity binding between Mona/Gads and SLP-76. *EMBO J.* **22,** 2571–2582

HMG Advance Access published April 15, 2014

Human Molecular Genetics, 2014 **1–13**
doi:10.1093/hmg/ddu148

Activating mutations in *RRAS* underlie a phenotype within the RASopathy spectrum and contribute to leukaemogenesis

Elisabetta Flex[1,†], Mamta Jaiswal[3,†], Francesca Pantaleoni[1,‡], Simone Martinelli[1,‡], Marion Strullu[4,7,‡], Eyad K. Fansa[3,‡], Aurélie Caye[4,7], Alessandro De Luca[8], Francesca Lepri[9], Radovan Dvorsky[3], Luca Pannone[1], Stefano Paolacci[1], Si-Cai Zhang[3], Valentina Fodale[1], Gianfranco Bocchinfuso[10], Cesare Rossi[11], Emma M.M. Burkitt-Wright[12], Andrea Farrotti[10], Emilia Stellacci[1], Serena Cecchetti[2], Rosangela Ferese[8], Lisabianca Bottero[1], Silvana Castro[13], Odile Fenneteau[5], Benoît Brethon[6], Massimo Sanchez[2], Amy E. Roberts[14], Helger G. Yntema[15], Ineke Van Der Burgt[15], Paola Cianci[16], Marie-Louise Bondeson[17], Maria Cristina Digilio[9], Giuseppe Zampino[18], Bronwyn Kerr[12], Yoko Aoki[19], Mignon L. Loh[20], Antonio Palleschi[10], Elia Di Schiavi[13,¶], Alessandra Carè[1], Angelo Selicorni[16], Bruno Dallapiccola[9], Ion C. Cirstea[3,21], Lorenzo Stella[10], Martin Zenker[22], Bruce D. Gelb[23,24,25], Hélène Cavé[4,7,§], Mohammad R. Ahmadian[3,§] and Marco Tartaglia[1,§,*]

[1]Dipartimento di Ematologia, Oncologia e Medicina Molecolare and [2]Dipartimento di Biologia Cellulare e Neuroscienze, Istituto Superiore di Sanità, Rome 00161, Italy, [3]Institut für Biochemie und Molekularbiologie II, Medizinische Fakultät der Heinrich-Heine Universitat, Düsseldorf 40225, Germany, [4]Genetics Department, [5]Biological Hematology Department and [6]Pediatric Hematology Department, Robert Debré Hospital, Paris 75019, France, [7]INSERM UMR_S940, Institut Universitaire D'Hématologie (IUH), Université Paris-Diderot Sorbonne-Paris-Cité, Paris 75010, France, [8]Laboratorio Mendel, Istituto di Ricovero e Cura a Carattere Scientifico-Casa Sollievo Della Sofferenza, Rome 00198, Italy, [9]Ospedale Pediatrico 'Bambino Gesù', Rome 00165, Italy, [10]Dipartimento di Scienze e Tecnologie Chimiche, Università 'Tor Vergata', Rome 00133, Italy, [11]UO Genetica Medica, Policlinico S.Orsola-Malpighi, Bologna 40138, Italy, [12]Genetic Medicine, Academic Health Science Centre, Central Manchester University Hospitals NHS Foundation Trust, Manchester M13 9WL, UK, [13]Istituto di Genetica e Biofisica 'A. Buzzati Traverso', Consiglio Nazionale Delle Ricerche, Naples 80131, Italy, [14]Department of Cardiology and Division of Genetics, and Department of Medicine, Boston Children's Hospital, Boston, MA 02115, USA, [15]Department of Human Genetics, Radboud University Medical Centre, and Nijmegen Centre for Molecular Life Sciences, Radboud University, Nijmegen 6500, The Netherlands, [16]Genetica Clinica Pediatrica, Clinica Pediatrica Università Milano Bicocca, Fondazione MBBM, A.O. S. Gerardo, Monza 20900, Italy, [17]Department of Immunology, Genetics and Pathology, Uppsala University, Uppsala 75237, Sweden, [18]Istituto di Clinica Pediatrica, Università Cattolica del Sacro Cuore, Rome 00168, Italy, [19]Department of Medical Genetics, Tohoku University School of Medicine, Sendai 980-8574, Japan, [20]Department of Pediatrics, Benioff Children's Hospital, University of California School of Medicine, and the Helen Diller Family Comprehensive Cancer Center, San Francisco, CA 94143, USA, [21]Leibniz Institute for Age Research, Jena 07745, Germany, [22]Institute of Human Genetics, University Hospital of

*To whom correspondence should be addressed at: Dipartimento di Ematologia, Oncologia e Medicina Molecolare, Istituto Superiore di Sanità, Viale Regina Elena, 299, 00161 Rome, Italy. Tel: +39 0649902569; Fax: +39 0649902850; Email: marco.tartaglia@iss.it
†These authors contributed equally to this project.
‡These authors contributed equally to this project.
¶Present address: Institute of Bioscience and BioResources, Consiglio Nazionale delle Ricerche, Naples 80131, Italy.
§These authors contributed equally as the senior investigators for this project.

Magdeburg, Otto-von-Guericke-University, Magdeburg 39120, Germany, [23]Department of Pediatrics and [24]Department of Genetics and [25]Department of Genomic Sciences, Mindich Child Health and Development Institute, Icahn School of Medicine at Mount Sinai, New York, NY 10029, USA

Received December 10, 2013; Revised and Accepted March 4, 2014

RASopathies, a family of disorders characterized by cardiac defects, defective growth, facial dysmorphism, variable cognitive deficits and predisposition to certain malignancies, are caused by constitutional dysregulation of RAS signalling predominantly through the RAF/MEK/ERK (MAPK) cascade. We report on two germline mutations (p.Gly39dup and p.Val55Met) in *RRAS*, a gene encoding a small monomeric GTPase controlling cell adhesion, spreading and migration, underlying a rare (2 subjects among 504 individuals analysed) and variable phenotype with features partially overlapping Noonan syndrome, the most common RASopathy. We also identified somatic *RRAS* mutations (p.Gly39dup and p.Gln87Leu) in 2 of 110 cases of non-syndromic juvenile myelomonocytic leukaemia, a childhood myeloproliferative/myelodysplastic disease caused by upregulated RAS signalling, defining an atypical form of this haematological disorder rapidly progressing to acute myeloid leukaemia. Two of the three identified mutations affected known oncogenic hotspots of *RAS* genes and conferred variably enhanced RRAS function and stimulus-dependent MAPK activation. Expression of an RRAS mutant homolog in *Caenorhabditis elegans* enhanced RAS signalling and engendered protruding vulva, a phenotype previously linked to the RASopathy-causing SHOC2^{S2G} mutant. Overall, these findings provide evidence of a functional link between RRAS and MAPK signalling and reveal an unpredicted role of enhanced RRAS function in human disease.

INTRODUCTION

Signalling elicited by activated cell surface receptors and transduced through RAS proteins to the RAF/MEK/ERK and PI3K/AKT cascades is central to cell proliferation, survival, differentiation and metabolism (1,2). Owing to this nodal role, enhanced traffic through RAS proteins and their downstream effectors has been established to have a major impact on oncogenesis (3,4). This signalling network also controls early and late developmental processes (e.g. organogenesis, morphology determination, synaptic plasticity and growth), and germline mutations in a number of genes encoding transducers and modulatory proteins participating in the RAS/MAPK signalling pathway have been causally linked to Noonan syndrome (NS) (5), one of the most common diseases affecting development and growth, and a group of clinically related syndromes, the so-called RASopathies (6–8). In this family of disorders, constitutional dysregulation of RAS signalling can be caused by enhanced activation of HRAS, KRAS and NRAS (RAS proteins hereafter), aberrant function of upstream signal transducers or effectors (PTPN11/SHP2, SOS1, SHOC2, RAF1, BRAF, MAP2K1/MEK1 and MAP2K2/MEK2) or inefficient down modulation by feedback mechanisms (CBL, NF1 and SPRED1). More recently, *RIT1*, encoding a monomeric GTPase structurally linked to RAS proteins, was identified as disease gene implicated in NS (9), extending the concept of 'RASopathy gene' to a transducer that contributes to signal propagation through RAS effector pathways but does not belong to the RAS/MAPK signalling backbone.

Clinical manifestations of RASopathies include postnatal reduced growth, a wide spectrum of cardiac defects, facial dysmorphism, ectodermal and skeletal anomalies and variable cognitive deficits (5,8,10). Consistent with the key role of most RASopathy genes in oncogenesis, these disorders are also characterized by variably increased risk for certain haematologic malignancies and other paediatric cancers (6,7,11,12). Most of these conditions are genetically heterogeneous, and the underlying disease gene has not been identified yet for a still significant fraction of cases. Based on the strict mechanistic link between the molecular events controlling development and contributing to oncogenesis, these 'missing' genes represent excellent candidate oncogenes/tumour suppressors.

Here, we report that constitutional dysregulation of RRAS function is associated with a Mendelian trait within the RASopathy spectrum and that somatically acquired mutations in the same gene occur in an aggressive form of juvenile myelomonocytic leukaemia (JMML), a rare childhood myeloproliferative/myelodysplastic neoplasm representing the archetypal somatic RASopathy (13), rapidly progressing to acute myeloid leukaemia (AML). We also demonstrate that RASopathy-causing *RRAS* mutations are activating and promote signalling perturbation by enhancing stimulus-dependent MEK, ERK and, at a lower extent, AKT phosphorylation.

RESULTS

Identification of candidate disease genes and *RRAS* mutation analysis

While the core of the machinery implicated in RAS signalling has been characterized comprehensively, signal propagation through this network is likely to include a larger number of proteins playing a modulatory or structural role (14), whose aberrant or defective function is expected to perturb development and

contribute to oncogenesis. Based on this assumption, we used a protein interaction/functional association network analysis to select a panel of genes encoding proteins functionally linked to the RAS signalling network as candidates for NS or a related RASopathy (15). Candidate gene selection was based on the use of the previously identified RASopathy genes as 'seed' proteins (i.e. proteins used to build the interaction/functional networks), and considering a panel of databases to construct functional subnetworks (Supplementary material, Table S1 and Fig. S1). Sequence scanning of the best candidates in a RASopathy cohort including 96 unrelated subjects negative for mutations in known disease genes allowed the identification of a functionally relevant *RRAS* change (c.163G>A, p.Val55Met) (Supplementary material, Fig. S2) in an adult subject with clinical features suggestive of NS but lacking sufficient characteristics to allow a definitive diagnosis (Supplementary material, Table S2). Parental DNA was not available for segregation analysis. The mutation was not identified among >400 population-matched unaffected individuals, indicating that it did not represent a common polymorphic nucleotide substitution. This change, rs368625677 (dbSNP 138), had been described in 1/13,006 alleles in the NHLBI Exome Sequencing Project (http://evs.gs.washington.edu/EVS/). Of note, similar frequencies have been reported in the same database for recurrent RASopathy-causing mutations (e.g. c.922A>G in *PTPN11*, and c.1259G>A in *CBL*). Mutation analysis was extended to additional 408 patients with NS or a clinically related phenotype tested negative for mutations in the major NS disease genes (see Materials and Methods), allowing to identify one sporadic case heterozygous for a three-nucleotide duplication (c.116_118dup, p.Gly39dup) (Supplementary material, Fig. S2). Parental DNA sequencing of the relevant exon demonstrated the *de novo* origin of the variant, and STR genotyping confirmed paternity. In this subject, the duplication was documented in DNA obtained from skin fibroblasts, excluding a somatic event restricted to haematopoietic cells. The subject had features reminiscent of NS (Fig. 1A and Supplementary material, Table S2), with onset of AML suspected to represent a blast crisis of JMML (Supplementary material, Table S3 and Fig. S3). In this patient, exome sequencing performed on leukaemic and non-leukaemic DNA failed to disclose any additional relevant germline/somatic change affecting genes known to be mutated in RASopathies and JMML, as well as genes directly linked to the RAS signalling network, further supporting the causal role of the identified *RRAS* lesion. Based on this association, the occurrence of *RRAS* mutations was also explored in a panel of genomic DNAs obtained from bone marrow aspirates/circulating leukocytes of 110 subjects with JMML. Heterozygosity for the previously identified Gly^{39} duplication and the c.260A>T (p.Gln87Leu) change was observed in two patients with JMML rapidly progressing to AML (Supplementary material, Table S3 and Fig. S3). Both lesions were absent in non-leukaemic DNA, indicating their somatic origin (Supplementary material, Fig. S2). These subjects also carried a somatic *NRAS* mutation, suggesting that the two hits might cooperate with this particularly severe form of disease. Sequencing of isolated JMML myeloid colonies in patient 14385 showed that *NRAS* and *RRAS* mutations coexisted in the same progenitors but failed to establish their sequence of appearance during leukaemogenesis, not allowing to discriminate whether the latter was involved in initiation or progression of disease.

Structural analyses

RRAS encodes a 23-kD a membrane-bound monomeric GTPase with 55–60% amino acid identity to RAS proteins (16). This highly conserved structure is flanked by a unique 26-amino acid region at the *N*-terminus (Fig. 1B). Similarly to the other RAS family proteins, RRAS binds to GTP and GDP with high affinity and specificity and functions as a molecular switch by cycling between active, GTP-bound and inactive, GDP-bound states (17). RRAS is activated by guanine nucleotide exchange factors (GEFs) in response to signals elicited by cell surface receptors. In the GTP-bound state, two functionally conserved regions, switch I and switch II (Fig. 1B), undergo a conformational change enabling RRAS to bind to and activate effector proteins. This interaction is terminated by hydrolysis of GTP to GDP, which is promoted by GTPase-activating proteins (GAPs) and results in switching towards the inactive conformation. Disease-associated *RRAS* mutations affected residues highly conserved among orthologs and paralogs (Supplementary material, Fig. S4) residing in the GTP-binding pocket (Fig. 1C) and were predicted to be damaging with high confidence (Supplementary material, Table S4). Among them, Gln^{87}, homolog of Gln^{61} in RAS proteins, is directly involved in catalysis (18,19). The p.Gln87Leu substitution had previously been reported as a rare somatic event in lung carcinoma, and mutations affecting Gln^{61} are among the most recurrent oncogenic lesions in *RAS* genes (COSMIC database, http://cancer.sanger.ac.uk/cancergenome/projects/cosmic/). Likewise, p.Gly39dup altered the G1 motif participating in GTP/GDP binding and GTPase activity (Fig. 1B). Within this motif, Gly^{12} and Gly^{13} (Gly^{38} and Gly^{39} in RRAS) represent major mutation hot-spots in human cancer (COSMIC database) and account for the majority of germline *HRAS* mutations causing Costello syndrome (20). Of note, analogous insertions in RAS proteins have been reported in JMML and other malignancies (21–24). In contrast, no somatic/germline *RAS* mutation affecting Val^{29}, homolog of Val^{55} in RRAS, had previously been reported. Val^{55} side-chain is not directly involved in GTP/GDP binding, GTP hydrolysis or interaction with effectors. However, it has been reported that H-bonds are possible between the backbone of Val^{29} in HRAS and GDP/GTP (25). Furthermore, it has been suggested that Val^{29} can play a role in the transition between the GDP- and GTP-bound states (26), as supported by the evidence that the Val29Gly substitution in HRAS accelerates the GDP/GTP exchange *in vitro* (27).

Molecular dynamics (MD) simulations were performed to predict *in silico* the effects of p.Val55Met on the structure and dynamics of RRAS (Fig. 2). The mutation was introduced in the available crystallographic structure of RRAS in complex with GDP and Mg^{2+}, and the system was simulated in water for 200 ns. For comparison, MD simulations were also performed using the wild-type protein, which maintained a stable structure along the whole simulation, as expected (Fig. 2A, left panel). In contrast, a dramatic local structural transition extending up to the switch I region (residues 58–64), which mediates effector binding, was documented for the $RRAS^{V55M}$ mutant, after ~80 ns (Fig. 2A, right panel). This conformational transition resulted in an increased solvent exposure of Met^{55}, in agreement with the higher hydrophilicity of this residue compared with Val, and was accompanied by the formation of a stable

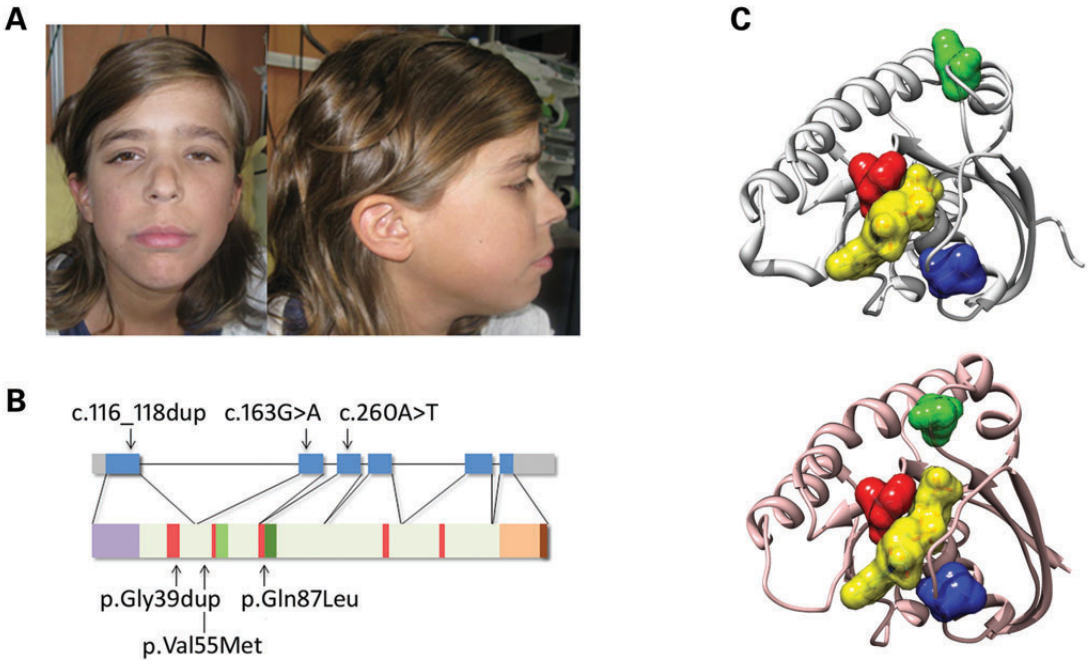

Figure 1. RASopathy-causing and leukaemia-associated *RRAS* mutations. (**A**) Facial features of the affected subject (9802) heterozygous for the *de novo* germline c.116_118dup. (**B**) *RRAS* exon–intron arrangement with coding exons as blue boxes. RRAS functional motifs include the GTP/GDP binding domain (G1 to G5, starting from the *N*-terminus) (red), switch I (light green), switch II (dark green) and hypervariable region (light brown) with the *C*-terminal CAAX motif (dark brown). The unique *N*-terminal region is also shown (violet). Location of disease-associated mutations is reported. (**C**) Position of affected residues on the three-dimensional structure of RRAS in its GDP-bound, inactive state (PDB: 2FN4) (above) and that of non-hydrolysable GTP analogue (GppNHp)-bound, active HRAS (PDB: 5P21) (below). The red surface indicates Gly^{39} and Val^{40} (Gly^{13} and Val^{14}, in HRAS), whereas Val^{55} (Val^{29}) and Gln^{87} (Gln^{61}) are shown in blue and green, respectively. GDP is reported as semi-transparent yellow surface.

cluster involving residues Ile^{50}, Met^{55} and Tyr^{58} (Fig. 2A and Supplementary material, Table S5) permitted by the unbranched and long side-chain of Met^{55}. No further significant conformational changes were observed for the remaining interval of the simulation. The major effect of this structural rearrangement was to increase exposure of GDP to the solvent (Fig. 2B), with an almost doubled solvent accessible surface area of the nucleotide after the conformational transition. This structural rearrangement was accompanied by a perturbation of the intermolecular H-bond network stabilizing GDP binding, with loss of the H-bonds between residues at codons 55 and 56, and GDP (Supplementary material, Table S5). Of note, a possible impact of the described structural transition on RRAS binding to GEF proteins, which bind to this region and mediate GDP release, was also noticed. Specifically, we observed that after the conformational rearrangement, the $RRAS^{V55M}$ region implicated in GEF binding populated a structure similar to that assumed in RAS/GEF complexes (Fig. 2C), suggesting a possible enhanced interaction of the disease-associated RRAS mutant with GEFs. In particular, Tyr^{58} was observed to adopt a side-chain orientation very similar to that of the RAS homolog Tyr^{32} in the HRAS/SOS1 complex, which has been shown to contribute to the structural rearrangements of switch I and interaction with GEFs (28–30).

Overall, these data supported an activating role of p.Val55Met through enhanced GDP release as a result of a decreased affinity for the nucleotide and/or enhanced interaction with a GEF.

Biochemical and functional characterization of RRAS mutants

Previous studies documented the gain-of-function role of p.Gln87Leu on RRAS function, and MAPK and PI3K/AKT signalling (31). To characterize the impact of p.Val55Met and p.Gly39dup on protein function, we analysed the intrinsic and GEF-accelerated nucleotide exchange reaction of these mutants. Dissociation kinetics analysis demonstrated a dramatically increased intrinsic ($RRAS^{G39dup}$) and GEF-stimulated ($RRAS^{G39dup}$ and $RRAS^{V55M}$) dissociation rate of mantGDP, indicating a facilitated nucleotide release in both mutants (Fig. 3A). RAS proteins exhibit low intrinsic GTPase activity that is enhanced by GAPs (32). Assessment of $RRAS^{G39dup}$ and $RRAS^{V55M}$ GTPase activity documented a significantly reduced intrinsic and GAP-stimulated GTP hydrolysis in the former (Fig. 3B and Supplementary material, Fig. S5). Finally, the interaction of RRAS proteins with various effectors was analysed by fluorescence polarization (Fig. 3C). While $RRAS^{WT}$ was found to bind to RAF1, RALGDS, RASSF5 and PLCE1 less efficiently than HRAS, an increased binding affinity to PIK3CA was observed. Compared with $RRAS^{WT}$, aberrant binding behaviour of the two RRAS mutants was demonstrated, with $RRAS^{G39dup}$ exhibiting an increased binding affinity towards PIK3CA, RAF1, PLCE1 and RASSF5, and $RRAS^{V55M}$ to RALGDS.

To gain further insights into the impact of disease-causing mutations on RRAS functional dysregulation and explore their effects on RAS signalling, the activation state of RRAS proteins

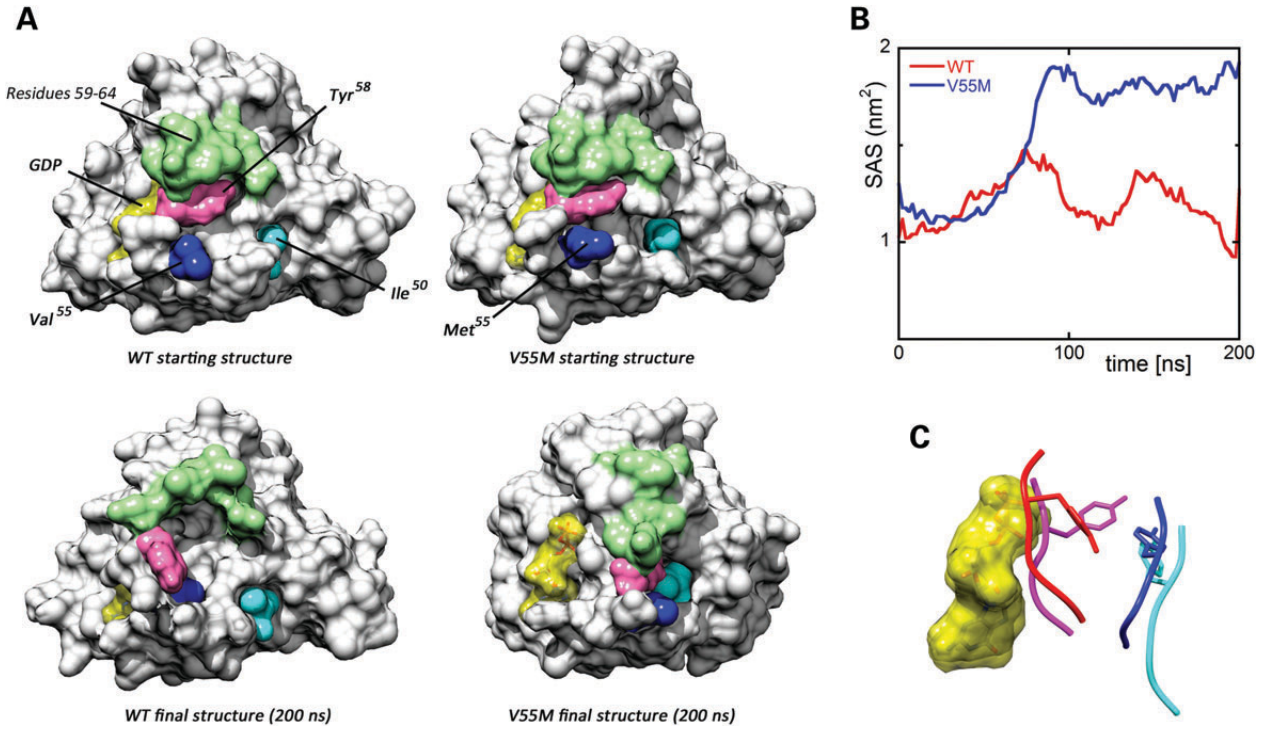

Figure 2. Molecular dynamics (MD) simulations. (**A**) Structural perturbations promoted by the p.Val55Met substitution as obtained from MD simulations of the RRAS/GDP complex. The wild-type (WT) protein is also shown for comparison. Top panels report the protein structures at the beginning of simulations, whereas the final structures (200 ns) are shown at the bottom. The final structure of $RRAS^{V55M}$ is well representative of the last 120 ns of the trajectory. The protein surface of RRAS is shown with GDP (yellow). The mutated residues and those forming a cluster in the simulation of mutated RRAS are coloured as follows: Val^{55}/Met^{55} (blue), Tyr^{58} (pink) and Ile^{50} (cyan). Residues 59–64, which, together with Tyr^{58}, form the switch I region, are coloured in green. (**B**) Solvent accessible surface of GDP in the MD simulations of wild-type (red) and mutant (blue) RRAS/GDP complexes. (**C**) Conformation of the loop comprised between Val^{55}/Met^{55} and Asp^{59} in wild-type (red) and mutant (blue) RRAS/GDP complexes obtained from MD simulations. GDP is reported as semi-transparent yellow surface. Superimposed conformations of the corresponding loop (residues 29–33) in GDP-bound HRAS (violet) (PDB: 4Q21) and GDP-bound HRAS complexed with SOS1 (cyan) (PDB: 1BKD) are shown for comparison. The side chains of Tyr^{58} and the corresponding residue in HRAS, Tyr^{32}, are displayed as sticks.

and extent of signalling through the MAPK and PI3K/AKT cascades were evaluated using transient expression in COS-7 cells. Consistent with the above-mentioned findings, pull-down assays revealed a variably higher proportion of active, GTP-bound form for both mutants (Fig. 4A). Moreover, similarly to what observed under cell-free conditions, $RRAS^{G39dup}$ was resistant to GAP stimulation. Expression of both mutants promoted enhanced serum-dependent MEK, ERK and AKT phosphorylation (Fig. 4B), which was more evident in cells expressing the $RRAS^{G39dup}$ mutant.

Caenorhabditis elegans studies

To explore further the functional impact of the RASopathy causative RRAS mutants on RAS signalling *in vivo*, we used the nematode *C. elegans* as an experimental model. In *C. elegans*, the role of *ras-1*, the *RRAS* ortholog (33), has not been characterized yet. On the contrary, proper signalling through LET-60, the *C. elegans* ortholog of RAS proteins, has been established to play a crucial role in vulval development (34). In particular, LET-60/RAS is known to mediate the priming signal (LIN-3/EGF) released by the anchor cell to induce the three nearby vulval precursor cells (VPCs), P5.p, P6.p and P7.p, to generate a normal vulva. Enhanced and decreased signalling through LET-60 and the MAPK cassette results in multiple ectopic pseudovulvae (multivulva phenotype) and a failure in VPC induction (vulvaless phenotype), respectively (34,35).

Multiple transgenic lines were generated to conditionally express the wild-type *ras-1* cDNA ($ras\text{-}1^{WT}$) or the allele homologous to the disease-associated three-nucleotide duplication ($ras\text{-}1^{G27dup}$), which was identified to occur both as a germline and somatic event. Exogenous RAS-1 expression was induced by heat shock at early L3 larval stage to investigate the effects of the mutant protein on vulval development. Animals expressing $ras\text{-}1^{G27dup}$ displayed abnormal vulval morphogenesis resulting in the formation of a protruding vulva (Pvl) (Fig. 5A and B and Supplementary Material, Table S6), a phenotype associated with aberrant traffic through different signalling cascades (36,37). Of note, this phenotype had previously been reported in worms expressing the RASopathy causative $SHOC2^{S2G}$ mutant (38). Like those animals, $ras\text{-}1^{G27dup}$ worms showed decreased egg-laying efficiency (Egl phenotype), and accumulation of larvae inside the mother (Bag-of-worms phenotype). A significantly less penetrant phenotype was observed in animals expressing $ras\text{-}1^{WT}$. These findings, together with the observation that animals lacking *ras-1* do not exhibit any vulval defect (WormBase, http://www.wormbase.org/, and our personal assessment), supported the gain-of-function role of the mutation on RAS-1 function. At the late L3/early L4 larval stage, vulva

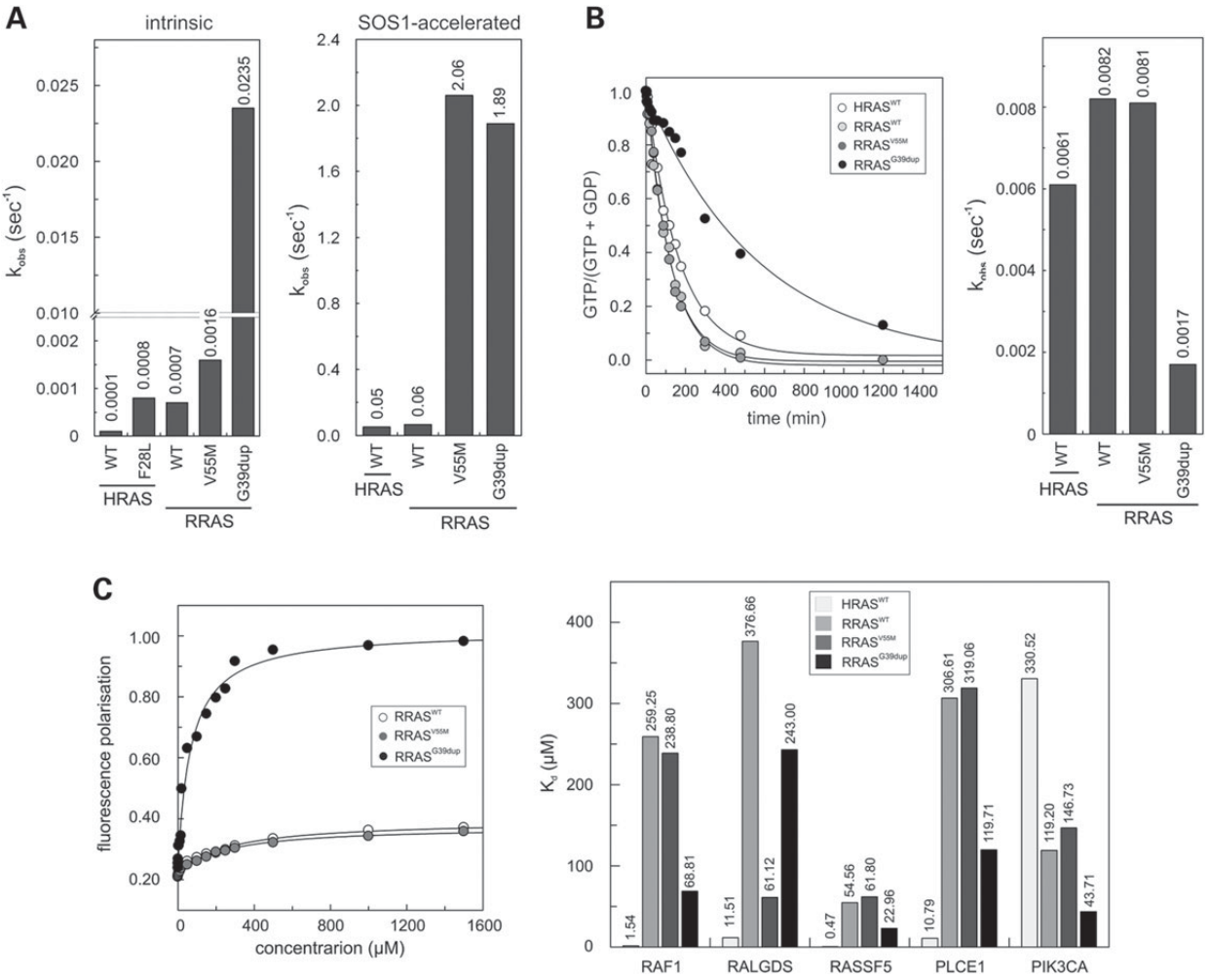

Figure 3. *In vitro* biochemical characterization of the RRAS^{G39dup} and RRAS^{V55M} mutants. (**A**) Intrinsic (left) and SOS1-accelerated (right) mantGDP nucleotide dissociation measured in the presence of 20-fold excess of non-labelled GDP. The decrease in mant fluorescence was fitted by single exponentials to obtain k_{obs} values for nucleotide dissociation. RRAS^{G39dup} exhibited a 35-fold increased intrinsic dissociation of mantGDP, whereas SOS1-accelerated mantGDP dissociation was augmented by ~30-fold for both mutants, compared with RRAS^{WT} and HRAS^{WT}. The K_{obs} values are an average of five to seven independent measurements. (**B**) Intrinsic GTP hydrolysis kinetics (left) and rate constants (right) of RRAS^{G39dup} and RRAS^{V55M} proteins, documenting the impaired catalytic activity in the former. The K_{obs} values are an average of five to seven independent measurements. (**C**) Binding of RRAS^{WT}, RRAS^{V55M} and RRAS^{G39dup} to the RAS-binding domain of RAF1 measured as variation in fluorescence polarization of each mantGppNHp-bound RRAS protein at increasing concentrations of RAF1-RBD (left), and dissociation constants (K_d) for the interaction of HRAS^{WT} and RRAS proteins to the RBDs of RAF1, RALGDS, PLCE1, PIK3CA and RASSF5 (right). K_d values were obtained by quadratic fitting of the concentration-dependent binding curves from fluorescence polarization measurement as exemplified for RAF1-RBD. Of note, RRAS^{WT} binds to RAF1, RALGDS, RASSF5 and PLCE1 less efficiently than HRAS, whereas an increased binding affinity to PIK3CA is observed.

morphogenesis normally begins with the descendants of VPC P6.p detaching from the cuticle and forming a symmetric invagination (Fig. 5C) (34). Animals in which the expression of *ras-1*^{WT} had been induced at early L3 largely maintained this pattern (17/20). In contrast, in larvae expressing *ras-1*^{G27dup}, descendants of VPCs P5.p and/or P7.p more frequently detached from the cuticle, resulting in larger and more asymmetric invaginations (10/30). This morphogenesis defect was the earliest detectable effect of the *ras-1*^{G27dup} allele on vulval development, similarly to that previously documented in transgenic lines expressing SHOC2^{S2G} (38).

Genetic interaction between the RAS-1/RRAS mutant and LET-60/RAS was also investigated. While expression of the RAS-1^{G27dup} mutant was able to exacerbate the multivulva phenotype associated with a hyperactive *let-60* allele (*n1046*), expression of wild-type RAS-1 failed to do so (Table 1). Similarly, a significant, although partial rescue of the VPC induction defect associated with a *let-23/EGFR* hypomorphic allele (*sy1*) was observed in animals expressing the activating RAS-1^{G27dup} mutant, but not in worms expressing the wild-type counterpart (Table 1). Overall, these experiments provided evidence of a positive modulatory role of the RAS-1/RRAS mutant on LET-60/RAS signalling.

DISCUSSION

Mutations of genes coding for proteins with role in RAS signalling and the RAF/MEK/ERK cascade have been identified as the

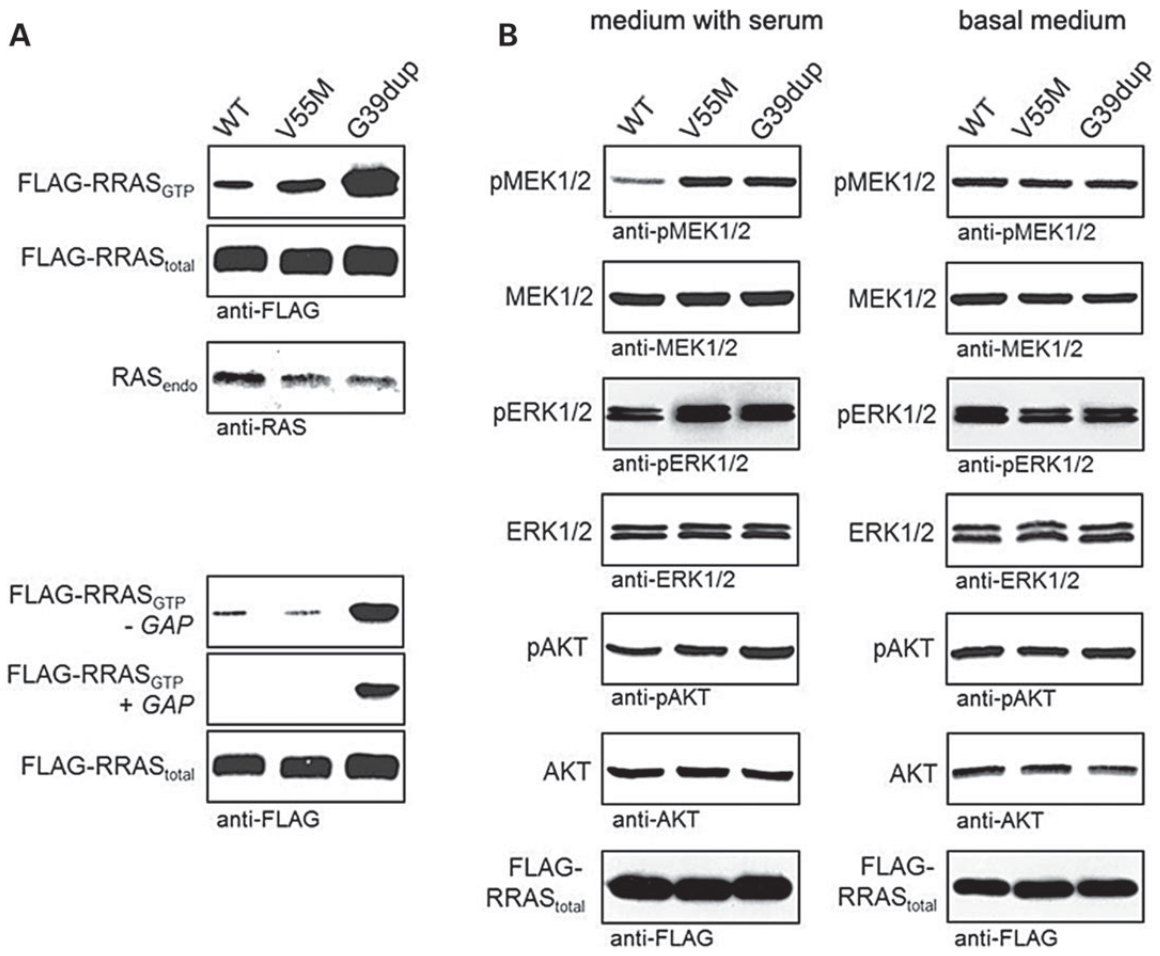

Figure 4. RRAS^{G39dup} and RRAS^{V55M} signalling activities in cells. (**A**) Determination of GTP-bound RRAS levels in COS-7 cells transiently expressing wild-type or mutant FLAG-tagged RRAS proteins. Assays were performed in the presence of serum (above), and in serum-free conditions (−GAP) or in the presence of the neurofibromin GAP domain (+GAP) (below). RRAS^{G39dup} was predominantly present in the active GTP-bound form and was resistant to GAP stimulation, whereas a slightly increased level of GTP-bound RRAS^{V55M} was observed in the presence of serum. Representative blots of three performed experiments are shown. (**B**) Determination of MEK, ERK and AKT phosphorylation levels (pMEK, pERK and pAKT) in transiently transfected COS-7 cells cultured in medium with serum (left) or basal medium (right). Expression of each RRAS mutant resulted in variably enhanced MEK, ERK and also partially AKT phosphorylation after stimulation. Total MEK, ERK and AKT in cell lysates are shown for equal protein expression and loading. Expression levels of exogenous, FLAG-tagged RRAS in cell lysates are shown for each experiment. Representative blots of three performed experiments are shown.

molecular cause underlying a group of clinically related developmental disorders, the RASopathies. Here, we used a gene candidacy approach based on large-scale protein–protein interaction/functional network analysis to identify *RRAS* as a novel gene implicated in a condition with features within the RASopathy spectrum. Disease-causing *RRAS* mutations are activating and act by maintaining the GTPase in its GTP-bound active state. Aberrant RRAS function was demonstrated to perturb variably intracellular signal flow through the RAF/MEK/ERK cascade, and to a certain extent also the PI3K/AKT pathway. Of note, these gain-of-function mutations are likely to define a novel leukaemia-prone condition. Consistent with this view, the same class of *RRAS* lesions was identified to occur as acquired somatic event in JMML, characterizing a subset of this myeloproliferative/myelodysplastic disorder with rapid progression to AML.

RRAS shares several biochemical properties with HRAS, NRAS and KRAS, as well as some common function, including stimulation of cell proliferation, survival and transformation (19,39). Despite these similarities, however, previous observations have emphasized the role of RRAS in cell adhesion, spreading and migration, and its modulatory function on effectors distinct from those used by 'classical' RAS proteins (40,41). While PI3K/AKT has been recognized as a major effector pathway of RRAS, only a minor impact on MAPK signalling had been reported (41,42). The present *in vitro* findings provide evidence that disease-associated RRAS mutants enhance the activation of the MAPK cascade, at least in response to specific stimuli. On the other hand, the identification of *RRAS* as a novel disease gene implicated in a RASopathy disorder further emphasizes the relevance of dysregulated signalling controlling cell spreading and migration in certain features of NS (e.g. congenital heart defects and lymphedema) and JMML (leukocyte infiltration in non-haematopoietic tissues) (43–45).

Caenorhabditis elegans studies provided evidence for a genetic interaction between the RAS-1^{G27dup}/RRAS^{G39dup} and

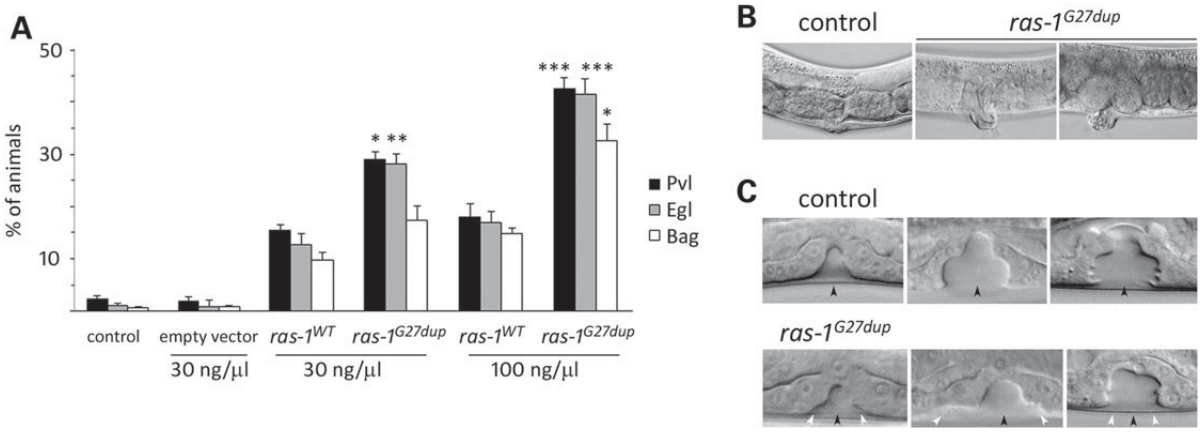

Figure 5. Consequences of *ras-1*^{G27dup} expression on *C. elegans* vulval development. (**A**) Heat-shock-driven expression of *ras-1*^{WT} and *ras-1*^{G27dup} at early L3 stage results in protruding vulva (Pvl), egg laying defective (Egl) and bag-of-worms (Bag) phenotypes. Isogenic animals that had lost the transgene (control group) and worms expressing the heat shock-inducible vector (empty vector) were subjected to heat shock and scored in parallel for comparison. The dose at which the transgene has been injected is reported at the bottom. Error bars indicate SD of three independent experiments. Asterisks indicate significant differences compared with *ras-1*^{WT} at the corresponding dose of injection ($^{*}P < 0.05$; $^{**}P < 0.005$; $^{***}P < 0.0005$; Fisher's Exact Test). (**B**) A proper vulva develops in heat-shocked control animals (left), whereas a protruding vulva is observed in heat-shocked *ras-1*^{G27dup} young adults (middle) and adult worms (right). (**C**) Nomarski images of vulval precursor cells in late L3 (left), early L4 (middle) and mid-late L4 (right) stages from synchronized animals heat-shocked at early L3. In control animals ($N = 48$), only P6.p descendants invaginate (upper panel), whereas in 10 of 30 analysed *ras-1*^{G27dup}-expressing worms, P5.p and/or P7.p descendants also detach from the cuticle, generating asymmetric invaginations (lower panel). Black arrowheads point to P6.p descendant invagination, whereas white arrowheads point to P5.p and P7.p descendant invagination. Anterior is to the left and dorsal is up, in all images.

LET-60/RAS *in vivo*. Specifically, expression of the RAS-1 mutant protein was able to rescue, in part, the VPC induction defect resulting from a hypomorphic LET-23 mutant and enhanced the multivulva phenotype associated with a LET-60 gain-of-function genetic background. No impact of wild-type RAS-1/RRAS expression was observed in both models. We also observed that worms expressing *ras-1*^{G27dup} displayed abnormal vulval morphogenesis (protruding vulva), possibly resulting from aberrant morphogenetic movements of the VPC descendant cells. Of note, we observed an equivalent phenotype in transgenic lines expressing SHOC2^{S2G} (38) and a PTPN11/SHP2 gain-of-function mutant (our unpublished data), suggesting functional equivalence of these mutants. Genetic studies support the view that these vulva defects arise, in part, through perturbation of signalling mediated by the RHO-related GTPase, RAC, which plays a critical role in vulval morphogenesis (37). This finding is in line with the established role of RRAS on RAC signalling (40,41) and with preliminary data indicating enhanced migration and chemotactic capabilities in cells stably expressing the disease-associated RRAS mutants (our unpublished data).

The biochemical characterization of disease-associated *RRAS* mutations provided strong evidence for the existence of distinct structural and mechanistic effects resulting in an overall enhancement of RRAS signalling. Function of RAS family proteins in signal transduction is controlled by two events, the GDP/GTP exchange and GTP hydrolysis. Any perturbation of these processes can affect dramatically the fine-tuned balance of the GTPase interaction with effectors and signal output. The majority of gain-of-function mutations affecting RAS proteins, including those contributing to oncogenesis, trigger the accumulation of these GTPases in the active state by impairing intrinsic GTPase activity, and/or conferring resistance to GAPs (17). This is also the case of two of the three mutations identified in this study, p.Gly39dup and p.Gln87Leu, the latter corresponding to the p.Gln61Leu in RAS proteins (present study and ref. 18,19). The characterization of the biochemical behaviour of RRAS^{G39dup}, however, also demonstrated a dramatic increase in both the intrinsic and GEF-catalysed nucleotide exchange as a process contributing to the accumulation of this mutant in its GTP-bound state. Aberrant GEF-accelerated nucleotide exchange dynamics was identified as the event driving functional dysregulation in the RRAS^{V55M} mutant, which was documented to be hyper responsive to GEF stimulation, but retained stimulus-dependency. Remarkably, the RRAS^{G39dup} and RRAS^{V55M} mutants were demonstrated to exhibit a diverse binding behaviour to effectors suggesting a differential impact of mutations on downstream signalling cascades, including PI3K/AKT and RALGDS/RAL, whose biological significance and impact, however, require further studies.

The clinical phenotype of the two subjects with germline *RRAS* mutations was reminiscent of NS. The individual with the Gly^{39} duplication displayed pulmonic stenosis, reduced growth, café-au-lait spots, mild motor delay and low-set ears, which recur in NS (5). Facial features, however, were distinctive, and not typical of NS. In contrast, the patient heterozygous for the p.Val55Met substitution exhibited a very mitigated phenotype characterized by suggestive facial characteristics (triangular face, downslanting palpebral fissures and low-set ears), low posterior hairline, broad chest and borderline cognitive abilities, without cardiac involvement or defective growth, indicating that clinical features associated with *RRAS* mutations might be quite subtle. Of note, the milder phenotype associated with the p.Val55Met change is consistent with the weaker perturbing effect of the RRAS^{V55M} mutant on MAPK and PI3K/AKT signalling compared with the RRAS^{G39dup} protein. Additional information on the spectrum of germline *RRAS* mutations, their associated phenotype and their functional impact on signalling,

Table 1. Vulva phenotypes in *C. elegans* mutant strains expressing wild-type RAS-1 or the disease-associated RAS-1^{G27dup} mutant

Genotype	Transgene	*N*	Muv (%)	Vul (%)	Pvl (%)	*N*	P6.p induction (%)
wild-type	none	207	0	0	1.0	48	100
let-60(*n1046*)	none	201	77.9	–	0.5	50	100
let-60(*n1046*)	*ras-1*^{wt}	244	76.4	–	2.8	43	100
let-60(*n1046*)	*ras-1*^{G27dup}	231	87.1[a]	–	3.0	50	100
let-23(*sy1*)	none	194	–	87.8	3.6	178	13.4
let-23(*sy1*)	*ras-1*^{WT}	169	–	84.3	4.1	156	14.0
let-23(*sy1*)	*ras-1*^{G27dup}	282	–	83.3	10.3[b]	128	24.2[c]

Strains: *let-60(n1046)* is a gain-of-function allele of *let-60* (ortholog of the human *HRAS*, *KRAS* and *NRAS* genes); *let-23(sy1)* is a hypomorphic allele of *let-23* (ortholog of the human *EGFR* gene). *ras-1*^{WT} and *ras-1*^{G27dup} indicate *hsp-16.41::ras-1*^{WT}- and *hsp-16.41::ras-1*^{G27dup}-containing constructs injected at 100 ng/µl, respectively. After each cross, isogenic worms that had lost the transgene were cloned separately and used as controls.
Animals were grown at 20°C and heat-shocked in parallel at early L3 stage. *N* indicates the number of animals scored. Multivulva (Muv), vulvaless (Vul) and protruding vulva (Pvl) phenotypes are expressed as percentage of worms with ectopic pseudovulvae, animals lacking a vulva and adults with a protruding vulva, respectively. Induction of vulval cell fate is expressed as percentage of P6.p that has been induced to invaginate.
In all comparisons, *P*-values were calculated using two-tailed Fisher's exact test.
[a]Significantly different from *let-60(n1046)* ($P < 0.02$).
[b]Significantly different from *let-23(sy1)* ($P < 0.01$) and *let-23(sy1);ras-1*^{WT} ($P < 0.02$).
[c]Significantly different from *let-23(sy1)* ($P = 0.02$) and *let-23(sy1);ras-1*^{WT} ($P < 0.05$).

however, is necessary to establish clinically relevant genotype–phenotype correlations.

JMML is a clonal myeloproliferative/myelodysplastic disorder of childhood characterized by overproduction of immature myeloid cells that variably retain the capacity to differentiate. Upregulation of RAS/MAPK signalling owing to germline and somatic mutations in *PTPN11*, *NRAS*, *KRAS*, *NF1* and *CBL* is a major event implicated in this malignancy (13,46,47). Our data document that upregulated RRAS function represents a novel event contributing to JMML pathogenesis and/or disease progression. Notably, somatic *RRAS* mutations co-occurred with acquired *NRAS* lesions in atypical JMML characterized by late onset and rapid progression to AML. While JMML is generally an aggressive malignancy, a subset of *NRAS*/*KRAS* mutation-positive patients has been reported to exhibit a mild course, with spontaneous remission despite the *RAS*-mutated clone persisting for years (48–50, our unpublished data). This suggests that in some instances, certain *NRAS* mutations are not sufficient to support full leukaemogenesis, requiring synergism with a second RAS signalling targeting event. In line with this view, *NRAS* mutations have been documented to co-exist with defects in other RASopathy genes (e.g. *PTPN11*) in some cases resulting in a particularly aggressive disease resembling AML with myelodysplasia-related changes (51,52), as that observed in the present cases. Other studies, however, are required to appreciate more precisely the role of enhanced RRAS function in leukaemogenesis as well as its clinical relevance in haematological malignancies.

In conclusion, our findings document that germline activating mutations in *RRAS* underlie a condition within the RASopathy family that may resemble NS phenotypically. In the examined cohorts, *RRAS* lesions were found to account for only a small portion of cases, which might be related to their severe consequences on embryonic/foetal development and/or to the biased selection of the subjects included in this study. Based on the present findings, however, *RRAS* mutations are expected to be more common among subjects with clinical features only partially overlapping NS, and particularly in patients with syndromic JMML/AML not associated with mutations in the *PTPN11*, *NF1*, *CBL*, *KRAS* and *NRAS* genes. While further efforts are required to characterize more precisely the clinical impact of germline and somatic mutations affecting *RRAS*, our findings suggest an unpredicted role of this GTPase in development and haematopoiesis. Consistent with the recent identification of *RIT1* as disease gene implicated in a significant proportion of NS (9), our findings further extend the concept of 'RASopathy gene' to a transducer whose dysregulated function perturbs signal flow through the MAPK cascade but does not belong to the core RAS/MAPK signalling cassette.

MATERIALS AND METHODS

Selection of RASopathy candidate genes

A web-based tool, Genes2FANs (http://actin.pharm.mssm.edu/genes2FANs), using a large-scale protein–protein interaction network coupled to a panel of functional association networks (FANs) was utilized to build a subnetwork connecting proteins to the known RASopathy genes (i.e. *PTPN11*, *SOS1*, *NF1*, *SPRED1*, *CBL*, *NRAS*, *KRAS*, *HRAS*, *RAF1*, *BRAF*, *SHOC2*, *MAP2K1* and *MAP2K2*), as seed proteins. Gene Ontology (biological process tree), mammalian phenotype browser, and Connectivity Map (drug-associated gene expression signatures), ChEA and TRANSFAC (transcription factor networks) databases were selected to construct the functional subnetworks utilized for prioritization of candidates (15). The programme allows to calculate z-scores for intermediate nodes (i.e. candidates), which are ranked based on their connections to the seed proteins.

Subjects and mutation analysis

Three cohorts of patients were considered in the study. A first group including 96 subjects with clinical features within the RASopathy spectrum and without mutation in previously identified RASopathy genes (i.e. *CBL*, *PTPN11*, *SOS1*, *KRAS*, *HRAS*, *NRAS*, *RAF1*, *BRAF*, *SHOC2*, *MAP2K1* and *MAP2K2*) was screened for a selected panel of candidates. A second cohort including 408 subjects with NS or a closely related phenotype previously tested negative for mutations in a heterogeneous subset

of RASopathy genes was scanned for *RRAS* mutations. All subjects included in this cohort had been screened for mutations in *PTPN11*, *SOS1* and *RAF1* genes. In both cohorts, the clinical diagnosis was made on the basis of standardized clinical criteria assessed by experienced clinical geneticists and paediatricians. Clinical features for the majority of subjects satisfied diagnostic criteria reported for NS, LEOPARD syndrome and cardiofaciocutaneous syndrome (53–57), but individuals who lacked sufficient features for a definitive diagnosis were also included. *RRAS* mutation analysis was also carried out on a cohort including 110 subjects with non-syndromic JMML that had prospectively been collected and genotyped (58). Mutation screening was performed on the entire *RRAS* coding sequence and flanking intronic stretches (NC_000019.10, 49635295.. 49640143, complement; NM_006270.3; NP_006261.1) on genomic DNA extracted from circulating leukocytes (cohorts I, II and III) or bone marrow aspirates (cohort III) by denaturing high-performance liquid chromatography (DHPLC) (3100 or 3500HT WAVE DNA fragment analysis system, Transgenomic, Omaha, NE, USA) and/or direct bidirectional sequencing (ABI Prism 3130, 3730 and 3500 Genetic Analyzers; Applied Biosystems, Foster City, CA, USA). Primer pairs, PCR and DHPLC conditions are available upon request. dbSNP137 (http://www.ncbi.nlm.nih.gov/projects/SNP/snp_summary.cgi), HapMap (rel.27) (http://hapmap.ncbi.nlm.nih.gov/) and 1000 Genomes (http://www.1000genomes.org/) databases were used to annotate the identified sequence variants. SIFT (http://sift.jcvi.org/), PolyPhen-2 (http://genetics.bwh.harvard.edu/pph2/) and MutationTaster (http://www.mutationtaster.org/) were used to predict the functional impact of the identified variants. Paternity was confirmed by STR genotyping, using the PowerPlex 16 System (Promega). DNA from leukocytes, hair bulb cells, bone marrow aspirates and skin fibroblasts was extracted using standard protocols. DNA specimens were collected under Institutional Review Board-approved protocols. Informed consent for DNA storage and genetic analyses was obtained from all subjects. Permission was obtained to publish picture of patient 9802, whereas subject NS1166 denied consent for picture publication.

Exome sequencing

Targeted enrichment and massively parallel sequencing were performed on genomic DNA extracted from circulating leukocytes and fibroblasts of patient 9802. Exome capture was carried out using the SureSelect Human All Exon V4+UTRs (Agilent), and sequencing with a HiSeq2000 instrument (Illumina). Image analysis and base calling were performed using the Real Time Analysis (RTA) pipeline v. 1.14 (Illumina). Paired-end reads alignment to the reference human genome (UCSC GRCh37/hg19) and variant calling were carried out using the CASAVA v. 1.8 pipeline (Illumina). Variant annotation, SNP filtering (dbSNP135, 1000 Genomes, HapMap and IntegraGen Exome databases) and patient-matched germline variant filtering were attained using an in-house pipeline by IntegraGen (Evry, France).

Molecular dynamics analyses

Starting coordinates for MD simulations were obtained from the RRAS crystallographic structure in complex with GDP and Mg^{2+} (PDB: 2FN4; RCSB Protein Data Bank, http://www.rcsb.org/pdb/home/home.do). The *N*-terminus and *C*-terminus of RRAS, absent in the crystal, were not considered in simulations. Deep View software was used to add atoms missing in the PDB file, belonging to residues 31, 96, 114, 121 and 192 as well as to substitute residue 55 (simulation of the p.Val55Met mutant) (59). All MD simulations were performed with GROMACS 4.5 package, by using the GROMOS96 43a1 force field parameters for the protein. Parameters for GDP were taken from the GROMACS website (http://www.gromacs.org). Simulations were performed as previously described (60,61), except for some details. Briefly, the proteins were initially placed in a dodecahedral box, solvated with ~6700 SPC water molecules, and six Na^+ ions were added to neutralize the protein charge. Following initial energy minimization and a 100-ps MD run, during which the protein atoms were position restrained, the temperature of solute and solvent was raised from 50 to 300 K in a stepwise manner. 200-ns-long simulations were performed for wild-type RRAS and the RASopathy causative mutant. The particle mesh Ewald method was used to evaluate electrostatic interactions (62), whereas a cut-off scheme was employed for Van der Waals interactions. Temperature and pressure were kept constant at 300 K and 1 bar by using the Berendsen weak-coupling method (63), using separate temperature baths for protein–GDP complex and solvent, with a relaxation time of 0.1 ps for temperature and 1 ps for pressure. A time step of 2 fs was employed. Root mean square deviations were calculated according to standard definitions. UCSF Chimera (http://www.cgl.ucsf.edu/chimera/) was used for molecular graphics and structures superposition, by using the MatchMaker option.

Biochemical and functional characterization of RRAS mutants

The generation of constructs, and preparation and purification of proteins were as previously described (64). The intrinsic activities of the RAS proteins, their modulation by GEFs and GAPs and their interaction with different effector proteins were determined as described earlier (65,66). Dissociation of mantGDP from RAS proteins (0.1 μM) was measured in the presence of 20 μM GDP in 30 mM Tris–HCl, pH 7.5, 10 mM KH_2PO_4/K_2HPO_4, 5 mM $MgCl_2$, 3 mM dithioerythritol (DTE), at 25 °C, using a Perkin Elmer fluorimeter at 366 nm (excitation wavelength) and 450 nm (emission wavelength). Observed rate constants (k_{obs}) of dissociation were obtained by single exponential fitting of the data. GEF-accelerated mantGDP dissociation from RAS proteins (0.1 μM) was measured as mentioned earlier, in the presence of the catalytic domain of SOS1, Cdc25 (5 μM), using stopped-flow instrument.

The intrinsic GTPase reaction was performed by mixing 70 μM nucleotide-free RAS proteins (HRAS, $RRAS^{WT}$, $RRAS^{V55M}$ and $RRAS^{G39dup}$) with 50 μM GTP in 30 mM Tris–HCl, pH 7.5, 10 mM KH_2PO_4/K_2HPO_4, 10 mM $MgCl_2$, 3 mM DTE, at 25°C, using HPLC assay as previously described (67). Samples were taken at different time points and analysed by HPLC for their GDP and GTP contents to determine the relative GTP content [(GTP)/(GDP + GTP)]. Intrinsic GTP hydrolysis k_{obs} of proteins were obtained by single exponential fitting of the data. For determination of GAP (neurofibromin, residues

1–333)-stimulated GTPase activity, GDP bound to HRAS and RRAS proteins was exchanged with excess mantGTP in the presence of alkaline phosphatase. Unbound nucleotides were removed by NAP5 column, and the RAS/mantGTP proteins were snap-frozen in liquid nitrogen (66). GAP-stimulated GTP hydrolysis of RAS proteins (0.2 μM) was measured in 30 mM Tris–HCl, pH 7.5, 10 mM $MgCl_2$, 3 mM DTE at 25°C using a Hightech TgK Scientific stopped-flow instrument. Reactions measured the decrease in fluorescence owing to hydrolysis of mantGTP. This decay was fit by a single exponential.

Effector binding assays were performed in 30 mM Tris–HCl, pH 7.5, 100 mM NaCl, 5 mM $MgCl_2$, 3 mM DTE at 25°C using a Fluoromax 4 fluorimeter in polarization mode. Increasing amounts of GST-tagged RAS-binding domains (RBD) of RAS effectors were titrated to 0.3 μM mantGppNHp-bound RAS proteins resulting in an increase of polarization (64). The dissociation constants (K_d) were calculated by fitting the concentration-dependent binding curve using a quadratic ligand binding equation.

For cell-based assays, COS-7 cells were transiently transfected with FLAG-tagged $RRAS^{WT}$, $RRAS^{V55M}$ or $RRAS^{G39dup}$ by the DEAE-dextran method. For serum conditions, cells were incubated for 48 h in 10% FCS. In serum-starved conditions, serum was changed to basal medium midway between the transfection and harvesting. Transfected COS-7 cells were harvested and lysed in fishing buffer [50 mM Tris–HCl, pH 7.5, 2 mM $MgCl_2$, 100 mM NaCl, 1% IGEPAL CA-630, 10% glycerol, EDTA-free protease inhibitor cocktail (Roche, 1 tablet/50 ml buffer), 20 mM disodium β-glycerol phosphate and 1 mM Na_3VO_4]. Cleared cell lysates were incubated with GSH-beads loaded with GST-RAF1-RBD. GTP-bound proteins and total recombinant proteins were analysed by immunoblotting with anti-FLAG antibody. Antibodies against MEK1/2, ERK1/2, AKT, phospho-MEK1/2 (Ser217/221), phospho-ERK1/2 (Thr202/Tyr204) and phospho-AKT (Thr308) were purchased from Cell Signaling Technology (68).

Caenorhabditis elegans studies

Culture and maintenance of animals were as previously described (69). The *let-60(n1046)* (*let-60*/*RAS* gain-of-function allele) and *let-23(sy1)* (*let-23*/*EGFR* hypomorphic allele) strains were provided by the *Caenorhabditis Genetics Center* (University of Minnesota). The three-nucleotide insertion, c.81_82insGGC *(ras-1^{G27dup})*, corresponding to c.116_118dup in *RRAS*, was introduced in the wild-type cDNA (*ras-1^{WT}*) (*C. elegans* ORF clone AAB03320, Thermo Scientific) by site-directed mutagenesis (QuikChange Site-Directed Mutagenesis Kit, Stratagene). *ras-1* cDNAs were subcloned into the pPD49.83 heat shock-inducible vector (a gift of A. Fire, Stanford University School of Medicine). Germline transformation was performed as described (70). pJM371 plasmid [p*elt-2*::NLS::*RFP*] (a gift from J.D. McGhee, University of Calgary), which drives red fluorescent protein (RFP) expression in intestinal cell nuclei, was used as co-injection marker (30 ng/μl). Two different doses of constructs were injected (30 and 100 ng/μl). Animals from at least three independent transgenic lines for each construct and each dose of injection (i.e. six lines expressing *ras-1^{WT}* and six lines expressing *ras-1^{G27dup}*) were heat-shocked in parallel and scored blindly at a Leica MZ10F dissecting microscope to check for the presence of protruding vulvae (Pvl phenotype) and multiple ectopic pseudovulvae (Muv phenotype), count the number of eggs retained in the uterus (Egl phenotype) and identify animals that had become bag-of-worms (Bag phenotype). Isogenic worms that had lost the transgene were cloned separately and used as controls. Following heat shock, all the transgenic lines expressing *ras-1^{WT}* or *ras-1^{G27dup}* showed a variable degree of these phenotypes. Lines *gbEx555a*[*hsp-16.41*::*ras-1^{WT}*;*pelt-2*::NLS::*RFP*] and *gbEx557a*[*hsp-16.41*::*ras-1^{G27dup}*;*pelt-2*::NLS::*RFP*] were scored quantitatively in triplicate experiments at the compound microscope and used for further analyses. Genetic crosses were performed according to standard methods (69). The genotype of individual alleles was confirmed by direct sequencing of the appropriate genomic region. After each cross, isogenic worms that had lost the transgene were used as controls.

To investigate VPCs induction and vulva morphogenesis, synchronized hermaphrodites carrying each transgene and the corresponding isogenic controls were heat-shocked in parallel at early L3 stage (33°C, 1 h, followed by 30°C, 1 h). Animals were scored at the compound microscope for vulval induction at late L3 and L4 stages, and for Pvl/Egl/Bag phenotypes at the adult stage. Microscopy observations were performed with a Nikon Eclipse 80i instrument equipped with Nomarski differential interference contrast optics on live animals mounted on 2% agarose pads containing 10 mM sodium azide as anaesthetic.

SUPPLEMENTARY MATERIAL

Supplementary Material is available at *HMG* online.

ACKNOWLEDGEMENTS

We are grateful to the participating patients and their families. We thank Serenella Venanzi (Istituto Superiore di Sanità, Rome, Italy), Michela Bonaguro (Policlinico S.Orsola-Malpighi, Bologna, Italy), Federica Consoli (Istituto Mendel, Rome, Italy) and Cédric Vignal and Sabrina Pereira (Hôpital Robert Debré, Paris, France) for skilful technical assistance, and the Open Laboratory (IGB-CNR, Naples, Italy) for experimental support. We also thank Paolo Bazzicalupo (IGB-CNR) for critical reading of the manuscript, paediatricians from the *Société Française des Cancers de l'Enfant* (SFCE) for providing biological material from their patients and CINECA for computational resources. Some nematode strains used in this work were provided by the *Caenorhabditis Genetics Center* (University of Minnesota, Minneapolis, MN, USA) funded by the NIH Office of Research Infrastructure Programs (P40OD010440).

Conflict of Interest statement. None declared.

FUNDING

This work was supported by grants from the ERA-Net for research programmes on rare diseases 2009 (NSEuroNet to M.Z., H.C., M.R.A. and M.T.), Telethon-Italy (GGP10020 and GGP13107 to M.T.), AIRC (IG 13360 to M.T.), NGFNplus program of the German Ministry of Science and Education (01GS08100 to M.R.A.), German Research Foundation through the Collaborative Research Center 974 (Communication and Systems Relevance

during Liver Injury and Regeneration to M.R.A.) and NIH (HL071207 to B.D.G.). F.P. was recipient of a research fellowship from '*Associazione Italiana Sindromi di Costello e cardiofaciocutanea*'. Funding to pay the Open Access publication charges for this article was provided by Telethon-Italy.

REFERENCES

1. Mitin, N., Rossman, K.L. and Der, C.J. (2005) Signaling interplay in Ras superfamily function. *Curr. Biol.*, **15**, R563–R574.
2. Mendoza, M.C., Er, E.E. and Blenis, J. (2011) The Ras-ERK and PI3K-mTOR pathways: cross-talk and compensation. *Trends Biochem. Sci.*, **36**, 320–328.
3. Harris, T.J.R. and McCormick, F. (2010) The molecular pathology of cancer. *Nat. Rev. Clin. Oncol.*, **7**, 251–265.
4. Pylayeva-Gupta, Y., Grabocka, E. and Bar-Sagi, D. (2011) RAS oncogenes: weaving a tumorigenic web. *Nat. Rev. Cancer*, **11**, 761–774.
5. Roberts, A.E., Allanson, J.E., Tartaglia, M. and Gelb, B.D. (2013) Noonan syndrome. *Lancet*, **381**, 333–342.
6. Schubbert, S., Shannon, K. and Bollag, G. (2007) Hyperactive Ras in developmental disorders and cancer. *Nat. Rev. Cancer*, **7**, 295–308.
7. Tartaglia, M. and Gelb, B.D. (2010) Disorders of dysregulated signal traffic through the RAS-MAPK pathway: phenotypic spectrum and molecular mechanisms. *Ann. N. Y. Acad. Sci.*, **1214**, 99–121.
8. Rauen, K.A. (2013) The RASopathies. *Annu. Rev. Genomics Hum. Genet.*, **14**, 355–369.
9. Aoki, Y., Niihori, T., Banjo, T., Okamoto, N., Mizuno, S., Kurosawa, K., Ogata, T., Takada, F., Yano, M., Ando, T. *et al.* (2013) Gain-of-function mutations in RIT1 cause Noonan syndrome, a RAS/MAPK pathway syndrome. *Am. J. Hum. Genet.*, **93**, 173–180.
10. Tartaglia, M., Gelb, B.D. and Zenker, M. (2011) Noonan syndrome and clinically related disorders. *Best Pract. Res. Clin. Endocrinol. Metab.*, **25**, 161–179.
11. Kratz, C.P., Rapisuwon, S., Reed, H., Hasle, H. and Rosenberg, P.S. (2011) Cancer in Noonan, Costello, cardiofaciocutaneous and LEOPARD syndromes. *Am. J. Med. Genet. C Semin. Med. Genet.*, **157C**, 83–89.
12. Gripp, K.W. (2005) Tumor predisposition in Costello syndrome. *Am. J. Med. Genet. C Semin. Med. Genet.*, **137C**, 72–77.
13. Loh, M.L. (2011) Recent advances in the pathogenesis and treatment of juvenile myelomonocytic leukaemia. *Br. J. Haematol.*, **152**, 677–687.
14. McKay, M.M. and Morrison, D.K. (2007) Integrating signals from RTKs to ERK/MAPK. *Oncogene*, **26**, 3113–3121.
15. Dannenfelser, R., Clark, N.R. and Ma'ayan, A. (2012) Genes2FANs: connecting genes through functional association networks. *BMC Bioinformatics*, **13**, 156.
16. Lowe, D.G., Capon, D.J., Delwart, E., Sakaguchi, A.Y., Naylor, S.L. and Goeddel, D.V. (1987) Structure of the human and murine R-ras genes, novel genes closely related to ras proto-oncogenes. *Cell*, **48**, 137–146.
17. Wennerberg, K., Rossman, K.L. and Der, C.J. (2005) The Ras superfamily at a glance. *J. Cell Sci.*, **118**, 843–846.
18. Krengel, U., Schlichting, I., Scherer, A., Schumann, R., Frech, M., John, J., Kabsch, W., Pai, E.F. and Wittinghofer, A. (1990) Three-dimensional structures of H-ras p21 mutants: molecular basis for their inability to function as signal switch molecules. *Cell*, **62**, 539–548.
19. Saez, R., Chan, A.M., Miki, T. and Aaronson, S.A. (1994) Oncogenic activation of human R-ras by point mutations analogous to those of prototype H-ras oncogenes. *Oncogene*, **9**, 2977–2982.
20. Aoki, Y., Niihori, T., Kawame, H., Kurosawa, K., Ohashi, H., Tanaka, Y., Filocamo, M., Kato, K., Suzuki, Y., Kure, S. *et al.* (2005) Germline mutations in HRAS proto-oncogene cause Costello syndrome. *Nat. Genet.*, **37**, 1038–1040.
21. Bollag, G., Adler, F., elMasry, N., McCabe, P.C., Conner, E. Jr, Thompson, P., McCormick, F. and Shannon, K. (1996) Biochemical characterization of a novel KRAS insertion mutation from a human leukemia. *J. Biol. Chem.*, **271**, 32491–32494.
22. Reimann, C., Arola, M., Bierings, M., Karow, A., van den Heuvel-Eibrink, M.M., Hasle, H., Niemeyer, C.M. and Kratz, C.P. (2006) A novel somatic K-Ras mutation in juvenile myelomonocytic leukemia. *Leukaemia*, **20**, 1637–1638.
23. Murugan, A.K., Hong, N.T., Cuc, T.T., Hung, N.C., Munirajan, A.K., Ikeda, M.A. and Tsuchida, N. (2009) Detection of two novel mutations and relatively high incidence of H-RAS mutations in Vietnamese oral cancer. *Oral. Oncol.*, **45**, e161–e166.
24. Sartori, G., Cavazza, A., Sgambato, A., Marchioni, A., Barbieri, F., Longo, L., Bavieri, M., Murer, B., Meschiari, E., Tamberi, S. *et al.* (2009) EGFR and K-ras mutations along the spectrum of pulmonary epithelial tumors of the lung and elaboration of a combined clinicopathologic and molecular scoring system to predict clinical responsiveness to EGFR inhibitors. *Am. J. Clin. Pathol.*, **131**, 478–489.
25. Milburn, M.V., Tong, L., deVos, A.M., Brünger, A., Yamaizumi, Z., Nishimura, S. and Kim, S.-H. (1990) Molecular switch for signal transduction: structural differences between active and inactive forms of protooncogenic ras proteins. *Science*, **247**, 939–945.
26. Diaz, J.F., Wroblowski, B., Schlitter, J. and Engelborghs, Y. (1997) Calculation of pathways for the conformational transition between the GTP- and GDP-bound states of the Ha-ras-p21 protein: calculations with explicit solvent simulations and comparison with calculations in vacuum. *Proteins*, **28**, 434–451.
27. Kuppens, S., Díaz, J.F. and Engelborghs, Y. (1999) Characterization of the hinges of the effector loop in the reaction pathway of the activation of ras-proteins. Kinetics of binding of beryllium trifluoride to V29G and I36G mutants of Ha-ras-p21. *Prot. Sci.*, **8**, 1860–1866.
28. Ma, J. and Karplus, M. (1997) Molecular switch in signal transduction: reaction paths of the conformational changes in ras p21. *Proc. Natl. Acad. Sci. USA*, **94**, 11905–11910.
29. Gorfe, A.A., Grant, B.J. and McCammon, J.A. (2008) Mapping the nucleotide and isoform-dependent structural and dynamical features of Ras proteins. *Structure*, **16**, 885–896.
30. Hall, B.E., Yang, S.S., Boriack-Sjodin, P.A., Kuriyan, J. and Bar-Sagi, D. (2001) Structure-based mutagenesis reveals distinct functions for Ras switch 1 and switch 2 in Sos-catalyzed guanine nucleotide exchange. *J. Biol. Chem.*, **276**, 27629–27637.
31. Suzuki, J., Kaziro, Y. and Koide, H. (1997) An activated mutant of R-Ras inhibits cell death caused by cytokine deprivation in BaF3 cells in the presence of IGF-I. *Oncogene*, **15**, 1689–1697.
32. Scheffzek, K., Ahmadian, M.R., Kabsch, W., Wiesmüller, L., Lautwein, A., Schmitz, F. and Wittinghofer, A. (1997) The Ras-RasGAP complex: structural basis for GTPase activation and its loss in oncogenic Ras mutants. *Science*, **277**, 333–338.
33. Lundquist, E.A. (2006) Small GTPases. In *WormBook*. The *C. elegans* Research Community, WormBook (ed.), http://www.wormbook.org. doi:/10.1895/wormbook.1.67.1.
34. Sternberg, P.W. (2005) Vulval development. In *Wormbook*. The *C. elegans* Research Community (ed.), http://www.wormbook.org. doi:10.1895/wormbook.1.6.1.
35. Sundaram, M.V. (2006) RTK/Ras/MAPK signaling. In *Wormbook*. The *C. elegans* Research Community (ed.), http://www.wormbook.org. doi/10.1895/wormbook.1.80.1.
36. Eisenmann, D.M. and Kim, S.K. (2000) Protruding vulva mutants identify novel loci and Wnt signaling factors that function during *Caenorhabditis elegans* vulva development. *Genetics*, **156**, 1097–1116.
37. Kishore, R.S. and Sundaram, M.V. (2002) ced-10 Rac and mig-2 function redundantly and act with unc-73 trio to control the orientation of vulval cell divisions and migrations in *Caenorhabditis elegans*. *Dev. Biol.*, **241**, 339–348.
38. Cordeddu, V., Di Schiavi, E., Pennacchio, L.A., Ma'ayan, A., Sarkozy, A., Fodale, V., Cecchetti, S., Cardinale, A., Martin, J., Schackwitz, W. *et al.* (2009) Mutation of SHOC2 promotes aberrant protein N-myristoylation and causes Noonan-like syndrome with loose anagen hair. *Nat. Genet.*, **41**, 1022–1026.
39. Cox, A.D., Brtva, T.R., Lowe, D.G. and Der, C.J. (1994) R-Ras induces malignant, but not morphologic, transformation of NIH3T3 cells. *Oncogene*, **9**, 3281–3288.
40. Wozniak, M.A., Kwong, L., Chodniewicz, D., Klemke, R.L. and Keely, P.J. (2005) R-Ras controls membrane protrusion and cell migration through the spatial regulation of Rac and Rho. *Mol. Biol. Cell*, **16**, 84–96.
41. Osada, M., Tolkacheva, T., Li, W., Chan, T.O., Tsichlis, P.N., Saez, R., Kimmelman, A.C. and Chan, A.M. (1999) Differential roles of Akt, Rac, and Ral in R-Ras-mediated cellular transformation, adhesion, and survival. *Mol. Cell. Biol.*, **19**, 6333–6344.
42. Marte, B.M., Rodriguez-Viciana, P., Wennström, S., Warne, P.H. and Downward, J. (1997) R-Ras can activate the phosphoinositide 3-kinase but not the MAP kinase arm of the Ras effector pathways. *Curr. Biol.*, **7**, 63–70.

43. Jopling, C., van Geemen, D. and den Hertog, J. (2007) Shp2 knockdown and Noonan/LEOPARD mutant Shp2-induced gastrulation defects. *PLoS Genet.*, **3**, e225.
44. Wang, S., Yu, W.M., Zhang, W., McCrae, K.R., Neel, B.G. and Qu, C.K. (2009) Noonan syndrome/leukemia-associated gain-of-function mutations in SHP-2 phosphatase (PTPN11) enhance cell migration and angiogenesis. *J. Biol. Chem.*, **284**, 913–920.
45. Chen, P.C., Wakimoto, H., Conner, D., Araki, T., Yuan, T., Roberts, A., Seidman, C., Bronson, R., Neel, B., Seidman, J.G. *et al.* (2010) Activation of multiple signalling pathways causes developmental defects in mice with a Noonan syndrome-associated Sos1 mutation. *J. Clin. Invest.*, **120**, 4353–4365.
46. Emanuel, P.D. (2008) Juvenile myelomonocytic leukemia and chronic myelomonocytic leukemia. *Leukemia*, **22**, 1335–1342.
47. Niemeyer, C.M. and Kratz, C.P. (2008) Paediatric myelodysplastic syndromes and juvenile myelomonocytic leukaemia: molecular classification and treatment options. *Br. J. Haematol.*, **140**, 610–624.
48. Matsuda, K., Shimada, A., Yoshida, N., Ogawa, A., Watanabe, A., Yajima, S., Iizuka, S., Koike, K., Yanai, F., Kawasaki, K. *et al.* (2007) Spontaneous improvement of hematologic abnormalities in patients having juvenile myelomonocytic leukemia with specific RAS mutations. *Blood*, **109**, 5477–5480.
49. Flotho, C., Kratz, C.P., Bergsträsser, E., Hasle, H., Starý, J., Trebo, M., van den Heuvel-Eibrink, M.M., Wójcik, D., Zecca, M., Locatelli, F. *et al.* (2008) Genotype-phenotype correlation in cases of juvenile myelomonocytic leukemia with clonal RAS mutations. *Blood*, **111**, 966–967.
50. Takagi, M., Piao, J., Lin, L., Kawaguchi, H., Imai, C., Ogawa, A., Watanabe, A., Akiyama, K., Kobayashi, C., Mori, M. *et al.* (2013) Autoimmunity and persistent RAS-mutated clones long after the spontaneous regression of JMML. *Leukaemia*, **27**, 1926–1928.
51. Park, H.D., Lee, S.H., Sung, K.W., Koo, H.H., Jung, N.G., Cho, B., Kim, H.K., Park, I.A., Lee, K.O., Ki, C.S. *et al.* (2012) Gene mutations in the Ras pathway and the prognostic implication in Korean patients with juvenile myelomonocytic leukemia. *Ann. Hematol.*, **91**, 511–517.
52. Sakaguchi, H., Okuno, Y., Muramatsu, H., Yoshida, K., Shiraishi, Y., Takahashi, M., Kon, A., Sanada, M., Chiba, K., Tanaka, H. *et al.* (2013) Exome sequencing identifies secondary mutations of SETBP1 and JAK3 in juvenile myelomonocytic leukemia. *Nat. Genet.*, **45**, 937–941.
53. Van der Burgt, I., Berends, E., Lommen, E., van Beersum, S., Hamel, B. and Mariman, E. (1994) Clinical and molecular studies in a large Dutch family with Noonan syndrome. *Am. J. Med. Genet.*, **53**, 187–191.
54. Allanson, J.E. (1987) Noonan syndrome. *J. Med. Genet.*, **24**, 9–13.
55. Sarkozy, A., Digilio, M.C. and Dallapiccola, B. (2008) LEOPARD syndrome. *Orphanet J. Rare Dis.*, **3**, 13.
56. Voron, D.A., Hatfield, H.H. and Kalkhoff, R.K. (1976) Multiple lentigines syndrome: case report and review of the literature. *Am. J. Med.*, **60**, 447–456.
57. Roberts, A., Allanson, J., Jadico, S.K., Kavamura, M.I., Noonan, J., Opitz, J.M., Young, T. and Neri, G. (2006) The cardiofaciocutaneous syndrome. *J. Med. Genet.*, **43**, 833–842.
58. Pérez, B., Kosmider, O., Cassinat, B., Renneville, A., Lachenaud, J., Kaltenbach, S., Bertrand, Y., Baruchel, A., Chomienne, C., Fontenay, M. *et al.* (2010) Genetic typing of CBL, ASXL1, RUNX1, TET2 and JAK2 in juvenile myelomonocytic leukaemia reveals a genetic profile distinct from chronic myelomonocytic leukaemia. *Br. J. Haematol.*, **151**, 460–468.
59. Guex, N. and Peitsch, M.C. (1997) SWISS-MODEL and the Swiss-PdbViewer: an environment for comparative protein modeling. *Electrophoresis*, **18**, 2714–2723.
60. Martinelli, S., Torreri, P., Tinti, M., Stella, L., Bocchinfuso, G., Flex, E., Grottesi, A., Ceccarini, M., Palleschi, A., Cesareni, G. *et al.* (2008) Diverse driving forces underlie the invariant occurrence of the T42A, E139D, I282V and T468M SHP2 amino acid substitutions causing Noonan and LEOPARD syndromes. *Hum. Mol. Genet.*, **17**, 2018–2029.
61. Bocchinfuso, G., Stella, L., Martinelli, S., Flex, E., Carta, C., Pantaleoni, F., Pispisa, B., Venanzi, M., Tartaglia, M. and Palleschi, A. (2007) Structural and functional effects of disease-causing amino acid substitutions affecting residues Ala72 and Glu76 of the protein tyrosine phosphatase SHP-2. *Proteins*, **66**, 963–974.
62. Darden, T., York, D. and Pedersen, L. (1993) Particle mesh Ewald: an N · log(N) method for Ewald sums in large systems. *J. Chem. Phys.*, **98**, 10089–10092.
63. Berendsen, H.J.C., Postma, J.P.M., van Gunsteren, W.F., Di Nola, A. and Haak, J.R. (1984) Molecular dynamics with coupling to an external bath. *J. Chem. Phys.*, **81**, 3684–3690.
64. Gremer, L., Merbitz-Zahradnik, T., Dvorsky, R., Cirstea, I.C., Kratz, C.P., Zenker, M., Wittinghofer, A. and Ahmadian, M.R. (2011) Germline KRAS mutations cause aberrant biochemical and physical properties leading to developmental disorders. *Hum. Mutat.*, **32**, 33–43.
65. Hemsath, L. and Ahmadian, M.R. (2005) Fluorescence approaches for monitoring interactions of Rho GTPases with nucleotides, regulators, and effectors. *Methods*, **37**, 173–182.
66. Jaiswal, M., Dubey, B.N., Koessmeier, K.T., Gremer, L. and Ahmadian, M.R. (2012) Biochemical assays to characterise Rho GTPases. *Methods Mol. Biol.*, **827**, 37–58.
67. Eberth, A. and Ahmadian, M.R. (2009) In vitro GEF and GAP assays. *Curr. Protoc. Cell Biol.*, **43**, 14.9.1–14.9.25.
68. Cirstea, I.C., Gremer, L., Dvorsky, R., Zhang, S.C., Piekorz, R.P., Zenker, M. and Ahmadian, M.R. (2013) Diverging gain-of-function mechanisms of two novel KRAS mutations associated with Noonan and cardio-facio-cutaneous syndromes. *Hum. Mol. Genet.*, **22**, 262–270.
69. Sulston, J.E. and Hodgkin, J. (1988) Methods. In Wood, W.B. and The Community of *C. elegans* Researchers (ed.), *The Nematode Caenorhabditis Elegans*. Cold Spring Harbor Laboratory Press, Cold Spring Harbor, NY, pp. 587–606.
70. Mello, C.C., Kramer, J.M., Stinchcomb, D. and Ambros, V. (1991) Efficient gene transfer in *C. elegans*: extrachromosomal maintenance and integration of transforming sequences. *EMBO J.*, **10**, 3959–3970.

Activating mutations in *RRAS* underlie a phenotype within the RASopathy spectrum and contribute to leukaemogenesis

Elisabetta Flex[1,24], Mamta Jaiswal[2,24], Francesca Pantaleoni[1,25], Simone Martinelli[1,25], Marion Strullu[3,4,25], Eyad K. Fansa[2,25], Aurélie Caye[3,4], Alessandro De Luca[5], Francesca Lepri[6], Radovan Dvorsky[2], Luca Pannone[1], Stefano Paolacci[1], Si-Cai Zhang[2], Valentina Fodale[1], Gianfranco Bocchinfuso[7], Cesare Rossi[8], Emma M.M. Burkitt-Wright[9], Andrea Farrotti[7], Emilia Stellacci[1], Serena Cecchetti[10], Rosangela Ferese[5], Lisabianca Bottero[1], Silvana Castro[11], Odile Fenneteau[12], Benoît Brethon[13], Massimo Sanchez[10], Amy E. Roberts[14], Helger G. Yntema[15], Ineke van der Burgt[15], Paola Cianci[16], Marie-Louise Bondeson[17], Maria Cristina Digilio[6], Giuseppe Zampino[18], Bronwyn Kerr[9], Yoko Aoki[19], Mignon L. Loh[20], Antonio Palleschi[7], Elia Di Schiavi[11], Alessandra Carè[1], Angelo Selicorni[16], Bruno Dallapiccola[6], Ion C. Cirstea[2,21], Lorenzo Stella[7], Martin Zenker[22], Bruce D. Gelb[23], Hélène Cavé[3,4,26], Mohammad R. Ahmadian[2,26] & Marco Tartaglia[1,26]

[1]Dipartimento di Ematologia, Oncologia e Medicina Molecolare, Istituto Superiore di Sanità, Rome, Italy. [2]Institut für Biochemie und Molekularbiologie II, Medizinische Fakultät der Heinrich-Heine Universitat, Düsseldorf, Germany. [3]Genetics Department, Robert Debré Hospital, Paris, France. [4]INSERM UMR_S940, Institut Universitaire d'Hématologie (IUH), Université Paris-Diderot Sorbonne-Paris-Cité, Paris, France. [5]Laboratorio Mendel, Istituto di Ricovero e Cura a Carattere Scientifico-Casa Sollievo della Sofferenza, Rome, Italy. [6]Ospedale Pediatrico "Bambino Gesù", Rome, Italy. [7]Dipartimento di Scienze e Tecnologie Chimiche, Università "Tor Vergata", Rome, Italy. [8]UO Genetica Medica, Policlinico S.Orsola-Malpighi, Bologna, Italy. [9]Genetic Medicine, Academic Health Science Centre, Central Manchester University Hospitals NHS Foundation Trust, Manchester, UK. [10]Dipartimento di Biologia Cellulare e Neuroscienze, Istituto Superiore di Sanità, Rome, Italy. [11]Istituto di Genetica e Biofisica "A. Buzzati Traverso", Consiglio Nazionale delle Ricerche, Naples, Italy. [12]Biological Hematology Department, Robert Debré Hospital, Paris, France. [13]Pediatric Hematology Department, Robert Debré Hospital, Paris, France. [14]Department of Cardiology and Division of Genetics, and Department of Medicine, Boston Children's Hospital, Boston, MA. [15]Department of Human Genetics, Radboud University Medical Centre, and Nijmegen Centre for Molecular Life Sciences, Radboud University, Nijmegen, The Netherlands. [16]Genetica Clinica Pediatrica, Clinica Pediatrica Università Milano Bicocca, Fondazione MBBM, A.O. S. Gerardo, Monza, Italy. [17]Department of Immunology, Genetics and Pathology, Uppsala University, Uppsala, Sweden. [18]Istituto di Clinica Pediatrica, Università Cattolica del Sacro Cuore, Rome, Italy. [19]Department of Medical Genetics, Tohoku University School of Medicine, Sendai, Japan. [20]Department of Pediatrics, Benioff Children's Hospital, University of California School of Medicine, and the Helen Diller Family Comprehensive Cancer Center, San Francisco, CA. [21]Leibniz Institute for Age Research, Jena, Germany. [22]Institute of Human Genetics, University Hospital of Magdeburg, Otto-von-Guericke-University, Magdeburg, Germany. [23]Mindich Child Health and Development Institute and Departments of Pediatrics and Genetics and Genomic Sciences, Icahn School of Medicine at Mount Sinai, New York, NY. [24]These authors contributed equally to this project. [25]These authors contributed equally to this project. [26]These authors contributed equally as the senior investigators for this project.

SUPPLEMENTARY MATERIAL

Supplementary Table S1. Leading RASopathy gene candidates predicted by mammalian protein interaction/functional association network analysis.

Supplementary Table S2. Clinical features of the subjects heterozygous for germline *RRAS* mutations.

Supplementary Table S3. Haematological features associated with germline or somatically acquired *RRAS* mutations.

Supplementary Table S4. *In silico* prediction of the functional impact of *RRAS* disease-associated mutations.

Supplementary Table S5. Molecular dynamics (MD) analyses.

Supplementary Table S6. *C. elegans* phenotypes resulting from expression of wild-type RAS-1 or the disease-associated RAS-1^{G27dup} mutant.

Supplementary Figure S1. Mammalian protein interaction/functional association network analysis constructed by using proteins known to be mutated in RASopathies as seed proteins.

Supplementary Figure S2. Germline and somatic disease-associated *RRAS* mutations.

Supplementary Figure S3. May-Grünwald-Giemsa stained bone marrow smears from *RRAS* mutation-positive patients at diagnosis of myeloid malignancies.

Supplementary Figure S4. Partial amino acid sequence alignment of human RRAS, KRAS, NRAS and HRAS proteins, together with representative RRAS orthologs showing conservation of mutated residues.

Supplementary Figure S5. Abolished GAP-stimulated GTP hydrolysis of the RRAS^{G39dup} mutant.

Supplementary Table S1. Leading RASopathy gene candidates predicted by mammalian protein interaction/functional association network analysis.

Gene name	Links	Links in background	Links to seed	Links in subnetwork	z-score
KSR2	10	373330	3	1169	16.80292
KSR1	60	373330	7	1169	15.74081
RALGDS	37	373330	5	1169	14.37168
SPRY2	17	373330	3	1169	12.79210
RRAS	69	373330	6	1169	12.46291
FRS2	18	373330	3	1169	12.41847
PARK7	32	373330	4	1169	12.33921
RGL2	53	373330	5	1169	11.88482
PIK3CA	71	373330	5	1169	10.14864
SPRY1	27	373330	3	1169	10.04257
EPB42	14	373330	2	1169	9.35753
BRAP	14	373330	2	1169	9.35753
RGS12	31	373330	3	1169	9.33203
RALB	56	373330	4	1169	9.14782
PLAU	15	373330	2	1169	9.02576
RET	35	373330	3	1169	8.74470
SGSM3	61	373330	4	1169	8.72902
ARAF	65	373330	4	1169	8.42836
SPRY4	40	373330	3	1169	8.13561
ITSN1	42	373330	3	1169	7.92225
SHC2	74	373330	4	1169	7.84058
RASGRP3	43	373330	3	1169	7.82104
PIK3R5	76	373330	4	1169	7.72387
BCR	47	373330	3	1169	7.44813
FLT1	22	373330	2	1169	7.36913
FARP2	85	373330	4	1169	7.24881
RRAS2	53	373330	3	1169	6.96769
GRB10	25	373330	2	1169	6.87923
RASSF2	25	373330	2	1169	6.87923
VAV1	96	373330	4	1169	6.75796
PLCE1	26	373330	2	1169	6.73465
RAP1GDS1	58	373330	3	1169	6.62379
NEK10	28	373330	2	1169	6.46849
MET	64	373330	3	1169	6.26363
SYNGAP1	65	373330	3	1169	6.20831
RASSF1	31	373330	2	1169	6.11733

Supplementary Table S2. Clinical features of the subjects heterozygous for germline *RRAS* mutations.

Patient #	NS1166	9802
Nucleotide change	c.163G>A	c.116_118dup
Amino acid change	p.Val55Met	p.Gly39dup
Sporadic/familial	unknown	sporadic
Origin of mutation	-	*de novo*
Age at last evaluation (years)	51	16
Sex	female	female
Prenatal findings	NA	polyhydramnios
Feeding difficulties	NA	+
Growth failure	NA	+
Short stature (<3rd centile)	-[1]	+
Facial features	triangular face, downslanting palpebral fissures, low-set ears, thick lips	triangular face, downslanting palpebral fissures, ptosis[2], low-set ears, thick lips
Low posterior hairline	+	+
Congenital heart defect	-	pulmonic stenosis
Hypertrophic cardiomyopathy	-	-
Short/webbed neck	-	-
Broad chest	+	+
Pectus deformity	-	-
Coagulation defects	-	-
Postnatal lymphedema	-	-
Ophthalmological problems	-	-
Motor delay / muscular hypotonia	-	Delayed acquisition of walking (20 months)
Cognitive deficits	-[3]	-
Ectodermal anomalies	-	-
Lentigines	-	-
Nevi	-	-
café-au-lait spots	-	+
Malignancy	+[4]	+[5]
Other		Crowded teeth, pyloric stenosis, glomerulonephritis, arthritis

NA, not available.
[1]10th centile.
[2]Congenital, surgically treated.
[3]Borderline cognitive abilities.
[4]Unspecified bone tumour (left leg) diagnosed during childhood.
[5]AML suspected to be secondary to JMML, with onset at 13 years (Supplementary Table S3). The condition was not associated with any germline/somatic mutation affecting previously identified RASopathy genes. Several complications occurred during treatment (renal failure, pulmonar infection, vein-occlusive disease), without complete remission. Death occurred at age of 16 by recurrence of the disease after 2 years of palliative treatment.

Supplementary Table S3. Haematological features associated with germline or somatically acquired *RRAS* mutations. Mutations characterise a subset of myeloid neoplasms with classical features of JMML (*i.e.*, monocytosis, low blast counts, presence of circulating myeloid progenitors, and elevated basophil counts) combined with atypical features, including late onset and rapid progression to AML. The latter, along with monosomy 7, are reminiscent of AML with myelodysplasia-related changes.

Patient	**9802**	**7615**	**14385**
Diagnosis	AML[1]	JMML[2]	JMML[2]
Gender	F	F	F
Age at onset (years)	13	10	13
Splenomegaly	yes	yes	no
Peripheral blood cell counts ($x10^9$/L)			
Platelets	663	47	180
White blood cells	11	7.4	14
Monocytes	1.3	1.5	4.6
Basophils	0.2	0.18	0.77
Myeloid precursors in peripheral blood (%)	14	15	10
Circulating undifferentiated myeloid blasts (%)	8	3.5	10
Bone marrow smear cytomorphology			
Undifferentiated myeloid blasts (%)	38	12	18
Myelodysplasia	+	+	+
In vitro growth of myeloid progenitors	microclusters only	microclusters only	+
Haemoglobin (g/L)	86	104	120
Fetal Haemoglobin	NA	5%	-
RRAS mutation	c.116_118dup p.Gly39dup (germline)	c.116_118dup p.Gly39dup (somatic)	c.260A>T p.Gln87Leu (somatic)
Concomitant RAS pathway mutations	-	*NRAS*, c.82A>G p.Q61R (somatic)	*NRAS*, c.35G>A[3] p.G12D (somatic)
BCR-ABL transcript	-	-	-
Karyotype (blasts)	46,XX,t(3;6)(q26;q26)[24] /46,XX[4]	45,XX -7[20] /46,XX[1]	45,XX -7

NA, not available.
[1]Secondary to JMML.
[2]Rapidly progressed to AML.
[3]The clonal architecture was investigated by sequencing the somatic *RRAS* and *NRAS* mutations in 62 individual colonies obtained by *in vitro* culture of myeloid precursors (30 CFU-GM and 32 CFU-M). All colonies exhibited both mutations.

Supplementary Table S4. *In silico* prediction of the functional impact of *RRAS* disease-associated mutations.

Nucleotide substitution	Amino acid change	SIFT	Mutation Taster	PolyPhen-2
c.163G>A	p.Val55Met	deleterious (Score = 0)	disease causing (P = 0.999999)	probably damaging ($Score_{HumVar}$ = 0.962)
c.116_118dup	p.Gly39dup	*not analyzable*	*not analyzable*	*not analyzable*
c.260A>T	p.Gln87Leu	deleterious (Score = 0)	disease causing (P = 0.999999)	probably damaging ($Score_{HumVar}$ = 0.975)

Supplementary Table S5. Molecular dynamics (MD) analyses. Structural properties of the p.Val55Met RRAS mutant (V55M) assessed before and after the structural transition observed in the MD simulation. Comparison with corresponding parameters of wild-type RRAS (WT) documents that the mutation affects the H-bonding network stabilising the GDP-RRAS complex, increases the solvent accessibility of the mutated residue, and promotes formation of a stable cluster involving Met^{55}, Tyr^{58} and Ile^{50} (Fig. 2).

Properties	WT		V55M	
	0-50 ns	100-200 ns	0-50 ns	100-200 ns
Number of H-bonds with GDP[1]	1.3 ± 0.7	1.0 ± 0.7	1.4 ± 0.6	0.01 ± 0.08
% of SAS[2] for the side-chain of residue Val^{55}/Met^{55}	27 ± 11	28 ± 11	25 ± 12	36 ± 11
% of contacts[3] between residues Val^{55}/Met^{55} and Ile^{50}	0.0	0.0	0.0	10.9
% of contacts[3] between residues Val^{55}/Met^{55} and Tyr^{58}	79.10	84.53	95.90	84.71
% of contacts[3] between residues Tyr^{58} and Ile^{50}	0.04	0.02	0.03	49.19

SAS, solvent accessible surface.
[1]Average number of the H-bonds between residues Val^{55}/Met^{55}, and Ser^{56} and GDP.
[2]The solvent accessible surface of the side-chain for residue Val^{55} (wild-type) or Met^{55} (mutant) is normalised as percentage with respect to the maximum values of 117 $Å^2$ (valine) and 160 $Å^2$ (methionine).
[3]Percentage of the simulation time with the two residues at a minimum distance lower than 4 Å.

Supplementary Table S6. *C. elegans* phenotypes resulting from expression of wild-type RAS-1 or the disease-associated RAS-1^{G27dup} mutant.

Transgene (dose of injection)	*N*	Pvl (%)	Egl (%)	Bag (%)
none	175	1.1	0.6	0.6
empty vector $_{(30\ ng/\mu l)}$	106	1.9	0.9	0.9
ras-1^{WT} $_{(30\ ng/\mu l)}$	103	15.5	12.7	9.7
ras-1^{G27dup} $_{(30\ ng/\mu l)}$	103	29.1[1]	28.2[2]	17.5
ras-1^{WT} $_{(100\ ng/\mu l)}$	94	18.1	17.0	14.9
ras-1^{G27dup} $_{(100\ ng/\mu l)}$	89	42.7[3]	41.6[3]	32.6[4]

Injections were carried out on N2 worms (wild-type background).
Strains: *ras-1*^{WT} and *ras-1*^{G27dup} indicate *hsp-16.41::ras-1*^{WT} and *hsp-16.41::ras-1*^{G27dup}, respectively; *ras-1*^{G27dup} results from the three-nucleotide insertion, c.82_83insGCG, corresponding to the RASopathy causative c.116_118dup in *RRAS*.
The concentration at which the plasmid has been injected is reported in parenthesis.
Worms were grown at 20 °C and heat-shocked at early L3 stage. Isogenic worms that had lost the transgene were cloned separately and used as controls.
N indicates the number of animals scored.
Pvl is the percent of adult worms with a protruding vulva.
Egl is the percent of animals with an increased number of eggs retained in the uterus (N > 22).
Bag is the percent of bag-of-worms animals counted up to 6 days post-fertilisation.
[1-4]Statistical significance of comparisons with worms expressing *ras-1*^{WT} at the corresponding dose of injection ([1]$P < 0.05$; [2]$P < 0.005$; [3]$P < 0.0005$; [4]$P < 0.01$). *P* values were calculated using 2-Tail Fisher's Exact Test.

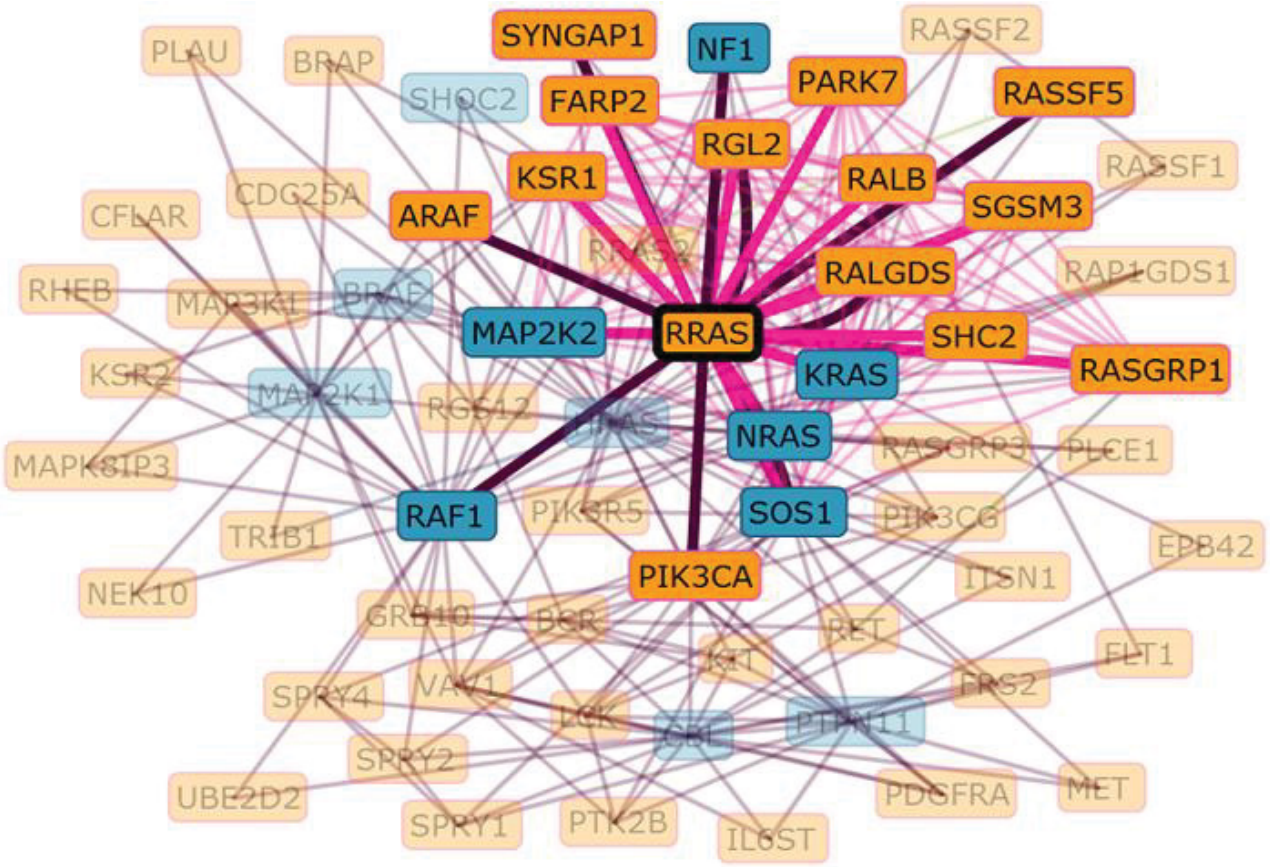

Supplementary Figure S1. Mammalian protein interaction/functional association network analysis constructed by using proteins known to be mutated in RASopathies as seed proteins. The analysis was performed by using Genes2FANs (15) (http://actin.pharm.mssm.edu/genes2FANs). Connections are based on Protein-Protein Interaction (PPI) and Connectivity Map (CMAP) networks, Mammalian Phenotype (MP) Browser, and Gene Ontology (GO), ChIP Enrichment Analysis (ChEA) and TRANSFAC databases. Connections involving RRAS are highlighted. Purple lines indicate protein-protein interactions; magenta lines indicate GO-biological process links. RASopathy genes are in blue. Leading candidates and relative z-scores are reported in Supplementary Table S1.

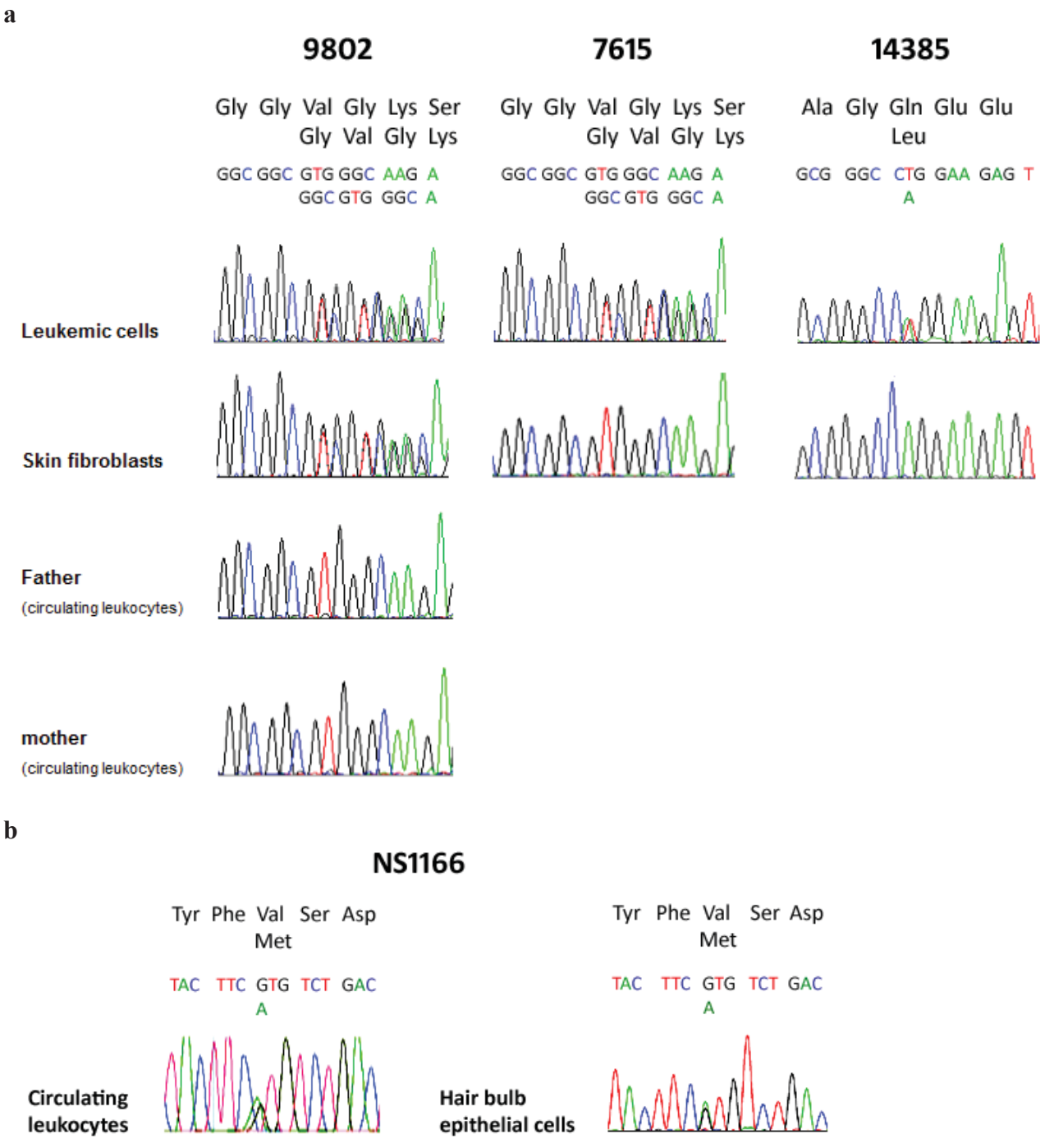

Supplementary Figure S2. Germline and somatic disease-associated *RRAS* mutations. (**a**) Electropherograms showing the *de novo*, germline origin of the c.116_118dup change (p.Gly39dup) in sporadic case 9802 (RASopathy with AML), and the somatic origin of the same in-frame duplication and the c.260A>T missense substitution (p.Gln87Leu) in subjects 7615 and 14385 (non-syndromic JMML). (**b**) Electropherograms of the germline c.163G>A missense substitution (p.Val55Met) in subject NS1166.

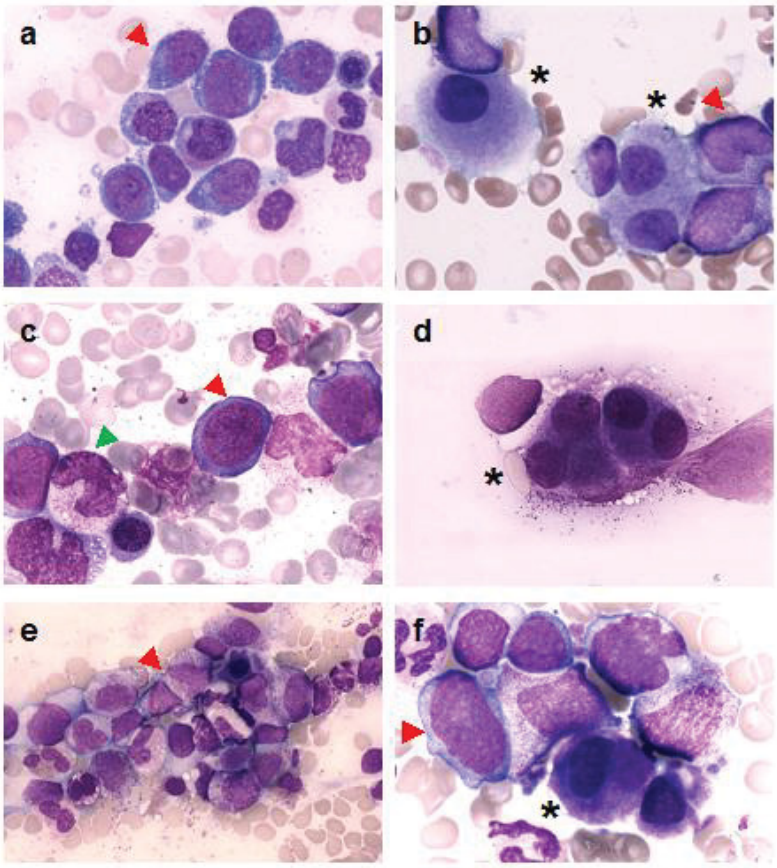

Supplementary Figure S3. May-Grünwald-Giemsa stained bone marrow smears from *RRAS* mutation-positive patients at diagnosis of myeloid malignancy. (**a**, **b**) Patient 9802 at the time of AML. (**c**, **d**) Patient 7615 with JMML. (**e**, **f**) patient 14385 with JMML. Morphological evidence of multilineage dysplasia together with excess of undifferentiated myeloid blasts is observed in all patients. Red arrowheads show undifferentiated myeloid blasts, while green arrowheads and black asterisks indicate dysplastic granulocytes and dysplastic micromegakaryocytes, respectively.

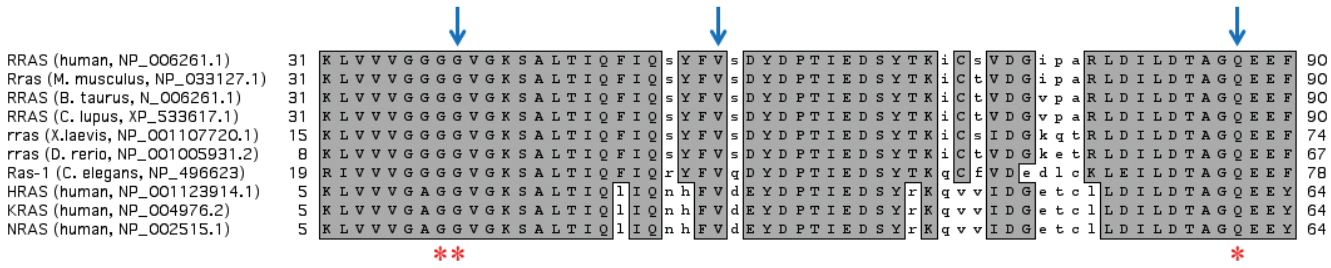

Supplementary Figure S4. Partial amino acid sequence alignment of human RRAS, KRAS, NRAS and HRAS proteins, together with representative RRAS orthologs showing conservation of the RRAS mutated residues. Blue arrows on top of the alignment mark amino acids affected by disease-associated *RRAS* mutations, while the red asterisks below the alignment indicate the positions of the cancer-associated mutation hot spots in RAS proteins.

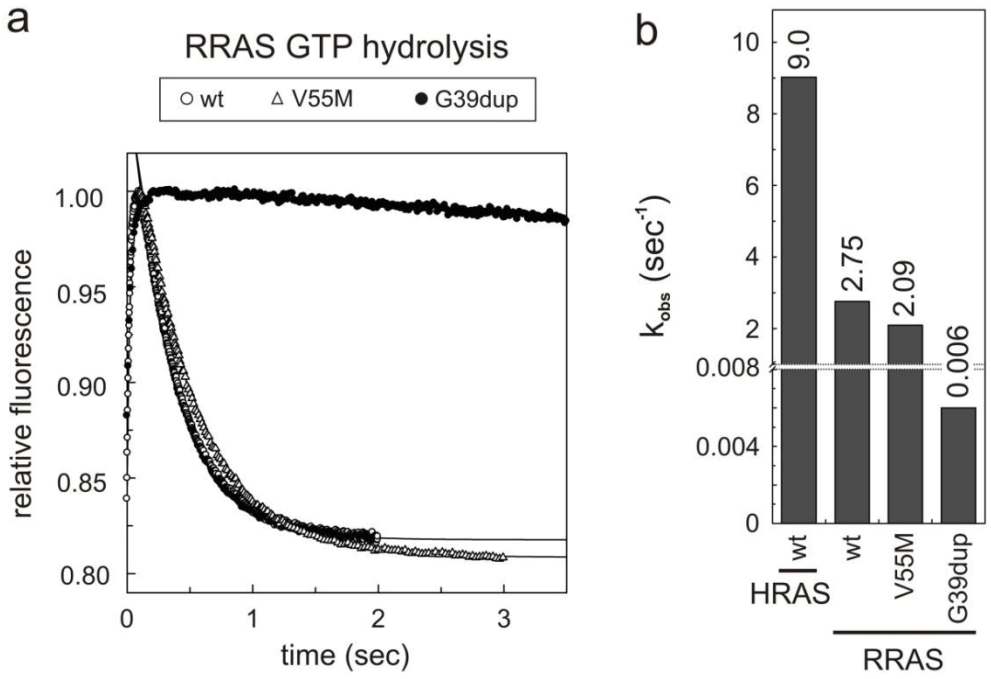

Supplementary Figure S5. Abolished GAP-stimulated GTP hydrolysis of $RRAS^{G39dup}$ mutant. (**a**) Kinetics of mantGTP hydrolysis of mantGTP-bound $RRAS^{WT}$, $RRAS^{V55M}$, and $RRAS^{G39dup}$ in presence of the GAP domain of neurofibromin. The decrease in fluorescence is directly correlated with the stimulated GTP hydrolysis reaction with an observed rate constant k_{obs} obtained by single exponential fitting and represented here as a bar chart (**b**). For comparison, the k_{obs} value for the GAP stimulated GTP hydrolysis of HRAS is shown.